

N O T I C E

THIS DOCUMENT HAS BEEN REPRODUCED FROM
MICROFICHE. ALTHOUGH IT IS RECOGNIZED THAT
CERTAIN PORTIONS ARE ILLEGIBLE, IT IS BEING RELEASED
IN THE INTEREST OF MAKING AVAILABLE AS MUCH
INFORMATION AS POSSIBLE

CR134839

K.O. 11/15/77
2/78
5/78
6-78
8-78
10-78



QUIET CLEAN SHORT-HAUL EXPERIMENTAL ENGINE
(QCSEE)

Preliminary Analyses and Design Report

Volume II

October 1974

by

Advanced Engineering & Technology Program Department
General Electric Company

(NASA-CR-134839) QUIET CLEAN SHORT-HAUL
EXPERIMENTAL ENGINE (QCSEE). PRELIMINARY
ANALYSES AND DESIGN REPORT, VOLUME 2
(General Electric Co.) 330 p HC A15/MF A01

N80-15124

CSCL 21E G3/07

Unclas
33508

Prepared For

National Aeronautics and Space Administration

NASA Lewis Research Center
Contract NAS3-18021



R74AEG479

**QUIET CLEAN SHORT-HAUL EXPERIMENTAL ENGINE
(QCSEE)**

Preliminary Analyses and Design Report

Volume II

October 1974

FOREWORD

The Quiet Clean Short-haul Experimental Engine (QCSEE) Program is currently being conducted by the General Electric Company, Aircraft Engine Group under NASA Contract NAS3-18021. The preliminary design work was performed under the direction of the NASA Project Manager, Mr. Raymond J. Rulis, Lewis Research Center.

This report covers the preliminary design effort of under-the-wing (UTW) and over-the-wing (OTW) propulsion systems. Preliminary designs of experimental and flight versions of both propulsion systems were completed during the first six months of the contract, and an oral review of the designs was conducted at Lewis Research Center on June 25 and 26, 1974.

The preliminary design phase was approved by the NASA Project Manager on July 3, 1974, permitting the program to proceed through the detail design phase.

The report is covered in two volumes plus a separate appendix (Appendix B) containing information for government use only.

PRECEDING PAGE BLANK NOT FILMED

TABLE OF CONTENTS

VOLUME I

<u>Section</u>		<u>Page</u>
1.0	INTRODUCTION	1
2.0	SUMMARY	2
2.1	Program Objectives	2
2.2	Specific Technical Objectives	3
2.2.1	Noise	3
2.2.2	Pollution	3
2.2.3	Thrust-to-Weight	3
2.2.4	Thrust Reversal	4
2.2.5	Engine Bleed	4
2.2.6	Power Extraction	4
2.2.7	Dynamic Thrust Response	5
2.2.8	Distortion Tolerance	5
2.2.9	Oil Consumption	5
2.2.10	Dumping	5
2.2.11	General Design Criteria	5
2.3	Operating Requirements	6
2.3.1	Life and Duty Cycle	7
2.3.2	Flight Maneuvers	9
2.3.3	Flight Attitudes	9
2.4	UTW Experimental Propulsion System	9
2.5	UTW Flight Propulsion System	13
2.6	OTW Experimental Propulsion System	17
2.7	OTW Flight Propulsion System	20
3.0	ACOUSTIC DESIGN	23
3.1	Summary	23
3.2	Design Requirements	24
3.3	UTW Preliminary Design	30
3.3.1	System Acoustic Design Considerations (UTW)	30
3.3.2	Takeoff Noise Constituents	31
3.3.3	Takeoff Suppression	35
3.3.4	Approach Noise Constituents	58
3.3.5	Approach Suppression	63
3.3.6	Reverse Thrust Noise Constituents	69
3.3.7	Reverse Thrust Suppression	69
3.3.8	Effect of Constituents on System Noise	74
3.4	OTW Preliminary Design	76
3.4.1	System Acoustic Design Considerations (OTW)	76
3.4.2	Takeoff Noise Constituents	76
3.4.3	Takeoff Suppression	80

TABLE OF CONTENTS (Continued)

<u>Section</u>	<u>Page</u>
3.4.4 Approach Noise Constituents	85
3.4.5 Approach Suppression	88
3.4.6 Reverse Thrust Noise Constituents	88
3.4.7 Reverse Thrust Suppression	94
3.4.8 Effect of Constituents on System Noise	94
3.5 Effect of Field Length on Engine Design	99
 4.0 EMISSIONS CONTROL	 108
4.1 Summary	108
4.2 Exhaust Emissions Design Goals	108
4.3 Selected Combustor Design for QCSEE Engines	111
4.4 Predicted UTW and OTW Engines Emissions Characteristics - With Unmodified F101 MQT Combustor	115
4.4.1 Smoke Emissions	115
4.4.2 Gaseous Emissions	117
4.5 Pertinent Emissions Reductions Design Technology	122
4.6 Predicted UTW and OTW Emissions Characteristics - With Added Emissions Control Features	126
 5.0 ENGINE CYCLE & PERFORMANCE	 128
5.1 Summary	128
5.2 Cycle Selection Criteria	128
5.3 UTW Experimental Engine and System Performance	131
5.4 UTW Flight Engine and System Performance	141
5.5 OTW Experimental Engine and System Performance	141
5.6 OTW Flight Engine and System Performance	147
 6.0 FAN AERODYNAMIC DESIGN	 149
6.1 Summary	149
6.2 UTW Fan	149
6.2.1 Operating Requirements	149
6.2.2 Basic Design Features	151
6.2.3 Reverse Flow	153
6.2.4 Performance Representation with Variable Pitch	154
6.2.5 Detailed Configuration Design	157
6.2.6 Rotor Blade Design	158
6.2.7 Core OGV Design	165
6.2.8 Transition Duct Strut Design	171
6.2.9 Vane-Frame Design	171

TABLE OF CONTENTS (Continued)

<u>Section</u>	<u>Page</u>
6.3 OTW Fan	183
6.3.1 Operating Requirements	183
6.3.2 Basic Design Features	183
6.3.3 Detailed Configuration Design	188
6.3.4 Rotor Blade Design	194
6.3.5 Core OGV Design	199
7.0 QCSEE VARIABLE-PITCH ACTUATION SYSTEMS	206
7.1 Design Requirements and Criteria	206
7.2 General Electric Actuation System	208
7.2.1 Design Studies	211
7.2.2 Ball Spline Mechanical Design	215
7.2.3 Brake Drive and Differential Gearing	217
7.2.4 Feedback Mechanism	219
7.2.5 Weight	219
7.3 Hamilton Standard Actuation System	220
7.3.1 Blade Trunnion and Roller	223
7.3.2 Cam Drive Harmonic Actuator	223
7.3.3 Cam	225
7.3.4 Harmonic Drive	225
7.3.5 Spring Clutch	231
7.3.6 Differential Gearing	231
7.3.7 Blade Pitch Stops	233
7.3.8 Input Shafting	233
7.3.9 Beta Regulator	233
7.3.10 Hydraulic Motor	235
7.3.11 LVDT and EHV	235
7.3.12 Lubrication	235
7.3.13 Accuracy	235
7.3.14 Test Hardware Consideration	236
7.3.15 Weight	236
8.0 FAN ROTOR MECHANICAL DESIGN	238
8.1 Summary	238
8.2 UTW Fan Rotor	238
8.2.1 Composite Fan Blades	240
8.2.2 Fan Disk	263
8.2.3 Blade Support Bearing	263
8.2.4 Blade Retention Trunnion	269
8.2.5 Fan Spinner	273
8.3 OTW Fan Rotor	273
8.3.1 OTW Fan Blade	275
8.3.2 OTW Fan Disk Design	281
8.3.3 OTW Fan Spinner	281

TABLE OF CONTENTS (Continued)

<u>Section</u>	<u>Page</u>
9.0 FAN FRAME MECHANICAL DESIGN	287
9.1 Summary	287
9.2 Design Requirements	291
9.2.1 Loads	291
9.3 Structural Description	291
9.4 Structural Functions	295
9.5 Structural Concept	300
9.6 Design Analysis	303
9.6.1 Weight	309
9.7 Supporting Test Data	309
9.8 Differences Between the UTW and OTW Frames	314
10.0 REDUCTION GEAR DESIGN	316
10.1 Summary	316
10.2 Design Requirements	316
10.2.1 Lubrication	319
10.2.2 Envelope	319
10.2.3 Interface	319
10.3 Gear Ratio Selection (UTW and OTW)	319
10.4 Reduction Gear Design for UTW and OTW	320
10.4.1 Description of Gear Configuration, UTW and OTW	320
10.4.2 Design Approach	323
10.4.3 Reduction Gear Design Conditions	323
10.4.4 Materials	328
10.4.5 Reduction Gear Design	328
10.5 Supporting Data	336
VOLUME II	
11.0 ENGINE CORE AND LOW PRESSURE TURBINE DESIGN	339
11.1 Summary	339
11.2 Design Requirements	339
11.3 Engine Core Modifications (UTW and OTW)	339
11.3.1 Accessory Drive Gear Mount	340
11.3.2 Compressor IGV Inner Flowpath	340
11.3.3 Compressor Stator Actuator	340
11.3.4 Compressor Stator Feedback	345
11.3.5 Combustor	345
11.3.6 HP Turbine Diaphragm Area	345

TABLE OF CONTENTS (Continued)

<u>Section</u>	<u>Page</u>
11.3.7 LP Turbine Diaphragm Area	347
11.3.8 Low Pressure Turbine No. 2 Blade	347
11.3.9 Turbine Frame	347
11.3.10 Balance Piston	347
11.4 Low Pressure Turbine Frame Aerodynamic Design	350
11.4.1 Introduction	350
11.4.2 Design	350
11.5 Low Pressure Turbine Frame Mechanical Design, UTW and OTW	354
11.5.1 Summary	354
11.5.2 Design Requirements	359
11.5.3 Design Description	359
11.5.4 Design Analysis	365
 12.0 BEARINGS AND SEALS DESIGN	 380
12.1 Summary	380
12.2 Design Requirements	381
12.3 UTW/OTW Lubrication System	382
12.3.1 Oil Supply Subsystem	382
12.3.2 Scavenge Subsystem	384
12.3.3 Seal Pressurization Subsystem	385
12.3.4 Vent Subsystem	385
12.3.5 Thermal Balance	386
12.3.6 Hydraulic System	389
12.4 UTW/OTW Thrust Balance System	389
12.5 Bearings, Seals, and Sump Design	392
12.5.1 Forward Sump Definition	394
12.5.2 Aft Sump Definition	394
12.6 Accessory Drive Design, UTW and OTW	398
 13.0 CONTROLS AND ACCESSORIES DESIGN	 405
13.1 Summary	405
13.2 Design Requirements, UTW and OTW	406
13.3 Engine Control System, UTW and OTW	407
13.3.1 General Description	407
13.3.2 Automatic Control	407
13.3.3 Manual Control	411
13.3.4 Failure Detection and Correction	412
13.3.5 Hydromechanical Control	412
13.3.6 Digital Control	419
13.4 Fuel Delivery System	430
13.5 Variable Geometry Actuation Systems	434
13.5.1 Hydraulic Supply System	434
13.5.2 QCSEE Fan Nozzle (A18) Actuation	438
13.5.3 Core Stator Actuation and Feedback	440

TABLE OF CONTENTS (Continued)

<u>Section</u>	<u>Page</u>
13.6 Sensors	441
13.6.1 Low Pressure Turbine (LPT) Speed Sensor	441
13.6.2 Core Engine Speed Sensor	443
13.6.3 Fan Inlet Temperature (T2) Sensor	445
13.6.4 Absolute and Differential Pressure Sensors	447
13.6.5 Position Feedback Sensors	450
13.7 Advanced Technology Elements	454
13.7.1 Inductive Connector	454
13.7.2 High Reliability Electronic Module	456
13.7.3 Fail-Fixed Servovalve	458
13.7.4 Magnetic Shaft Encoder	460
13.8 Variations for Flight Engines	461
 14.0 NACELLE AERODYNAMIC DESIGN	 464
14.1 Summary	464
14.2 Design Requirements	464
14.3 UTW Nacelle Aerodynamic Design	466
14.4 OTW Nacelle Aerodynamic Design	476
14.5 Supporting Data	481
 15.0 NACELLE MECHANICAL DESIGN	 494
15.1 Summary	494
15.1.1 UTW Flight Propulsion System	494
15.1.2 OTW Flight Propulsion System	496
15.1.3 UTW Experimental Propulsion System	498
15.1.4 OTW Experimental Propulsion System	501
15.2 Design Requirements	501
15.3 Material Selection	503
15.4 UTW Composite Nacelle Design	504
15.4.1 Inlet	505
15.4.2 Fan Bypass Duct and Fan Nozzle Design	513
15.4.3 Core Cowl Design	525
15.4.4 Core Nozzle Design	530
15.4.5 Mounting System	532
15.4.6 Engine System Dynamics	540
15.4.7 Accessories	546
15.5 OTW and UTW Boiler Plate Nacelle Design	549
15.5.1 Inlet	549
15.5.2 Fan Bypass Duct	553
15.5.3 Core Cowl	553
15.5.4 Core Nozzle	553
15.5.5 Pylon - Boiler Plate and Composite	554

TABLE OF CONTENTS (Concluded)

<u>Section</u>	<u>Page</u>
15.5.6 OTW Target Thrust Reverser	554
15.5.7 OTW Containment Ring	554
15.5.8 Mounting System	554
15.5.9 OTW Engine System Dynamics	563
15.5.10 Accessories	568
16.0 WEIGHT	569
16.1 UTW Engine	569
16.2 UTW Propulsion System	569
16.3 OTW Engine	569
16.4 OTW Propulsion System	569
17.0 AIRCRAFT SYSTEMS DESIGN	574
17.1 Summary	574
17.2 Study Objective	574
17.3 Mission Scenario	574
17.4 Preliminary DOC Ground Rules	579
17.5 UTW Aircraft Characteristics	579
17.6 OTW Baseline Aircraft Characteristics	590
APPENDIX A - Inflight and Reverse Thrust Noise Calculation Procedure	607

LIST OF ILLUSTRATIONS

<u>Figure</u>	<u>Page</u>
2-1. QCSEE Operating Envelope.	8
2-2. QCSEE Design Loads.	10
2-3. QCSEE Flight Attitudes.	11
2-4. UTW Experimental Engine System.	12
2-5. UTW Experimental Propulsion System.	14
2-6. UTW Flight Engine System.	15
2-7. UTW Flight Propulsion System.	16
2-8. OTW Experimental Engine System.	18
2-9. OTW Experimental Propulsion System.	19
2-10. OTW Flight Engine System.	21
2-11. OTW Flight Propulsion System.	22
3-1. QCSEE UTW Engine.	25
3-2. QCSEE OTW Engine - Preliminary Design.	26
3-3. QCSEE Acoustic Requirements.	27
3-4. Forward Radiated Fan Noise.	App B
3-5. Aft Radiated Fan Noise.	App B
3-6. UTW Takeoff Noise Constituents.	33
3-7. Suppression due to Accelerated Inlets.	App B
3-8. Design Suppression Curve - Maximum Attenuation Level.	App B
3-9. Suppression Spectrum Relative to Maximum Attenuation.	38
3-10. Effect of Duct Curvature on Suppression Bandwidth.	39
3-11. Typical Phased Treatment Test Results.	40
3-12. UTW Unsuppressed Fan Spectra.	42

LIST OF ILLUSTRATIONS (Continued)

<u>Figure</u>		<u>Page</u>
3-13.	UTW Fan Exhaust Duct Treatment.	43
3-14.	UTW Total and Segmented Fan Exhaust Duct Suppression.	44
3-15.	UTW Suppressed and Unsuppressed Fan Spectra.	45
3-16.	Normalized Spectrum of Struct Noise.	47
3-17.	UTW Suppressed Fan and Flow Generated Noise Spectra.	49
3-18.	UTW Takeoff Unsuppressed Core Spectra.	51
3-19.	SDOF Predicted Transmission Loss.	53
3-20.	Predicted Transmission Loss of Phased SDOF.	54
3-21.	Folded Quarter Wave Predicted Transmission Loss.	55
3-22.	Predicted Transmission Loss of Side Branch Resonators with Phased SDOF.	56
3-23.	UTW Core Treatment (Conceptual Design).	59
3-24.	QCSEE Compressor Treatment.	60
3-25.	Effect of Stagger Angle on Fan Noise.	App B
3-26.	UTW Approach Noise Constituents.	61
3-27.	UTW Inlet Treatment Configuration.	64
3-28.	UTW Unsuppressed Fan Spectra.	65
3-29.	UTW Inlet Suppression.	66
3-30.	UTW Suppressed and Unsuppressed Engine Spectra.	67
3-31.	UTW Suppressed and Unsuppressed Fan Spectra.	68
3-32.	UTW Reverse Thrust Noise Constituents.	70
3-33.	UTW Reverse Thrust Fan Noise.	71
3-34.	UTW Fan Inlet Suppression Spectra - Approach and Reverse Thrust.	73

LIST OF ILLUSTRATIONS (Continued)

<u>Figure</u>		<u>Page</u>
3-35.	UTW Fan Exhaust Suppression Spectrum - Forward and Reverse Thrust.	75
3-36.	Effect of Constituent Suppression on System Noise - UTW.	77
3-37.	OTW Takeoff Noise Constituents.	79
3-38.	OTW Unsuppressed Fan Spectra.	82
3-39.	OTW Fan Exhaust Duct Treatment.	83
3-40.	OTW Total and Segmented Fan Exhaust Duct Suppression.	84
3-41.	OTW Takeoff Unsuppressed Core Spectra.	86
3-42.	OTW Approach Noise Constituents.	87
3-43.	OTW Inlet Treatment Configuration.	90
3-44.	OTW Fan Inlet Suppression.	91
3-45.	OTW Suppressed and Unsuppressed Engine Spectra.	92
3-46.	OTW Suppressed and Unsuppressed Fan Spectra.	93
3-47.	OTW Jet Noise Increase due to Thrust Reverser.	95
3-48.	OTW Reverse Thrust Noise Constituents.	96
3-49.	Effect of Constituent Noise Suppression on System Noise - OTW.	98
3-50.	UTW and OTW Core Noise Suppressor Configuration.	102
4-1.	EPA Smoke Emission Standards.	110
4-2.	QCSEE Engines Combustor.	112
4-3.	F101 Combustor Central Fuel Injection Dome Cutaway - Side View.	App B
4-4.	F101 Combustors.	App B
4-5.	F101 PFRT Engine Combustor.	113
4-6.	F101 PFRT Engine Combustor.	114

LIST OF ILLUSTRATIONS (Continued)

<u>Figure</u>		<u>Page</u>
4-7.	F101 Central Fuel Injection Combustor Exit Temperature Characteristics.	116
4-8.	F101 Central Fuel Injection Combustor Altitude Relight Performance.	App B
4-9.	Comparison of Typical Commercial and Military Relight Envelopes.	App B
4-10.	Peak Smoke Emissions Characteristics of AEG Commercial Engines (Class T2).	App B
4-11.	Estimated Gaseous Exhaust Emission Characteristics of QCSEE Engines, Based on F101 PFRT Engine and Combustor Test Data.	118
4-12.	NO _x Emissions Characteristics of AEG Commercial Engines (Class T2).	App B
4-13.	C _x H _y Emissions Characteristics of AEG Commercial Engines (Class T2).	App B
4-14.	CO Emissions Characteristics of AEG Commercial Engines (Class T2).	App B
4-15.	C _x H _y and CO Reductions in CF6-6 Engine - with Localized Fuel Injection.	App B
4-16.	C _x H _y and CO Reductions in CF6-6 Engine with Increased CDP Bleed Air Extraction.	App B
4-17.	Fuel Staging Methods at Idle in the CF6 Engine.	125
4-18.	C _x H _y and CO Reductions in a CF6-50 Engine Combustor.	App B
5-1.	QCSEE Ram Recovery Characteristics.	129
5-2.	QCSEE Inlet Characteristics.	130
5-3.	UTW Cooling Flow Schematic.	133
5-4.	Station Designations - Separated Flow Turbofan Cycle.	137
5-5.	UTW Component Operating Characteristics During Approach.	139
5-6.	OTW Cooling Flow Schematic.	142

LIST OF ILLUSTRATIONS (Continued)

<u>Figure</u>		<u>Page</u>
5-7.	Station Designations - Mixed Flow Turbofan Cycle.	146
6-1.	UTW Variable Pitch Fan.	150
6-2.	Cross Section of UTW Variable Pitch Fan.	152
6-3.	UTW Blade Geometry at Different Pitch Angle Settings.	155
6-4.	UTW Stage Characteristics at 100% Speed for Various Pitch Settings.	156
6-5.	UTW Radial Distribution of Rotor Total Pressure Ratio.	159
6-6.	UTW Radial Distribution of Rotor Efficiency.	160
6-7.	UTW Radial Distribution of Rotor Diffusion Factor.	161
6-8.	UTW Radial Distribution of Rotor Relative Mach Number.	162
6-9.	UTW Radial Distribution of Rotor Relative Air Angle.	163
6-10.	UTW Radial Distribution for Core OGV.	164
6-11.	UTW Rotor Incidence, Deviation, and Empirical Adjustment Angles.	166
6-12.	UTW Rotor, Percent Throat Margin.	167
6-13.	UTW Fan Blade Plane Sections.	168
6-14.	UTW Camber and Stagger Angle Radial Distribution.	169
6-15.	UTW Rotor Thickness Distributions.	170
6-16.	UTW Core OGV.	172
6-17.	QCSEE UTW.	173
6-18.	Cylindrical Section of UTW OGV at the Pitch Line Radius.	174
6-19.	Transition Duct Flowpath.	175
6-20.	Transition Duct Strut.	176

LIST OF ILLUSTRATIONS (Continued)

<u>Figure</u>		<u>Page</u>
6-21.	Vane Frame Aerodynamic Environment.	178
6-22.	Vane Frame Nominal Vane Configuration.	179
6-23.	Vane Frame Unwrapped Section at I.D.	181
6-24.	Vane Frame Unwrapped Section at I.D., 32 Vanes Plus Pylon L.E. Fairing.	182
6-25.	QCSEE Vane Frame.	184
6-26.	QCSEE Vane Frame.	185
6-27.	Major Operating Requirements for OTW Fan.	186
6-28.	Cross Section of OTW Fan.	187
6-29.	OTW Radial Distribution of Rotor Total Pressure Ratio.	189
6-30.	OTW Radial Distribution of Rotor Efficiency.	190
6-31.	OTW Radial Distribution of Rotor Diffusion Factor.	191
6-32.	OTW Radial Distribution of Rotor Relative Mach Number.	192
6-33.	OTW Radial Distribution of Rotor Relative Air Angle.	193
6-34.	OTW Radial Distribution for Core OGV.	195
6-35.	OTW Rotor Chord Distribution.	196
6-36.	OTW Rotor Thickness Distribution.	197
6-37.	OTW Rotor Incidence, Deviation, and Empirical Adjustment Angles.	198
6-38.	OTW Rotor, Percent Throat Margin.	200
6-39.	OTW Fan Blade Plane Sections.	201
6-40.	OTW Camber and Stagger Radial Distribution.	202
6-41.	OTW Core OGV.	203

LIST OF ILLUSTRATIONS (Continued)

<u>Figure</u>		<u>Page</u>
6-42.	OTW Core OGV.	204
6-43.	Cylindrical Section of OTW OGV at the Pitch Line Radius.	205
7-1.	UTW Mission Duty Cycle.	207
7-2.	UTW Fan Maximum Net Twisting Moment.	210
7-3.	Reverse Pitch Fan Cross Section.	212
7-4.	GE Ball Spline Actuator System.	213
7-5.	UTW Ball Spline Actuator.	216
7-6.	Brake Drive and Differential Gearing.	218
7-7.	QCSEE Variable Pitch Actuation System.	221
7-8.	Hamilton Standard Actuation System Schematic.	222
7-9.	Blade Retention and Actuation System.	224
7-10.	Cam Output Characteristics Reverse Through Feather.	226
7-11.	Cam Output Characteristics Reverse Through Flat Pitch.	227
7-12.	Harmonic Drive Schematic.	228
7-13.	Spring Clutch (No-Back) Schematic.	232
7-14.	Blade Angle or Beta Regulator.	234
8-1.	UTW Variable Pitch Fan.	239
8-2.	QCSEE Stage I Molded Fan Blade.	243
8-3.	QCSEE Fan Blade.	244
8-4.	QCSEE Composite Blade.	247
8-5.	QCSEE Orientation (Design Number 1).	250
8-6.	QCSEE UTW Composite Blade.	252

LIST OF ILLUSTRATION (Continued)

<u>Figure</u>		<u>Page</u>
8-7.	Limit Cycle Boundaries.	253
8-8.	QCSEE UTW Composite Blade.	254
8-9.	UTW Blade Resultant Radial Stress - 3157 rpm.	255
8-10.	Blade Life (Goodman Diagram).	256
8-11.	UTW Blade Displacements and Twist - 3157 rpm.	257
8-12.	Allowable Stress Range Diagram - Dovetail Normal Stress.	259
8-13.	Allowable Stress Range Diagram - Dovetail Shear (PRD/Glass/Graphite Epoxy).	260
8-14.	Eighteen Blade QCSEE Impacted by a 1.81 kg (4 lb) Bird.	261
8-15.	QCSEE Composite Blade Predicted Gross Impact Capability.	262
8-16.	UTW Fan Rotor Disk.	264
8-17.	UTW Bearing and Disk Seat.	265
8-18.	Blade Thrust Bearing.	267
8-19.	Bearing Test Rig.	268
8-20.	UTW Keyhole Blade Attachment.	App B
8-21.	UTW Variable Pitch Fan with GE Actuation System.	271
8-22.	UTW Variable Pitch Fan with Hamilton Standard Actuation Arms.	272
8-23.	QCSEE OTW Fan Rotor.	274
8-24.	QCSEE OTW Fan.	277
8-25.	QCSEE OTW Fan Campbell Diagram - First Flexural Frequency.	278
8-26.	QCSEE OTW Fan Blade Campbell Diagram.	279
8-27.	Limit Cycle Boundaries.	280

LIST OF ILLUSTRATION (Continued)

<u>Figure</u>		<u>Page</u>
8-28.	OTW Fan Blade.	282
8-29.	QCSEE OTW Fan Blade Chord Vs. Span.	284
8-30.	OTW Fan Blade Maximum Thickness/Chord Vs. Span.	285
8-31.	OTW Fan Rotor.	286
9-1.	QCSEE Fan Frame.	288
9-2.	Simulated Composite Frame.	289
9-3.	QCSEE Composite Frame.	290
9-4.	QCSEE Fan Design Bypass OGV/Frame Aero Design Air Loads - Closed 2°, Open 2°, and Nominal Vanes.	294
9-5.	Fan Frame Service Areas.	296
9-6.	Fan Frame Service Areas.	297
9-7.	Fan Frame Service Areas.	298
9-8.	QCSEE Composite Frame.	299
9-9.	Fan Frame, Looking Aft.	301
9-10.	Fan Frame, Looking Forward.	302
9-11.	Fan Blade Containment Ring.	304
9-12.	Process for Iterative Structural Computer-Aided Design (PISCAD).	305
9-13.	Computer Analytical Model of Composite Frame.	306
9-14.	Finite Element Model - Composite Frame.	307
9-15.	Finite Element Model - Composite Frame.	308
9-16.	Subcomponent Test Regions.	315
10-1.	YT49-W-1 Reduction Gear.	317
10-2.	UTW Reduction Gear Assembly.	321
10-3.	QCSEE Main Reduction Gear - UTW.	324

LIST OF ILLUSTRATIONS (Continued)

<u>Figure</u>		<u>Page</u>
10-4.	Preliminary Design, Main Reduction Gear - OTW.	325
10-5.	Star Arrangement - UTW.	326
10-6.	Star Gear Bearings.	334
Volume II		
11-1.	Accessory Drive Gear Mount.	341
11-2.	Compressor IGV Inner Flowpath.	342
11-3.	F101 Compressor Characteristics (SLS Operating Line).	343
11-4.	F101 Compressor Vane Travel.	344
11-5.	Compressor Characteristics.	346
11-6.	High Pressure Turbine Stator Stage 1 Nozzle Assembly.	348
11-7.	Low Pressure Turbine Stator Stage 1 Assembly.	349
11-8.	QCSEE OGV/Frame Flowpath.	352
11-9.	QCSEE Turbine Frame Axisymmetric Flow Analysis.	353
11-10.	QCSEE Vane Modification.	355
11-11.	CASC Mach Number Distributions.	356
11-12.	CASC Mach Number Distributions.	357
11-13.	QCSEE Turbine Frame Modifications.	358
11-14.	QCSEE Turbine Exit Gas Profile (OTW).	360
11-15.	Rear Mounting System.	361
11-16.	QCSEE and F101 Mounting System.	362
11-17.	Outer Ring Support.	363
11-18.	QCSEE Turbine Frame Strut.	364

LIST OF ILLUSTRATIONS (Continued)

<u>Figure</u>		<u>Page</u>
11-19.	Turbine Frame Fishmouth Seal.	366
11-20.	Turbine Frame Stresses and Loads - Max. Sea Level Steady State plus 10 G Landing.	368
11-21.	Turbine Frame Transient Average Temperatures for Start to Max. Sea Level.	370
11-22.	Turbine Frame Stresses and Loads - 50 sec Transient plus 1 G Load.	371
11-23.	QCSEE Frame Stress Range Diagram - Foot/Skin Weld Line.	373
11-24.	QCSEE Frame Stress Range Diagram - Hub.	374
12-1.	Lube/Hydraulic System Schematic.	383
12-2.	Maximum Allowable Lube Supply Temperature of OTW Flight Engine for 150° C (300° F) Gear Temperature.	387
12-3.	OTW Flight Heat Load.	388
12-4.	Schematic of Conventional and Geared Drives.	390
12-5.	Low Pressure Turbine Thrust Balance System.	391
12-6.	Schematic of Main Shaft Bearing Arrangement.	393
12-7.	UTW Foreward Sump.	395
12-8.	Aft Sump.	396
12-9.	Accessory Drive System.	399
12-10.	Accessory Gearbox System.	400
12-11.	Inlet Gearbox Assembly.	401
12-12.	Comparison of IGB Mounting.	402
12-13.	Cross Section of Scavenge Pump Drive.	404
13-1.	Control System Schematic.	408
13-2.	F101 Fuel System Schematic.	415
13-3.	F101 Fuel Pump.	420

LIST OF ILLUSTRATIONS (Continued)

<u>Figure</u>		<u>Page</u>
13-4.	Digital Control Schematic.	421
13-5.	Central Processor Unit.	427
13-6.	Typical Control Module Cross Section.	429
13-7.	Digital Electrical Control.	431
13-8.	Fuel Delivery System.	432
13-9.	Hydraulic Supply System Schematic.	435
13-10.	Hydraulic Pump.	437
13-11.	UTW Variable Nozzle.	439
13-12.	Low Pressure Turbine (LPT) Shaft Speed Sensor.	442
13-13.	Alternating Current Generator.	444
13-14.	Fan Inlet Temperature (T_2) Sensor.	446
13-15.	Pressure Sensor.	448
13-16.	Variable Differential Transformer Schematic.	451
13-17.	Inductive Connector.	455
13-18.	High Reliability Electronic Module.	457
13-19.	Fail-Fixed Servovalve Schematic.	459
13-20.	Magnetic Shaft Encoder.	462
14-1.	Flight Placard Airflow Characteristics for QCSEE and CTOL Aircraft.	467
14-2.	Inlet Threat Mach Number Selection.	468
14-3.	Definition of Inlet Contraction Ratio to Satisfy Operational Requirements.	469
14-4.	QCSEE Inlet Lip Design.	470
14-5.	Cowl Geometries that Satisfy Low-Speed Nose Shape Requirements.	472

LIST OF ILLUSTRATIONS (Continued)

<u>Figure</u>		<u>Page</u>
14-6.	UTW and OTW Inlet.	473
14-7.	UTW Fan Duct Mach Number Distribution.	474
14-8.	UTW Fan Duct Mach Number Distribution - Reverse Thrust/Flow Operation.	475
14-9.	QCSEE OTW Fan Duct and Nozzle System.	478
14-10.	OTW Exhaust System Parameters.	479
14-11.	STOL Aircraft Design Envelope.	482
14-12.	QCSEE 30.48 cm (12 in.) Inlet Model in NASA Lewis 2.74 x 4.57 m (9 x 15 ft) Wind Tunnel.	484
14-13.	QCSEE 30.48 cm (12 in.) Inlet Test Results from NASA Lewis 2.74 x 4.57 m (9 x 15 ft) Wind Tunnel.	485
14-14.	QCSEE 30.48 cm (12 in.) Inlet Test Results, NASA Lewis 2.74 x 4.57 m (9 x 15 ft) Wind Tunnel - Inlet Separation Boundaries.	486
14-15.	On Line Dynamic Transducer Results from NASA Lewis 2.74 x 4.57 m (9 x 15 ft) Wind Tunnel Tests.	487
14-16.	Inlet Flow Separation Bounds - $V_{\infty} = 41.18$ m/sec (80 knots) - Preliminary Data.	489
14-17.	QCSEE 13.97 cm (5.5 in.) Exlet Model, Typical Tunnel Installation.	490
14-18.	QCSEE Exlet Test Matrix.	491
14-19.	Effect of Nozzle Deflection on Turning Angle.	493
15-1.	Under the Wing Flight Propulsion System.	495
15-2.	Over the Wing Flight Propulsion System.	497
15-3.	OTW Flow Paths.	499
15-4.	QCSEE Inlet Physical Properties.	506
15-5.	UTW Inlet Design.	507
15-6.	Sensitivity of Composite Wall to Local Loads.	512

LIST OF ILLUSTRATIONS (Continued)

<u>Figure</u>		<u>Page</u>
15-7.	Outer Cowl Cross Section.	514
15-8.	UTW Nacelle Cross Section.	515
15-9.	Fan Frame/Outer Cowl Joint.	516
15-10.	Outer Cowl Lower Latch and Seal.	519
15-11.	Outer Cowl Hinge and Seal.	520
15-12.	Flare Nozzle Flap Schematic.	522
15-13.	Variable Flap Nozzle.	523
15-14.	Flare Nozzle Flap Tradeoff Study.	524
15-15.	Nozzle Flap Loads Vs. Flap Length.	526
15-16.	Splitter Cross Section.	527
15-17.	Splitter End View.	528
15-18.	Splitter Joints.	529
15-19.	Core Exhaust Nozzle, UTW Experimental Engine.	533
15-20.	Stacked Acoustic Treatment Core Exhaust Nozzle, UTW Flight Engine.	534
15-21.	Side Branch Resonator Type Core Exhaust Nozzle, UTW Flight Engine.	535
15-22.	Engine Change Unit.	537
15-23.	Mounting System used for UTW and OTW Experimental Engines and UTW Flight Engine.	538
15-24.	Rear Engine Mount and Thrust Link Assembly.	539
15-25.	Load Locations.	541
15-26.	QCSEE Vibration Model, Configuration No. 1 (Typical UTW and OTW).	543
15-27.	UTW Experimental Engine Accessories.	547
15-28.	Inlet Configuration.	550

LIST OF ILLUSTRATIONS (Continued)

<u>Figure</u>		<u>Page</u>
15-29.	Inlet Mounted on Test Stand at Peebles Proving Grounds.	551
15-30.	Boiler Plate Inlets.	552
15-31.	Fan Cowl Door Attachment.	555
15-32.	Fan Core Cowl Door Attachment.	556
15-33.	OTW Experimental Core Exhaust.	557
15-34.	Facility Pylon.	558
15-35.	OTW Thrust Reverser Assembly.	559
15-36.	OTW Containment Ring.	561
15-37.	OTW Engine Change Unit.	562
15-38.	OTW Flight Type Mounting System.	564
17-1.	Short-Haul Network.	576
17-2.	QCSEE Baseline UTW Aircraft.	581
17-3.	Engine/Flap Relationship, Inboard Station.	582
17-4.	150 Passenger Interior Arrangement.	584
17-5.	Mission Profile Used for Aircraft Sizing.	585
17-6.	Baseline Aircraft Sizing Parameters.	586
17-7.	Payload Range Performance.	589
17-8.	DOC Vs. Stage Length.	591
17-9.	QCSEE Baseline OTW Aircraft.	594
17-10.	OTW Mission Performance.	597
17-11.	OTW Direct Operating Cost.	600
17-12.	Operating Cost Sensitivities to Airframe and Engine Price.	601
17-13.	Operating Cost Sensitivities to Fuel Price and Aircraft Utilization.	602
17-14.	Indirect Operating Cost Sensitivities.	605

LIST OF ILLUSTRATIONS (Concluded)

<u>Figure</u>		<u>Page</u>
A-1.	UTW Propulsion System Takeoff Configuration.	621
A-2.	UTW Propulsion System Approach Configuration.	622
A-3.	OTW Propulsion System Takeoff Configuration.	623
A-4.	OTW Propulsion System Approach Configuration.	624
A-5.	Doppler Frequency Shift.	625
A-6.	Dynamic Effect - Correction Curves.	626
A-7.	In-Flight Clean-Up and Upwash Angle Correction.	627
A-8.	Correction to OTW and UTW Jet/Flap Noise for In-Flight Effect.	627
A-9.	Curve for Adding Constituents PNdB Levels with Similar Spectra.	628
A-10.	Curve for Adding Constituent PNdB with Nonsimilar Spectra.	629
A-11.	PNdB to EPNdB Conversion for Highly Suppressed Engines.	630

LIST OF TABLES

<u>Table</u>	<u>Page</u>
2-I. Flight Duty Cycle.	7
2-II. Experimental Duty Cycle.	8
3-I. Summary of UTW and OTW Noise Levels.	23
3-II. UTW and OTW Engine and Aircraft Flight Characteristics for Acoustic Calculations.	28
3-III. Propulsion System Reverse Thrust Static Test Conditions.	29
3-IV. UTW Design Parameters.	32
3-V. QCSEE UTW Status Noise Levels.	34
3-VI. UTW Fan Exhaust Duct Suppression.	41
3-VII. Core Suppression.	52
3-VIII. QCSEE UTW Status Noise Levels.	62
3-IX. UTW Fan Exhaust Duct Suppression.	63
3-X. QCSEE UTW Status Noise Levels.	72
3-XI. OTW Design Parameters.	78
3-XII. OTW Status Noise Levels.	81
3-XIII. OTW Fan Exhaust Duct Suppression.	85
3-XIV. OTW Status Noise Levels.	89
3-XV. OTW Fan Exhaust Duct Suppression.	94
3-XVI. OTW Engine Status Noise Level.	97
3-XVII. UTW - Effect of Runway Length on Noise.	100
3-XVIII. OTW - Effect of Runway Length on Noise.	101
3-XIX. QCSEE UTW Status Noise Levels.	103
3-XX. QCSEE UTW Status Noise Levels.	104
3-XXI. QCSEE OTW Status Noise Levels.	105
3-XXII. QCSEE OTW Status Noise Levels.	106

LIST OF TABLES (Continued)

<u>Table</u>		<u>Page</u>
4-I.	EPA Gaseous Emissions Standards for Class T2 Engines.	109
4-II.	EPA Gaseous Emissions Standards - Turbojets and Turbofans.	109
4-III.	Emissions Calculations Using Prescribed EPA Landing-Takeoff Cycle.	119
4-IV.	Emissions Calculations Using Prescribed EPA Landing-Takeoff Cycle.	120
4-V.	Predicted QCSEE Engines Emissions Characteristics.	121
5-I.	QCSEE Performance Objectives.	132
5-II.	UTW Experimental Engine Performance.	134
5-III.	Separated Flow Turbofan Nomenclature.	135
5-IV.	UTW Experimental Engine Reverse Mode Performance.	140
5-V.	UTW Flight Engine Performance.	140
5-VI.	OTW Experimental Engine Performance.	143
5-VII.	Mixed Flow Turbofan Nomenclature.	144
5-VIII.	OTW Flight Engine Performance.	148
6-I.	QCSEE UTW Variable-Pitch Fan.	151
6-II.	QCSEE OTW Fan.	183
7-I.	Variable Pitch System Design Requirements.	209
7-II.	Weight Summary - General Electric Variable-Pitch Fan System.	220
7-III.	Harmonic Drive Application - Design Characteristics.	229
7-IV.	Comparison of Harmonic Drives.	230
7-V.	Weight Summary - Hamilton Standard Variable Pitch Fan System.	237

LIST OF TABLES (Continued)

<u>Table</u>		<u>Page</u>
8-I.	QCSEE UTW Composite Blade Preliminary Design Summary.	245
8-II.	PR288/AU Prepreg Properties.	248
8-III.	Composite Material Properties.	249
8-IV.	UTW Fan Disk Design Data.	266
8-V.	Bearing Load and Life Summary.	270
8-VI.	QCSEE OTW Fan Design Criteria.	276
8-VII.	QCSEE OTW Fan Blade.	283
9-I.	QCSEE Engine Loads	292
9-II.	QCSEE Frame Radial Bearing Loads.	293
9-III.	Frame Component Stresses.	310
9-IV.	Band Shear Stresses.	311
9-V.	Geometry and Material Properties of Various Composite Frame Components.	312
9-VI.	QCSEE Composite Frame Weight Breakdown.	313
10-I.	Design Requirements.	318
10-II.	Reduction Gear Requirements for Flight Duty Cycle.	318
10-III.	Lubrication Requirements for UTW Reduction Gears.	319
10-IV.	Reduction Gear Design Conditions.	327
10-V.	Gear Set Materials.	328
10-VI.	Gear Data UTW.	329
10-VII.	Gear Data OTW.	329
10-VIII.	Gear Contact Stress Data.	330
10-IX.	Gear Bending Stress Data.	330
10-X.	Gear Scoring Index for the Experimental Test Cycle.	332

LIST OF TABLES (Continued)

<u>Table</u>		<u>Page</u>
10-XI.	UTW Gear Scoring Index for the Flight Duty Cycle.	332
10-XII.	Preliminary Overall UTW Reduction Gear Efficiency and Losses for Selected Flight Conditions.	333
10-XIII.	Preliminary Heat Rejection - OTW.	333
10-XIV.	Total Oil Flows for Reduction Gears at Takeoff.	333
10-XV.	Bearing Data.	335
10-XVI.	Comparison of YT49, UTW, and OTW Gear Sets.	336
10-XVII.	Roller Bearing Comparison.	337

VOLUME II

11-I.	Fan Turbine Operating Point Data.	351
11-II.	Summary of Design Changes.	354
11-III.	Turbine Frame Maneuver Stresses, Maximum Steady State Plus 10 G Down Landing.	369
11-IV.	Turbine Frame Stresses Thermal Loading and 1 G Engine Loading, Start to Maximum S.L. Thrust.	372
11-V.	Reaction Load for Blade-Out Condition.	375
11-VI.	UTW Engine Mount Reaction Load Due to Maneuver, 2.54 cm (1 in.) Mount Pin.	376
11-VII.	OTW Engine Mount Reaction Load Due to Maneuver, 2.54 cm (1 in.) Mount Pin.	377
11-VIII.	Engine Mount Reaction Loads for 2.54 cm (1 in.) Pin.	378
11-IX.	Turbine Frame Flight Weight Design Study.	379
12-I.	QCSEE Lube Flows.	384
12-II.	Comparison of F101 and QCSEE Engine Heat Loads.	386
13-I.	Digital Control Instrumentation Signals.	423

LIST OF TABLES (Continued)

<u>Table</u>		<u>Page</u>
13-II.	Digital Control Engine Sensor and Transducer Signals.	424
13-III.	Alternator and Digital Signals to Digital Control.	424
13-IV.	Outputs.	425
13-V.	Pump Characteristics (F101 Pump).	433
14-I.	Propulsion System Exhaust Area Requirements.	465
14-II.	30.48 cm (12 in.) Inlet Test Matrix.	483
15-I.	Inlet Weight Comparison.	508
15-II.	Estimated Forces and Moments on QCSEE Inlet Cowl Based on Potential-Flow Theory, Left-Hand Cowl.	509
15-III.	Stresses from Shear, Moment, and Axial Loads.	510
15-IV.	Critical Buckling Loads.	511
15-V.	Latch Loads.	513
15-VI.	Fan Duct Hinge/Skin Stresses.	518
15-VII.	UTW Experimental Propulsion System Mount Loads with Composite Nacelle.	542
15-VIII.	Basic Engine Weight and Moment Data, UTW Configuration No. 1.	544
15-IX.	System Critical Speeds, Maximum Response Due to Fan Rotor.	544
15-X.	System Critical Speeds, Maximum Response Due to LP Turbine Rotor.	545
15-XI.	System Critical Speeds, Maximum Response Due to HP Rotor.	546
15-XII.	OTW Flight Engine Mount Reaction Loads.	565
15-XIII.	Basic Engine Weight and Moment Data, OTW Configuration No. 1.	566

LIST OF TABLES (Continued)

<u>Table</u>		<u>Page</u>
15-XIV.	System Critical Speeds, Maximum Response Due to Fan Rotor.	566
15-XV.	System Critical Speeds, Maximum Response Due to LP Turbine Rotor.	567
15-XVI.	System Critical Speeds, Maximum Response Due to HP Rotor.	567
16-I.	Engine Detail Weight Breakdown.	570
16-II.	UTW Propulsion System Weight Status.	572
16-III.	OTW Propulsion System Weight Status.	573
17-I.	QCSEE Preliminary Aircraft System Definition.	575
17-II.	QCSEE Preliminary Aircraft System Definition.	577
17-III.	Typical Trunk Airline Departures.	578
17-IV.	Preliminary Data for Economic Studies.	580
17-V.	UTW Aircraft Characteristics.	587
17-VI.	Group Weight Statement.	588
17-VII.	Direct Operating Cost Breakdown.	592
17-VIII.	Engine Trade Factors.	592
17-IX.	Design Conditions.	593
17-X.	Propulsion System.	593
17-XI.	Basic Weights.	596
17-XII.	Baseline Aircraft Characteristics.	598
17-XIII.	Data for Economic Analysis.	599
17-XIV.	Direct Operating Cost Comparison.	603
17-XV.	Indirect Operating Cost Comparison.	604

LIST OF TABLES (Concluded)

<u>Table</u>		<u>Page</u>
A-I.	UTW and OTW Engine and Aircraft Design Flight Characteristics for Acoustic Calculations.	609
A-II.	Propulsion System Reverse Thrust Static Test Conditions.	609

PRECEDING PAGE BLANK NOT FILMED

SECTION 11.0

ENGINE CORE AND LOW PRESSURE TURBINE DESIGN

11.1 SUMMARY

In order to minimize development risk and expense in the QCSEE program, the F101 core and low pressure turbine were selected. Moreover, to capitalize on the advanced state of development of these components, the qualified PFRT, or YF101, design was specified insofar as practical. Several exceptions to this approach exists. The following components are different from the PFRT configuration.

1. Accessory Drive Gear Mount
2. Compressor IGV Inner Flowpath
3. Compressor Stator Actuator
4. Compressor Stator Feedback
5. Combustor
6. HP Turbine Diaphragm Area
7. LP Turbine Diaphragm Area
8. LP Turbine No. 2 Blade
9. Turbine Frame
10. Balance Piston

11.2 DESIGN REQUIREMENTS

The F101 core and low pressure turbine were proposed for the QCSEE engines, because in addition to providing desirable cycle and thrust size, this core engine employs suitable advanced technology components.

A major consideration in the detail core selection has been the desire to retain as much "qualified" hardware as practical. Therefore, the qualified PFRT configuration has been specified in all areas except those discussed in the following paragraphs. It is also noted that the UTW and OTW engines incorporate identical core and LPT hardware, providing future program flexibility for parts interchange.

11.3 ENGINE CORE MODIFICATIONS (UTW AND OTW)

The following specific deviations from the PFRT configuration are planned for the QCSEE engines.

11.3.1 Accessory Drive Gear Mount

The F101 internal accessory drive bevel gears are mounted in a 17-4PH steel casting. This casting is bolted to the aft inner flange of the fan frame. Because of the higher bypass ratio of the QCSEE engines, the aft ring of the composite frame interferes with this gear mount casting.

The solution to this problem is to reverse the casting and bolt it to the forward ring of the frame as shown in Figure 11-1.

In addition, the QCSEE experimental engines will have two radial drive shafts; one driving the top-mounted accessories and another driving the scavenge pump, located in the lower core cowl region. This requirement can be readily satisfied by using two sets of bevel gears and two support castings in each engine. (The casting occupies less than 180° of the mounting flange.) The flight UTW engine would require two sets of bevel gears whereas the OTW would only require one.

11.3.2 Compressor IGV Inner Flowpath

The F101 inner flowpath in the IGV region is shown as a dashed line in Figure 11-2. Because of the higher bypass ratio and lower fan exit radius ratio in the QCSEE engines, difficulty was encountered in fairing into this flowpath contour from the fan frame with acceptable aerodynamic flow lines. Therefore, a modification was made to the inner ring of the inlet guide vane as shown in the figure.

11.3.3 Compressor Stator Actuator

The F101 compressor has been developed to optimize efficiency and flow at reduced corrected speeds, as required by its higher Mach number mixed mission. As a result, it produces 27.3 kg/sec (60.3 lb/sec) at 100% corrected speed. For use in the QCSEE engines, a higher airflow is desired, consistent with existing rpm and T4 limits. Operation at greater than 100% corrected speed would result in a severe compressor efficiency loss.

Fortunately, as a part of the F101 compressor development, various other stator schedules have been tested. One of the demonstrated schedules delivers a significant increase in corrected flow at high corrected speeds as indicated by the dashed line in Figure 11-3. It may also be noted that this "high flow" schedule met the F101 objective stall margin of 22%.

The means of achieving the higher flow is illustrated in Figure 11-4. The IGV and Stage 1-3 vane setting angles are varied as a function of compressor corrected speed within the limits shown. The β schedule must be increased at the open end of travel as shown in the dashed line. The increase amounts to about 11° of additional IGV rotation and lesser amounts in the other stages.

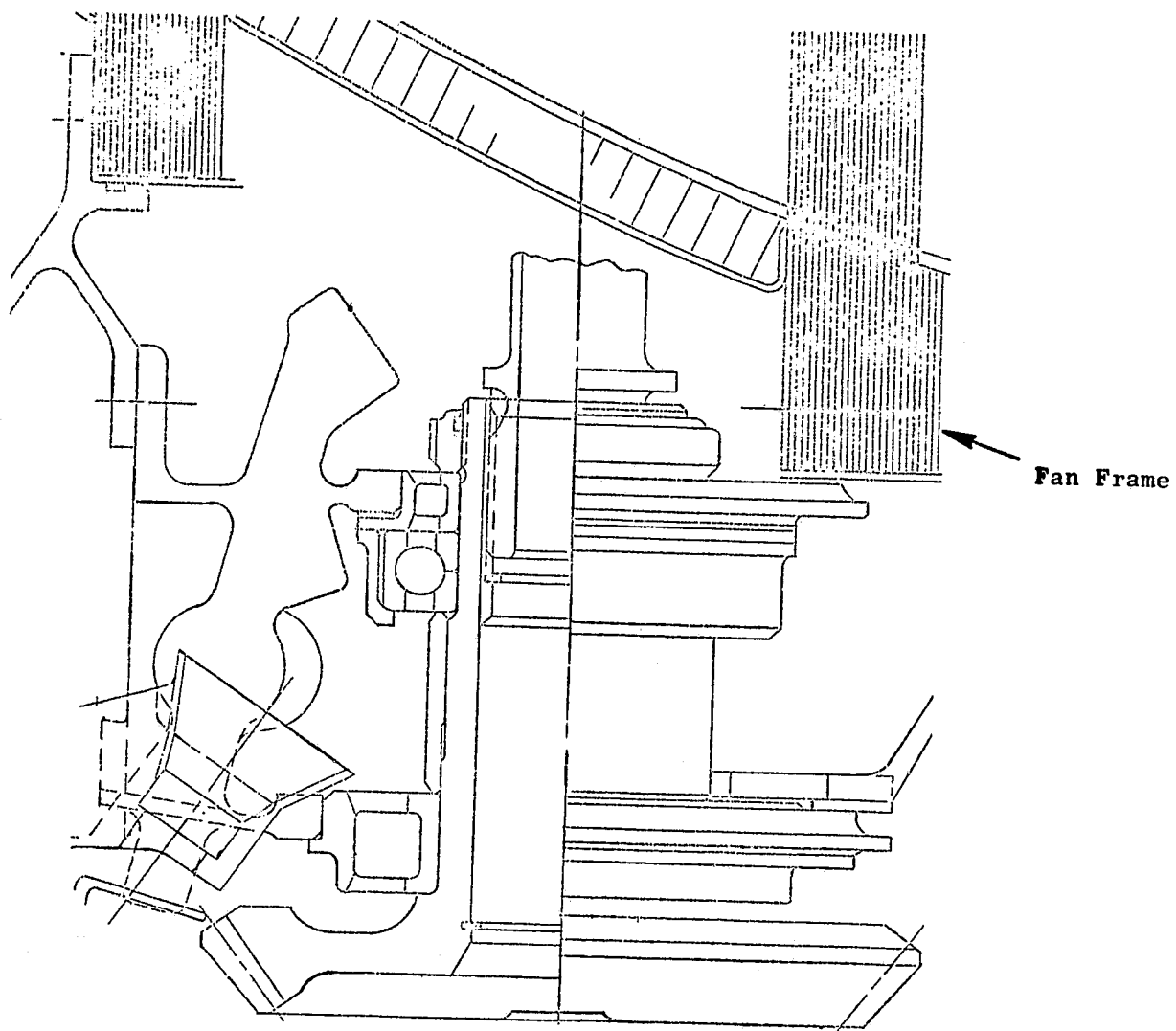


Figure 11-1. Accessory Drive Gear Mount.

ORIGINAL PAGE IS
OF POOR QUALITY

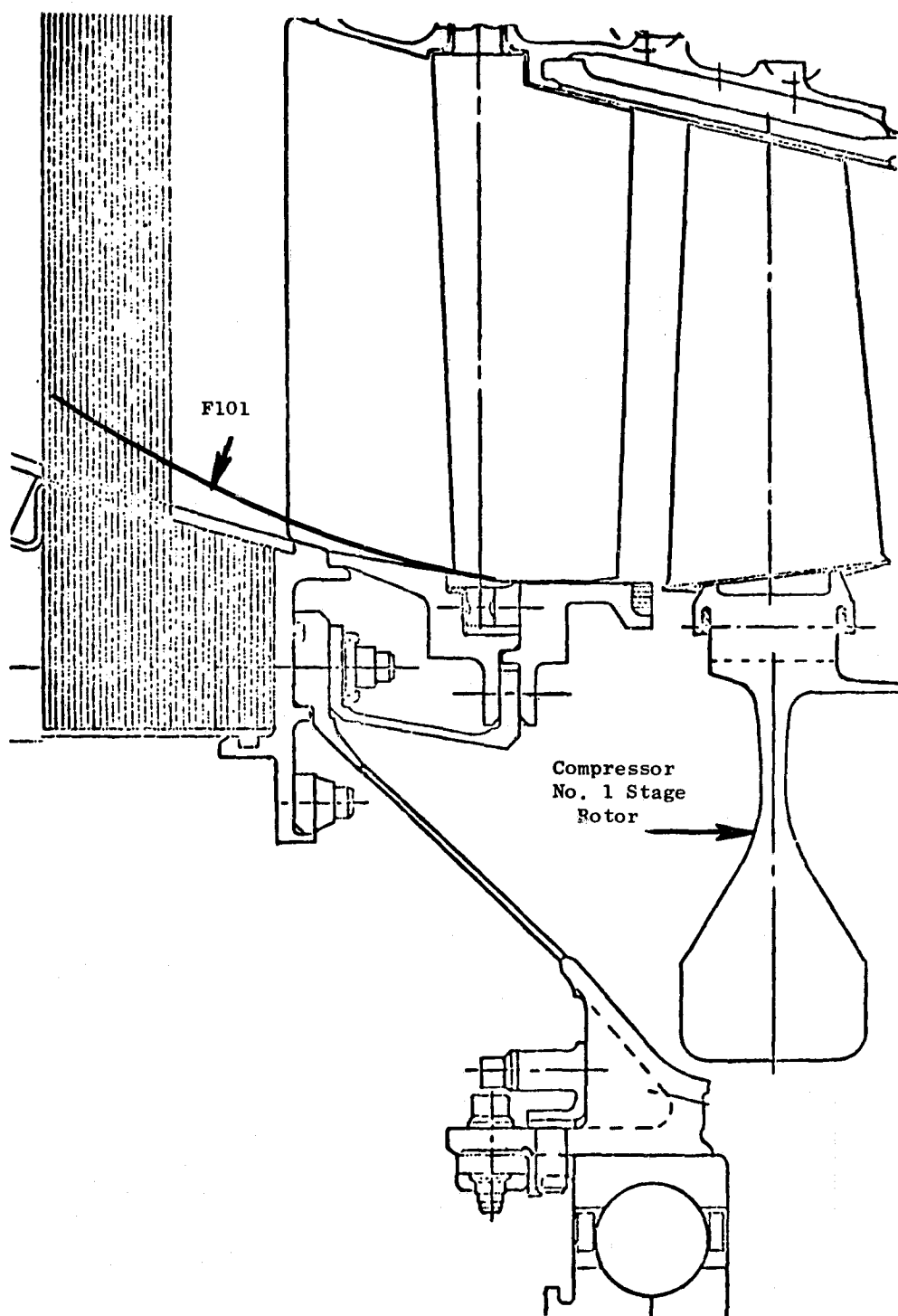


Figure 11-2. Compressor IGV Inner Flowpath.

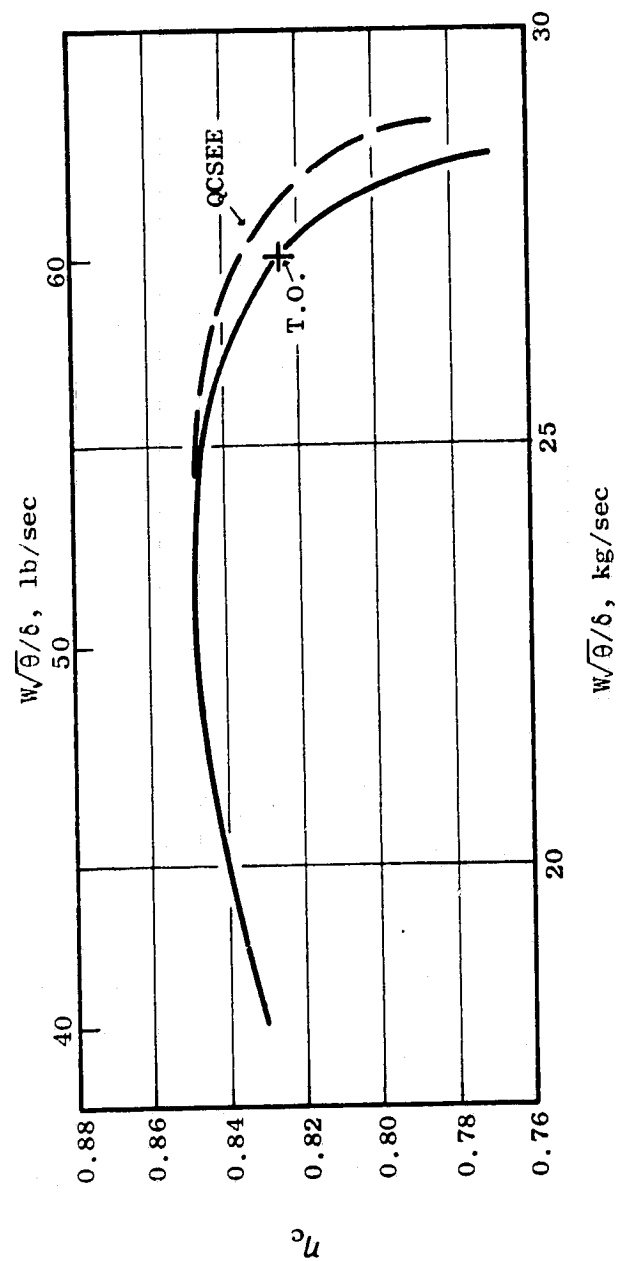


Figure 11-3. F101 Compressor Characteristics (SLS Operating Line).

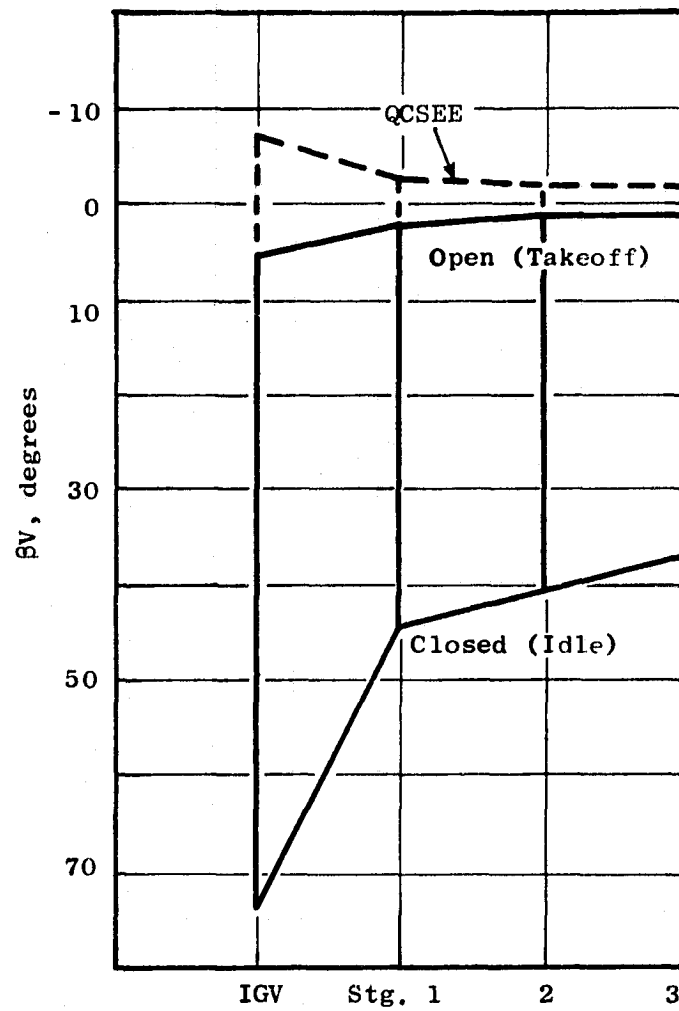


Figure 11-4. F101 Compressor Vane Travel.

In order to achieve the increase in vane travel, several minor modifications are required in the actuator and linkages.

1. The vane actuator stroke must be increased from 7.747 cm (3.05 in.) to 9.627 cm (3.79 in.).
2. A new Stage 3 bellcrank must be provided.
3. The rod end of the Stage 3 linkage must be shortened about 0.127 cm (0.050 in.).
4. Bolts and nuts in the bellcranks must be replaced with flathead pins and snap rings to permit them to pass between the actuation support members.

11.3.4 Compressor Stator Feedback

In the F101 engine, compressor stator angle is fed back to the control by means of a splined shaft, extending from the master bellcrank out through the bypass duct. This shaft is too short for use in the QCSEE engines and it will be replaced by a flex-cable leading from the master bellcrank, through the pylon to the control.

11.3.5 Combustor

The F101 PFRT engine contains a scroll carbureting combustor dome as illustrated in Figure 4-4 (Appendix B). While this design has been generally satisfactory, there have been isolated cases of flashback and carbon formation in the scroll. As a result, the F101 MQT design and other future engines have been changed to incorporate a "central injector dome". In this design the fuel is injected at low pressure through holes in the sides of the injector tubes. It impinges on the walls of a venturi where it is violently mixed with primary combustion air. This design eliminates the possibility of flashback by eliminating premixing.

Since a major objective of the QCSEE program is the development of low-emission combustor technology for future engines, it was deemed desirable to use the latest combustor dome design. Therefore, the MQT dome has been specified for the QCSEE engines, and the reduced emission effort described in Section 4.0 is based upon this design.

11.3.6 HP Turbine Diaphragm Area

Figure 11-5 again shows the "high flowed" compressor characteristic selected for the QCSEE engines. Because of the reduced pressure ratio compared to the F101 cycle, both the HP and LP turbine effective areas require adjustment. If the nominal F101 areas were used, the compressor would have to be operated at the point shown to deliver objective thrust levels. Again this would result in a severe efficiency penalty.

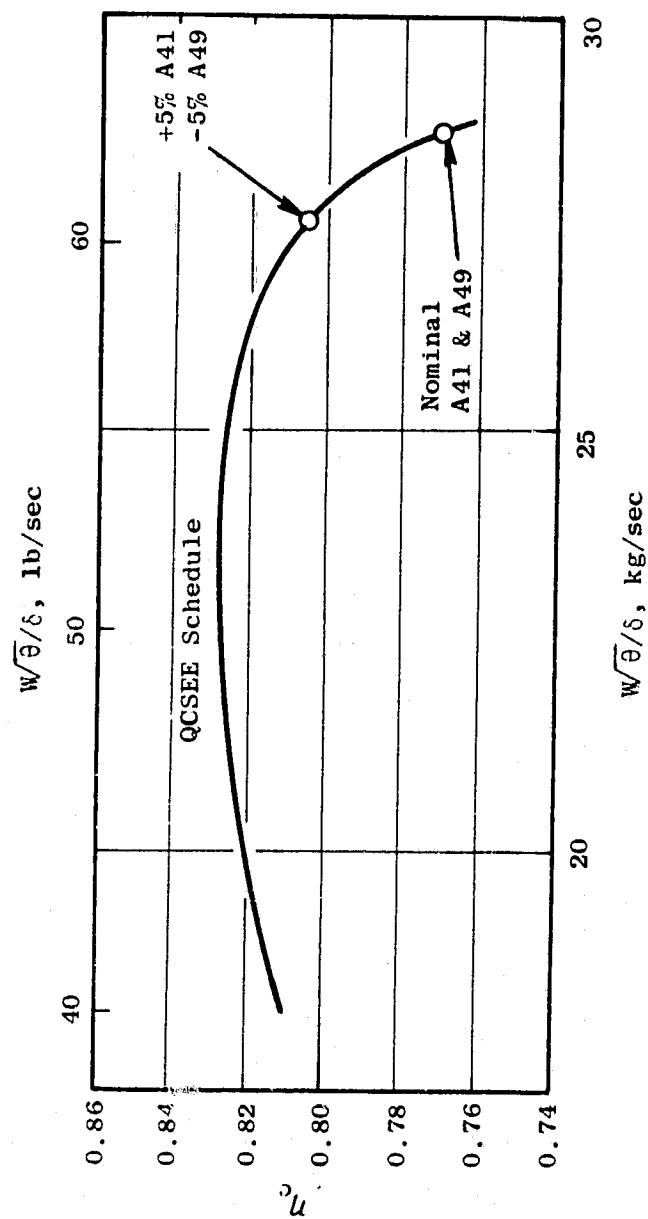


Figure 11-5. Compressor Characteristics.

By increasing the HP turbine effective area by 5% and decreasing the LP turbine effective area by 5%, the compressor can be made to operate at a much more favorable point, as shown.

The means for adjusting turbine area is to rotate the vanes slightly to open or close the throat dimension. Figure 11-6 illustrates the degree of rotation needed for a 5% increase in HP turbine area. This will be accomplished by rotating the tool used to EDM the vane slots in the bands. New inspection fixtures may also be required.

11.3.7 LP Turbine Diaphragm Area

In the case of the LP turbine, 5% reduction of area is accomplished by similar means. In either case the change in throat dimension (D_o) is less than 0.05 cm (0.020 in.). Figure 11-7 illustrates this adjustment in the LPT stage one diaphragm.

11.3.8 Low Pressure Turbine No. 2 Blade

Low pressure turbine aft running exit swirl has presented a development problem in the F101, in that the actual pitch line swirl values were approximately 8° greater than the design value of 20° . This has been corrected in development engines by "decambering" the No. 2 blade. This process consisted of bending the trailing edge open about 3° at the pitch line with no change at the hub or tip sections. The MQT blade is currently being redesigned to incorporate this change in the airfoil castings.

In the QCSEE engines, the increased LP energy extraction results in higher exit swirl, which will be removed by using longer straightening vanes in the turbine frame. However, to minimize the required turning in these vanes, and to provide more predictable angles of attack on the vanes, it was deemed advisable to incorporate the MQT No. 2 LPT blade.

11.3.9 Turbine Frame

Modifications to the F101 turbine frame to extract greater swirl and to adapt the frame structurally to meet QCSEE requirements are described in detail in Section 11.4 and 11.5.

11.3.10 Balance Piston

Introduction of a reduction gear between the low pressure turbine and the fan in the QCSEE engines effectively cuts the load path normally used to balance fan plus LPT low pressure rotor net thrust force. Therefore, the rear sump area will be modified to incorporate a pneumatic piston to balance part of the turbine rotor thrust. Without this, the turbine thrust bearing is impractical. The design of the balance piston is discussed in detail in Section 12.5.

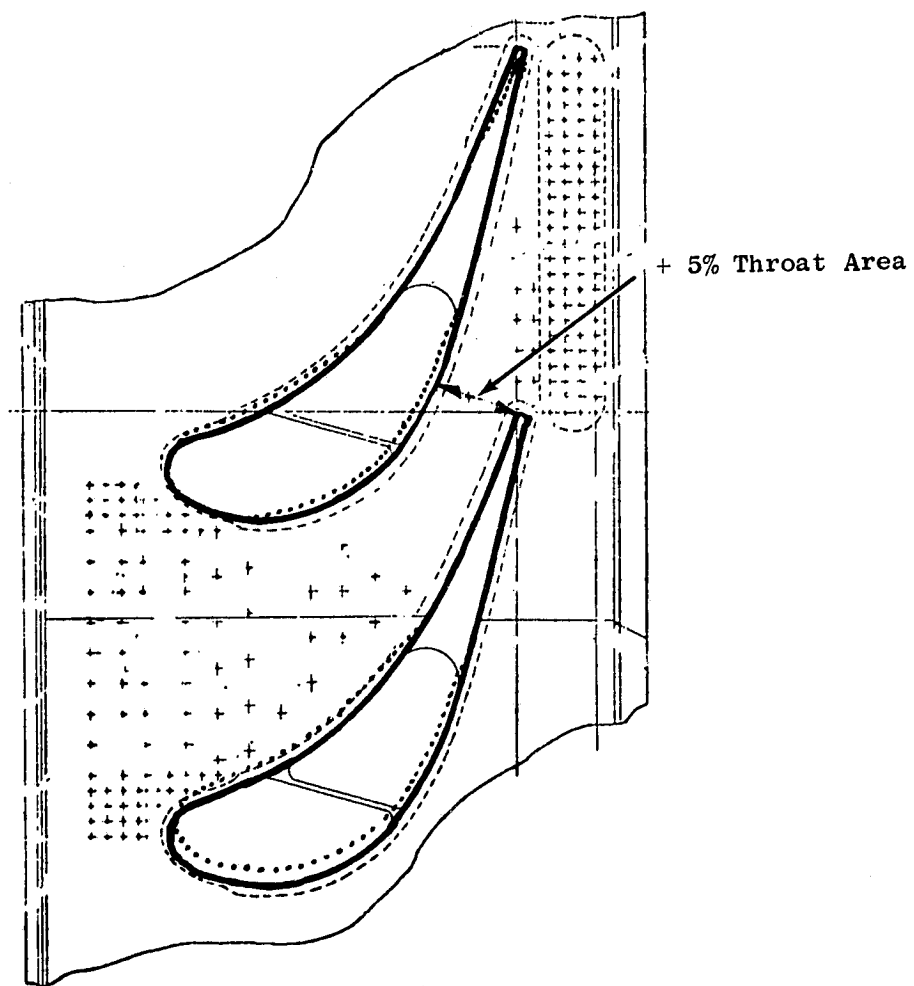


Figure 11-6. High Pressure Turbine Stator Stage I Nozzle Assembly.

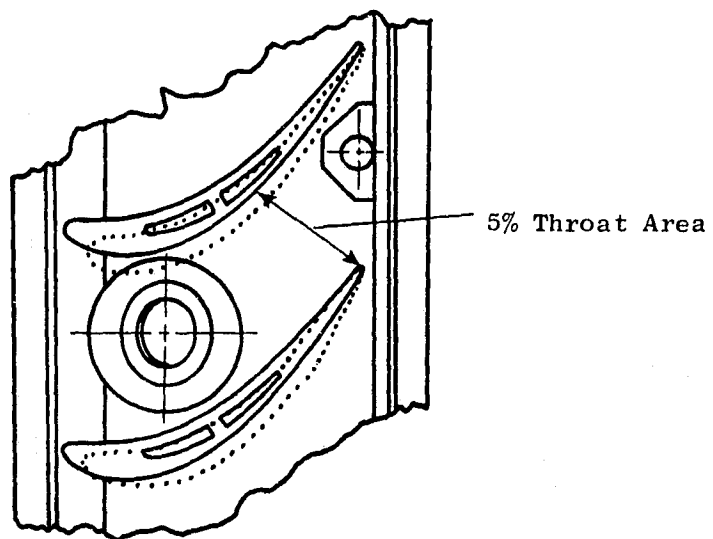


Figure 11-7. Low Pressure Turbine Stator
Stage I Nozzle Assembly.

11.4 LOW PRESSURE TURBINE FRAME AERODYNAMIC DESIGN

11.4.1 Introduction

The QCSEE low pressure turbine is a slight modification of the F101 low pressure turbine operating at an increased pressure ratio. The increased turbine exhaust swirl necessitated a modification to the present F101 frame/OGV aerodynamic geometry. The frame/OGV was redesigned for low noise and low loss characteristics.

11.4.2 Design

Design Point Selection

Turbine operating point for the frame/OGV aerodynamic design was selected to avoid off-design modes where separation and consequent core noise can occur at critical engine operating points. Turbine off-design vector diagram studies were made at significant QCSEE operating points using the Multi-Sector NASA Turbine Computer Program. These studies were based on cycle data contained in the Technical Requirements published April 1974. A summary of results is shown in Table 11-1. The OTW takeoff condition was chosen as the design point as this case represented the highest turbine exhaust swirl and Mach number conditions (excluding maximum cruise points). Subsequent cycle data indicated somewhat higher swirl points, but the OTW takeoff case shown was still considered to be a reasonable design condition.


Axisymmetric Analysis and Flowpath Modification

Axisymmetric analysis of the frame/OGV was done using the CAFD computer program. This calculation accounts for streamline slope and curvature as well as lean and sweep effects. The analysis was set up with many intrablade calculation stations in order to analyze endwall Mach number distributions. First, the F101 frame flowpath with an additional 2.54 cm (1 in.) of axial width in the OGV was analyzed. While the results of this analysis did not indicate any particular need to change the flowpath, a modified flowpath was designed which was considered an aerodynamic improvement (with reduced diffusion) and also satisfied frame mechanical design and exhaust system requirements. This flowpath is shown in Figure 11-8.

The results of the axisymmetric analysis are shown in Figure 11-9. Plotted versus radial height at the OGV inlet are the gas angle, OGV design angle (compared to the original F101 vane angle) and inlet absolute Mach number. Also shown is the absolute Mach number distributions on the inner and outer walls through the OGV. The NASA diffusion factors associated with this flowpath are:

$$\begin{aligned}D_{\text{Root}} &= 0.316 \\D_{\text{Pitch}} &= 0.440 \\D_{\text{Tip}} &= 0.183\end{aligned}$$

Table 11-I. Fan Turbine Operating Point Data.

Engine Condition	$\frac{F101}{T0}$	UTW		(1) TO		OTW	
		T0	APPR Max. Cruise	APPR Max. Cruise	(1) TO	APPR Max. Cruise	(1)
$\frac{\Delta h}{T} \sim \text{Btu}/^\circ \text{R}$	0.057	0.063	0.055	0.073	0.066	0.056	0.066
$\frac{\Delta h}{T} \sim J_{\text{sec}}/\text{gm-}^\circ \text{K}$	0.266	0.294	0.257	0.341	0.308	0.262	0.308
$\frac{N}{\sqrt{T}} \sim \text{rpm}/\sqrt{^\circ \text{R}}$	162	165	180	176	164	152	162
$\frac{N}{\sqrt{T}} \sim \text{rpm}/\sqrt{^\circ \text{K}}$	217	221	241	236	220	204	217
$\psi = \frac{\Delta V_u}{u}$	0.98	1.04	0.76	1.05	1.10	1.10	1.12
Swirl (Degrees)	23.7	25.8	8.2	33.5	29.6	24.1	29.9
Mach No.	0.42	0.47	0.34	0.68	0.53	0.40	0.52
 Design Point							

(1) Alt/Mach No. = 600 m/0.7 (20,000 ft/0.7)

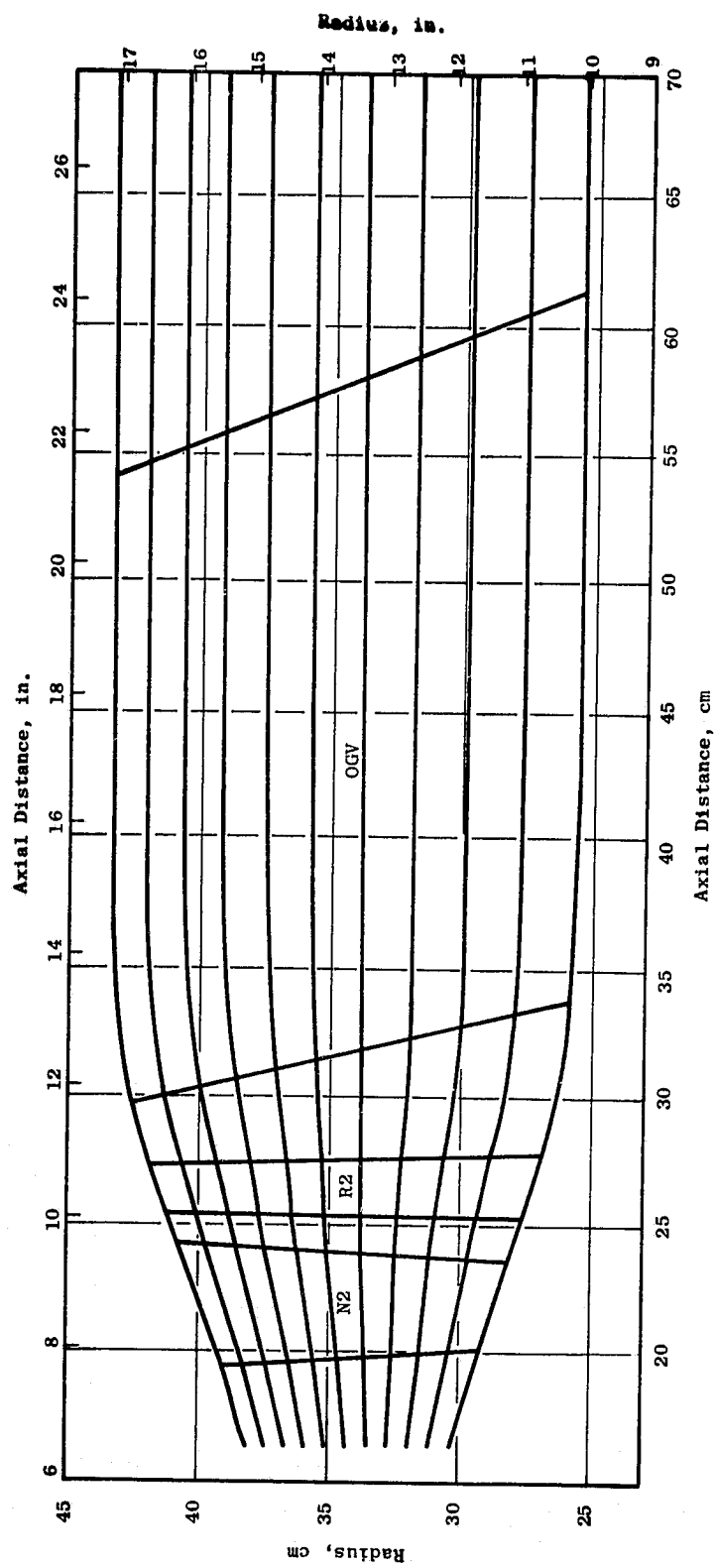


Figure 11-8. QCSEE OGV/Frame Flowpath.

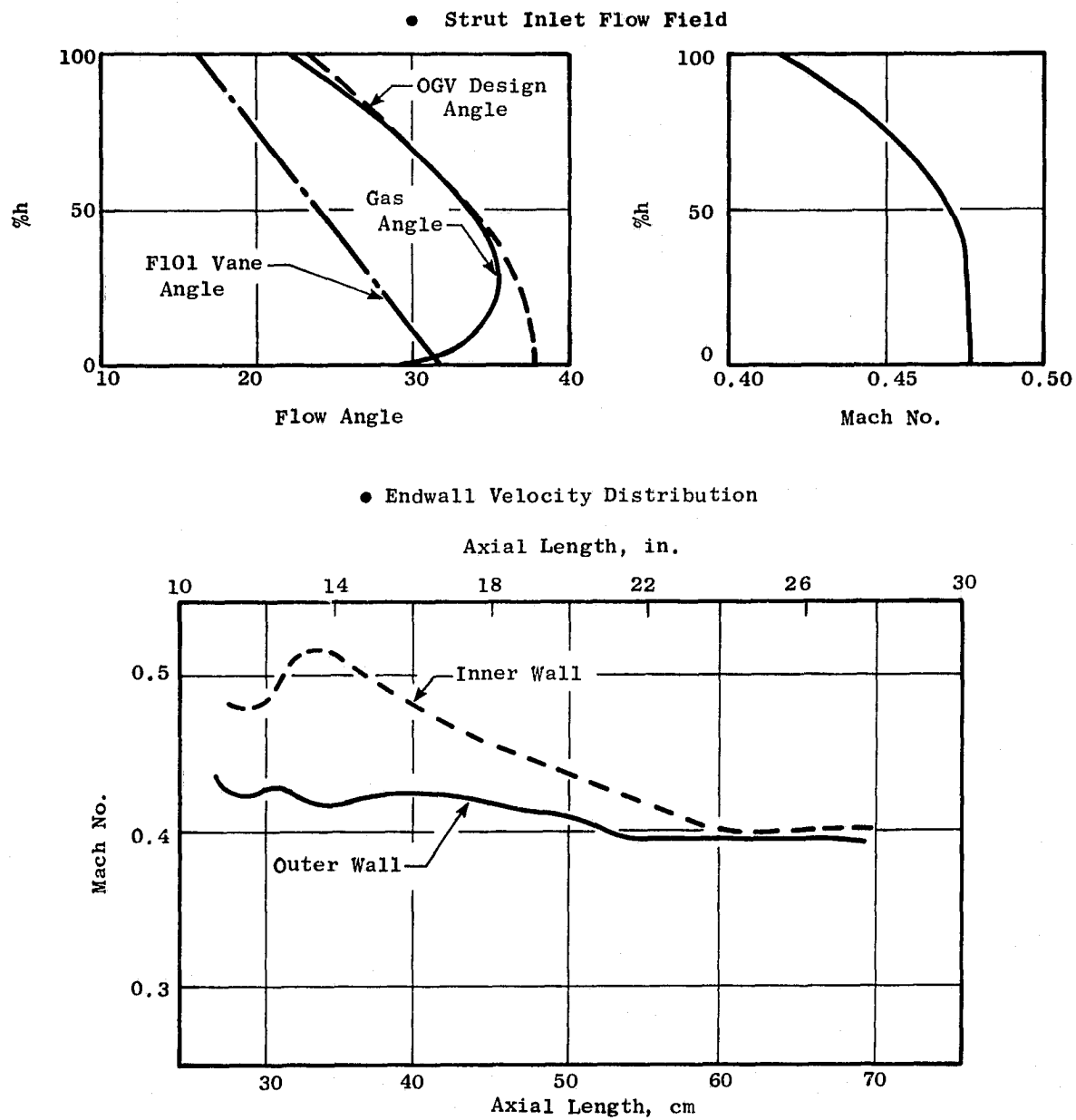


Figure 11-9. QCSEE Turbine Frame Axisymmetric Flow Analysis.

Vane Modification

The vane modification involved adding 2.54 cm (1 in.) of axial width to the present F101 OGV to remove the additional swirl. The change was made entirely in the false nose extension with the strut and aft strut extension remaining unchanged. Three vane sections at approximate root, pitch, and tip locations were designed and analyzed using both the CASC and CABIS programs. The CABIS (Cascade Analysis due to Beuckner, Isay, and Schnacker) program is an incompressible analysis while CASC (Cascade Analysis by Streamline Curvature) gives a compressible solution which accounts for radius change and streamtube thickness variation. The CASC Mach number distribution for the pitch section is given in Figure 11-10 for two different false nose extensions. Figure 11-10 shows that if the nose extension was designed to attach to the strut, as it presently does in the F101, there would be a distinct "bump" on the pressure surface. A smooth pressure surface was designed as shown and both configurations were analyzed with CASC. The resulting Mach number distributions clearly indicate the effect of the bump. Consultation with experienced OGV designers indicated only a small decrement in performance associated with this. However, it was decided (with Mechanical Design concurrence) to modify the OGV smoothly as shown. CASC Mach number distributions for the root and tip are shown in Figures 11-11 and 11-12. Other intermediate sections were designed to yield a smooth stack-up.

11.5 LOW PRESSURE TURBINE FRAME MECHANICAL DESIGN, UTW AND OTW

11.5.1 Summary

The turbine frame, used in both the UTW and OTW engines, is a modification of the F101 turbine frame. Changes are required to accommodate a longer vane/strut chord and to adapt the frame to a pylon mounting system. Figure 11-13 illustrates these modifications, which are summarized as follows in Table 11-II:

Table 11-II. Summary of Design Changes.

<u>Item</u>	<u>Change</u>	<u>Reason</u>
● Vane/Strut	Extended forward fairing	Remove additional swirl
● Outer ring	Larger section	Change mounting from 12, 0.792 cm (0.312 in.) diam pins to 3, 2.54 cm (1.00 in.) diam pins
● Flowpath liners	Recontour	Improve aero flowpath
● Outer casing	New structural part	Support exhaust nozzle
● Inner ring	Thicken and added flanges	Support centerbody

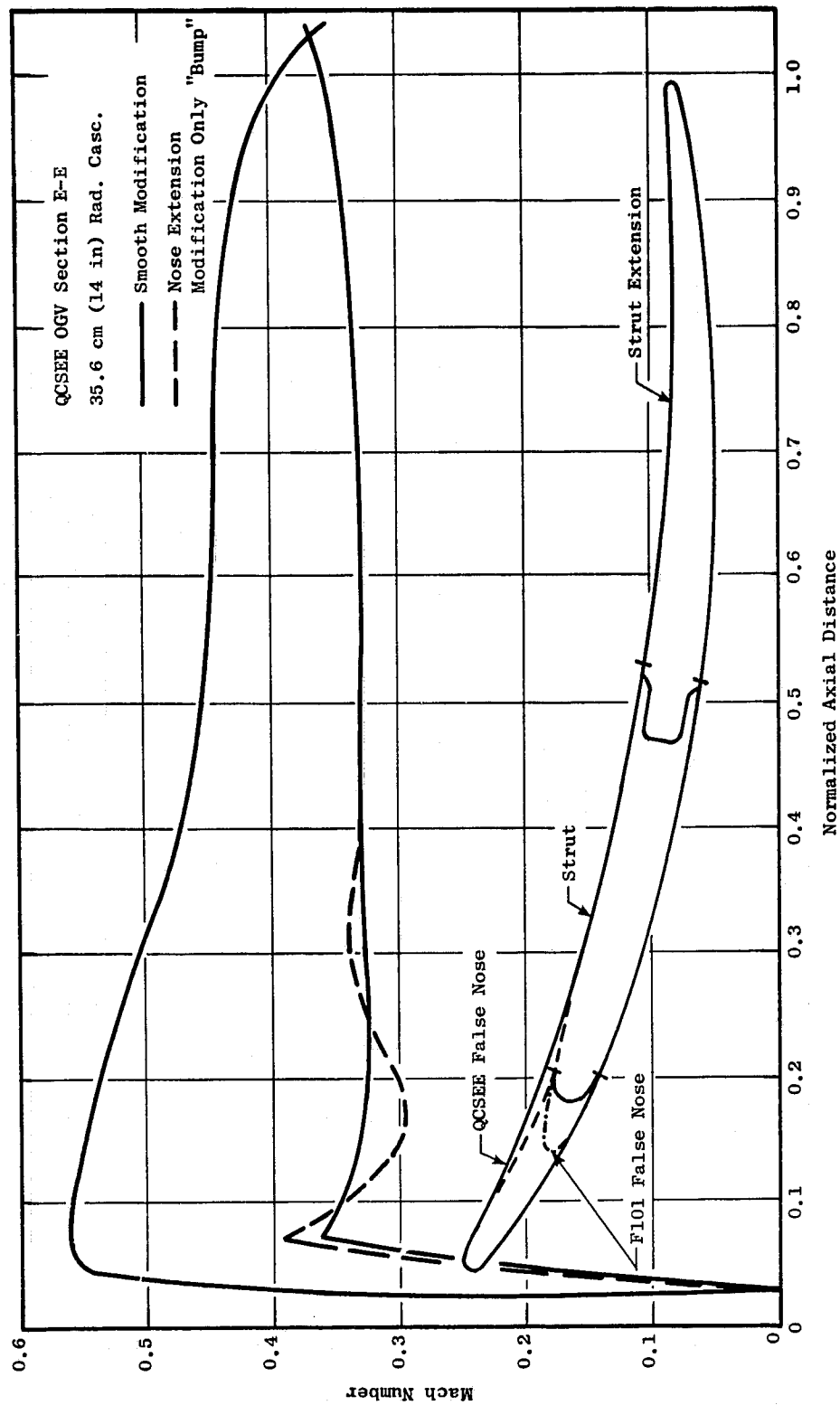


Figure 11-10. QCSEE Vane Modification.

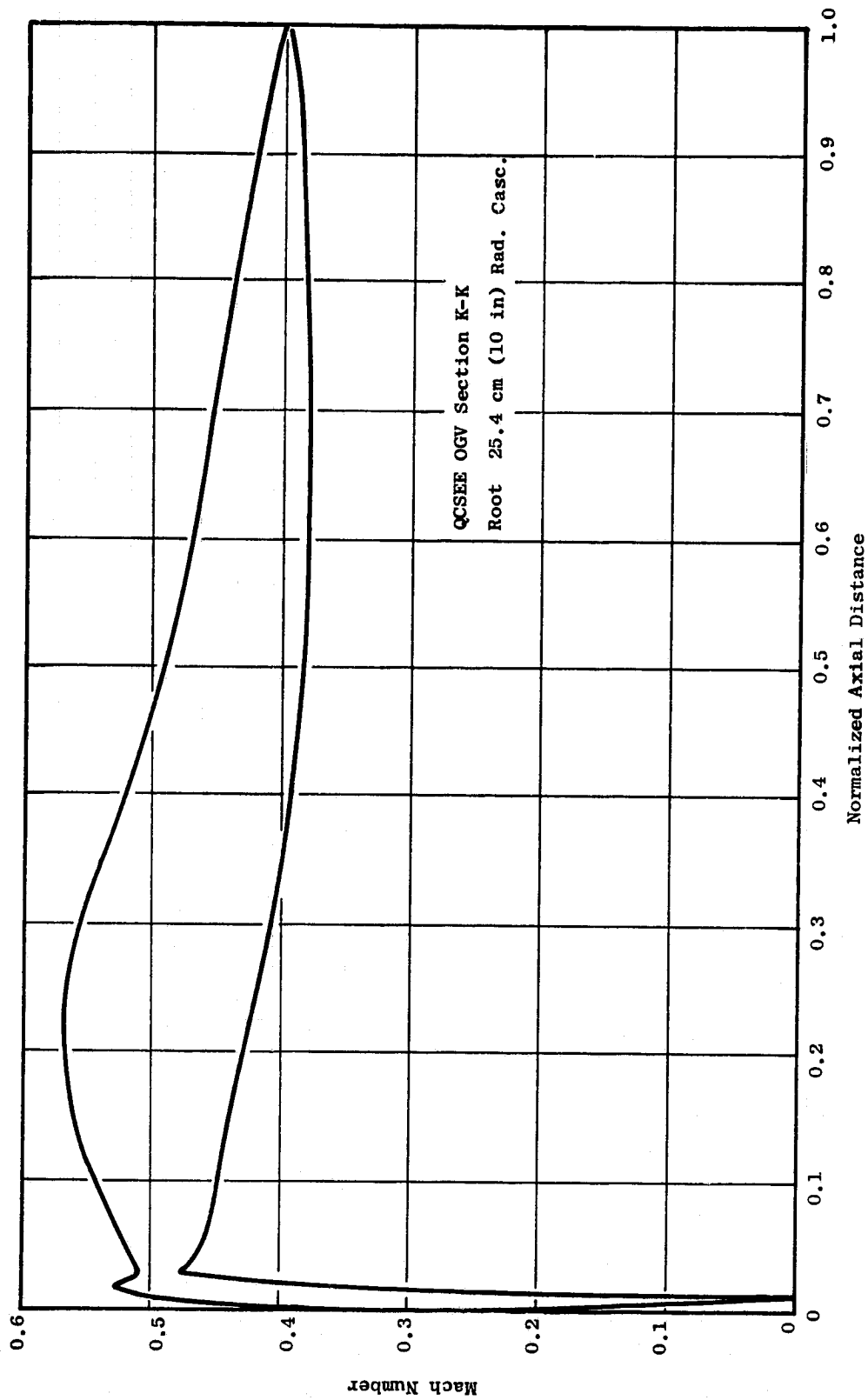


Figure 11-11. CASC Mach Number Distributions.

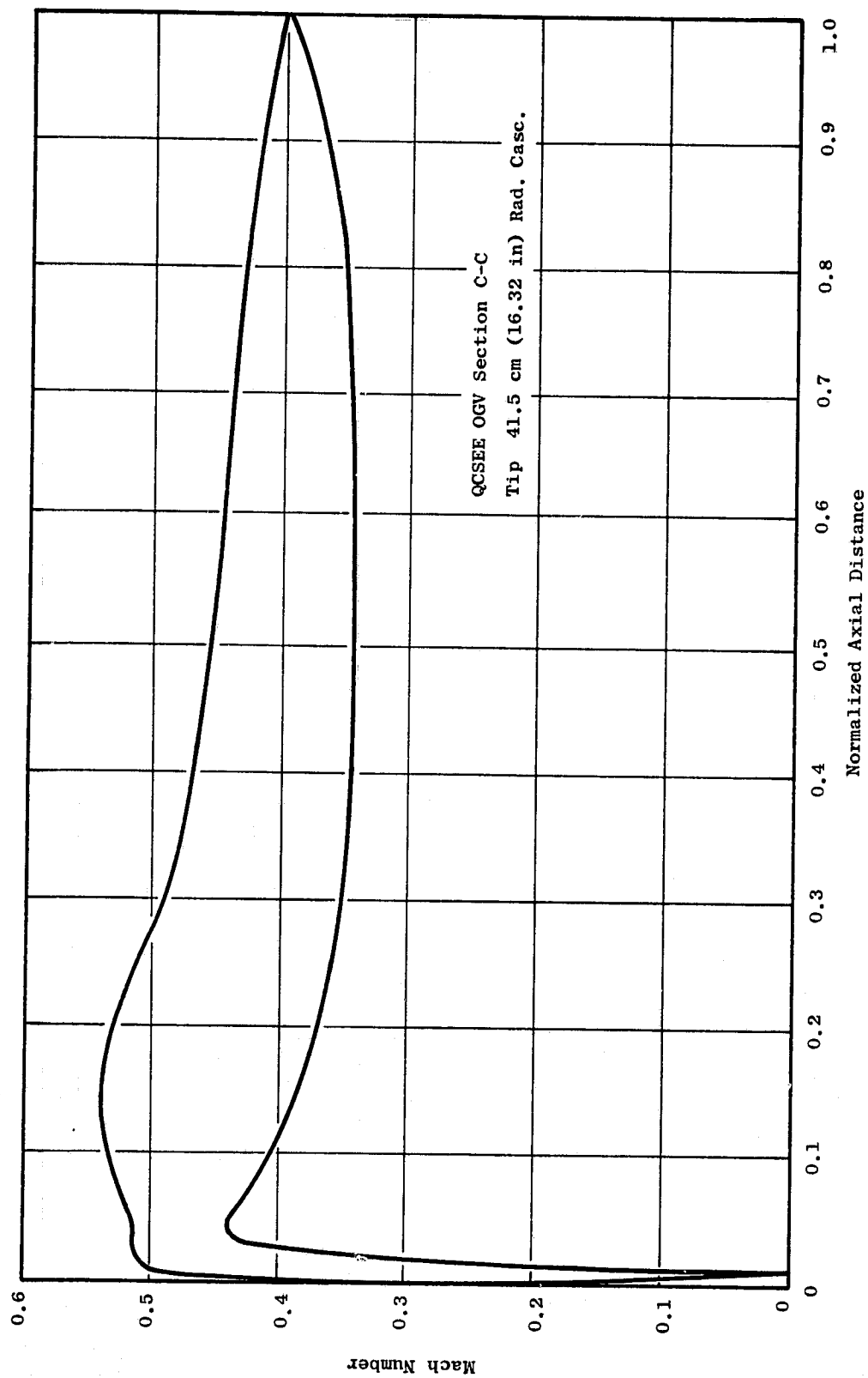


Figure 11-12. CASC Mach Number Distributions.

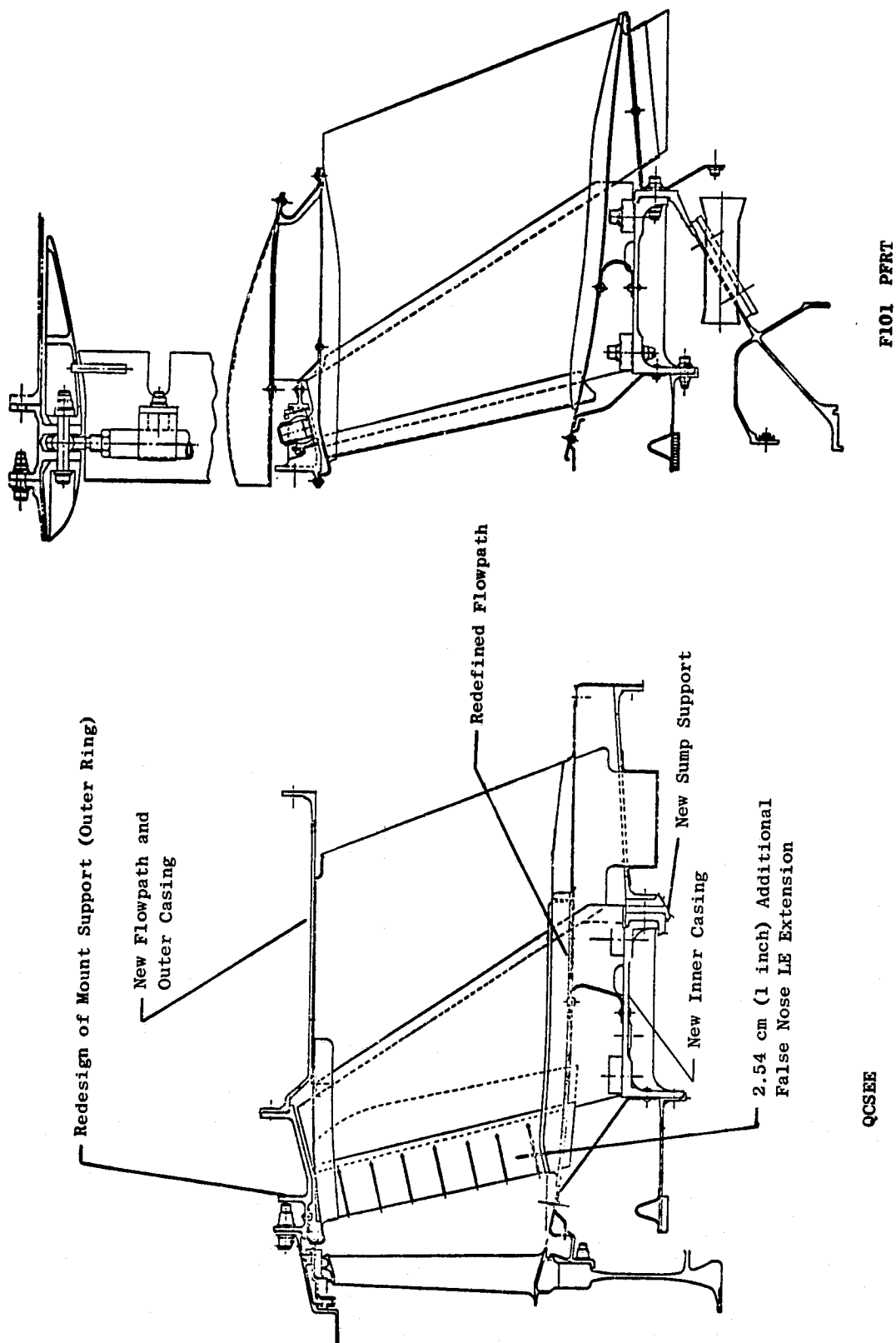


Figure 11-13. QCSEE Turbine Frame Modification.

11.5.2 Design Requirements

In addition to the maneuver loads shown in Figure 2-2, the following specific design criteria were established:

	<u>Stress</u>
Max. maneuver loads at operating temperatures	< 0.2% Y.S.
1-1/2 times max. maneuver loads at operating temp	< UTS
Blade out loads at operating temp	< UTS
1-1/2 times Buckling loads at operating temp	< 0.2% Y.S.
Transient thermal plus 1 g load	< 0.2% Y.S.
4 g vibratory load	< Goodman Diagram

In conjunction with the above limit loads, the primary gas temperature profile used for frame analysis is shown in Figure 11-14.

11.5.3 Design Description

The QCSEE turbine frame consists of an outer frame casing, 14 aerodynamic vane/struts, flow path liners, and a hub structure. The outer frame casing includes the outer ring which contains engine mounting provisions and outer casing. Figure 11-15 is a schematic of QCSEE and F101 rear engine mounting systems. In the F101 design, the turbine frame outer casing is supported from the outer bypass duct by 12 links as shown. Since the QCSEE pylon and short bypass duct necessitate a top-mounted frame configuration, a three-link system has been employed. These links take vertical and side loads and rolling moments.

Since the three-link configuration concentrates the mount reactions at the top of the frame, the outer ring section properties must be increased. This results in a larger ring section as shown in Figure 11-16. Details of the revised outer ring are shown in Figure 11-17.

In addition to engine mounting provisions, the outer frame casing extends aft from the turbine casing to support the core exhaust nozzle.

In order to straighten the exhaust gas, greater turning must be provided through the 14 vane/struts. These vane/struts are assemblies consisting of a central structural section with leading and trailing edge fairings having the cross section shown in Figure 11-18. The fairings are nonload carrying members, with the leading edge fairing sawcut at intervals to relieve thermal stress. Only the leading edge fairings need be modified to accept the higher turbine exit swirl in the QCSEE engines.

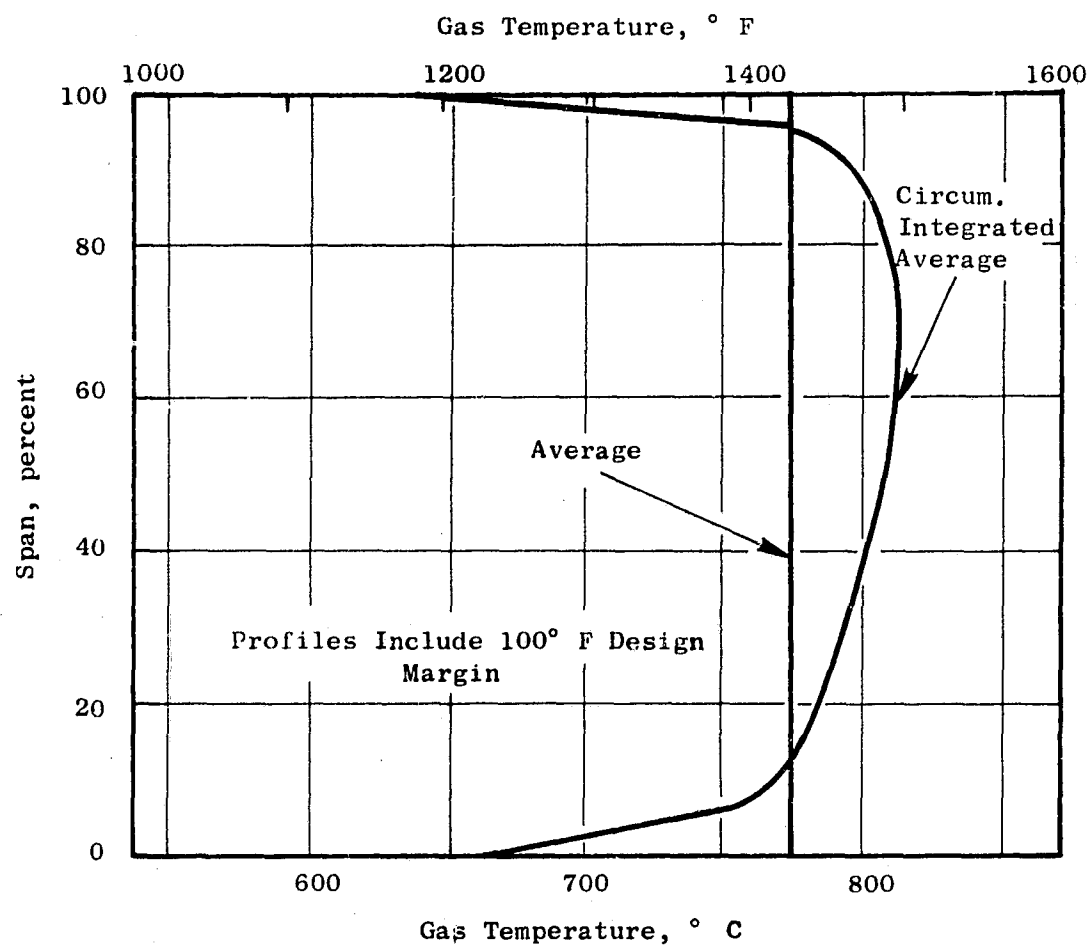


Figure 11-14. QCSEE Turbine Exit Gas Profile (OTW).

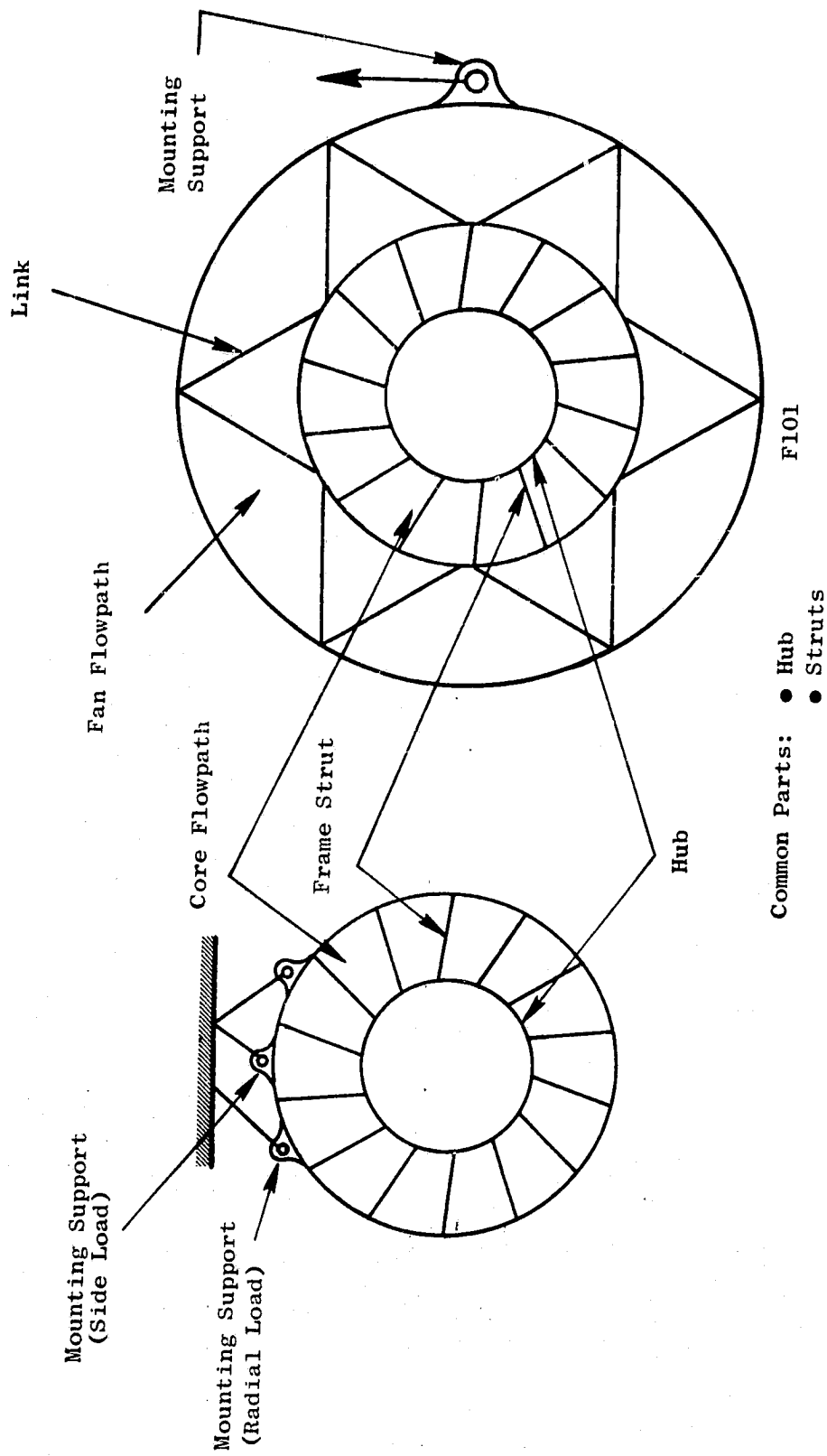
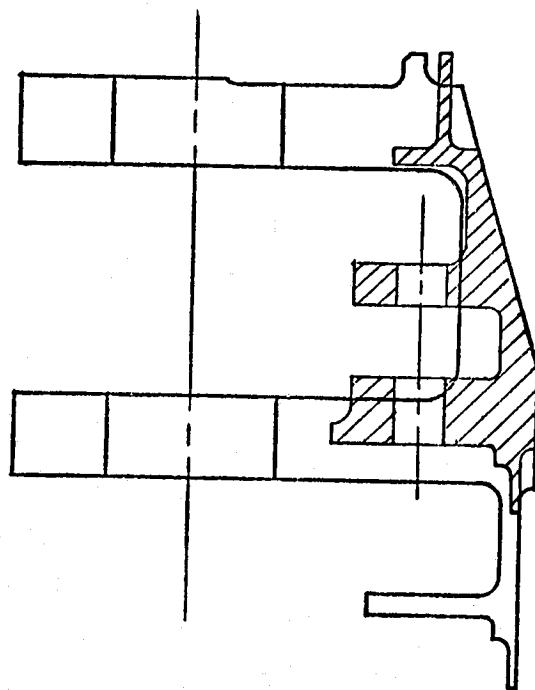


Figure 11-15. Rear Mounting System.

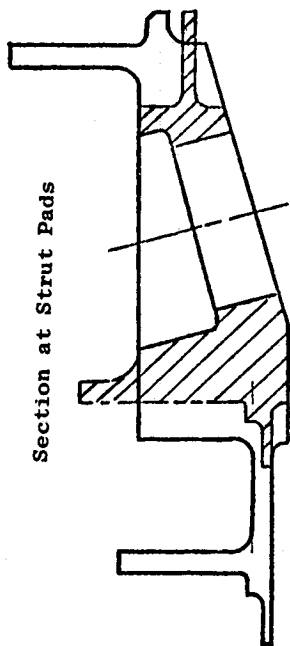
QCSEE 
 F101 

Section at Airframe Mounts



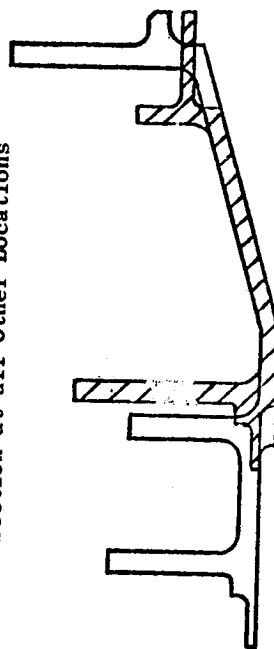
Section A-A

Section at Strut Pads



Section B-B

Section at all Other Locations



Section C-C

Figure 11-16. QCSEE and F101 Mounting System.

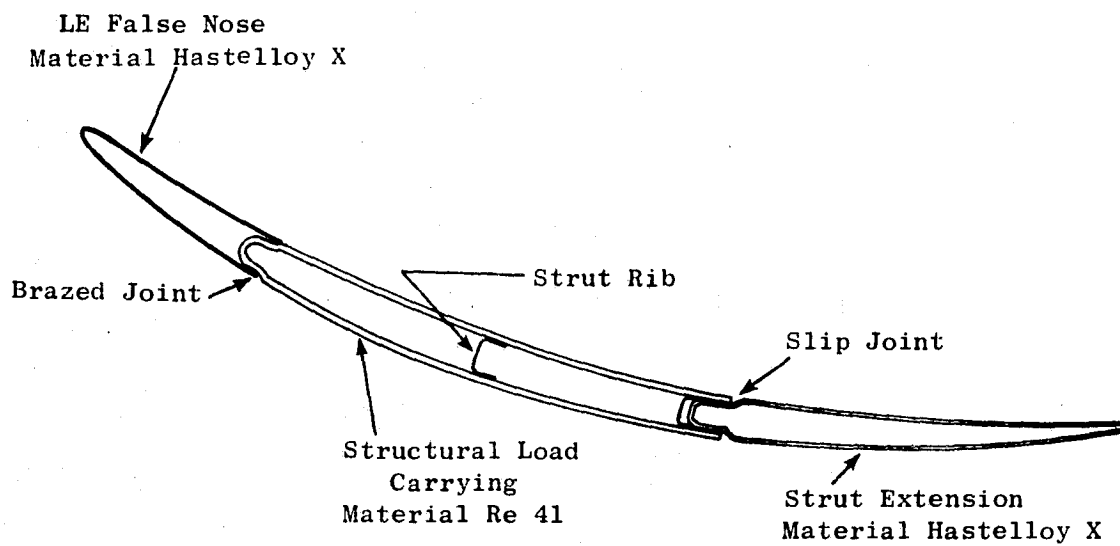


Figure 11-18. QCSEE Turbine Frame Strut.

Bearing loads are transferred through the central structural section of the struts. The inner ends of the struts are bolted to the hub through foot pad extensions. The outer ends are assembled to the outer casing through unibal connections designed to carry loads, but not moments, into the casing.

The rear fairings act as vane trailing edges and are attached to the central strut section by slip joints, providing for thermal expansion. The outer ends of the rear fairings are riveted to the casing and the inner ends are supported by pin joints.

A forged hub forms the inner structural member of the frame. It is composed of forward and aft flanges connected by a shear cylinder. Additional bending stiffness is provided by gussets. The forward flange mounts the outer and inner turbine seals, while the aft flange supports the bearing and sump housing, the balance piston assembly, and the nozzle centerbody.

Inner and outer flowpath liners are contoured to provide a smooth aerodynamic passage from the turbine to the exhaust nozzle and centerbody. In addition, the liners protect the hub from contact with hot gas, allowing better thermal growth matching with the outer structure.

The inner liner is formed in segments between struts. The liner is supported at three axial stations as shown in Figure 11-13. The outer liner is segmented between struts also, but is a separate continuous part behind the struts. The outer liner is supported from the outer casing. Liners are fabricated from Hastelloy X material.

Space between the flow path liners and structural struts is purged by turbine rotor cooling air. In order to minimize losses from purge air reentering the gas stream, a fish-mouth seal is brazed to the strut along the inner flowpath as shown in Figure 11-19. The purge air reenters the gas stream aft of the strut extensions.

11.5.4 Design Analysis

An analytical model depicting the turbine frame was made to represent the system. The GE computer program "MASS" was used to determine loads, stresses, and deflections. The model consisted of plates in the form of rectangles, squares, and trapezoids. These geometric sections were joined to form the cylindrical and conical surfaces of revolution. The struts were modeled as beams with variations of section properties along their length. The outer mount ring was modeled as beams. Variation of physical properties along the circumference was included in the analysis.

The forward and aft hub flanges were modeled as beams and connected to plates by a shear cylinder. The axial gussets in the hub were connected at joints in the shear cylinder and flanges. Connections to the strut from the hub were made through the foot pad. The outer strut ends were connected to the outer ring mount using a boundary condition that allows rotation with no moment transfer to the mount. The three locations at the outer mount system connect to ground through unbals.

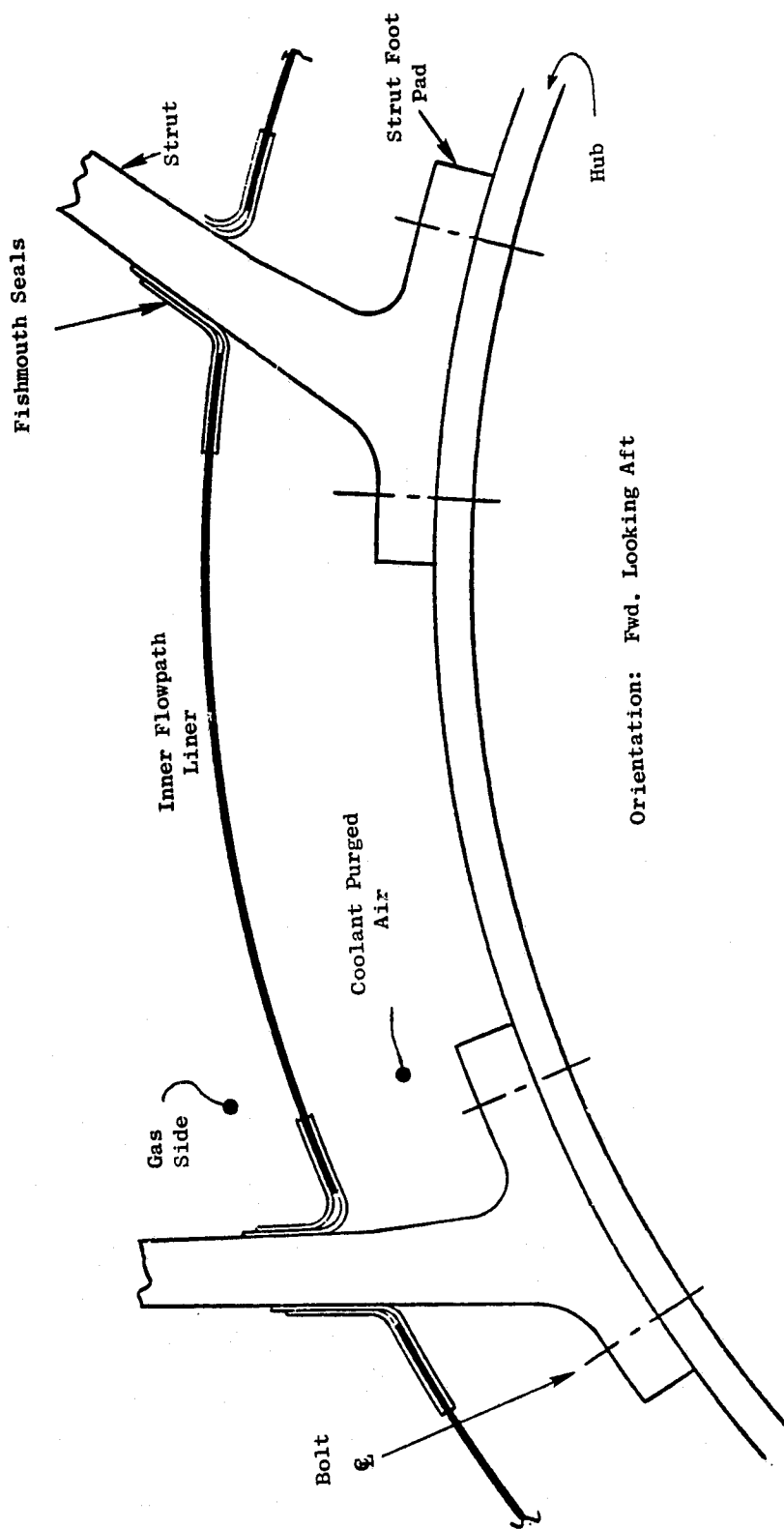


Figure 11-19. Turbine Frame Fishmouth Seal.

Results of the analysis were as follows:

Steady State Plus 10G Landing at Temperature

Loading and stresses are shown in Figure 11-20. Table 11-III summarizes the maximum effective stresses for the various components. All parts meet the design criteria under this loading condition.

Strut Buckling

This condition was based on establishing the transient time under which the maximum strut compression and bending would occur. This was based on a 50 second excursion from start to maximum sea level thrust based on Figure 11-21 temperatures. The strut skin/weld joint was found to be the most critical element. Interaction between the strut longitudinal compression and bending determined the effective buckling stress. The allowable stress in compression and bending established the margin of safety of 1.56.

Transient plus 1 G Load

Using the 50 second transient condition, the effective stresses and loads are presented in Figure 11-22. Table 11-IV summarizes the maximum effective stresses for the components, together with the resulting margins of safety. Maximum steady state plus 4 g vibratory are the combined loads existing under normal operating conditions. The Campbell diagrams shown in Figures 11-23 and 11-24 reflect these combined loads for the hub and struts. Maximum combined loads under temperature for the struts were found to be at the inner strut/weld line. Stress concentration factors (K_T) have been applied to the vibratory stress.

Pin Reaction and Link Attachment

A 2.54 cm (1 in.) diameter Inco 718 mounting pin has been selected for the QCSEE mount reactions. Pin load reactions for the UTW and OTW for the blade-out condition are shown in Table 11-V. Tables 11-VI and 11-VII reflect the pin mount loads due to maneuver. The frame loads shown in Table 11-VIII reflect the UTW and OTW unit loadings.

Flight Engine Turbine Frame

Although the F101 frame can be modified to meet all requirements of the QCSEE experimental engines, the result will not be an optimum design. For the flight engines, it has been assumed that time and cost pressures will be relaxed, permitting the design of a new optimized frame. This design is visualized as having eight structural struts and eight additional nonstructural turning vanes. A welded one piece construction would also be used to achieve a substantial weight saving over the experimental hardware. Major features of the flight and experimental designs are compared in Table 11-IX.

Note: Max. Hub Moment/Stresses Occur at the Aft Hub Flange for this Condition.

Strut	Loads		Stresses	
	N	lb	(N/m ²)	lb/in ² x 10 ⁻³
1	17100	3845	136	19.7
2	18200	4098	44	6.4
3	20600	4636	62	8.9
4	1170	263	131	19.0
5	3380	762	142	20.6
6	4640	1044	131	18.9
7	5850	1318	111	16.1
8	6640	1492	129	18.7
9	6600	1484	112	16.2
10	6350	1437	154	22.3
11	3560	800	61	8.8
12	2940	660	160	23.2
13	-1510	-339	226	32.8
14	18500	4158	158	22.8
Outer Support				
I	14000	1239	155	22.4
II	75300	6659	494	71.5
III	-	-	43	6.2
IV	4950	437	100	14.5
V	-	-	80	11.6
VI	71900	6352	467	67.8
Hub	Moment			
	Nm	lb in.		
a	3269	2893	180	26.0
b	3218	2848	180	26.0
c	1018	901	67	9.7

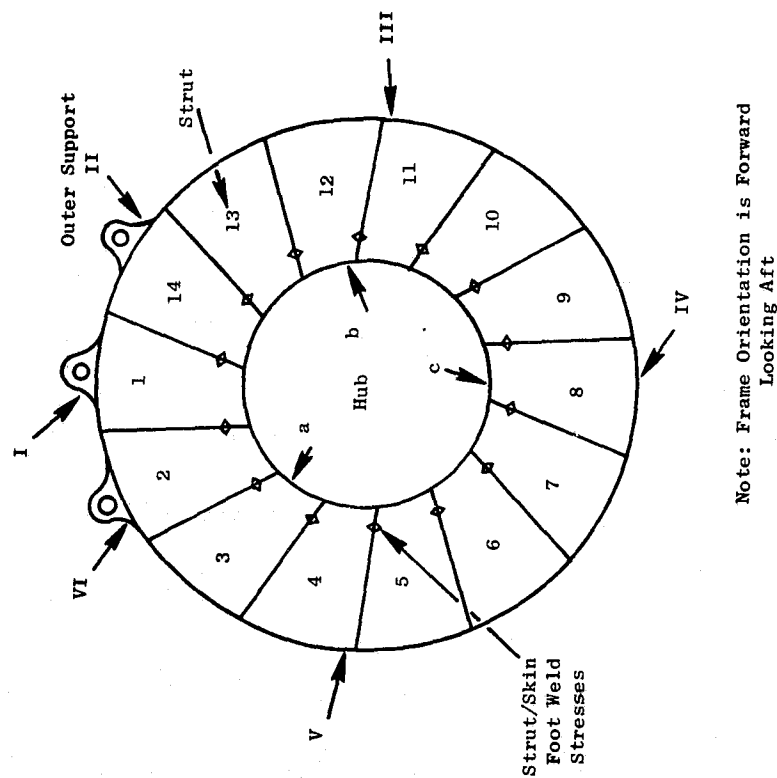


Figure 11-20. Turbine Frame Stresses and Loads - Max. Sea Level Steady State plus 10 G Landing.

Table 11-III. Turbine Frame Maneuver Stresses, Maximum Steady State
Plus 10 G Down Landing.

Item	Material	Eff. Stress/ys N/m^2 (ksi/ksi)	Ult. Eff. Stress/ Ult. Stress (2) N/m^2 (ksi/ksi)	MS (1) 0.2% ys	MS (2) Ult
Hub	Cast In 718	179/530 (26/77)	241/662 (35/96)	1.96	1.74
Outer Support	Forge In 718	493/814 (71.5/118)	895/1,241 (130/180)	0.65	0.38
Strut Foot/ Skin Weld	Cast Re 41	250/585 (36.2/85)	313/635 (45.2/92)	1.35	1.03
<p>(1) 0.2% yield strength at temperature</p> <p>(2) • Ultimate stress is (1.5 x mech) + thermal</p> <p>• Ultimate strength at temperature</p>					

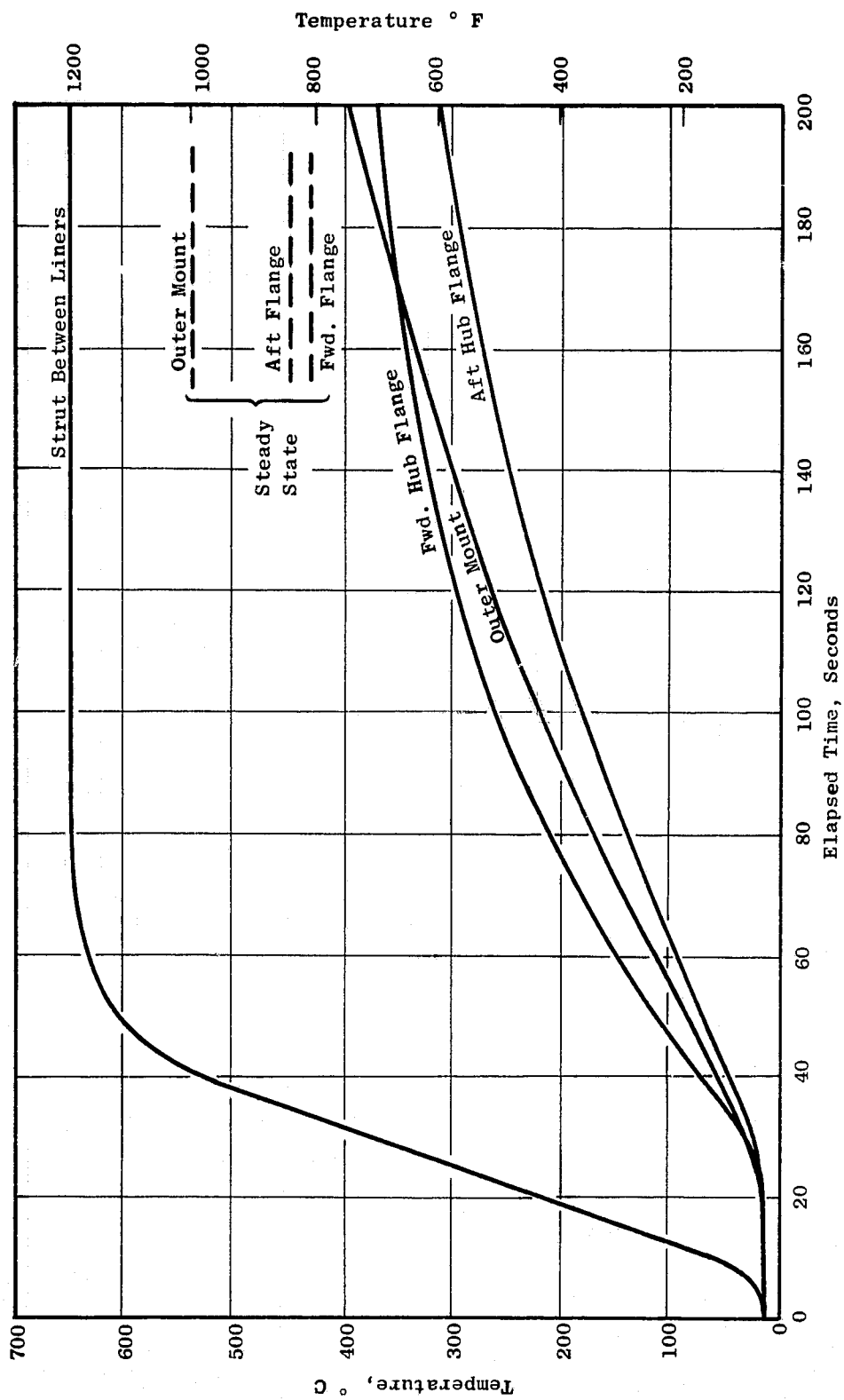
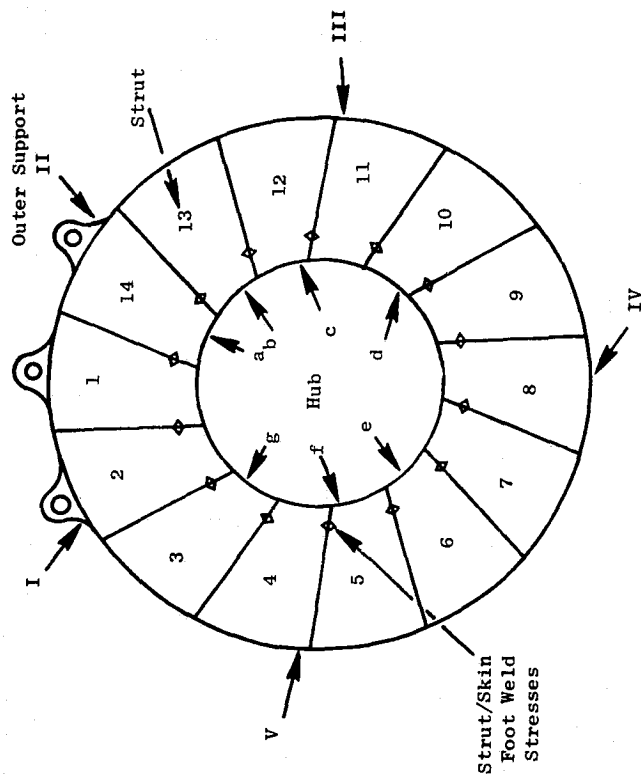


Figure 11-21. Turbine Frame Transient Average Temperatures for Start to Max. Sea Level.

Strut	Loads		Stresses	
	N	lb	(N/m ²)	lb/in ² x 10 ⁻³
1	-6085	-1368	302	43.7
2	-6032	-1356	297	44.0
3	-5764	-1296	307	44.5
4	-7460	-1677	311	45.0
5	-7264	-1633	309	44.7
6	-7028	-1580	308	44.6
7	-6912	-1554	308	44.6
8	-6872	-1545	308	44.6
9	-6899	-1551	309	44.7
10	-7273	-1635	309	44.7
11	-6828	-1535	307	44.5
12	-8193	-1842	312	45.1
13	-7513	-1689	302	43.7
14	-6041	-1358	301	43.6
Outer Support				
I	18553	4171	59	8.60
II	19359	4352	51	7.33
III	18290	4112	81	11.70
IV	17246	3877	62	9.03
V	17388	3909	63	9.12
Hub	Moment			
	Nm	lb in.		
a	5621	4974	178	25.7
b	5697	5042	183	26.6
c	5969	5282	191	27.7
d	5699	5043	185	26.8
e	5807	5139	186	26.9
f	5920	5239	186	26.9
g	5752	5090	178	25.7

Note: Max. Hub Moment/Stresses Occur at the Forward Flange for this Condition



Note: Frame Orientation is Forward Looking Aft

Figure 11-22. Turbine Frame Stresses and Loads - 50 sec Transient plus 1 G Load.

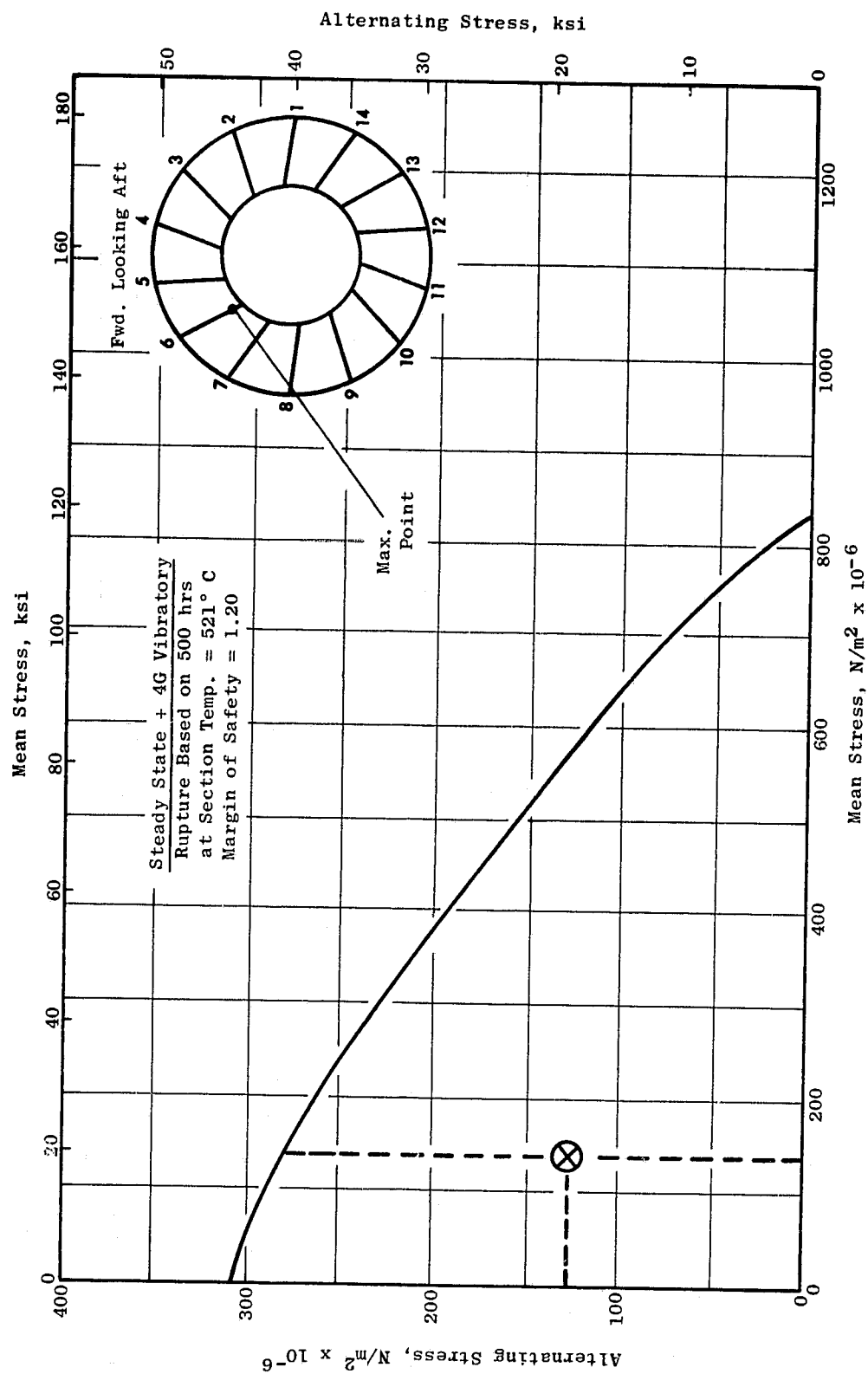


Figure 11-23. QCSEE Frame Stress Range Diagram - Foot/Skin Weld Line.

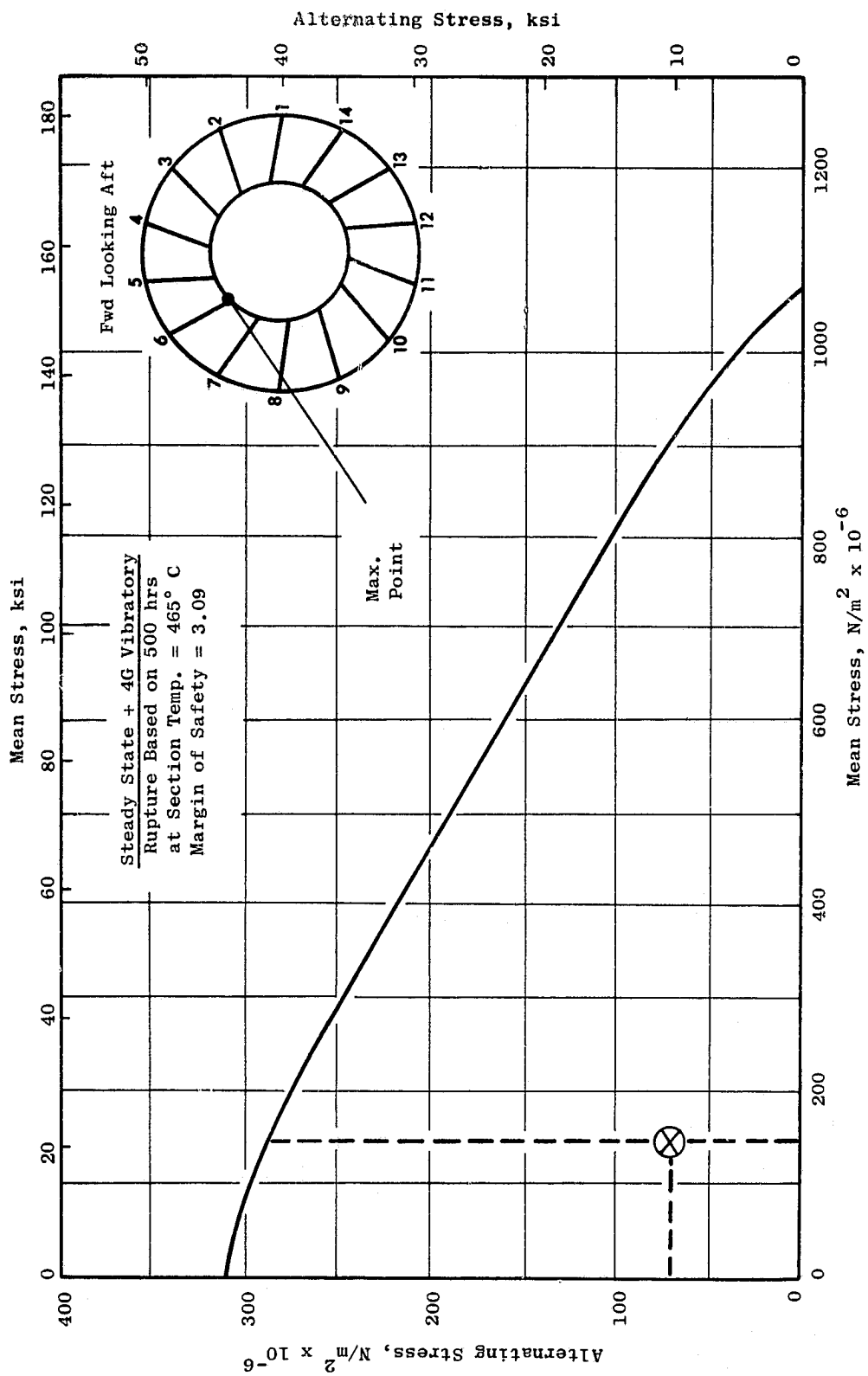


Figure 11-24. QCSEE Frame Stress Range Diagram - Hub.

Table 11-V. Reaction Load for Blade-Out Condition.

Condition	UTW				OTW		
	R _L N (1b)	R _R N (1b)	S N (1b)		R _L N (1b)	R _R N (1b)	S N (1b)
Blade Down	112,468 (25,285)	112,468 (25,285)	-		121,929 (27,412)	121,929 (27,412)	-
Blade Side	471,782 (106,066)	333,284 (74,929)	239,880 (53,930)		516,084 (116,026)	36,324 (81,750)	264,051 (59,364)

UTW reaction based on 2-1/2 airfoil blade-out load, 132,750 N
(29,845 lb) / blade

OTW reaction based on 1 airfoil blade-out load, 359,754 N
(80,890 lb)

2.54 cm (1 in.) mount pin meets margin of safety (MS) requirements of > 1

$$MS = \frac{\sigma_{ult}}{\sigma_{eff}} - 1 = 0.32$$

σ_{ult} = Ultimate strength on Inco 718 at 425° C (800° F)

σ_{eff} = Effective stress for 2.54 cm (1 in.) pin due to double shear

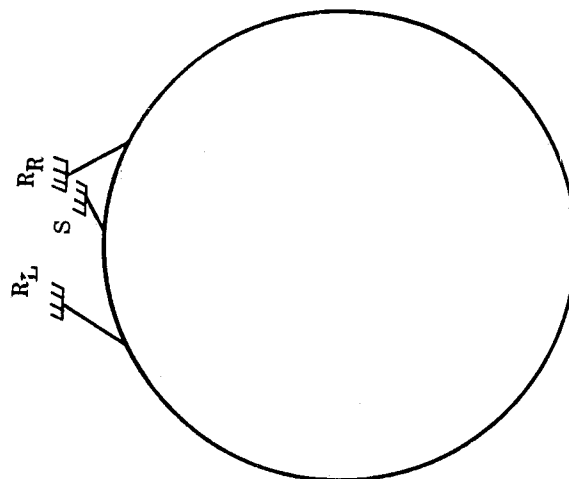


Table 11-VI. UTW Engine Mount Reaction Load Due to Maneuver,
2.54 cm (1 in.) Mount Pin.

Maneuver Condition (All Conditions Include 77,395 N, 17,400 lb Thrust)	R _{2L} N (lb)	R _{2R} N (lb)	S ₂ N (lb)
10 G Down, 2 G Side	52,357 (11,771)	56,365 (12,672)	76,270 (17,147)
10 G Down, 1.5 G Side, 2 G Fwd	28,178 (6,335)	53,363 (11,997)	57,201 (12,860)
6 G Down, 4 G Side, 2 G Fwd	137,154 (30,835)	80,295 (18,052)	155,346 (34,925)
6 G Down, 4 G Side, 3 G Aft	149,866 (33,693)	67,587 (15,195)	152,544 (34,295)
4 G Side, 4 G Fwd	152,317 (34,244)	65,132 (14,643)	152,544 (34,295)
4 G Side, 3 G Aft	170,109 (38,244)	47,340 (10,643)	152,544 (34,295)

UTW Engine Weight Used is 20,200 N (4,549 lb)

Table 11-VII. OTW Engine Mount Reaction Load Due to Maneuver,
2.54 cm (1 in.) Mount Pin.

Maneuver Condition (All Conditions Include 90,295 N, 20,300 lb Thrust)	R _{2L} N (lb)	R _{2R} N (lb)	S ₂ N (lb)
10 G Down, 2 G Side	49,858 (11,209)	45,125 (10,145)	66,057 (14,851)
10 G Down, 1.5 G Side, 2 G Fwd	28,770 (6,468)	42,465 (9,547)	49,542 (11,138)
6 G Down, 4 G Side, 2 G Fwd	123,192 (27,696)	66,778 (15,013)	132,119 (29,703)
6 G Down, 4 G Side, 3 G Aft	134,312 (30,196)	55,658 (12,513)	132,119 (29,703)
4 G Side, 4 G Fwd	135,575 (30,480)	54,395 (12,229)	132,119 (29,703)
4 G Side, 3 G Aft	151,139 (33,979)	38,831 (8,730)	132,119 (29,703)

OTW Engine Weight Used is 17,600 N (3,980 lb)

Table 11-VIII. Engine Mount Reaction Loads for 2.54 cm (1 in.) Pin.

Maneuver	UTW			OTW		
	R _L , N (1b)	R _R , N (1b)	S, N (1b)	R _L , N (1b)	R _R , N (1b)	S, N (1b)
1 G Down	+ 3,376 (759)	+ 3,376 (759)	-	+ 2,802 (630)	+ 2,802 (630)	-
1 G Side	+ 38,190 (8,586)	+ 16,168 (3,635)	+ 38,146 (8,576)	+ 33,280 (7,482)	+ 14,211 (3,195)	+ 33,026 (7,425)
1 G Aft	+ 2,340 (571)	- 2,340 (571)	-	+ 2,224 (500)	- 2,224 (500)	-
1 P Accel	+ 116 (26)	+ 116 (26)	-	+ 67 (15)	+ 67 (15)	-
1 P Vel	- 9,158 (2,059)	+ 4,270 (960)	+ 23,254 (5,228)	- 14,710 (3,307)	+ 6,859 (1,542)	+ 37,359 (8,399)
1 Y Accel	+ 102 (23)	+ 102 (10)	+ 258 (58)	+ 62 (14)	+ 27 (6)	+ 151 (34)
1 Y Vel	- 10,212 (2,296)	- 10,212 (2,296)	-	- 16,413 (3,690)	- 16,413 (3,690)	-
1 Thrust (Aft)	+ 9,719 (2,185)	+ 9,719 (2,185)	-	+ 2,550 (571)	+ 2,550 (571)	-

UTW Engine Weight - 20,200 N, (4,549 lb)
 OTW Engine Weight - 17,600 N, (3,980 lb)

Table 11-IX. Turbine Frame Flight Weight Design Study.

<u>Item</u>	<u>Nonflight Weight</u>	<u>Flight Weight</u>
Mount Ring	Forging	Castings/Fabrication
Strut Ends	(a) Uniball (outer) (b) Bolted (inner)	Weld Design
Hub	Cast	Castings/Fabrication
Liners	Flowpath Sheet Metal	Integral Part of Outer Mount Inner Flowpath Sheet Metal
Strut Extension	Fabricated	Fabricated
Strut Tan. Angle	8°	15°
Service Lines	None	Yes
No. of Struts	14	8 Structural and 8 Turning Vanes

SECTION 12.0

BEARINGS AND SEALS DESIGN

12.1 SUMMARY

This section deals with the QCSEE UTW/OTW bearings, seals, and accessory drives as well as their lubrication, thrust balancing, and cooling. The discussion details the requirements, shows the approach to the design, and presents a detailed description of the systems and their components.

Both engines utilize six main shaft bearings to support the rotating turbo-machinery. A main reduction gearbox located in the front sump reduces the high speed, low pressure turbine rotation to accommodate a large diameter low tip speed fan. Most of the hardware associated with the core engine is common to the General Electric F101.

An accessory gearbox mounted on the engine top vertical centerline is driven from the core by an F101 internal bevel gearset and a new radial drive shaft. Another F101 internal bevel gearset located on the bottom drives through a short shaft to a bevel gearset located in the core cowl area. This gearing drives a vane-type pump that scavenges oil from both the forward and aft sumps. Since the top-mounted accessory gearbox drains into the forward sump, this pump also scavenges the accessory gearbox.

The systems described in this section include the sumps, lube oil supply and scavenge, engine hydraulics, dynamic oil seals, venting and pressurizing systems, pump, oil coolers, filters, deaerators, magnetic chip detectors, static leak check valves, and the lube storage tank.

Lubrication system design is based on the use of current dry sump technology in which a circulating oil system is used with the bulk of the oil stored in the tank. Internal engine and gearbox passages are used wherever possible for oil delivery and return. Venting and pressurization functions also use internal engine passages when possible. Lubrication and hydraulic systems both use engine oil. The lube tank and accessories are located in the flight engine pylon to minimize the required space.

The short, stiff construction of the concentric QCSEE rotors permits a two-bearing support system for each rotor. The No. 1B and 1R bearings support the fan rotor. The No. 3 and No. 4 bearings support the high pressure rotor. The No. 2 and No. 5 bearings support the LP turbine and power shaft. Both the fan and low pressure turbine shaft are soft coupled to the main reduction gear to minimize induced loads. The problem of bearing skidding, associated with the absence of a finite load such as can occur in a three bearing system, is eliminated.

The thrust bearings have been located in the forward sump in order to provide precise control of fan and compressor blading clearances. Introduction of the main reduction gear requires that the axial "tie" between the fan and LP turbine be severed. The No. 2 thrust bearing must now handle the full aft loading of the turbine without any negating forward thrust from the fan. In order to relieve this load, a thrust balance cavity has been added to the rear sump. This cavity uses CDP air to pressurize a balance piston that tends to drive the rotor forward.

Since there is no practical method for thrust balancing the variable-pitch fan rotor, a high capacity CF6 No. 1 thrust bearing was chosen to handle the axial loads.

Careful attention has been given to fire-safe design features. Carbon seals are provided for minimal leakage of pressurization air into the sumps. During normal operation these seals also eliminate oil leakage from the sump and thus minimize oil consumption. Oil slingers or windbacks are provided with the objective of preventing coke formation in the moving parts of the seals. Each of the cavities adjacent to the sumps are pressurized with cool air to prevent the inflow of hot gases into the sumps. Adequate oil drains have been provided to remove inadvertent oil leakage and prevent fire damage. There are also no trapped oil pockets within the rotating hardware.

12.2 DESIGN REQUIREMENTS

The components to be used for the sumps and drive system for the QCSEE engine will meet the following requirements:

- Design loads for sumps and drives components shall be derived from the duty cycles given in Section 2.0. Design life based on these loads will meet established life requirements.
- Sumps are designed to scavenge at all steady-state attitudes shown in Figure 2-3.
- Design will be applicable to future airline use. Where slave hardware is designed, no compromises will be made that would not allow future adaptability to the airlines.
- Design will meet maintainability and reliability criteria.
- System will be designed to operate with Mil-L-7808 or Mil-L-23699 oil.
- All gearbox and sumps shall be vented to areas where temperatures are less than 371° C (700° F).
- No trapped oil will be allowed in rotors.

12.3 UTW/OTW LUBRICATION SYSTEM

The UTW/OTW Lubrication System contains the following four subsystems:

- Oil supply
- Oil scavenge
- Seal pressurization air
- Vent air.

A conventional dry sump system similar to that used on other General Electric engines is provided. The lube/hydraulic system schematic is shown in Figure 12-1. The bulk of the system oil supply is retained in the oil tank. Oil is pressure fed to each engine component requiring lubrication and/or cooling, and is removed from the gearbox and rear sump by scavenge pump elements for return to the oil tank.

12.3.1 Oil Supply Subsystem

The oil supply subsystem consists of the oil tank, the gearbox mounted oil supply pump, the oil supply filters, the static leak check valve, the oil supply nozzles, and associated piping. Oil is supplied from the modified TF39 oil tank by gravity to the inlet of the supply pump at all operating conditions. The 3350 cm³/sec (53 gpm) oil supply flow is achieved by combining the total scavenge element capacity of the CF6 lube supply pump and a scavenge pump. All scavenge elements discharge to a common discharge port to which the oil supply line is connected.

Mil-L-23699 Oil under pressure from the supply pump flows through the 74 micron nominal oil supply filters which protect the nozzles from contaminants. Each filter has a pressure relief bypass which opens when the pressure across the filter reaches 276 kN/cm² (40 psi). Thus, if the filter becomes plugged, full oil flow will be supplied to the engine. An automatic service shutoff valve is incorporated to allow removal of the filter without excessive loss of oil.

Oil drainage from the tank into the engine, during periods of shutdown, is prevented by a static leak check valve located downstream from the oil filter. The valve is set to crack and reseal at 34.5 kN/cm² (5 psid.)

Immediately downstream of the static leak check valve, a port is provided for sensing oil supply pressure. This pressure is referred to as the engine gearbox internal pressure, which provides a ΔP across the oil nozzles and piping.

Conventional nozzles, ranging from 0.089 to 0.216 cm (0.035 to 0.085 inches) diameter, meter the oil supply to the engine forward sump for lubrication and cooling of the bearings, seals, and sump walls. The rear sump oil is supplied into the bore of the low pressure turbine shaft, which distributes the oil

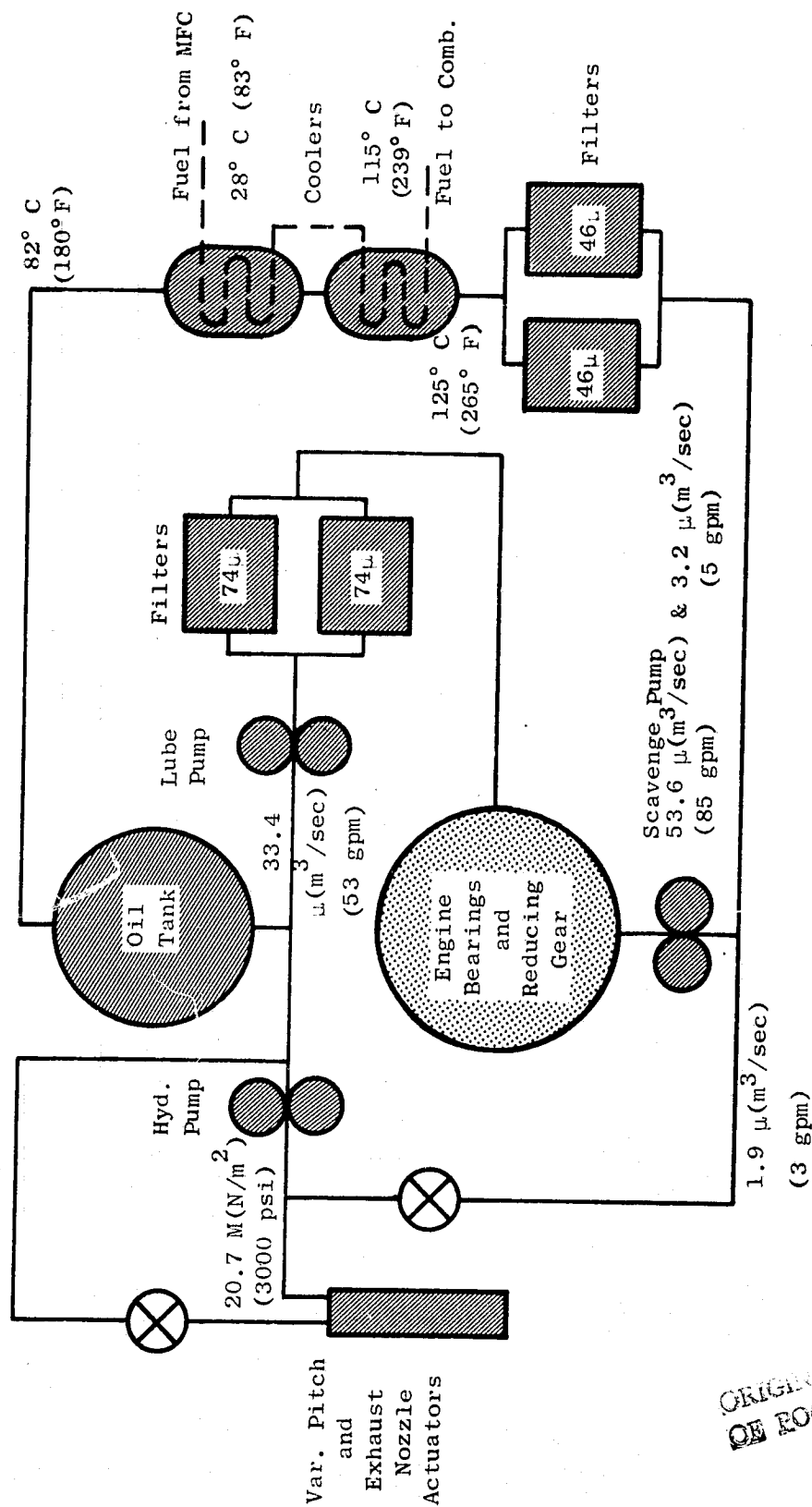


Figure 12-1. Lube/Hydraulic System Schematic.

ORIGINAL PAGE IS
OF POOR QUALITY

centrifugally through holes in the shaft and bearings to the seals. The oil supply piping has been sized to provide proper oil distribution throughout the range of oil supply temperatures. Table 12-I shows the oil flows to each area of the engines.

Table 12-I. QCSEE Lube Flows.				
	UTW		OTW	
	cm ³ /sec	(gpm)	Cm ³ /sec	(gpm)
No. 1B Bearing	126	2.00	126	2.00
No. 1R Bearing	63	1.00	63	1.00
No. 2 and No. 3 Bearings	161	2.56	161	2.56
Accessory GB & Drive	188	2.98	188	2.98
VP Actuator	32	.50	---	---
Main Reduction Gear	1510	24.00	2270	36.00
Aft Sump No. 4 and 5 Bearings	<u>164</u>	<u>2.60</u>	<u>164</u>	<u>2.60</u>
Total Flow	2290*	35.64*	2980	47.14*
Note: These are minimum required oil flows.				

12.3.2 Scavenge Subsystem

The scavenge subsystem consists of two scavenge pump elements, two scavenge filters, two oil coolers, the scavenge oil deaerator in the oil tank, and associated piping.

The oil in the accessory gearbox flows by gravity into the forward sump through drain pipes where it is combined with the sump scavenge oil. The combined oil is then scavenged by the bottom-mounted scavenge pump. The oil which drains down the scavenge pump radial drive shaft is scavenged by the speed reduction spur gears located within the pump. The aft sump scavenge oil is piped forward to the bottom-mounted scavenge pump and scavenged by a separate element.

The OTW flight engine does not have a top-mounted gearbox, hence the oil in the forward sump is drained by gravity through a pipe to the accessory gearbox driven scavenge pump. The accessory gearbox is scavenged by a separate element on the pump. The aft sump scavenge oil is piped forward to the accessory gearbox driven pump and scavenged by a third element.

The scavenge elements are provided with inlet screens and magnetic chip detectors. The inlet screens are provided to catch any debris which is larger than can pass through the pumping element without causing damage or excessive wear. The magnetic chip detectors collect ferrous particles which provide information on sump and gearbox component condition through spectrographic analysis.

The total engine scavenge flow is discharged through a common port and routed to the 46 micron scavenge filters. Each filter has a pressure relief bypass which opens when the pressure across the filter reaches 276 kN/cm^2 (40 psi). The valve allows bypassing flow if the filter element becomes plugged. The main function of the filter is to remove contaminants generated by the system components during normal engine operation. The filter incorporates a service shutoff valve to minimize the oil loss when the filter is removed for servicing.

The scavenge oil is piped through the two CF6 oil coolers which serve to transfer the heat generated by the main shaft bearings, seals, sump walls, gearboxes, piping, and other lube system components into the available engine fuel heat sink. The oil is then returned to the oil tank where a scavenge oil deaerator removes entrained air and conditions the oil for reuse by the oil supply subsystem.

12.3.3 Seal Pressurization Subsystem

Oil leakage can potentially contribute to seal coking and contamination of compressor bleed air, as well as increasing the engine oil consumption. In order to prevent oil leakage, the main shaft oil seals are pressurized to force air to flow across the seals into the sumps at all operating conditions.

The compressor stage for extraction of seal pressurization air has been selected to have adequate pressure to prevent the hot engine cycle air from entering the sumps and yet low enough in temperature during higher Mach number, hot day operation to permit the oil seals to meet their required life. Pressurization air is extracted at the hub of the third stage compressor rotor and routed internally within the engine to both the forward and rear sump oil seals. Air from the hub of the compressor is used because it contains the minimum contamination.

Oil seal drains are provided in the forward sump oil seals to remove any seal leakage which could contaminate the compressor. Since these drains carry fluid only in the case of a seal failure, the forward sump seal drains are routed overboard. The aft sump seal drains are routed to the flowpath aft of the low pressure turbine.

12.3.4 Vent Subsystem

The venting of the oil seal pressurization air from the sump cavities is accomplished through the gearbox. The rear sump is vented through the low pressure turbine shaft to the forward sump. The forward sump is vented to the accessory gearbox. The air in the gearbox is vented overboard through a rotating air/oil separator. The oil which is separated from the vent air is returned to the system as scavenge oil.

The vent flow areas have been sized to:

- Maintain the sump internal pressure below outside cycle air pressure
- Prevent reverse airflow across the oil seals during rapid power reductions
- Continue engine operation
 - With one seal failed from any cause including coking.
 - With the remaining seals at their maximum service leakage limit.

12.3.5 Thermal Balance

The flight engine lube oil is cooled by transferring heat to the engine fuel as well as the fuel bypass back to the fuel tanks. The engine heat balance study showed that on a 32° C (90° F) day at 100% rated reduction gear power, the system will provide the required 82° C (180° F) oil [needed to maintain 149° C (300° F) max gear temperature] with 27° C (80° F) fuel inlet temperature. The fuel bypass will absorb the 4.4° C (8° F) pumping temperature rise. If the fuel inlet temperature is maintained at 22° C (72° F) or below the engine is self cooling and no heat must be transferred to the fuel bypass flow. A comparison of engine heat loads is shown in Table 12-II.

Table 12-II. Comparison of F101 and QCSEE Engine Heat Loads.						
	F101		UTW		OTW	
	J/sec	(Btu/min)	J/sec	(Btu/min)	J/sec	(Btu/min)
Engine	70,500	4000	67,000	3800	67,000	3800
Red. Gear	---	---	86,000	4890	110,500	6276
Total	70,500	4000	153,000	8690	177,000	10,076

A plot of maximum allowable lube supply temperature for the OTW flight engine versus engine thrust is shown in Figure 12-2. The OTW flight engine heat load versus engine thrust is shown in Figure 12-3.

During testing of the UTW/OTW experimental engines for mapping, where it is planned to operate the reduction gear at 140% rated power, the fuel bypass will be simulated by means of a water cooler. In addition, an oil/water facility cooler will be provided for use if needed because of uncertainty in the heat rejection analysis.

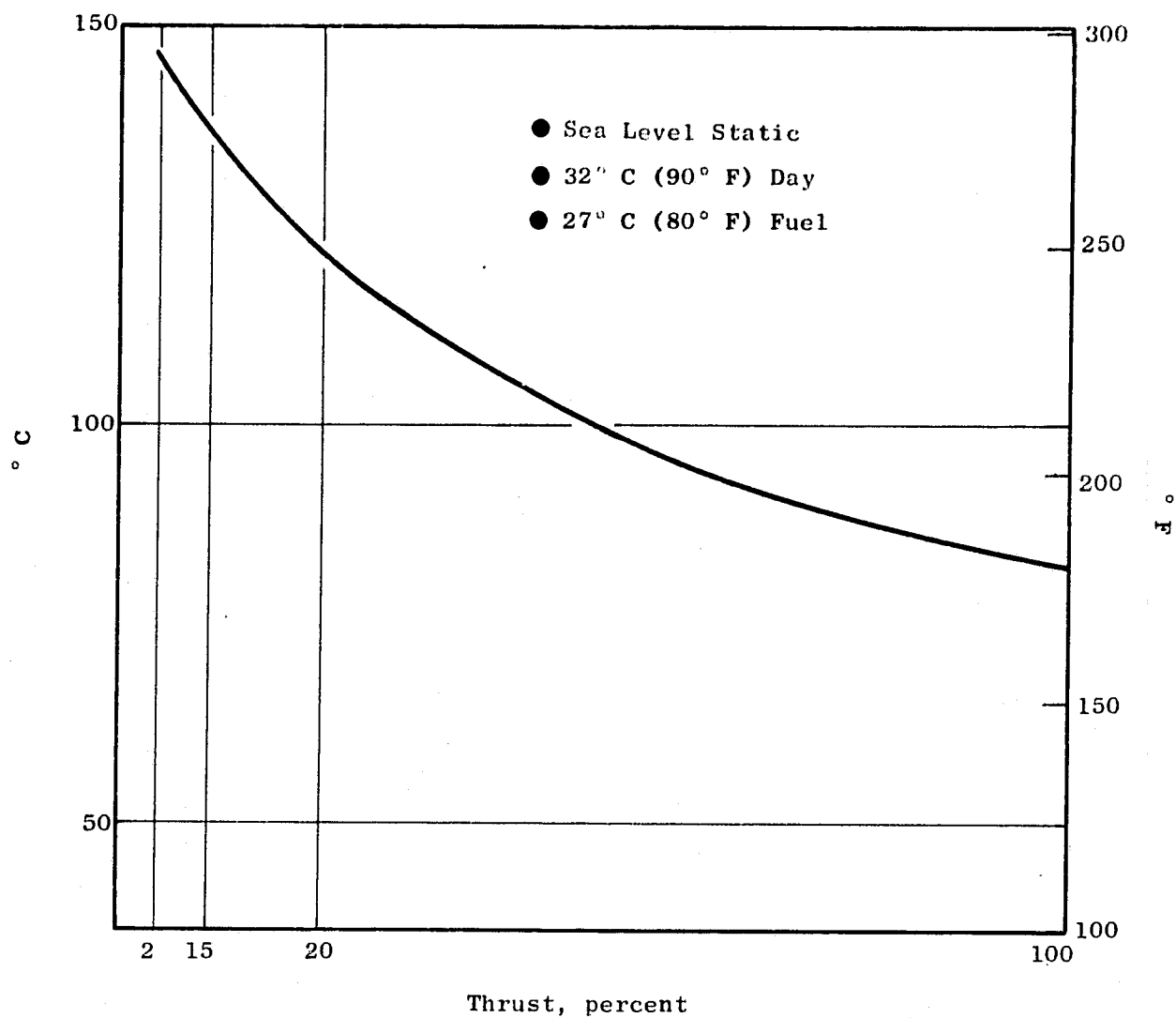


Figure 12-2. Maximum Allowable Lube Supply Temperature of OTW Flight Engine for 150° C (300° F) Gear Temperature.

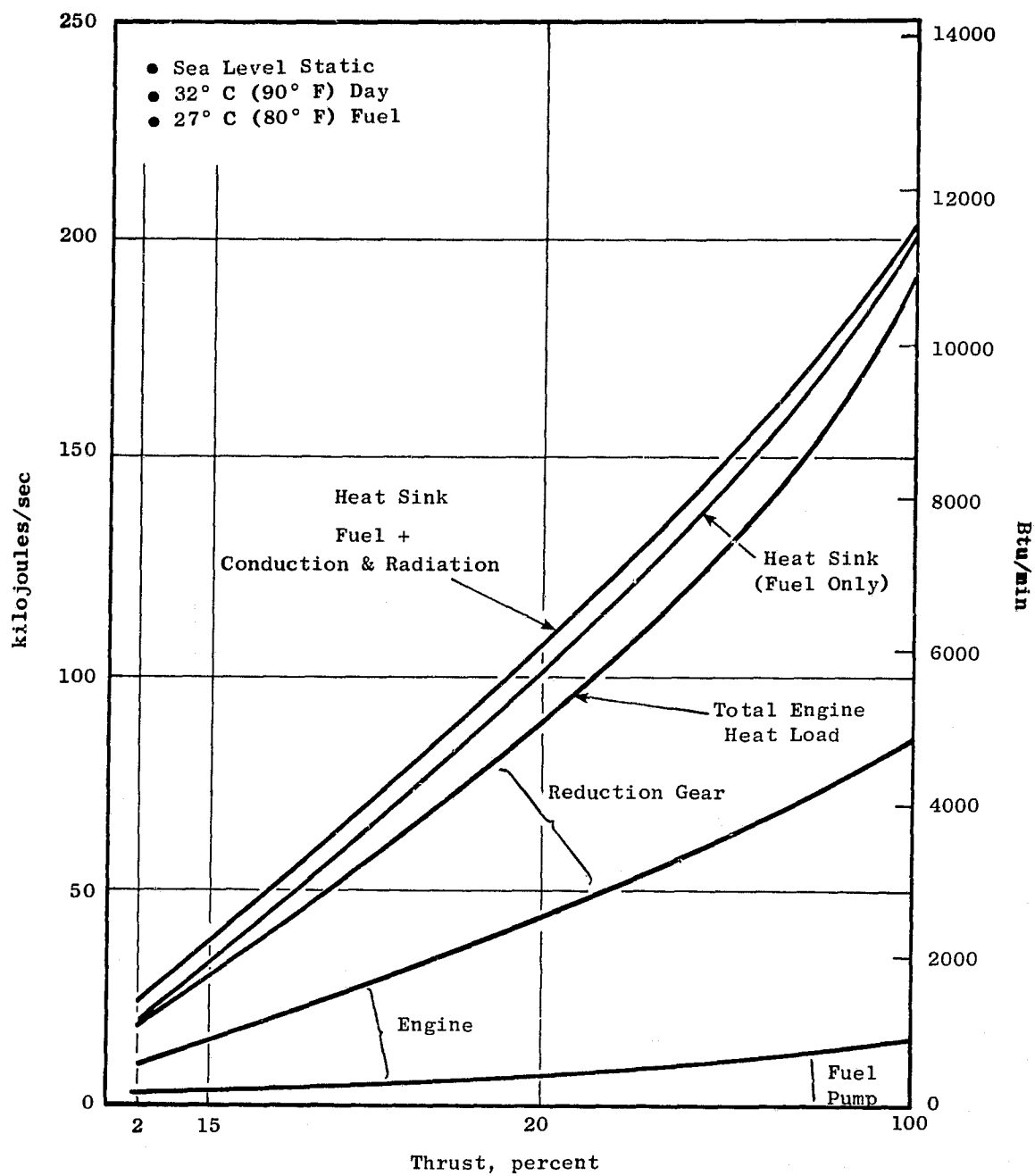


Figure 12-3. OTW Flight Heat Load.

12.3.6 Hydraulic System

The hydraulic system uses the same oil tank as the lube system. Oil is supplied from the oil tank through a boost element on the lube pump to the hydraulic pump. Case drain oil from the hydraulic pump is routed to the scavenge return line before the scavenge oil passes through the heat exchangers. This arrangement removes heat generated by the hydraulic system.

The hydraulic system will include a 10 micron filter at the pump inlet and a magnetic chip detector in the hydraulic system discharge line. The F101 hydraulic pump (which had an integral boost element) did not have sufficient capacity. A 47 gpm (340° psig) pump has been selected.

12.4 UTW/OTW THRUST BALANCE SYSTEM

In addition to the load components resulting from flight maneuver, misalignment, etc., the main shaft bearings are subjected to an axial load component. It is the result of the blade axial aerodynamic load and pressure forces on the rotor. A portion of this thrust load can be balanced by adjusting the radial location of one or more of the labyrinth seals.

The core engine thrust balance system (high pressure compressor and high pressure turbine) in the F101 uses a conventional method of thrust balancing, i.e., the forward compressor load and aft turbine load are balanced by radially adjusting the labyrinth seals to provide the balancing gas loads. The net axial thrust load is taken at the No. 3 ball bearing.

Figure 12-4 illustrates the difference between the low pressure system (fan and low pressure turbine) of a conventional engine and a geared drive engine. The loads shown are typical for a takeoff condition of the UTW engine. In the conventional engine, the low pressure shaft ties the turbine rotor to the fan rotor so that the thrust bearing feels only the difference in thrust between the rotors.

QCSEE engines have a geared drive which axially disconnects the fan from the LP turbine, therefore, each component is required to have its own thrust bearing. Both the OTW and UTW fans use a high thrust capacity ball bearing from the CF6 engine. The OTW engine (fixed-pitch fan blade) has a forward thrust load at all flight conditions where the UTW engine (variable-pitch fan blade) will change from forward to aft load as the fan blade is actuated from forward to reverse pitch.

The low pressure turbine thrust balance system is shown on Figure 12-5. The LP turbine aft load is balanced by the forward balance cavity load. The balance piston seal is located in the aft sump cavity, described in Section 12.5.2. Net aft load (aft LP turbine minus forward balance piston) is taken at the No. 2 ball bearing. Thrust balance air is supplied from the high pressure compressor 9th stage rotor tip and routed through a 5.09 cm (2 in.) ID pipe to a manifold connected below the bottom vertical strut, then through the strut in two 2.54 cm (1 in.) ID pipes to a manifold and forward to the pressure balance cavity in the aft sump. The amount of CDP air required for thrust balance is

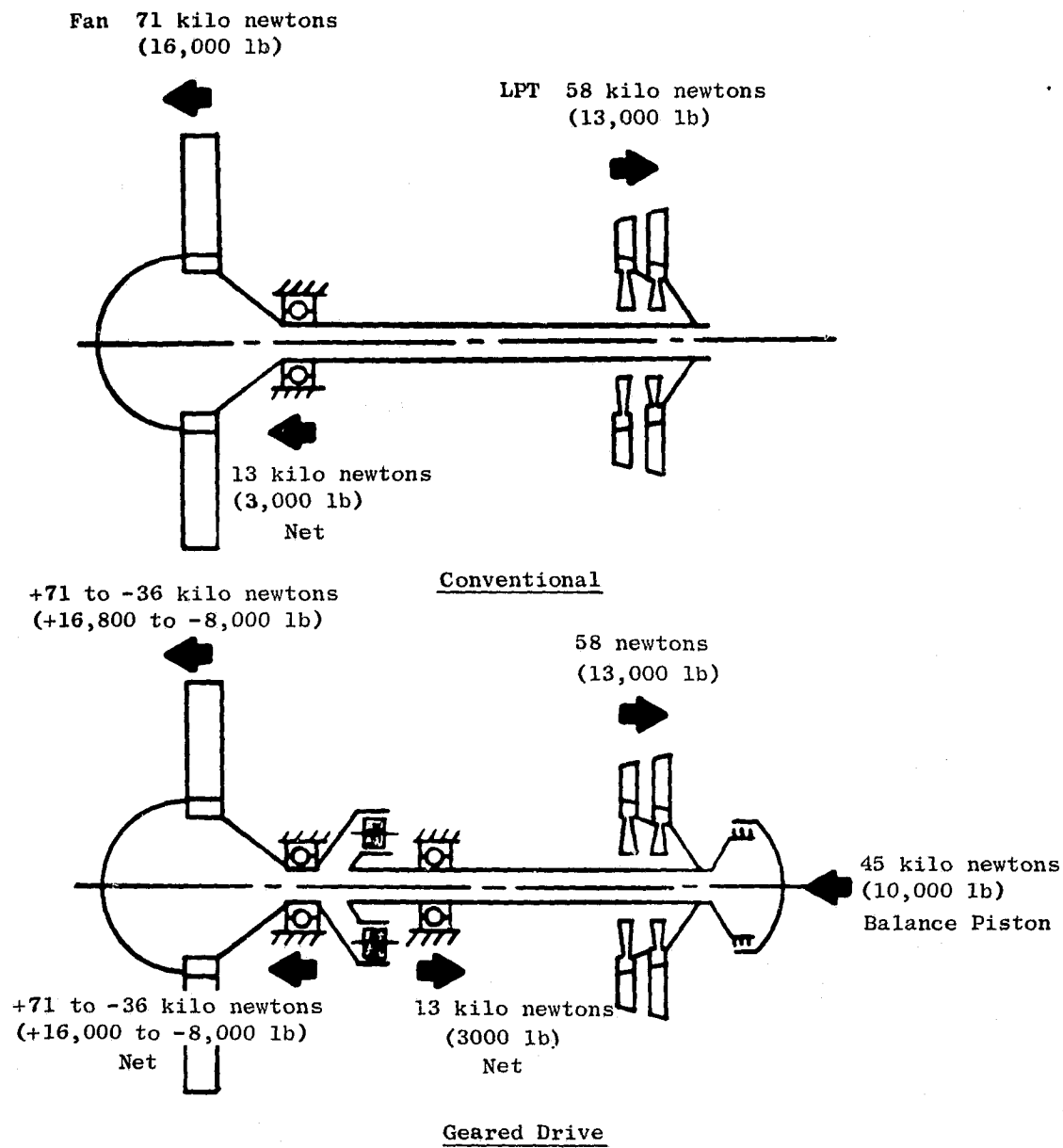


Figure 12-4. Schematic of Conventional and Geared Drives.

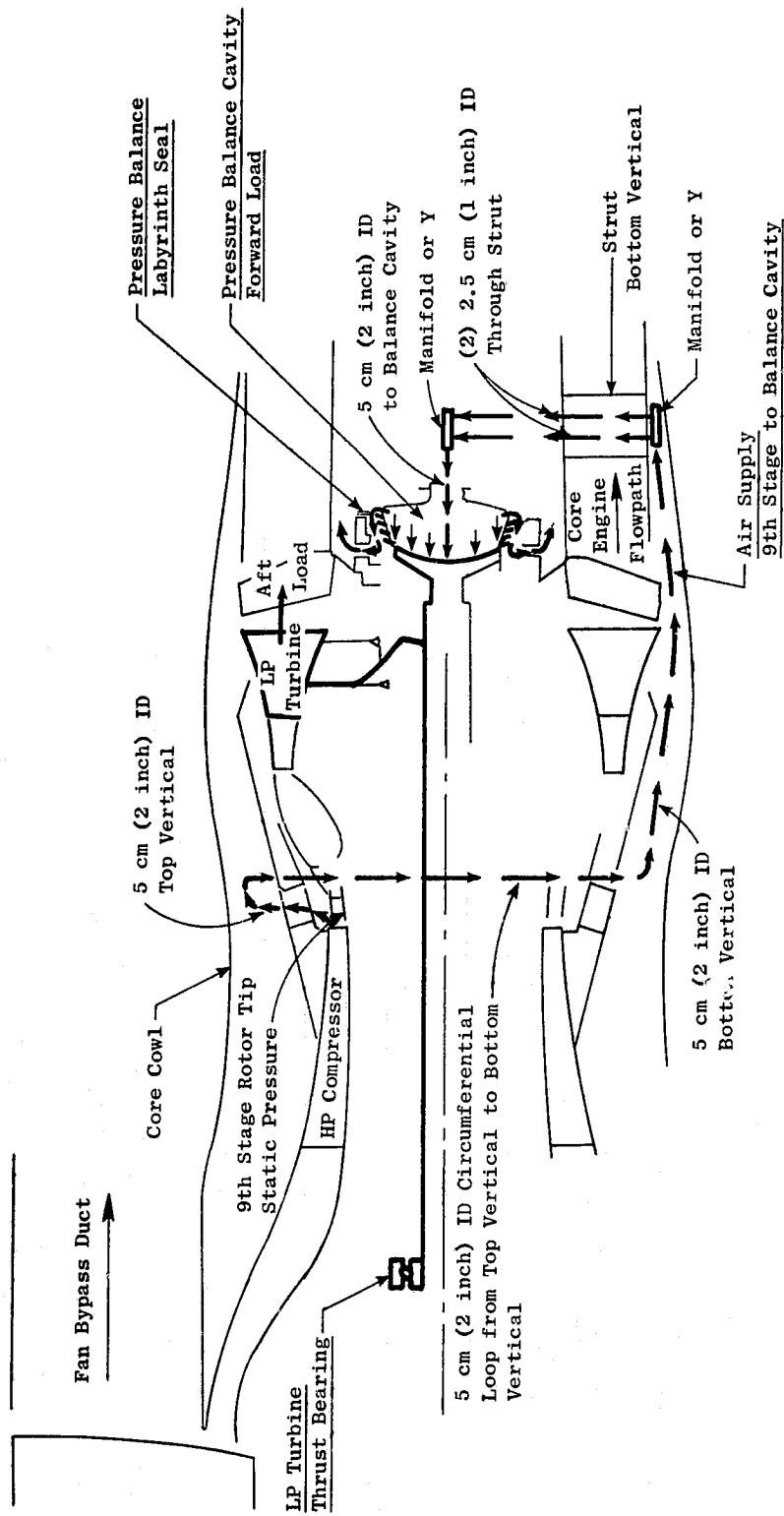


Figure 12-5. Low Pressure Turbine Thrust Balance System.

0.19 kg/sec (0.43 lb/sec) for a 0.038 cm (0.015 in.) seal clearance. A 0.152 cm (0.060 in.) seal clearance requires 0.52 kg/sec (1.15 lb/sec).

The No. 2 thrust balance cavity was sized to provide a minimum of 15,000 hours bearing life when subjected to the experimental engine life cycle defined below.

% N _F	% Fan HP	Time, hr	% Time	Net LP Turbine Load		LP Turbine Speed rpm
				kg	(lb)	
105	100	1	0.04	1580	3483	8359
100	140	1	0.04	2602	5736	7961
100	130	15	0.56	2196	4842	7961
100	110	15	0.56	1504	3315	7961
100	100	150	5.59	1190	2624	7961
90	80	500	18.64	910	2007	7165
75	50	1000	37.29	313	690	5971
30	10	1000	37.29	196	431	2388
		2682	100.0			

Bearing cubic mean load for this experimental cycle is 8287 N (1863 lb). Based on a dynamic capacity of 84,200 N (18,930), this bearing has a calculated B₁₀ life of 17,495 hours.

12.5 BEARINGS, SEALS, AND SUMP DESIGN

Figure 12-6 shows a schematic of the main shaft bearing arrangement and position designation.

The QCSEE engine will utilize the F101 core whose rotor is supported by two bearings. At the forward end is a ball thrust bearing (No. 3), which reacts the core unbalanced thrust load, and the radial load component. This bearing is supported from the aft flange of the fan frame. An intershaft roller bearing (No. 4) supports the rear of the core rotor on the low pressure turbine rotor shaft.

A face-type carbon seal is provided just aft of the No. 3 bearing and a circumferential carbon seal is used forward of the No. 4 bearing. The No. 3 and 4 bearings with their associated parts are identical to F101 hardware. QCSEE operating requirements are within the capability of this hardware.

The QCSEE low pressure rotor system is supported by four bearings. The low pressure turbine rotor is supported at the forward end by a ball thrust bearing (No. 2) and at the aft end by a roller bearing (No. 5). The fan rotor is cantilevered from a large ball thrust bearing (1B) and a roller bearing (1R). The low pressure turbine and fan rotors are coupled together through the reduction gear.

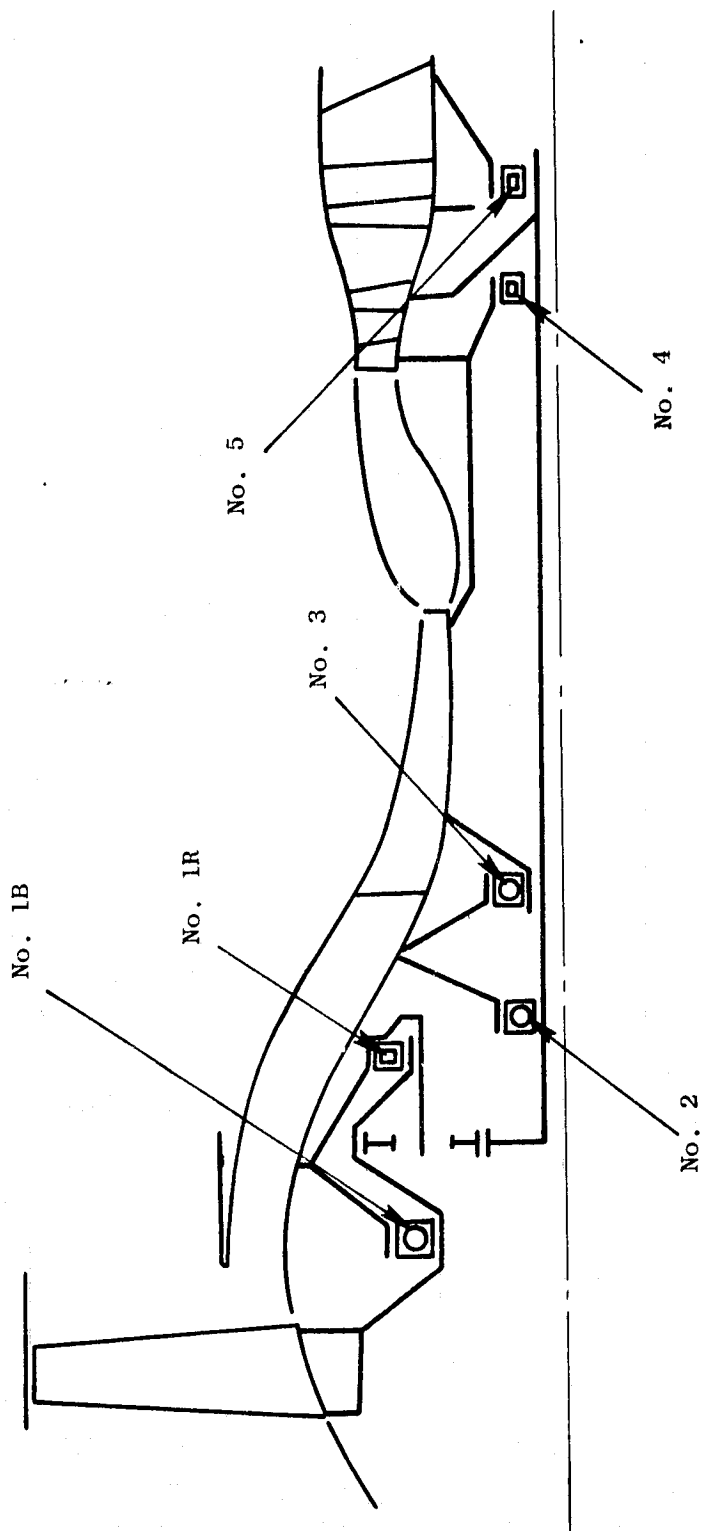


Figure 12-6. Schematic of Main Shaft Bearing Arrangement.

12.5.1 Forward Sump Definition

The forward sump, shown in Figure 12-7, contains the internal accessory drive bevel gearsets, reduction gears, variable pitch mechanism (for the UTW engine), and the No. 1B, 1R, 2, and 3 main shaft bearings and is enclosed by two carbon seals. A tandem circumferential carbon seal is being designed forward of the No. 1 bearing. This seal is pressurized by the same source as the other main shaft seals and cooled by oil flowing against the underside of the runner. A seal drain will be provided to collect any incipient leakage which will be directed overboard to prevent core engine contamination.

The balls and cage of the No. 1 bearing will be the same as used in the CF6. A new outer race, which will provide support over its entire length, will be designed and fitted to the common CF6 parts. A new inner race to handle thrust reversals, and slotted for under race lubrication, will be required. The races and balls are M50 and the cage is AMS 6414 (AISI 4340 Steel).

The No. 1B bearing and its seal are mounted in a 6Al-4V titanium housing which is bolted to the composite fan frame. Also mounted from this flange is the 6Al-4V titanium housing which supports the main reduction gear. Titanium was selected to be thermally compatible with the composite frame. The reduction gear is mounted to its support cone through a number of body-bound bolts. Mounting the main reduction gear and No. 1B bearing to a common frame flange allows modular assembly and disassembly of the fan and reduction gear assembly.

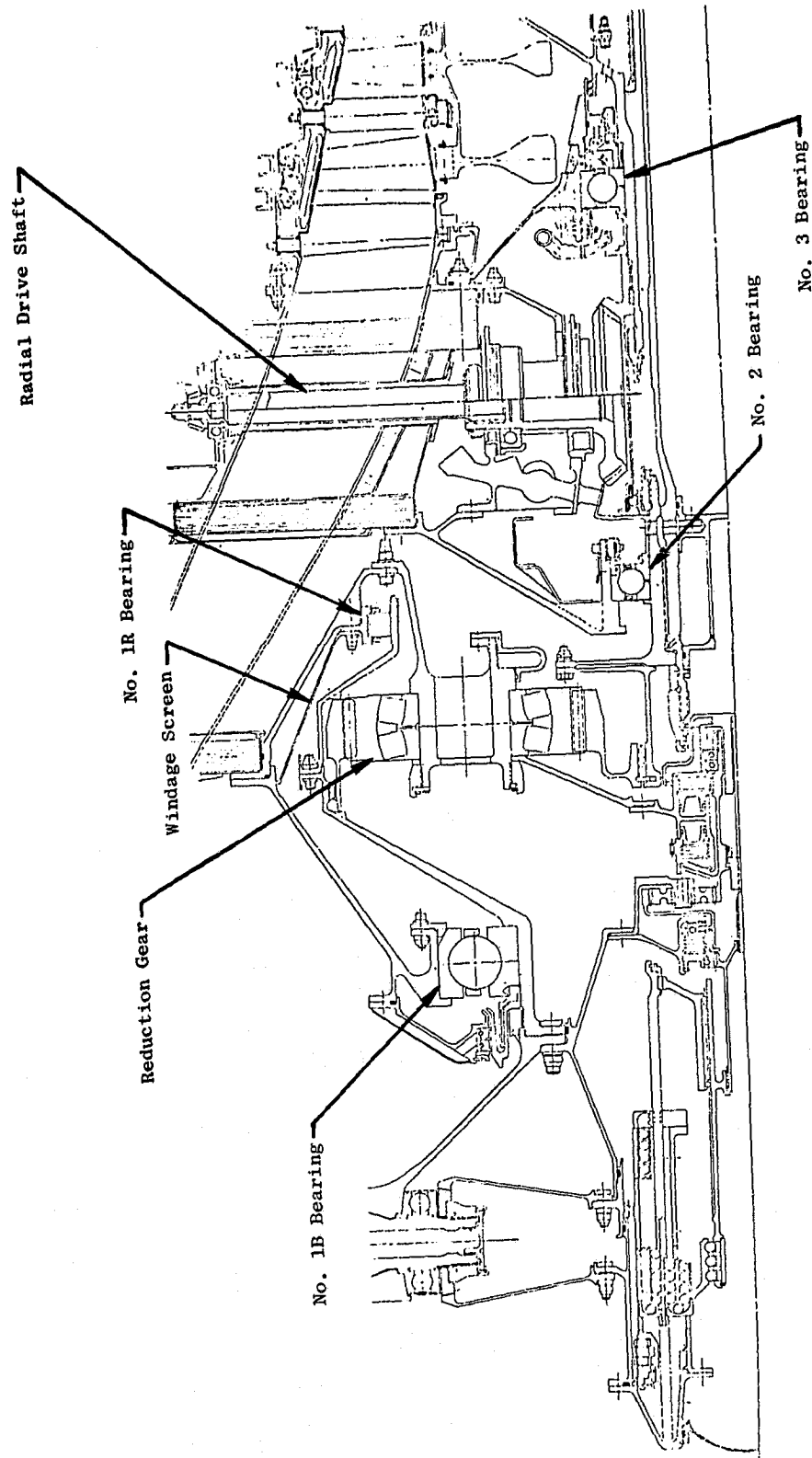
The No. 1R outer race and rollers are mounted in the reduction gear support cone and support the aft end of the fan stub shaft. This stub shaft will be manufactured from AISI 9310 material and the bearing journal will be case carburized to provide a hard contact surface for the No. 1R bearing rollers.

The No. 2 bearing is identical to the F101 bearing and is supported in a cone housing similar to that used in the F101 engine. For the UTW/OTW demonstrator engines, the F101 bevel gear assemblies will be mounted to a flange provided on the aft side of this bearing cone. This cone will be 6Al-4V titanium and the No. 2 bearing is M50 with a steel cage. The thrust load on this bearing is determined by the balance piston located in the aft sump.

A lubrication manifold, which is a modification to one used in the F101, will distribute oil to the No. 3 bearing, the bevel gears, and the No. 2 bearing. This manifold will provide a jumper tube to feed the reduction gear, the No. 1B and 1R bearings, and the variable-pitch mechanism.

12.5.2 Aft Sump Definition

The aft sump shown in figure 12-8 contains the intershaft roller bearing (No. 4) which supports the rear of the high pressure rotor on the low pressure rotor, and the aft roller bearing (No. 5) which supports the rear of the low pressure turbine shaft and stub shaft. This cavity is sealed on the forward side by a carbon piston ring intershaft seal and on the aft side by a single circumferential carbon oil seal.



ORIGINAL PAGE IS
OF POOR QUALITY

Figure 12-7. UTW Foreward Sump.

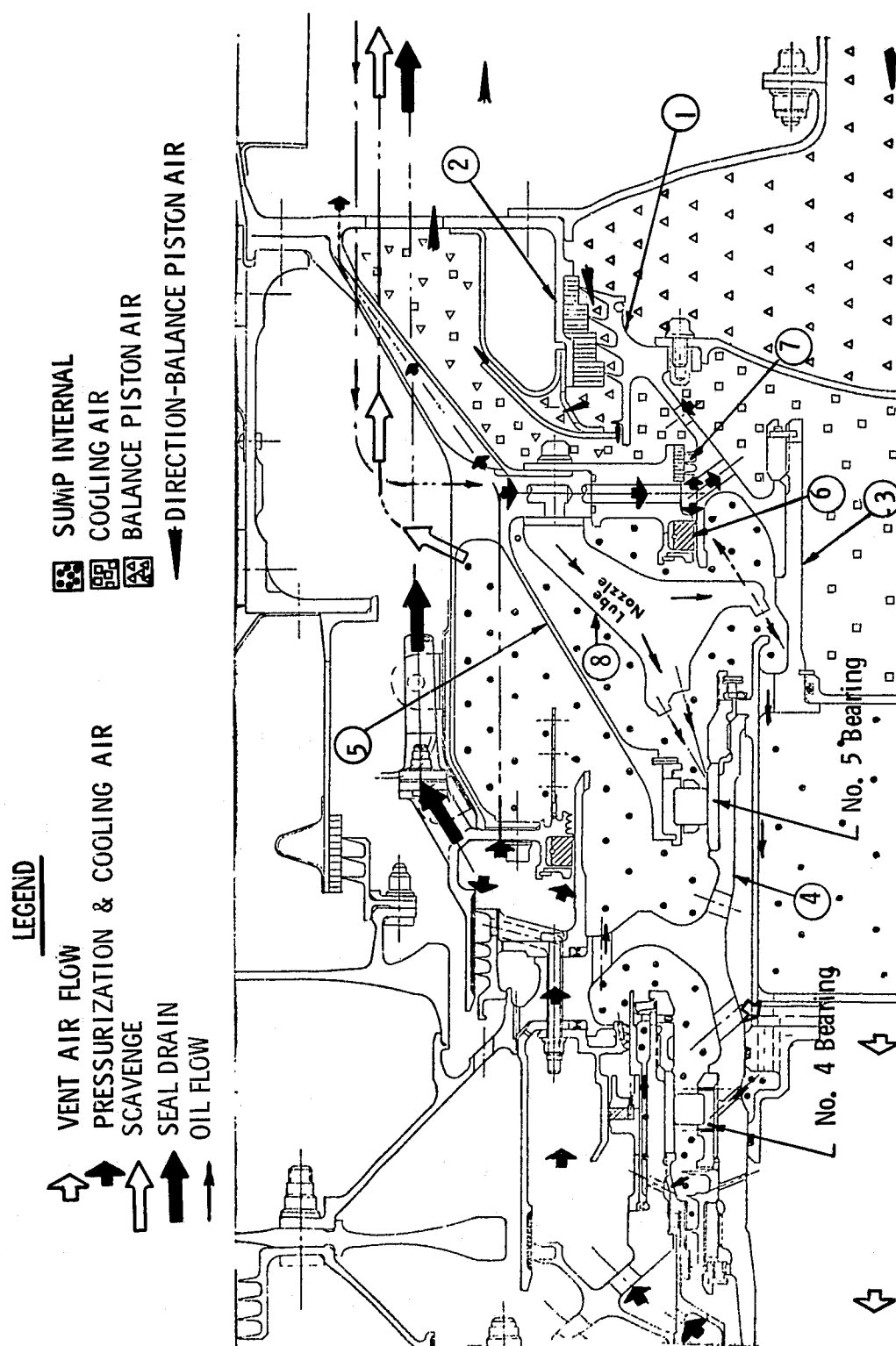


Figure 12-8. Aft Sump.

The same source air that pressurizes the aft carbon oil seal also has two other paths; one is inward through rotating holes for a buffer cooling cavity and out radially through rotating holes, and the second path is across the three-tooth labyrinth seal which continues outward and mixes with pressure balance exit air.

The pressurization air supply, oil supply, overboard seal drain, vent flow, and scavenge line are described in Section 12.3.

The pressure balance air flows across the slanted four-tooth labyrinth seal, with the majority of air exiting outward through the ejector and mixing with cooling air. A small percentage flows across the ejector skirt and mixes with cooling air.

Aft sump redesign includes the addition of a balance piston cavity and the removal of the F101 metering/scavenge pump. F101 existing hardware is retained where possible. New hardware and modifications to existing hardware are identified in figure 12-8 and are described as follows:

1. The rotating LP turbine thrust balance seal is a four-tooth stepped, labyrinth design 20.4 cm (8 in.) nominal diameter having slanted teeth tipped nominally 40° into the high pressure air with a minimum of one-to-one height-to-pitch ratio. Teeth are hard coated on rubbing surfaces. Axial tooth pitch is determined by proper axial spacing between rotating teeth and adjacent stator lands with allowance for tolerance stack-up, thrust bearing travel, and transient thermal movement. The small tooth at the discharge end deflects high velocity air radially outward through the eductor. A damper ring will be used if dictated by vibratory criteria.
2. The stationary labyrinth seal rub surface is abradable 1/32 hex-cell honeycomb made from 0.076 mm (0.003 in.) thick Hastelloy X material. The downstream end of the stator has an ejector to aspirate the pressurization air and prevent backflow into the sump. This type ejector is used on the CF6 and TF39 engines.
3. A new pressure balance cavity stub shaft is required to support the rotating pressure balance seal and adjacent hardware. The shaft is piloted to the low pressure turbine shaft. "O" rings are used on each side of the oil supply cavity. The stub shaft is locked to the LP turbine shaft end by a spanner nut.
4. Modifications will be made to the low pressure turbine shaft within the existing forging. The modifications will be in the area of the interface to the pressure balance cavity stub shaft.
5. The bearing sump housing is designed to transfer all loads from the existing No. 5 roller bearing to the LP turbine frame and accommodate all sump service lines.

6. The sump seal is a single circumferential carbon type with oil cooling the underside of the race. This design has been proven in many other General Electric engine applications.
7. The outer labyrinth seal is a straight three-tooth design with a height-to-pitch ratio of one-to-one.
8. The lube nozzle provides oil as described in Section 12.3. Redundant jets are designed in the nozzle.

12.6 ACCESSORY DRIVE DESIGN, UTW AND OTW

Engine accessory power is extracted from the core engine shaft through right angle bevel gearing, and transmitted through radial drive shafting to a top-mounted accessory gearbox and to a scavenge pump mounted in the core cavity area on the bottom vertical centerline. To minimize the frontal area projection of the engine, the accessory gearbox is configured to fit within the pylon strut. Mounted to and driven from the accessory gearbox are the following components:

- Fuel pump and control
- Lube supply pump
- Hydraulic pump
- Control alternator
- Starter drive pad.

The starter is remotely mounted to the engine support structure aft of the accessory gearbox. A shaft will be provided between starter and gearbox. The drive system is shown schematically in Figures 12-9 and 12-10.

To minimize program cost, the right angle bevel gearing presently proposed at the main engine shaft will utilize two sets of F101 bevel gears. Splined to the main engine shaft is a 47-tooth gear which will drive 35-tooth gears mounted in two individual gear housings. Figure 12-11 shows this gear housing assembly. Figure 12-12 compares the QCSEE method of mounting versus the F101. This configuration permits use of F101 housings without change. Larger moment loads associated with this system will require a support between the fan frame aft flange and the bevel gears as shown.

Gears and bearings are AISI 9310 and CEVM-M50, respectively, and the housing is investment cast 17-4PH. Lubrication is identical to the F101 and will be accomplished by modifying the internal lube manifold.

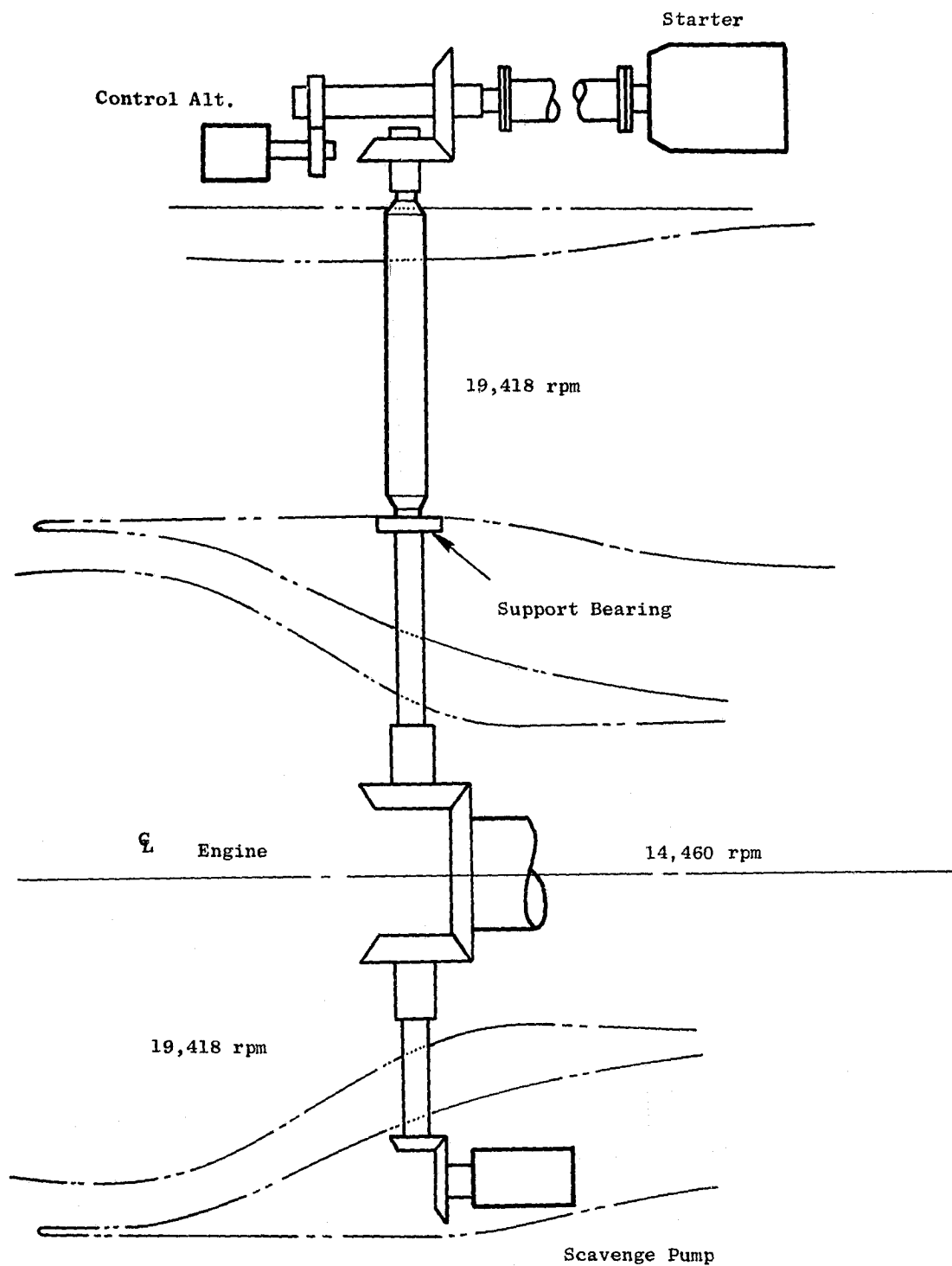


Figure 12-9. Accessory Drive System.

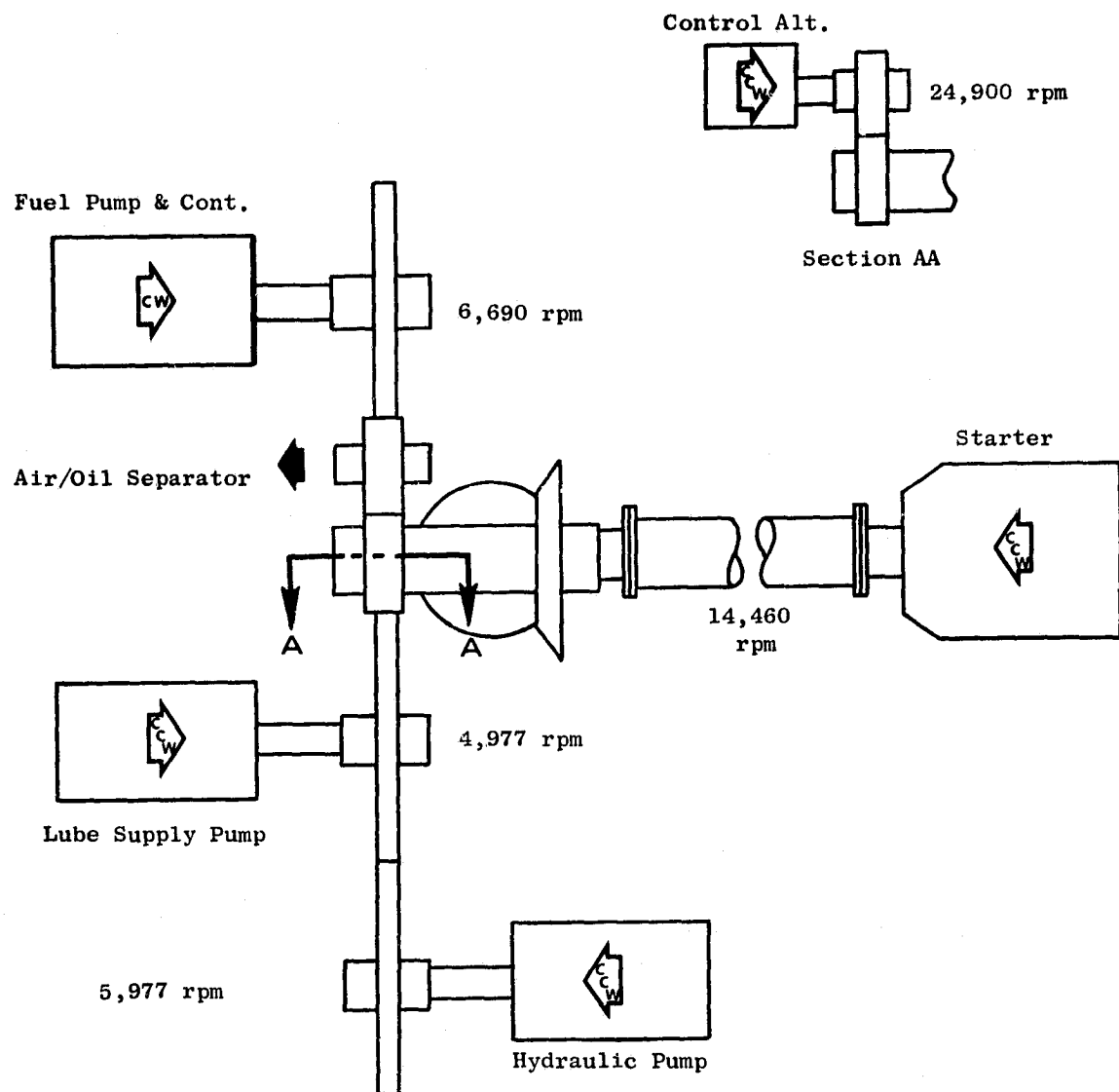


Figure 12-10. Accessory Gearbox System.

ORIGINAL PAGE IS
OF POOR QUALITY

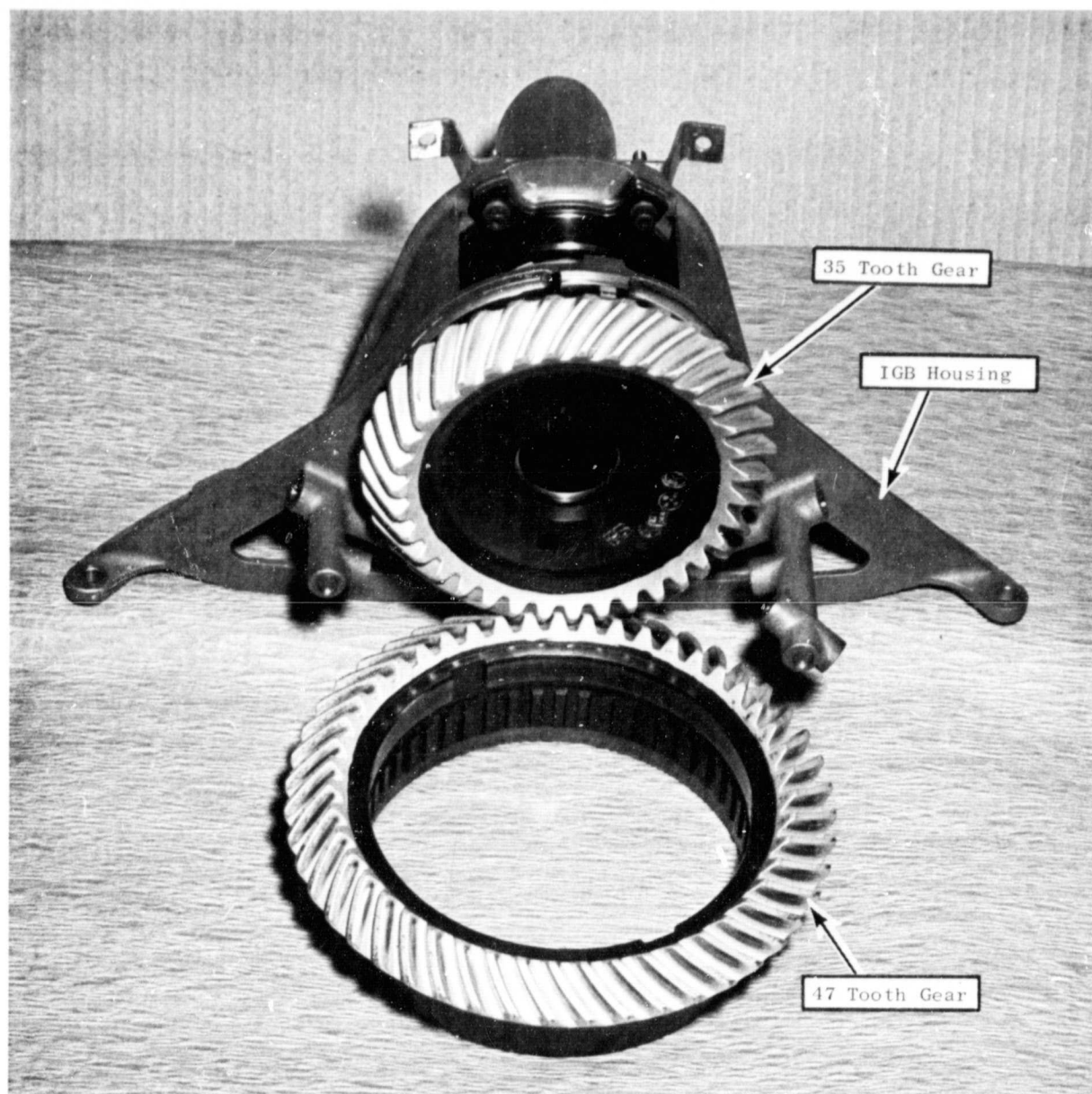


Figure 12-11. Inlet Gearbox Assembly.

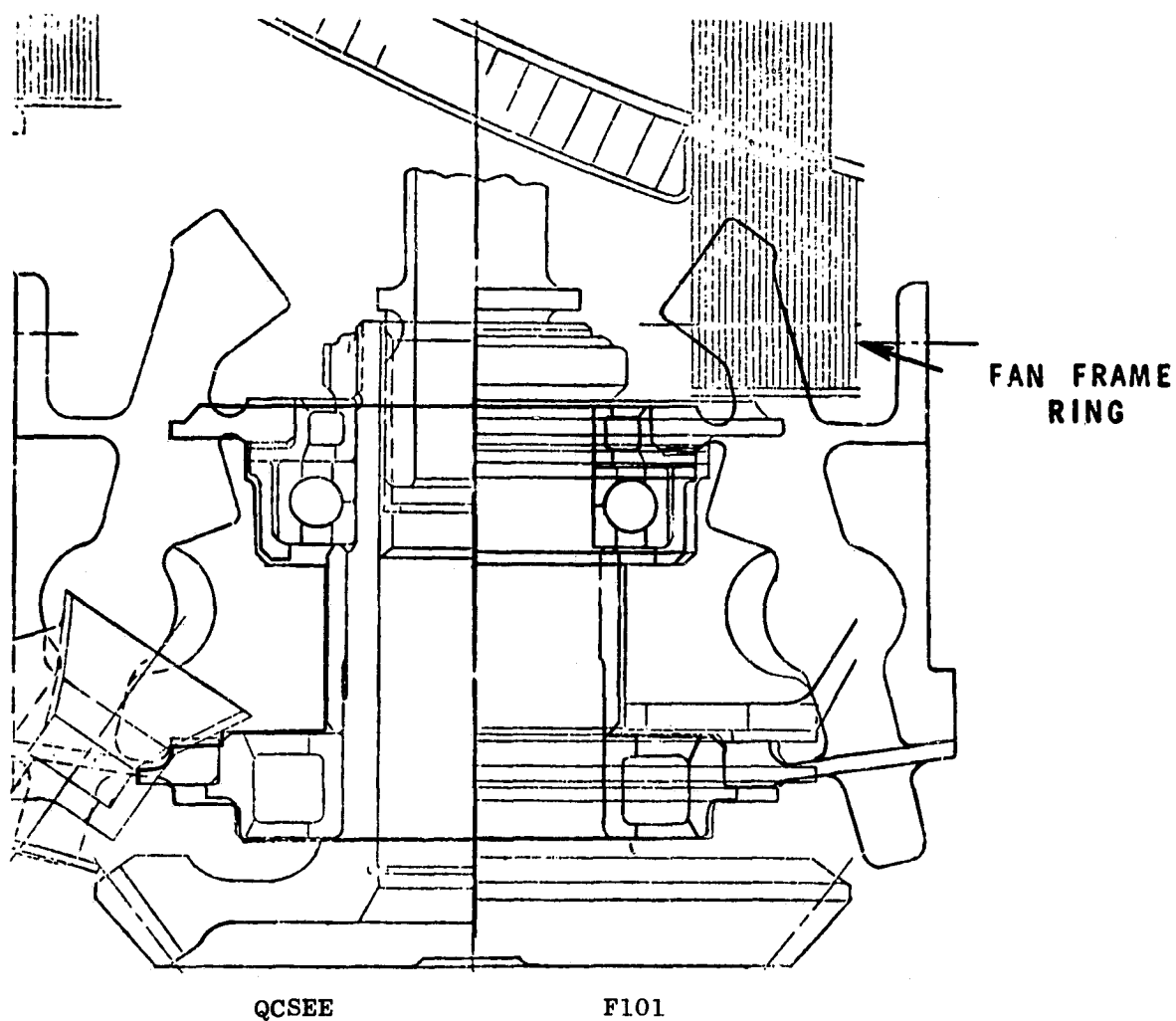


Figure 12-12. Comparison of IGB Mounting.

C-2

The bevel gears driving the bottom-mounted scavenge pump will be very lightly loaded in the demonstrator program and the design will require optimization for the flight design. For the UTW flight design, the 35-tooth gears driving the top accessory gearbox and the bottom scavenge pump will be mounted in a common housing. The flight OTW design will require a single drive to a bottom-mounted accessory gearbox where the scavenge pump would also be located.

The radial drive shaft between the internal bevel gear and the accessory gearbox will have a central support bearing located to keep the critical speed approximately 25% above the shaft operating speed. The location of this bearing is shown on the main engine cross sectional drawings. The arrangement is similar to that used on the CF6 and CFM56 engine.

The shaft between the internal bevel gears and bottom-mounted scavenge pump does not require a central support bearing because of its shorter overall length.

The top accessory gearbox will be designed to use the F101 bevel and spur gears and bearings. Efforts will be made to utilize other F101 hardware where applicable. Minor modifications may be required to this hardware to meet the requirements of the QCSEE gearbox. It is planned to use a CF6 lube supply pump which is compatible with the F101 lube pump drive speed and an idler gear will be relocated to make the direction of rotation compatible. Figure 12-10 shows the hydraulic pump driven by a separate gear which would be required if an F101 hydraulic pump is used. Another hydraulic pump being considered has opposite direction of rotation and would be mounted opposite the lube supply pump, thereby, eliminating a gear.

A new gearbox housing will be required to fit the pylon envelope available and will be fabricated or cast from aluminum. All gears and bearings are AISI 9310 and CEVM-M50 material, respectively.

Bevel gear meshes and associated bearings will be jet lubricated, and spur gears and their bearings will be splash lubricated.

The right angle gearbox provided to drive the bottom-mounted scavenge pump will require a new set of bevel gears. This bevel gear set will reduce the radial shaft speed from 19,418 rpm to 6700 rpm. This gearbox, shown in Figure 12-13, is located within the fan frame and provides an external drive for the scavenge pump. Access to the radial drive shaft is to be provided through the flowpath liner between adjacent vanes. Oil is scavenged from this gearbox by utilizing the drive gears in the scavenge pump.

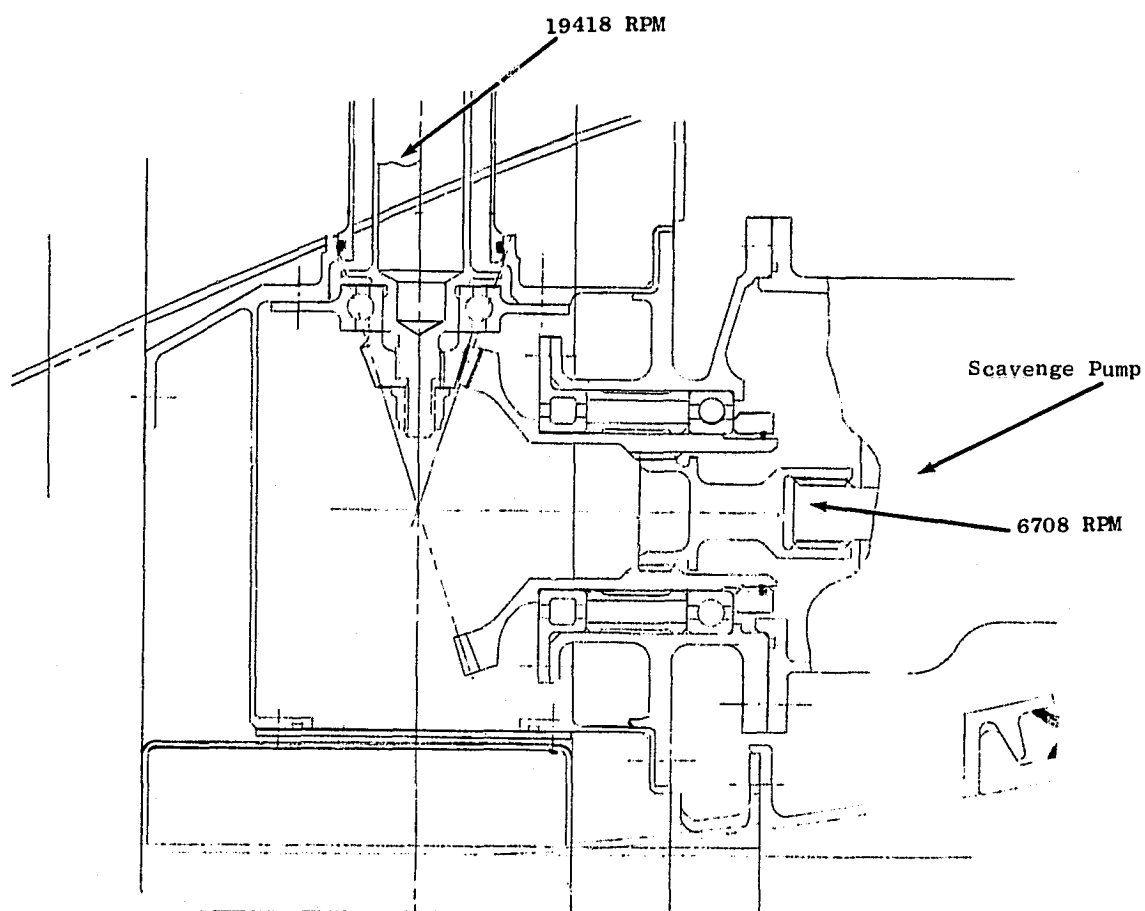


Figure 12-13. Cross Section of Scavenge Pump Drive.

ORIGINAL PAGE IS
OF POOR QUALITY

SECTION 13.0

CONTROLS AND ACCESSORIES DESIGN

13.1 SUMMARY

During the preliminary design phase, general requirements have been established for both the UTW and OTW control systems, and based on these requirements, basic system designs have been established. Components to be included in the systems have been identified and their inter-relationships generally defined.

The designs incorporate two basic control components; a modified F101 hydro-mechanical fuel control and a digital electronic control which is a new design. The digital electronic control provides the primary control of the engine variables with the hydromechanical acting as a backup and providing limits.

The systems include both automatic and manual operating modes. The automatic modes will provide control of all engine variables which will allow transient performance to be determined. The systems can be integrated with a remote computer simulating a STOL transport aircraft computer, thus allowing STOL propulsion system investigations to be performed. The manual operating mode is included since it allows independent manipulation of controlled variables so that engine characteristics can be completely explored. This is particularly applicable to the UTW engine with its variable-pitch fan and nozzle.

Studies are underway to define the automatic control modes. Naturally, more emphasis is on the UTW system because of its earlier timing and because of the added complexity resulting from the variable pitch fan. The mode studies are aimed at defining the best thrust control parameter for automatic power management and at evaluating various methods of interrelating and scheduling the controlled variables. Consultations have been held with NASA, McDonnell-Douglas, and Boeing relative to aircraft aspects of the mode studies. One of the tools being used in the studies is a recently completed hybrid computer model of the engine.

Detailed design of many system components is complete or nearly complete because existing designs are being used. Definition of the changes required in these existing components is proceeding. With regard to the digital control, the major emphasis has been on preliminary design of circuits. Final detailed design and programming of the digital control will proceed as control modes are defined.

Four advanced technology elements have been proposed for demonstration as a part of the QCSEE controls and accessories program and some preliminary work has been done on these. The elements are an inductive connector, a high reliability electronic module, a fail-fixed servovalve, and a magnetic shaft encoder.

Progress has also been made in the area of failure detection and correction which is another part of the QCSEE controls and accessories program. A survey has been made on use of Kalman filtering techniques in use in other fields for detection and correction of failures and, based on this survey, an approach has been chosen for QCSEE.

13.2 DESIGN REQUIREMENTS, UTW AND OTW

The control system designs are based on a number of requirements, some contractual and some resulting from the nature of the UTW and OTW engine designs. The major requirements are described below.

Components - General - The system shall utilize existing controls and accessories components as applicable except it shall utilize digital electronics to perform functions not now performed by existing hydromechanical controls.

Digital Control - General - The digital control shall be mounted on the engine and shall interface with a remotely located aircraft computer to provide selectable power management, failure indication, and failure corrective action.

Controlled Variables - UTW - The UTW control system shall control fuel flow, core compressor stator vanes, fan blade pitch, and fan exhaust nozzle area.

Controlled Variables - OTW - The OTW control system shall control fuel flow, core compressor stator vanes, fan exhaust nozzle area (flight systems only), and thrust reverser.

Experimental Engine Flexibility - The systems shall include capability for independently manipulating variables so that engine characteristics can be completely explored.

Automatic Control Capability - The systems shall be capable of coordinated control of variables so that STOL aircraft propulsion test investigations can be performed with the intent of achieving:

- Thrust control throughout specified flight map with minimum pilot workload
- Fast thrust response
 - 1.0 sec 62 to 95% forward thrust
 - 1.5 sec Takeoff to maximum reverse thrust
- Specified noise and pollution goals.

Engine Protection - The system shall protect the engine from rotor overspeeds, turbine overtemperature, and excessive compressor or fan back pressure.

13.3 ENGINE CONTROL SYSTEM, UTW AND OTW

13.3.1 General Description

The control systems for the UTW and OTW are basically quite similar with the UTW being somewhat more complex because it includes four variables (fuel flow, fan pitch, core stator angle, and fan nozzle area) which can be manipulated in the forward thrust regime to achieve an optimum balance between thrust, fuel consumption, noise, and exhaust pollution goals. On the OTW, only three variables are available for such manipulation (fan pitch not available). A schematic of the UTW system is shown on Figure 13-1. The OTW system is the same except variable-pitch actuation is deleted and reverser actuation added.

Both systems incorporate two major controlling components, a hydro-mechanical control and a digital electronic control. The hydromechanical control provides backup control of fuel flow, controls core compressor stator vane position, and provides several limits. The basic fuel flow control is provided by electrical signals from the digital control to a torque motor on the hydro-mechanical control. The digital control also controls fan nozzle area, fan pitch angle, core stator reset and the thrust reverser. More details on the hydromechanical and digital controls are given in subsequent sections of this report.

The control systems are being designed to be operated in several different modes. Both systems will have one or more automatic modes in which the system receives power demand inputs as it would with the engine integrated into a STOL transport propulsion system. These operating modes are discussed in the sections which follow. In addition, there will be a manual mode to explore engine characteristics.

13.3.2 Automatic Control

General

The control systems are being designed for automatic modes in which operation of the controlled variables is integrated to respond to input demand signals simulating those which would exist in a STOL transport propulsion system. Studies are currently in process exploring a variety of potential methods for interrelating the controlled variables. The majority of this effort currently is being applied to the UTW system.

As a guideline for automatic mode studies, a list of general principles was established. This has been modified some on the basis of discussions with NASA, McDonnell-Douglas, and Boeing and may be further modified as system design proceeds. The current list is as follows:

1. A mechanical power lever link is assumed from the aircraft to the engine to be used as an enable and for backup fuel control only.

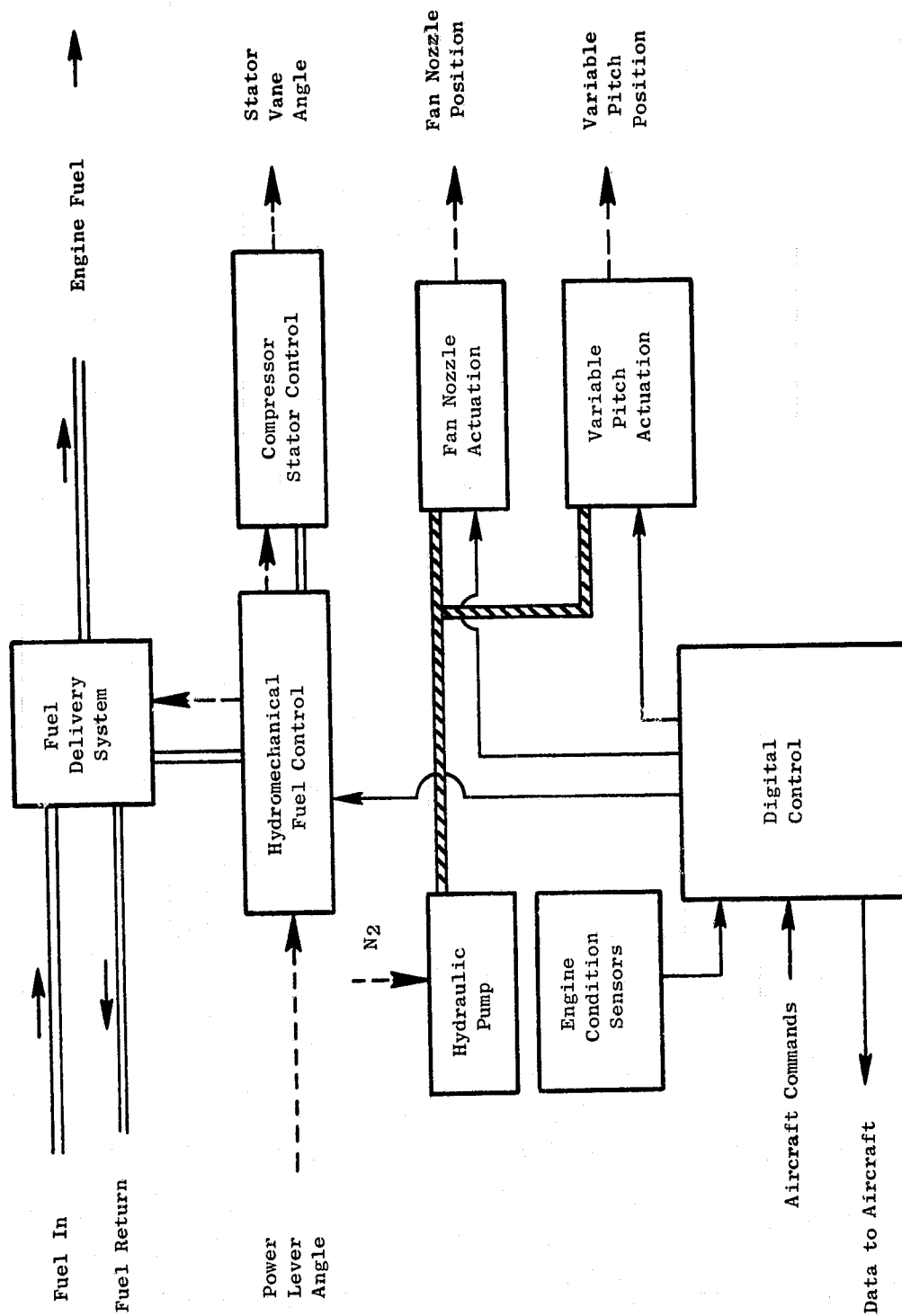


Figure 13-1. Control System Schematic.

2. A digital electrical thrust demand signal is assumed from the aircraft computer to the engine digital control demanding percent of available thrust.
3. A digital electrical mode signal is assumed from the aircraft computer to the engine digital control to select between available operating modes such as takeoff, climb, cruise, etc.
4. The engine digital control shall compute maximum available thrust at all flight conditions and shall be capable of setting this thrust or any portion of it as a function of a single aircraft thrust demand signal.
5. The engine control system shall provide selected engine safety limits, protecting against rotor overspeeds, fan or compressor stall, turbine overtemperature, and compressor discharge overpressure.
6. Manual control of thrust via the throttle shall be maintainable within safe limits if the engine digital control and/or aircraft digital control fails.
7. It is desirable that no throttle or thrust demand changes be required during takeoff except in the event of an abort.
8. It shall be an objective that fan pitch shall not change if the engine digital control fails.
9. It shall be an objective that fan nozzle area shall go to the takeoff position in the event of a failure.
10. Detection of engine failure to produce commanded thrust shall be achieved through a combined indication from engine parameters in the engine digital control and a signal shall be transmitted to the aircraft.

Thrust Control Parameter

One fundamental factor in designing for automatic control is the choice of a thrust control and indication parameter or parameters. This parameter must be an accurate measure of thrust in the takeoff regime, and must be related to other sensed engine variables in such a manner that the engine digital control can compute and set maximum available thrust or any portion thereof anywhere in the flight envelope.

To determine the thrust setting accuracy of various potential thrust control parameters, preliminary tolerance studies have been prepared. These studies combine typical control and measurement tolerances, engine component tolerances, and engine component deterioration experience with engine cycle characteristics into matrices which are manipulated by computer to determine thrust tolerances using the various potential thrust indication parameters.

Initial tolerance studies revealed that the thrust control parameter used on the CF6 engine, fan rpm corrected with inlet temperature, is not accurate on the QCSEE/UTW engine because of significant effects of fan pitch setting and

measuring tolerances. The initial studies showed airflow, thrust related pressure ratio parameters, and power indicating parameters to be best from a tolerance point of view.

Another important thrust parameter consideration is scheduleability over a wide range of operating conditions. This is evaluated by studying cycle data. A study of this nature using early cycle data showed that a power related parameter such as P_{49}/P_2 (LP turbine inlet/engine inlet pressure) which appeared favorable in the tolerance study also proved scheduleable. These results are currently being checked using cycle data which includes an improved representation of the variable pitch fan. Scheduleability is also being investigated using the hybrid computer engine model recently completed.

Accuracy of measurement is another factor to be considered in judging thrust control parameters. The previously mentioned parameter, P_{49}/P_2 , has been virtually eliminated because P_{49} , the pressure between the high and low pressure turbines, is difficult to measure in the F101 advanced configuration engine. Pressure nonuniformity across the flow path in this region requires multitap probes to achieve accuracy. Such probes create flow path disturbances, degrade turbine performance, and would be a maintenance problem due to high temperature, and would be costly to introduce into the hardware. Current studies indicate that compressor discharge static pressure (P_{S3}) can be substituted for P_{49} .

Still another factor to be considered is control loop stability with the various potential thrust control parameters. This will be investigated by means of the hybrid computer model of the engine and control system.

Thrust control parameter selection studies are continuing with emphasis on computed parameters which basically represent gas generator developed power or fan absorbed power. Such naturally integrated parameters are advantageous from a measuring accuracy standpoint. Similar studies on the OTW system, which will be simpler because fan pitch is not varied, will follow the UTW studies.

Control Modes

Another task necessary to definition of automatic control modes is the identification and evaluation of the modes themselves, that is, the inter-relationships between manipulated variables and controlled parameters.

Key operational requirements applicable to establishing automatic control modes at various conditions are:

- | | |
|----------------|---|
| <u>Takeoff</u> | <ul style="list-style-type: none">• Set guaranteed maximum static thrust or percent thereof• Set inlet throat Mach number for optimum noise/performance compromise |
| <u>Climb</u> | <ul style="list-style-type: none">• Set guaranteed maximum installed thrust or percent thereof• Control inlet Mach number for optimum performance |

- Cruise ● Attain minimum installed SFC at required thrust level
- Descent ● Maintain sufficient core speed for air conditioning and power extraction
- Approach ● Fast thrust response at readily controlled level up to guaranteed maximum
- Maximize inlet Mach number and airflow for low noise
- Ground Idle ● Minimum thrust
- Minimum exhaust pollution
- Low noise
- RPM sufficient for centrifugal anti-icing

Studies are currently underway using UTW engine cycle data and the UTW hybrid computer model to identify practical modes of control and to evaluate them. Currently data are being run at takeoff and approach conditions at a variety of thrust levels, fan pitch angles, and fan nozzle areas. These data are being analyzed to explore the various ways in which the variables can be combined and scheduled to achieve the requirements. The options are being judged relative to noise parameters, accuracy, response rate (particularly at approach), stability, and schedule practicality.

The above study efforts have not yet resulted in conclusive choice of control modes. The inherent flexibility of the digital control makes it possible to investigate experimentally several modes before a final choice is made.

13.3.3 Manual Control

In the manual operating mode, provisions will be made for manipulating the controlled variables independently. The control room throttle will serve as a manual input to the hydromechanical control to provide basic control of fuel flow by the core engine governor and various fuel flow limits in this component. In addition, potentiometers in the control room will serve as inputs to circuits and programs in the digital control which, through manipulation of the fuel flow trim signal to the hydromechanical control, trim fuel flow to provide closed loop control of such variables as fan speed, core pressure ratio, and calculated turbine temperature.

Additional potentiometers in the control room will serve as inputs to circuits and programs in the digital control which control the fan exhaust nozzle and the fan pitch angle.

Engine safety limits such as maximum rotor speeds, maximum internal temperatures, and maximum internal pressures or pressure ratios will be incorporated in either the hydromechanical or digital control and will be in effect at all times, thus protecting the engine during all exploratory testing in the manual control operating mode.

13.3.4 Failure Detection and Correction

In pursuing this aspect of the QCSEE control design requirement a thorough survey was made of current applications of Kalman filtering techniques for automatic failure detection and correction. For example, a detailed review was made of the NASA-Langley work done in defining Kalman filter techniques for detecting and compensating for faults in an aircraft flight control system.

Another unique and very impressive use of these techniques was uncovered in an industrial process control application. Lund University (Sweden) has developed a Kalman filtering type system for detecting and compensating for failures in automated machinery in a computer-controlled factory. This was observed in operation and a demonstration made in which key control elements were disconnected without noticeable effect on operation.

The Lund approach has tentatively been selected as the simplest for on-engine control mechanization and some preliminary work has been done on this. In general, this approach is to compute key engine and control system variables using engine equations and characteristics. Actual and computed values of the variables will be compared and any differences used to update the engine equations and thus correct the computed values of variables. If any of the directly sensed key variables deviates from the computed value to indicate a sensing system has failed, the control system will still function using the computed value of the variable which will be correct except for the relatively small error resulting from detection of the failed sensing system.

Work is continuing in this area to evaluate the above approach and prepare refined sets of engine equations for computing variables.

13.3.5 Hydromechanical Control

General Description

The QCSEE hydromechanical control is an F101 main engine control which will contain appropriate modifications applicable to the unique requirements of the QCSEE control system and engine. The control is capable of performing the computation (hydromechanical) and fuel metering necessary to control engine combustor fuel flow and compressor stator vane positioning. Woodward Governor Co. is the vendor source for this control.

The modified F101 control will perform the following subsystem functions:

- Modulates core engine fuel flow to govern core speed as a backup to the digital control
- Schedules acceleration and deceleration fuel flow limits
- Modifies acceleration fuel schedules for compressor discharge bleed conditions

- Schedules variable stator vane position
- Provides positive fuel flow shutoff and limits core engine overspeed
- Limits compressor discharge pressure
- Reduces fuel flow in proportion to electrical signals from the electronic control as the primary fuel control method
- Provides power lever position intelligence to the electronic control
- Provides minimum fuel system pressurization
- Provides fuel flow shutoff to limit fan overspeed in response to electrical control signals from the digital control
- Provides core stator vane reset in response to electrical control signals from the digital control
- Provides electrical metering valve position intelligence to the digital control

Hydromechanical Control Inputs and Outputs

The inputs to and outputs from the hydromechanical control are listed below.

INPUTS

- Pump discharge fuel flow
- Power lever angle
- Core engine drive speed
- Compressor discharge pressure
- Compressor bleed port pressure
- Core inlet air temperature
- Core stator actuator position
- Electrical fuel flow limit signal
- Electrical fan overspeed signal
- Electrical stator reset signal

OUTPUTS

- Metered engine fuel flow
- Bypass fuel flow
- Stator vane actuator control pressures
- Power level electrical position signal
- Metering valve electrical position signal

Hydromechanical Control Functional Description

The hydromechanical control mechanization arrangement which indicates implementation of the various control functions is depicted on Figure 13-2 for the existing F101 fuel control. QCSEE modifications to the schematic arrangement are identified in the following functional description which references Figure 13-2.

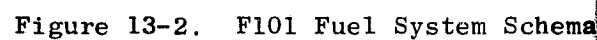
Backup engine speed control is accomplished with the same basic governing components that have been used in previous Woodward Governor Company units; a flyweight system that provides isochronous speed governing (zone C-14). In normal operation, this system is overridden by use of a two-stage torque motor servovalve to reduce engine speed in response to the electrical signal from the digital control (zone B-15). Engine speed can only be reduced by action of the electrical torque motor override system thereby requiring the throttle to be set at 100% to enable the system. This is important in that, should any malfunction occur in the electrical subsystem, complete control of engine speed is still available with the hydromechanical system.

The acceleration and deceleration limiting systems use a conventional W_f/P_3 3-D cam (zone E-12) limiting schedule generated as a function of engine speed (zone B-9), compressor inlet temperature (zone J-12), and compressor discharge pressure (zones F, H, J-13, and 14). The opposite side of this same 3-D cam also contains the reference schedule for the core stator vane servo. Stator servo position reference, a function of core speed and inlet temperature, is compared to actuator feedback position in a linkage system (zone E-11), and the error positions the stator servo pilot valve (zone E-11) to port flow and pressure to the stator actuation pistons.

The fuel metering system is designed to use simple control elements for multiple functions. The main metering valve is a variable area shoe and rotor (zone D-10). A constant pressure drop is maintained across the metering valve by a bypass-type proportional-plus-integral regulator (zones C, D, and E-10). The bypass system also provides the pump unloading function during shutdown (windmilling) conditions (zone B-12). For reliability purposes, the unloading function is positively locked out during normal engine operation between idle and maximum speed. The fuel shutoff valve (zone B-12), similar to the fuel valve rotor, is integral with and actuated by the power lever shaft (zone A-11). Movement of the power lever to the off position mechanically actuates the pump unloading function which provides a $1.72 \times 10^6 \text{ N/m}^2$ (250 psi) pump discharge pressure during windmilling conditions for servo system regulation purposes.

A pressurization valve (zone B-12), used to provide minimum back pressure to ensure adequate servo system pressure during low metered flow conditions, is provided as part of the control package.

The temperature sensor shown schematically (zone J-12) provides the control with a hydraulic signal that is proportional to temperature. The sensor will be located to sense core engine inlet temperature for the QCSEE engines. To meet the response speed requirements, a high conductivity zirconium alloy (Zircaloy II) is used for the gas-filled coil. The gas-filled coil



ORIGINAL PAGE IS
OF POOR QUALITY

senses temperature which expands a bellows inside the sensor body. The bellows applies a force at one end of the beam balance system which then changes the area at the variable metering orifice to produce a signal for control usage in acceleration and stator schedule computation. The sensor is designed for the following conditions:

- Temperature Range -53.9°C to 260°C (-65°F to 500°F)
- Response 0.5 sec @ $3.61 \times 10^2\text{ kg/sec/m}^2$ (74 pps/ft^2)
 airflow
- Accuracy $\pm 2.07 \times 10^4\text{ N/m}^2$ ($\pm 3\text{ psi}$) about a linear
 output schedule
- Sensitivity $2.02 \times 10^{-4}\text{ }^{\circ}\text{C/N/m}^2$ (2.5° F/psi)

The computation system is comprised of hydromechanical components. The hydraulic servos (conventional closed loop subsystems) use unique single-diameter, single-acting pistons. In each of the four sensing and computing subsystems, the modulated servo pressure is counterbalanced by a case reference pressure, thus eliminating the need for large double-diameter servos. This approach permits extension of the servo stroke within a given control envelope to achieve greater accuracy by more effective force multiplication.

The control mechanical design includes the following:

- Pilot Valve Assemblies - Pilot-to-sleeve diameter clearance, 5.08×10^{-6} to $20.32 \times 10^{-6}\text{ m}$ (0.0002 to 0.0008 inch). Pilot and sleeve are matched assemblies and of similar materials.
- Seals - Fluorsilicone for external static seals, Viton A for internal static seals. Tef-cap dynamic seals are used for the power lever, core static feedback lever, and metering valve position transducer.
- Position Servos - Aluminum pistons and sleeves, not matched, pressure balancing grooves along the piston. The pistons drive racks and pinions, made of 410 passivated steel, to perform computations.
- Cams - The 3-D and 2-D cams are 440 through-hardened steel; three 3-D cams are used.
- Cam Followers - Tungsten carbide.
- Springs - 17-7PH stainless steel is used except for temperature-sensitive functions where temperature-compensating material is used. For reduced cam loading, opposing (equilibrator) springs are used.

PRECEDING PAGE BLANK NOT FILLED

- Bearings - Roller, needle and thrust bearings are through-hardened 440 stainless steel. There are 22 carbon journal bearings. Double ball bearings are used in the governor and tachometer ball heads.
- Torque Motor - 2 stage, $5.05 \times 10^{-4} \text{ m}^3/\text{sec}$ (0.8 gpm) rated output.
- Gears - Through-hardened 410 steel except for two lightly loaded aluminum gears.

Modifications to the control planned for QCSEE use will include the following:

- 3-D Cams - Cam schedule contours will be changed to match QCSEE engine requirements (zone C-15 and E-12).
- Compressor Discharge Bleed Compensation - The acceleration schedule multiplier function of CDP/CBP ratio established by the CDP/CBP sensor (zone H-14) may have to be altered or extended for the high bleed flows planned for QCSEE.
- Emergency Fuel Shutoff - An electrical-to-hydraulic interface device will need to be added to the control to accomplish shutoff of engine fuel flow in response to an electrical fan overspeed signal. It is planned to accomplish this function by switching pump discharge pressure into the reference chamber of the system pressurizing valve (zone B-12). A similar action is taken in the event of core engine overspeed through the action of the existing overspeed shutoff valve (zone B-10). It is planned to provide a low-power, torque-motor-operated switching valve to be mounted on the pressurizing valve cover to accomplish the fan overspeed protection. The flow gain of the output stage of the shutdown device will be selected to cause closure of the pressurizing piston within 20 milliseconds after the electrical overspeed signal is sensed. This shutdown action will temporarily place the fuel pump on pressure relief during engine coastdown.
- Stator Reset - The existing Block I F101 controls contain provisions for an electrically operated reset of core stator vane position. The reset is presently initiated by energizing a solenoid (not shown on Figure 13-2) which is similar to the idle reset solenoid (zone F-15). The stator reset solenoid valve switches reference pressures to the VSV load piston (zone C-11) to reset the stator control valve feedback linkage. For the QCSEE controls it is planned to substitute a low-power, torque-motor-operated switching valve for the present solenoid valve.
- Metering Valve Position Signal - The present controls provide an electrical rotary rate transducer on the metering valve shaft to signal metering valve angular velocity (zone E-9). For the QCSEE units, a position transducer identical to the power lever position transducer (zone H-17) is planned to be substituted for the metering valve rate transducer.

- Electrical Fuel Override Authority - The present F101 controls provide a core speed floor limitation on the electrical fuel flow override through the action of a speed switch valve (zone C-14) which is actuated by the core speed tachometer (zone B-9). This speed floor setting will be changed to an engine ground idle speed value for QCSEE by remachining the actuating linkage detent on the tachometer output rack, thereby providing for full fuel control by the digital control.

Hydromechanical Control Installation

The hydromechanical control will be mounted on the F101 fuel pump similar to Figure 13-3. The pump is V-band flange mounted to an F101 gearbox pump drive pad. Through shafting is used to provide core speed input to the control drive spline.

For the QCSEE system it is desired to route control bypass fuel flow to the aircraft (or facility) fuel tank, in order to reduce fuel pump temperature rise and provide the system heat exchangers with a suitably low fuel entrance temperature for dissipation of oil system heat loads. Rerouting of bypass flow will require that a mount adapter sandwiched between the fuel control and pump interface flanges be provided. The adapter will block off the normal bypass return to the fuel pump interface and provide an external port to discharge the bypass flow. An extended-length drive quill shaft will be provided on the control and carried through the adapter to engage the pump output drive spline.

The core stator vane position mechanical feedback interface will be used identical to the F101 control installation. All hydraulic and pneumatic piping interfaces to the control will be identical to the F101 configuration with the exception of the bypass fuel flow adapter port.

13.3.6 Digital Control

General Description

The digital control accepts operational input demand and engine parameter information in the form of ac and dc analog signals and digital signals and uses this information to generate engine control signals and engine condition monitoring data. A simplified block diagram of the control is shown in Figure 13-4. The analog signals are conditioned to a standard voltage range and then multiplexed to an analog-to-digital (A/D) converter. The output of the A/D converter is fed to the central processor unit (CPU) where all necessary calculations are performed. The CPU output is fed into two circuits. One circuit is a multiplexer that sends data out to the aircraft. The other circuit is a digital to analog (D/A) converter circuit. The output of the D/A converter is fed to sample and hold circuits and subsequently to the output drive circuits. The drive circuits provide signals to the torque motors that are used to provide engine control. Power to the control is provided by an engine-mounted alternator. The alternator ac signal is converted to the necessary regulated dc voltages.

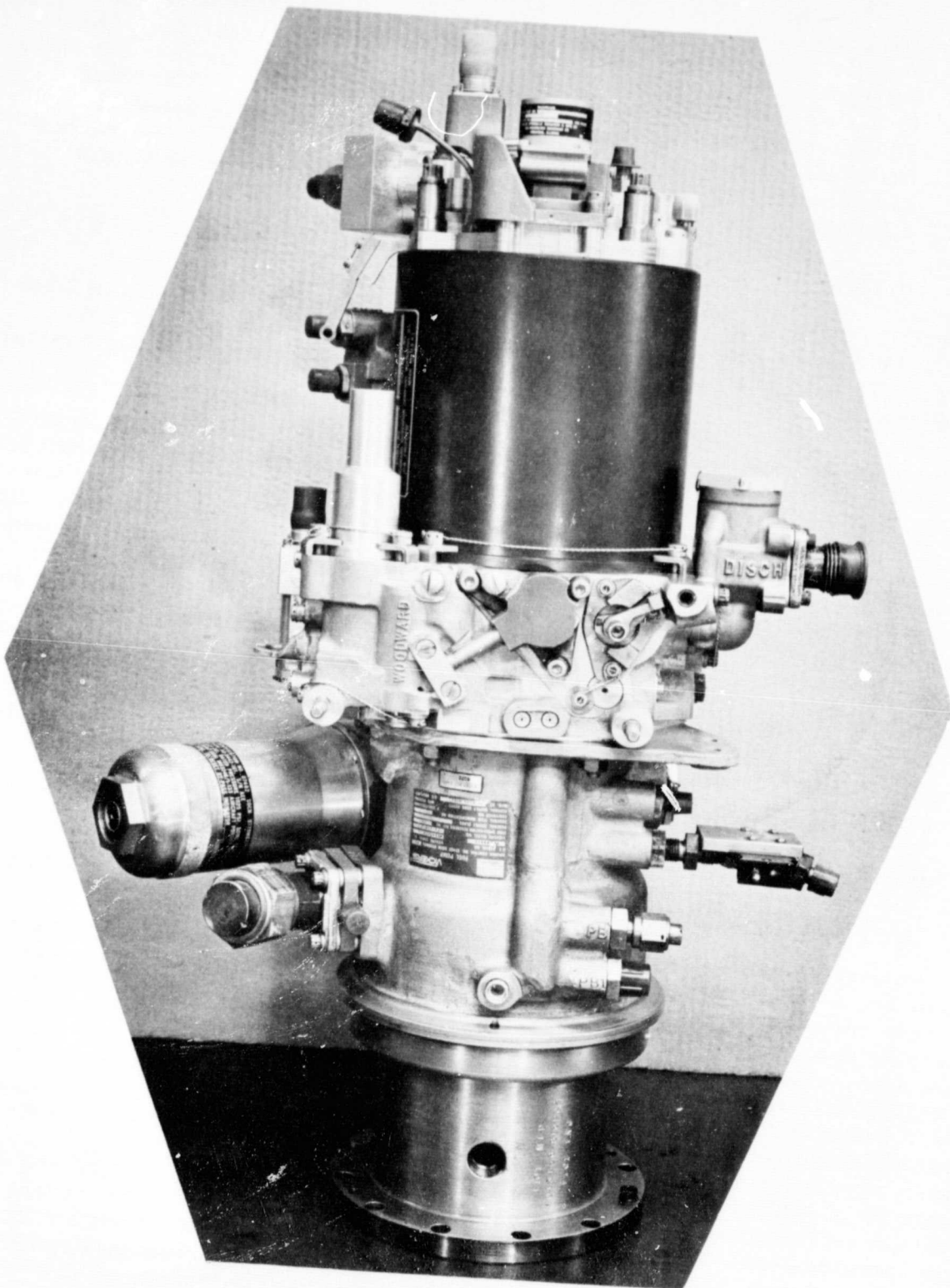


Figure 13-3. F101 Fuel Pump.

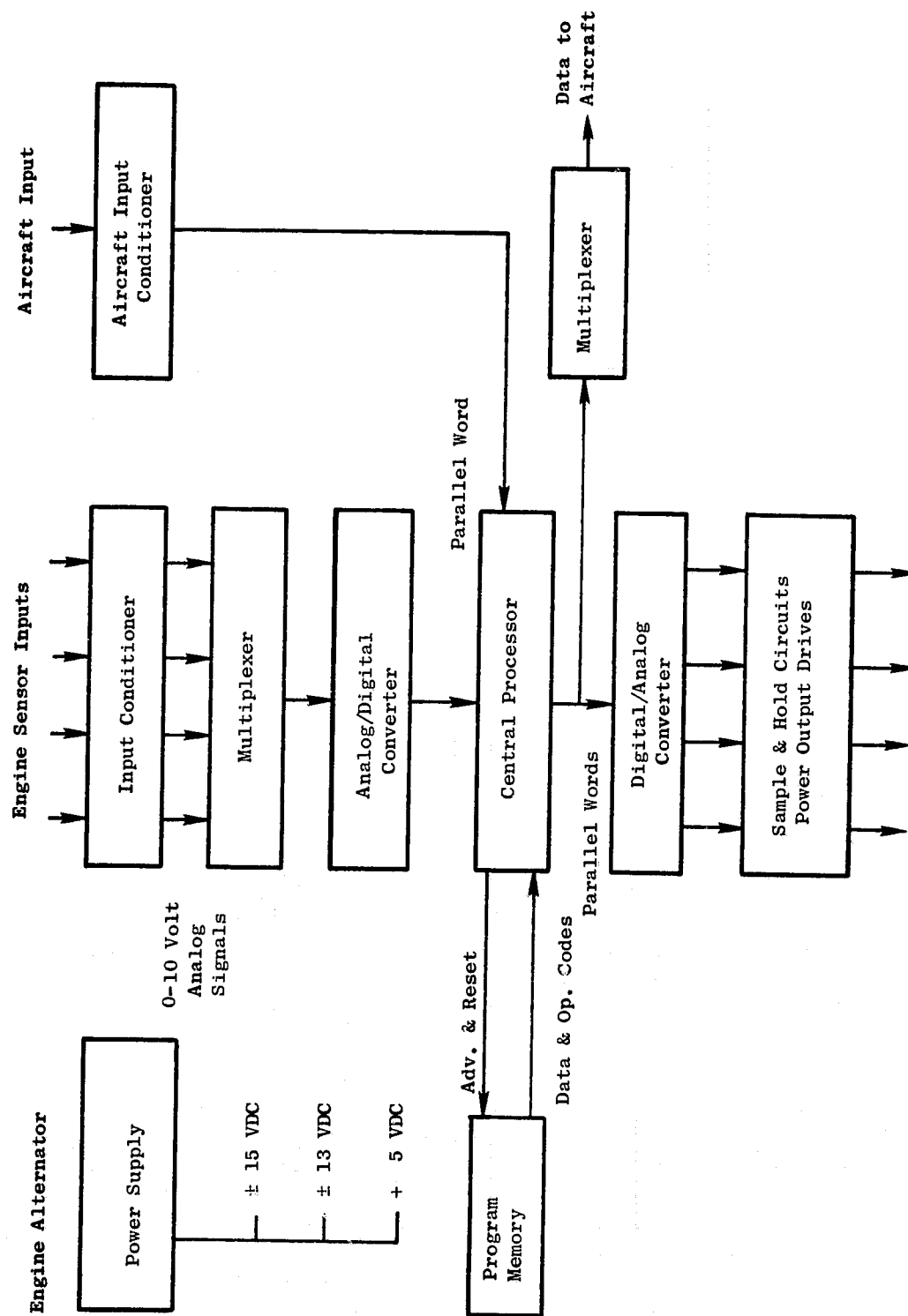


Figure 13-4. Digital Control Schematic.

Digital Control Inputs and Outputs

The QCSEE digital control inputs and outputs listed in Tables 13-I, 13-II, 13-III, and 13-IV are described below.

Inputs to the digital control consist of four classifications: (1) instrumentation signals, (2) sensor and transducer signals, (3) power signals, and (4) digital signals. Table 13-I is a list of the instrumentation signals. These signals are all 0-10 volt levels and the only signal conditioning required is an isolation amplifier in the digital control. Presently there are 16 instrumentation signals being used and there are four spare inputs that may be used if needed.

The sensor signals are shown in Table 13-II and come from various transducers and sensors located on the engine. Some signals are ac and some are dc and have various voltage ranges. These signals are conditioned to a standard 0-10 volt level in order to be used by the digital control.

The remaining inputs are the alternator signals that provide the power to the digital control and the digital signals that feed digital data to the control. These are listed in Table 13-III.

The QCSEE digital control outputs are of three types: (1) torque motor drive signals, (2) transducer and sensor excitation signals, and (3) digital signals. Table 13-IV lists these.

Digital Control Functional Description

Input Signal Conditioners

The input signal conditioning circuits are of two types: (1) isolation amplifiers and (2) processing amplifiers. The isolation amplifiers isolate the instrumentation output amplifiers from the control. These amplifiers prevent loading problems.

The signal processing amplifiers differ in design depending on the type of input signal. These consist of demodulating circuits, frequency to dc converters, and straight-gain setting amplifiers. These circuits condition all input signals to a standard 0-10 volt level over the signal range of interest. The proper gains and offsets to accomplish this are set in these amplifiers. The outputs of both isolation amplifiers and processing amplifiers are fed into an analog multiplexer.

Analog Multiplexer

The analog multiplexer circuit consists of three 16-channel multiplexer chips making a total of 48 signals which can be multiplexed. Each channel can be addressed separately depending on the signal needed by the digital control at any particular time. The outputs of the three multiplexer chips are connected together and are fed to a sample and hold circuit. The output of this circuit goes to an A/D converter circuit.

Table 13-I. Digital Control Instrumentation Signals.

- (1) Hydraulic Pump Pressure No. 1
- (2) No. 1 Fuel Temperature
- (3) Wf Manifold Pressure
- (4) EGT
- (5) Fuel Flow
- (6) Lube Pressure
- (7) Lube Scavenge Pressure
- (8) Lube Oil Temperature - Cooler In
- (9) Lube Oil Temperature - Cooler Out
- (10) T25 Sensor ΔP
- (11) Fan Discharge Pressure
- (12) P5 Pressure
- (13) Bearing Temperature
- (14) Horizontal Vib
- (15) Vertical Vib
- (16) Core Stator Position
- (17) Spare
- (18) Spare
- (19) Spare
- (20) Spare

Table 13-II. Digital Control Engine Sensor and Transducer Signals.

- (1) Power Lever LVDT (linear variable differential transformer)
- (2) Fuel Metering Valve LVDT
- (3) Fan Pitch LVDT
- (4) Fan Pitch LVDT
- (5) Fan Nozzle LVDT
- (6) N_{1T} (LP Turbine rpm No. 1)
- (7) N_{1T} (LP Turbine rpm No. 2)
- (8) T3 (Compressor Discharge Total Temperature)
- (9) T2 (Fan Inlet Total Temperature)
- (10) Ps3 (Compressor Discharge Stator Pressure)
- (11) P2 (Engine Inlet Total Pressure)
- (12) Ps 11 (Inlet Static Pressure)
- (13) Ps 14 (Fan Discharge Static Pressure)
- (14) P14 (Fan Discharge Total Pressure)

Table 13-III. Alternator and Digital Signals To Digital Control.

- (1) N2 Alternator Winding
- (2) N2 Alternator Winding
- (3) Data (Digital Signal from Aircraft)
- (4) Clock (Digital Signal from Aircraft)

Table 13-IV. Outputs.

- (1) Fuel Metering Valve Torque Motor Current (TMC)
 - (2) Fan Nozzle TMC
 - (3) Fan Pitch TMC
 - (4) Fan Pitch LVDT Excitation
 - (5) Fan Pitch LVDT Excitation
 - (6) Fuel Metering Valve LVDT Excitation
 - (7) Power Lever LVDT Excitation
 - (8) Fan Nozzle LVDT Excitation
 - (9) Core Stator Reset TMC
 - (10) Emergency Shutdown TMC
 - (11) Sync.
 - (12) Clock
 - (13) Reset
 - (14) Data
 - (15) Sync.
 - (16) Reset
 - (17) T2 Excitation
- } Digital Signals - 6 Twisted Pair to Control
Room Interconnect Unit

Analog To Digital (A/D) Converter

The A/D converter is a 12-bit successive approximation type circuit with a conversion time of 24 microseconds. The input to the A/D converter is a 0-10 volt dc signal and is converted to a digital word that corresponds to the particular voltage at the converter input. For 12 bits, there are 4096 possible words. The output of the A/D converter is fed to a serial digital multiplexer and from there to the central processor unit (CPU).

Central Processor Unit (CPU)

The CPU along with the program memory form the digital computer of the digital control. This circuit contains the arithmetic logic unit, the control and timing unit, the scratch pad memory, the accumulator, and other logic circuits necessary to carry out all calculations to generate the engine control signals and other functions. This unit accepts the A/D converter signals and the aircraft digital signals via the serial digital multiplexer. A block diagram of the CPU is seen in Figure 13-5. The output of the CPU is fed to a digital multiplexer whose output transmits data to the aircraft. The CPU output also goes to a digital-to-analog converter.

Digital-to-Analog (D/A) Converter

The D/A converter has a 12-bit digital word as an input and the output is one of 4096 possible voltage levels corresponding to the digital input. The output of the D/A is bipolar and will be in the -5 volt to +5 volt range. The D/A output is fed to the output drive circuits.

Output Drive Circuits

The output drive circuits consist of sample and hold circuits and the output circuits needed to power the valves, torque motors, etc. As the digital control performs the programmed calculations the output of the D/A converter is sampled at the proper time and stored in a sample and hold circuit. This value is held until the next time the program calls for this particular sample and hold circuit to be pulsed and the next value of the calculation to be stored. The output of each sample and hold circuit is fed to a driver amplifier. The outputs of the driver amplifiers are used to actuate the torque motors, and valves, that provide engine control.

Other Circuits

Transducer excitation circuits are also provided in the digital control. A 1.024 MHz clock signal is used to generate a 3011 Hz, 20 v p-p sine wave signal. This signal is fed to two transducer driver amplifiers whose outputs are used to provide the excitation voltage for the LVDT's. The 3011 Hz signal is also used to demodulate the outputs of the LVDT's.

The emergency shutdown and overspeed circuit performs two functions: (1) detects a failure in the low pressure system through speed rate of change and (2) detects a low pressure turbine overspeed. If either of these conditions exist, a fuel valve is closed to shut down the engine. This circuit is self contained and has its own power supply.

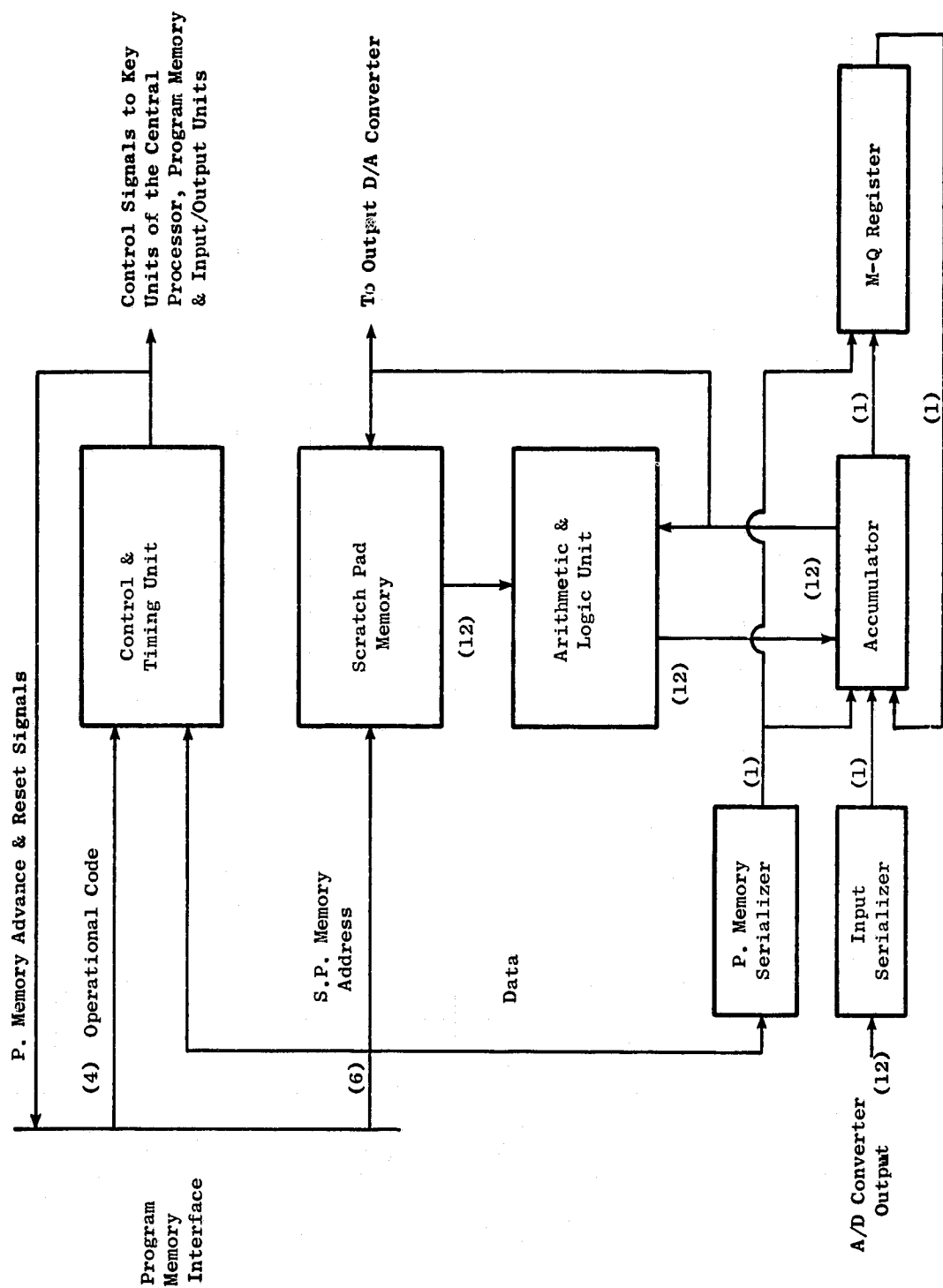


Figure 13-5. Central Processor Unit.

The QCSEE digital control power supply circuit accepts an AC signal from an engine-mounted alternator and converts it to the desired regulated voltages. There are three supplies: (1) a + and -15 volt supply, (2) a + and -11 volt supply, and (3) a +5 volt supply.

Digital Control

Mechanical Design

The QCSEE digital control is a solid-state, air-cooled, engine-mounted unit. The unit is made up of a chassis which provides mounting and which contains electrical connectors for external communications, and a series of individual modules which contain the electrical components and circuits.

The mechanical design or packaging approach for the digital control will use designs similar to existing on-engine electrical controls which have been proven on many military engine applications. To achieve the required reliability level, the control mechanical design must consider the unique turbine engine environment. Detail consideration is given to vibratory loads and cyclic temperature effects with respect to materials, mounting, potting, and interconnections. Structural integrity of the electrical components and interconnections is provided by installing the components in module cans which are filled with a soft potting compound. This approach provides vibration damping. The digital control will be designed to meet 12 g's. Vibration scans will be made on the complete assembly for the experimental engine. For the experimental program, life testing the digital control at its resonant frequency points is not planned.

Heat from the electrical components is dissipated by positive conduction and convection. A solid material path transfers component heat to a manifold which is cooled by fan discharge air. This positive heat transfer concept will result in a controlled environmental temperature. Details on module and chassis construction are presented below.

Electrical analog circuits are mounted to printed circuit boards (PCB's). A typical analog circuit requires two PCB's with copper runs on one side. An anodized aluminum heat sink, which provides the high conductivity heat path to the mounting flange, is bonded to the component side of the PCB. The electrical components are mounted so that they rest on the heat sink and their leads protrude through the plated holes. The board assemblies are wave soldered and then tested for performance. The two board assemblies are mounted in module cans as shown in Figure 13-6. The can is filled with a RTV potting material to a level covering the upper edge of the PCB's. Hookup wires are attached to the exposed pins at the upper edge of the PCB's and a clear RTV is used to fill the module can. The above potted assembly is called a module. Each module is a functionally discrete portion of the control. It is tested as an individual assembly and is directly interchangeable with a like module should replacement become necessary.

Digital circuits, which use dual in-line package (DIP) components, are mounted on wire-wrapped PCB's or multilayer PCB's. Wire-wrapped PCB's have terminal inserts. Interconnections are made by wire wrapping solid insulated wire as required for a point-to-point wiring arrangement on the inserts. These

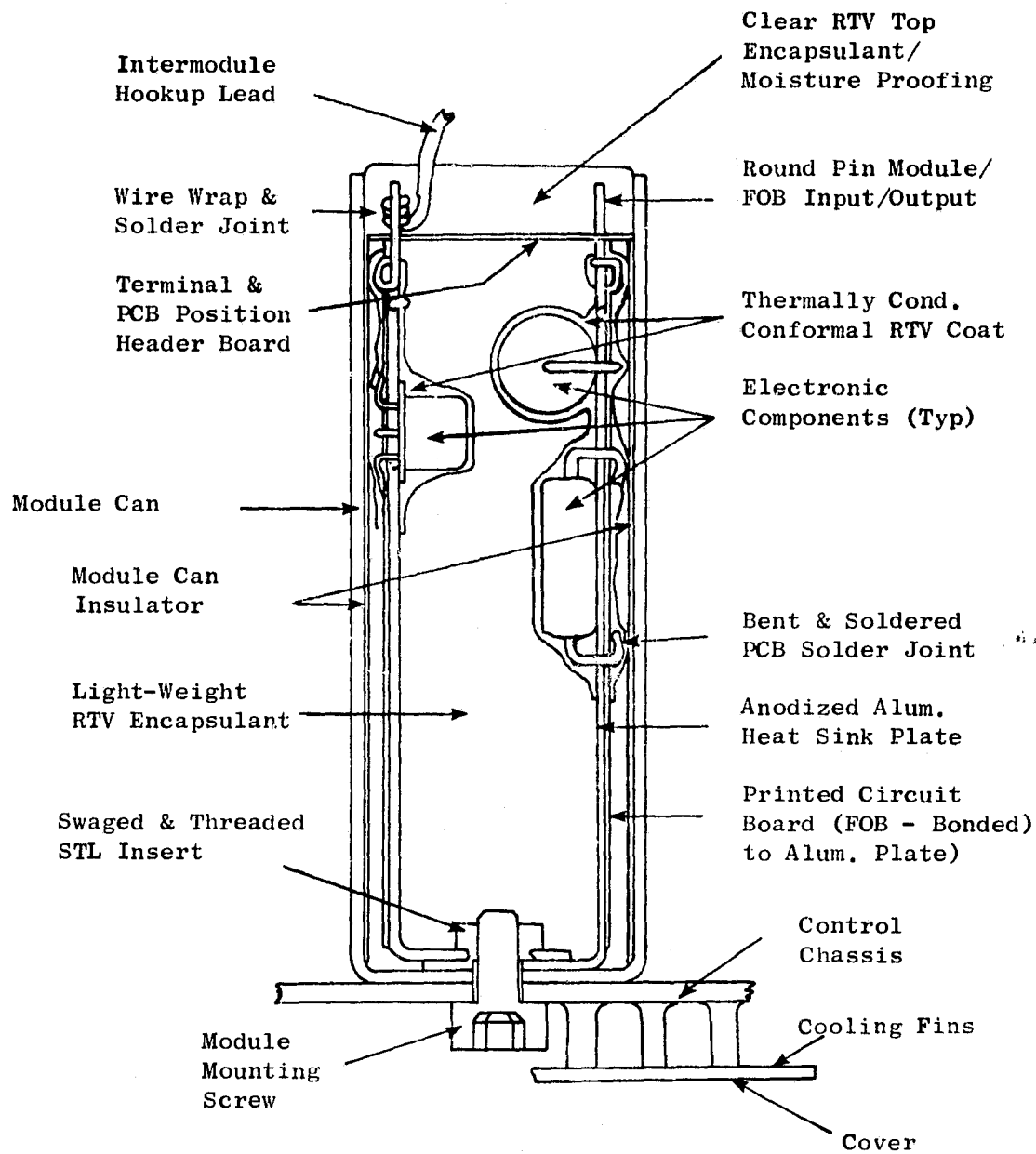


Figure 13-6. Typical Control Module Cross Section.

wire wraps and the DIP terminal interfaces are soldered to complete the electrical connections. The DIP's for the Central Processor will be mounted on multilayer PCB's. Multilayer PCB's are similar to one-sided PCB's except they have several internal circuit layers. The heat sink approach could be the same also, or, the outer surfaces may have a relatively thick layer of copper to improve conductivity to the mounting bracket. The DIP's are wave soldered to the plated-through-holes. The remainder of the module assembly, with either wire-wrapped or multilayer PCB's, is the same as for analog circuits (see Figure 13-6).

The chassis, which houses and engine mounts the modules, connectors, and pressure transducers, is a dip-brazed aluminum box (see Figure 13-7). Stiffening ribs are used both inside and outside the chassis to assure that the various loads can be safely carried to the mounting brackets. The connector panel and transducer mounting surfaces are also reinforced to resist the loads imposed by the electrical cables and the pressure lines. Surfaces subjected to handling are anodized while mating surfaces for connectors, modules, transducers, and grounding lugs are Ir-dited to maintain minimum electrical resistance and to provide improved EMI capability. The bottom of the chassis, is finned on the outside (see Figures 13-6 and 13-7). A cover is placed over the fins to provide channels through which fan discharge cooling air is directed. Since the modules are mounted to the inside surface, a minimum temperature drop is required to transfer the heat.

13.4 FUEL DELIVERY SYSTEM

The QCSSE fuel delivery system is primarily based on F101 engine main fuel system components including the hydromechanical control and temperature sensor described in Section 13.3.5. The fuel delivery system includes the following elements:

- Fuel Control (metering section)
- Main Fuel Pump
- Fuel Filter
- Fuel-Oil Heat Exchanger (2)

These elements are interconnected as shown in the schematic of Figure 13-8.

The fuel pump is a standard F101 main fuel pump unmodified. It is a balanced vane design of fixed displacement and contains an integral centrifugal booster stage to charge the vane intakes. Sizing of the fuel delivery system is indicated by the fuel pump characteristics listed in Table 13-V. A cross section view of the pump is shown on Figure 13-2 (zone F-7).

The lube oil heat exchangers are two standard CF6 engine fuel-oil heat exchangers connected in series.

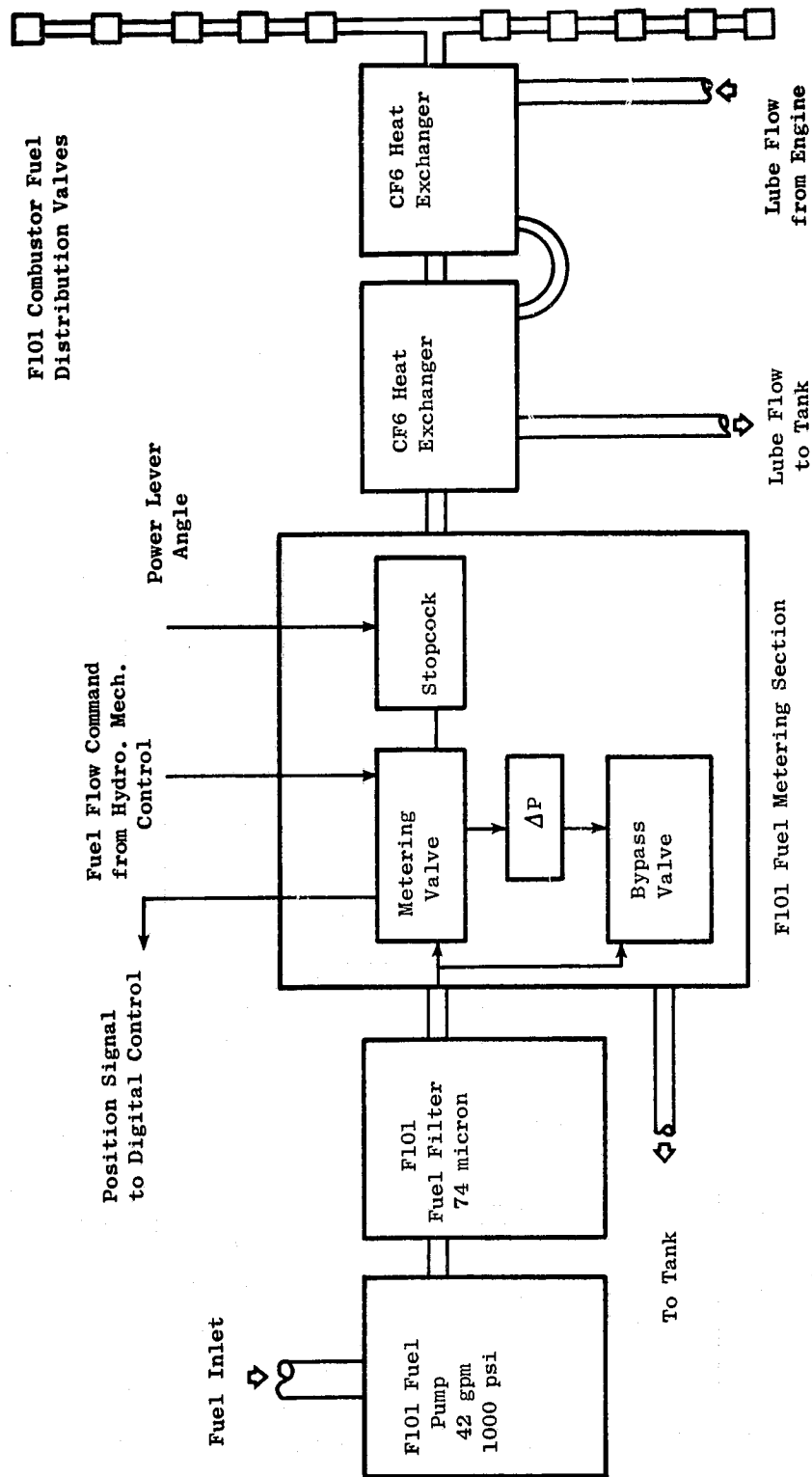


Figure 13-8. Fuel Delivery System.

Table 13-V. Pump Characteristics (F101 Pump).

	Main Fuel Pump	
	Boost Element	Vane Element
Rated Speed, rpm	6690	6690
Maximum S.S. Speed, rpm	6891	6891
Rated Flow (Delivered Flow @ Service Limit @ Rated Speed)	$2.7 \times 10^{-3} \text{ m}^3/\text{sec}$ (42.8 gpm) @ 107.2° C (225° F)	$2.7 \times 10^{-3} \text{ m}^3/\text{sec}$ (42.8 gpm) @ 107.2° C (225° F)
Rated ΔP @ Rated Flow	$2.76 \times 10^5 \text{ N/m}^2$ (40 psi) min.	$\approx 6.65 \times 10^6 \text{ N/m}^2$ (≈ 964 psi)
Power Loss @ Rated Speed	$1.49 \times 10^3 \text{ w}$ (2 hp) max	Overall Efficiency = 0.72 @ Design Point

13.5 VARIABLE GEOMETRY ACTUATION SYSTEMS

13.5.1 Hydraulic Supply System

Purpose

The hydraulic supply system provides hydraulic motive power to the fan duct nozzle (A18) actuators and fan blade variable pitch mechanism for UTW, and thrust reverser actuators for OTW. The system consists of a hydraulic pump, boost pump element, filter, and magnetic chip detector. These components are sized for the UTW application which is the most demanding in terms of flow and pressure. The same components will be used for the OTW engine.

System Description

The system is shown in Figure 13-9. A pressure-compensated hydraulic piston pump is driven by the accessory gearbox and provides varying flow output at constant pressure to servovalves which are part of the fan duct nozzle, variable-pitch, or thrust reverser systems. Pump output flow is determined by the demand from the servovalves, varying from zero at holding condition to maximum during the engine thrust reversal transient. The supply system is sized to provide peak transient flow for simultaneous operation of A18 and variable pitch at engine idle speed (65% of rated). Although pump maximum flow capability is proportional to engine speed, the output pressure is constant and virtually independent of speed or flow.

The hydraulic system receives and uses the same oil as the engine lube system. Once the hydraulic system is filled, however, it functions very nearly as an independent closed system. When oil leaves the pump to the servovalves at high pressure, oil is at the same time returning at low pressure from the servovalves. The servovalve incoming flow passes through a 1×10^{-5} m (10 micron) filter which provides servovalve protection from hydraulic pump and engine lube system contaminants.

As the A18 actuators slew from head-end to rod-end position, there is differential displaced volume equal to the volume represented by the actuator piston rods. For a one second slew, this amounts to somewhat less than 1.89×10^{-4} m³/sec (3 gpm) which must be made up from the engine lube system oil. Also, it is necessary to provide approximately 1.89×10^{-4} m³/sec (3 gpm) to the pump during steady-state holding for pump cooling. Both of these functions, makeup and pump cooling, are provided by using an element in the engine lube pump as a makeup and boost pump to the hydraulic pump. A relief valve across the lube pump element acts as a pressure regulator so that the hydraulic pump inlet pressure is sufficiently high to avoid cavitation in the pump piston cavities. Hydraulic pump cooling is provided by virtue of mixing hydraulic oil with lube oil which passes through the engine oil coolers. Incoming hydraulic system makeup and cooling flow has been filtered to the 46 micron level in the engine lube and scavenge oil filters, which minimizes the capacity required of the fine-micron-rated hydraulic filter. A magnetic chip detector is provided in the line returning hydraulic makeup and cooling flow to the engine lube system so that any ferrous metal contaminants generated in the hydraulic system can be identified.

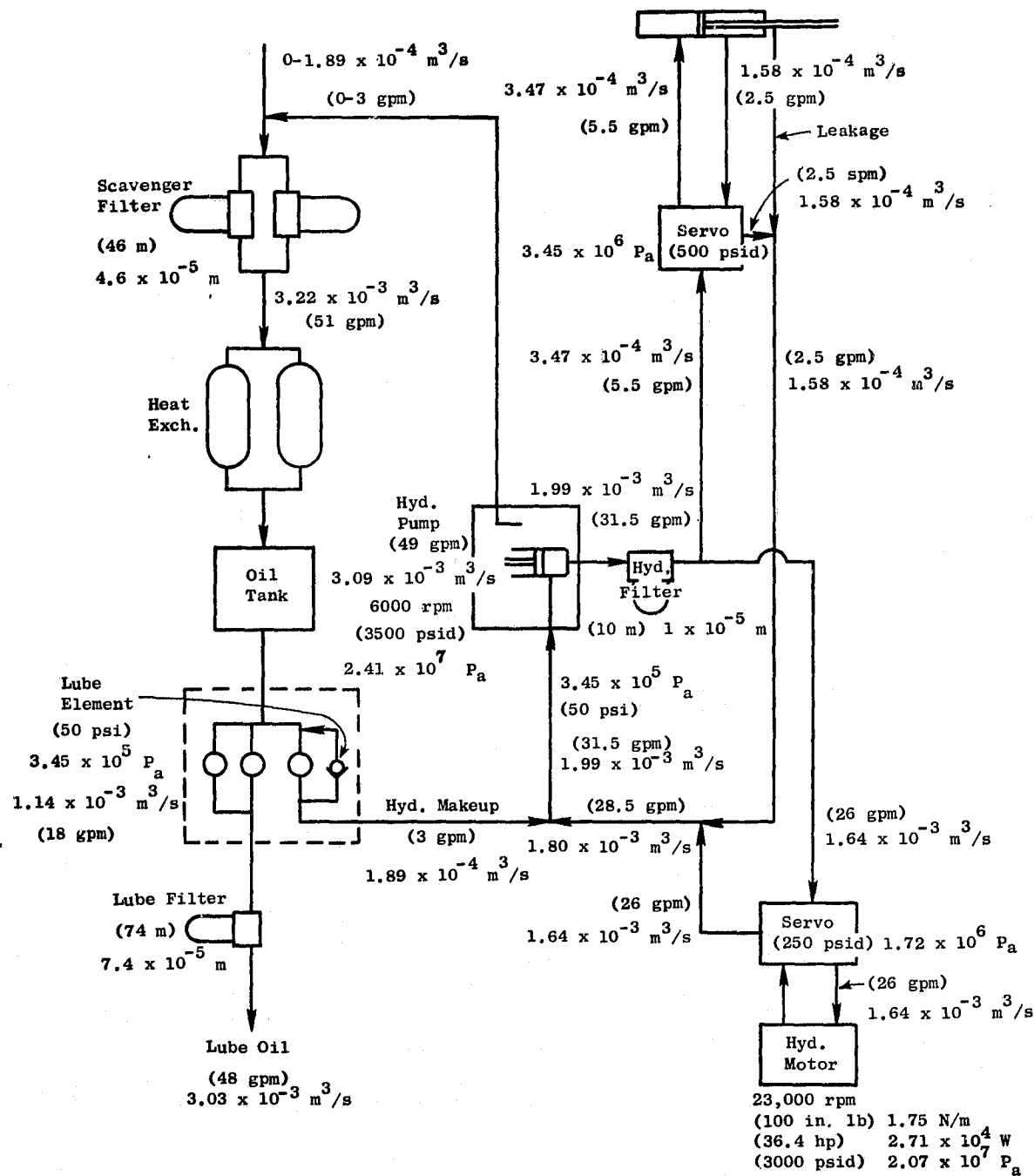


Figure 13-9. Hydraulic Supply System Schematic.

Hydraulic Pump

The pump slated for use on the demonstrator engines is an ABEX Model AP12V pressure-compensated piston pump. This pump is qualified and in production for the F-111 fighter aircraft and CH53 helicopter applications. The pump, shown in Figure 13-10, is compact in size and weighs 7.7 kg (17 pounds).

The pump contains a revolving cylinder barrel which contains nine pistons. By means of a hold-down plate and hydraulically balanced shoes, the pistons are supported on an inclined cam plate which causes them to reciprocate as the barrel revolves. The angle of the cam plate is varied by moving the trunnioned hanger on which it is mounted, thereby changing the displacement of the pump. The hanger, in turn, is controlled by the pressure compensator. Oil passes through the main inlet and then through porting in the end of the cylinder barrel to cylinders from which the pistons are being withdrawn. As the cylinder barrel revolves, these pistons are forced into their bores and discharge high pressure oil through porting in the end of the barrel to the outlet port. The cylinder barrel, supported by a radial bearing, is driven by an internal shaft that passes through the trunnioned hanger.

The pressure compensator regulates the volume delivered in accordance with the demand of the system, thereby maintaining a predetermined pressure. System pressure is directed to a compensating valve with a spool which is held in the closed position by an adjustable spring load. When system pressure exceeds the spring load, it moves the spool to admit system oil into a stroking cylinder. The stroking piston then moves the hanger to a lesser angle, which reduces the volume pumped sufficiently to maintain the desired pressure. When system pressure is less than the compensator spring load, the spring moves the spool to vent oil in the stroking cylinder to the pump case. The stroking piston then retracts and an inherent force assisted by the rate piston spring moves the hanger to a greater angle, increasing the volume pumped.

DESIGN FEATURES

Hydraulic Pump

Speed		5676 rpm (100%)
Output Flow	$3.09 \times 10^{-3} \text{ m}^3/\text{sec}$ $1.99 \times 10^{-3} \text{ m}^3/\text{sec}$	(49 gpm) at 100% speed (31.5 gpm) at 65% speed
Pressure Rise	$2.41 \times 10^7 \text{ N/m}^2$	(3500 psid)
Overall Efficiency		90%
Rated Shaft HP (at $1.99 \times 10^{-3} \text{ m}^3/\text{sec}$ demand)	$5.44 \times 10^4 \text{ w}$	(73 hp)
Inlet Oil Temperature	-40° to 123°C	(-40° to 250° F) at 100% speed

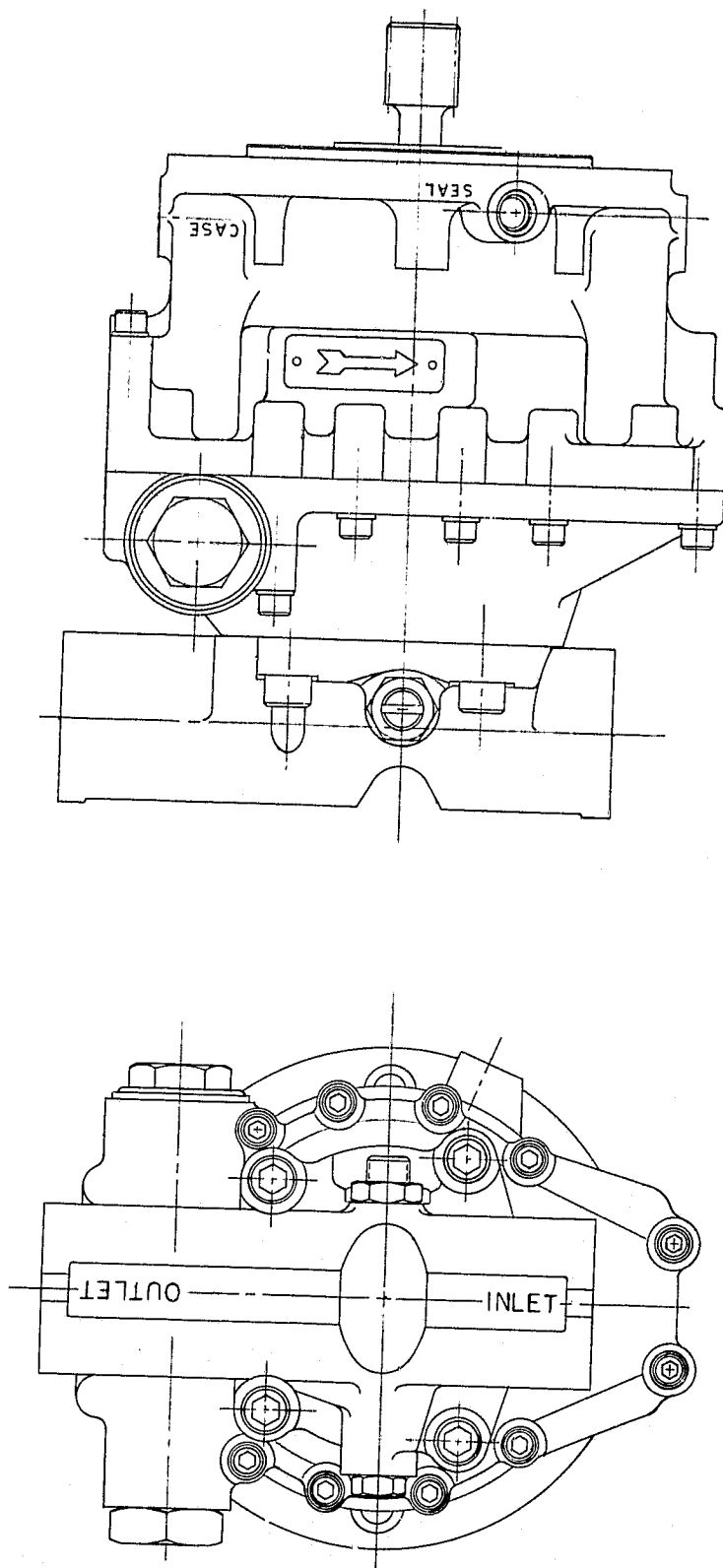


Figure 13-10. Hydraulic Pump.

Makeup and Cooling Flow	$1.89 \times 10^{-4} \text{ m}^3/\text{sec}$ at $3.45 \times 10^5 \text{ N/m}^2$	(3 gpm at 50 psid)
Heat Rejection	$4.13 \times 10^3 \text{ J/sec}$ $5.71 \times 10^3 \text{ J/sec}$	(235 Btu/min) steady-state (325 Btu/min) transient

Hydraulic Filter

Rating	$1 \times 10^{-5} \text{ m}$ $2.5 \times 10^{-5} \text{ m}$	(10 μ) nominal (25 μ) absolute
Capacity	$2.5 \times 10^{-3} \text{ kg}$	(2.5 gm) of contaminant
Pressure drop at	$1.99 \times 10^{-3} \text{ m}^3/\text{sec}$ (31.5 gpm)	$1.72 \times 10^5 \text{ N/m}^2$ (25 psid) maximum

13.5.2 QCSEE Fan Nozzle (A18) Actuation

Description, UTW

As shown in Figure 13-11 four interlocking flaps will be driven in a closed-loop system to provide a fully modulating exhaust nozzle. The interlocking flaps require positional synchronization and a linear stroke of 0.128 m (5.05 inches). Maximum loads are $1.10 \times 10^4 \text{ N}$ (2462 lb) in tension and $0.51 \times 10^4 \text{ N}$ (1150 lb) in compression at each of eight load points.

Several methods of A18 actuation for the UTW application were considered.

<u>METHOD</u>	<u>REMARKS</u>
(1) Hydraulic motor/ballscrews	Selected for study
(2) Reciprocating fuel motor/ballscrews	Rejected - High flow demand
(3) Hydraulic pump/synchronized actuators	Selected for study (Final system)
(4) Pneumatic motor/ballscrews	Rejected - High temperature modulating air motor
(5) Electric motor/ballscrews	Rejected - Weight and electrical power.
(6) Mechanical drive/ballscrews	Selected for study.

Results of a study of the three preferred systems showed no significant difference in cost and weight either in development or during production. The hydraulic pump/synchronized actuators was selected due to its low risk as a fully modulating, rapid responding system.

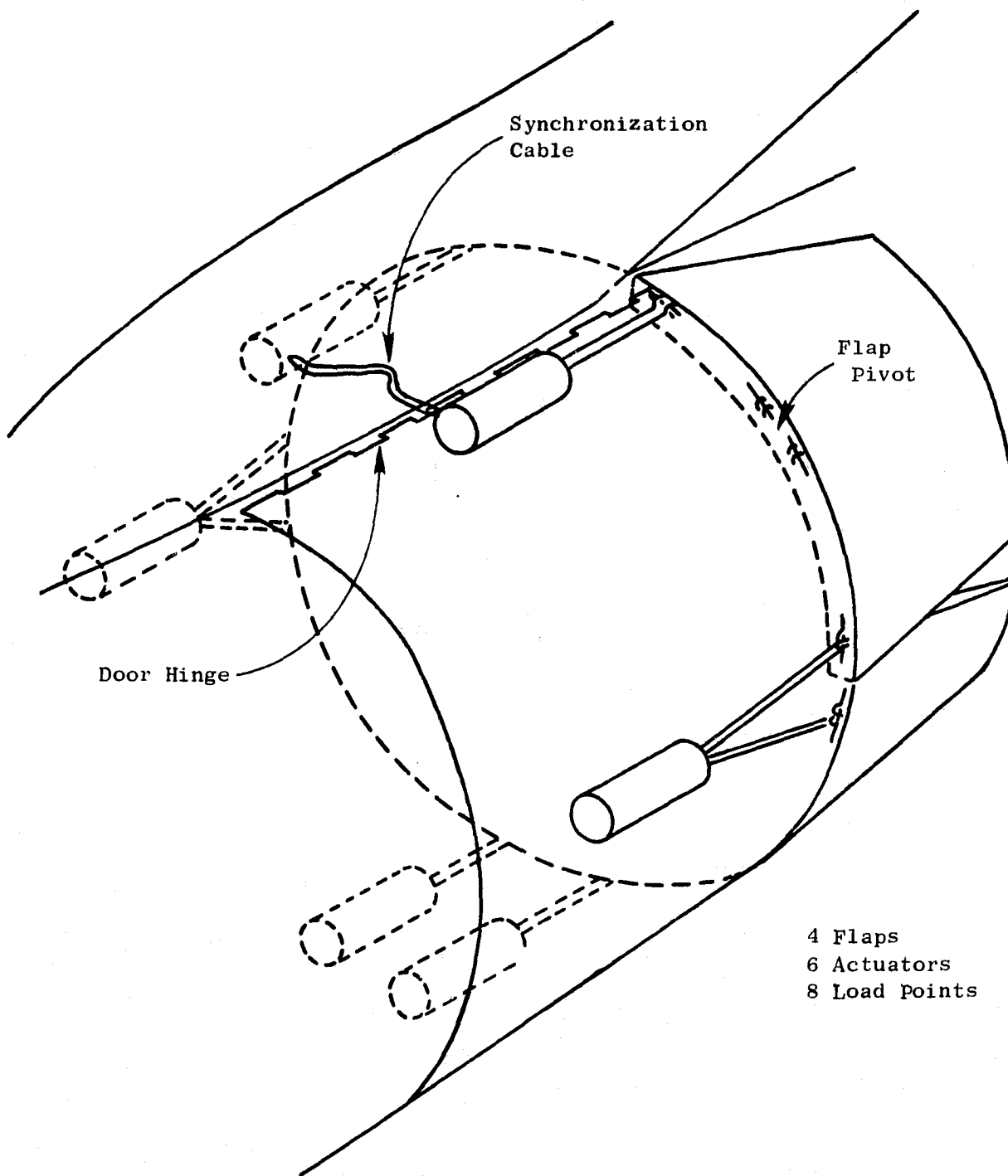


Figure 13-11. UTW Variable Nozzle.

Six actuators, three in each rear-cowling half, will be arranged circumferentially to hydraulically power the flaps through the eight load points. The center-mounted actuators in each half will each carry the load of two load points and thus be slightly larger in diameter than the remaining four. Synchronization in each cowl will be accomplished through the common center-mounted actuator and the structural rigidity of the flap-nozzle-flanges. Cross-synchronization between right and left halves will be by rotary-shaft coupling between two opposite actuators.

Hydraulic power, approximately $2.21 \times 10^{-4} \text{ m}^3/\text{sec}$ (3.5 gpm) at $2.41 \times 10^7 \text{ N/m}^2$ (3500 psi), will be supplied from the hydraulic pump common to the variable-pitch fan mechanism. Flow control will be by a conventional electrohydraulic servovalve.

Description, OTW

Due to configuration differences, the OTW variable exhaust nozzle/thrust reverser will require a different actuating mechanism than for the UTW. It will actually require two different actuation means, one for varying the side panels for a fully modulating exhaust nozzle system, and one for a two-position thrust reverser blocker door. At this preliminary stage, it appears that a rotary cable system and power-hinge powered by a hydraulic motor will be used for the fully modulating exhaust nozzle panels. Each panel will require $3.39 \times 10^8 \text{ N-m}$ (30,000 lb-in.) torque and rotate approximately 0.314 rad (18°). For thrust reversing, two 0.737 m (29 in.) stroke hydraulic actuators each working against a load of $3.47 \times 10^4 \text{ N}$ (7800 lb) are being considered. For the experimental engine, only the thrust reverser system is planned since there is no need to vary nozzle area for static testing.

13.5.3 Core Stator Actuation and Feedback

The core stator actuation control pressure output from the hydromechanical control is connected to a pair of linear hydraulic actuator pistons. A cross section view of the actuators is shown on Figure 13-2 (zone F-3).

The actuators will be F101 components modified to increase the linear stroke by $5.08 \times 10^{-3} \text{ m}$ (0.2 in.). The modification will be accomplished by shortening the piston head axial dimension to allow increased retraction when bottomed in the cylinder.

An F101-type core stator feedback cable provides the hydromechanical control with a stator position signal used for closed-loop stator scheduling. The cable is of the linear stroke type consisting of a fixed-length cable and a fixed-length conduit. The conduit provides a stroke path and protection for the cable. Rigging is obtained by adjusting the position of one end of the conduit.

It will be necessary to procure a cable of greater length, but of identical construction, for the QCSEE installation. Routing distance from the core stator feedback crank to the control location in the pylon is longer for the QCSEE installation. The F101 cable presently has sufficient stroke capability to accommodate the $5.08 \times 10^{-3} \text{ m}$ (0.2 in.) stroke increase for QCSEE.

13.6 SENSORS

The engine sensors are the devices which change the parameter to be measured into a form that can be used as an input signal to the engine digital or hydromechanical control or as an input signal to an indicator gage. The sensors include the following:

Low Pressure Turbine Speed Sensor

Core Engine Speed Sensor (AC Generator)

Fan Inlet Temperature Sensor

Static Pressure and Pressure Ratio Sensors

Position Feedback Sensors

13.6.1 Low Pressure Turbine (LPT) Speed Sensor

Purpose

The LPT shaft speed sensor produces two electrical signals that represent the rotational speed of the low pressure turbine shaft. One signal will be used for engine fan speed governing. The other signal will be used to limit the rate of speed change and maximum speed in the event of a loss of fan load, overspeed, or control failure.

Description

The speed sensor is nearly identical to that used on the F101 engine. As shown in Figure 13-12 the sensor consists of a curved metal tube containing lead wires, with a magnetic pickup at one end and an electrical connector at the other. The sensor is mounted on the fan frame outer surface. The pickup head and supporting tube extend through a fan frame strut to a point aft of the LPT shaft front bearing. The pickup is fixed in close proximity to a flanged ferromagnetic disk having equally spaced slots and teeth machined into the flange.

Operation

The magnetic pickup consists basically of a permanent magnet behind a soft iron pole piece around which a coil has been wound. The magnetic flux linking the coil is high when a ferrous metal object (tooth) is placed in front of the pole piece and is low with no ferrous metal in front of the pole piece (slot). The generated voltage is proportional to the rate of change of flux in the pole piece, and the frequency of the ac signal is proportional to the speed at which the ferrous material (teeth) passes in front of the pole piece. The wave form of the electrical signal is nearly sinusoidal depending upon the relative width of slots and teeth on the rotating disk and also the width of the pole piece relative to the slots and teeth. Signal output from the speed sensor is routed

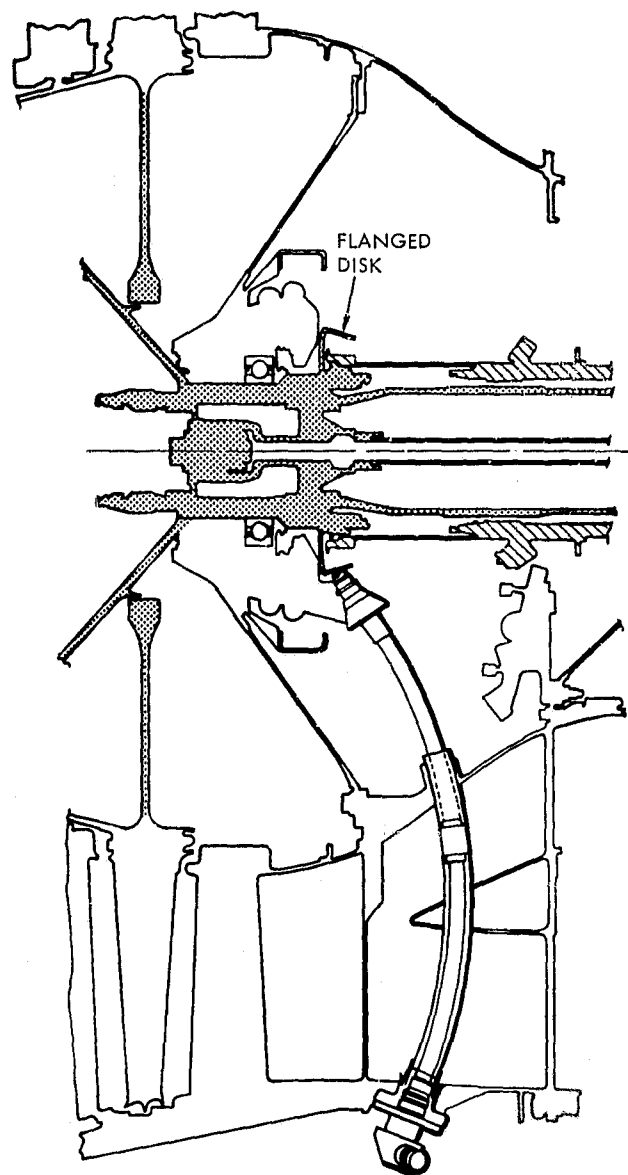


**Figure 13-12. Low Pressure Turbine (LPT)
Shaft Speed Sensor.**

to a conditioner device in the digital control which produces a uniform voltage amplitude and wave form at varying speed so that ultimately the conditioned signal is interpreted in terms of frequency rather than voltage amplitude.

Design Features

Speed range	0 to 9070 rpm (115%) UTW 0 to 8993 rpm (115%) OTW
Shaft speed acceleration	± 1200 rpm/sec
Environment temperature	-40 to 176.7° C (-40 to 350° F)
Acceleration loads	3.048 m/sec ² (10 G's)
Thermal shock	-40 to 93.3° C (-40 to 200° F) in 24 DS (4 minutes)
Vibration	5.08 x 10 ⁻⁴ m (0.020 inch) DA maximum 30.48 m/sec ² (100 G's) maximum
Signal frequency	0.2 Hz/rpm
Signal amplitude	0.2 volts peak-to-peak minimum at 10% LPT shaft speed
Air gap	3.56 x 10 ⁻³ to 5.08 x 10 ⁻³ m (0.140 to 0.200 inches)

13.6.2 Core Engine Speed Sensor

Purpose

An alternating current generator driven by the engine gearbox provides electrical power to the engine digital control. In addition, a signal source is generated which represents core engine speed and is used for engine control and indicating purposes.

Description

The generator is a 12-pole, high-speed, four-winding, alternating current generator. The generator, shown in Figure 13-13, is identical to that used on the F101 engine. The generator rotor is mounted to a drive shaft which is supported by bearings in the accessory gearbox. Each winding on the stator functions as an independent power source with independent leads and pins in a single connector.

A shaft seal in the gearbox permits the rotor to run in an essentially dry environment, reducing heat generation and avoiding the possibility of metallic particle pickup on the Alnico-9 magnetic rotor. The rotor is shielded for retention of the magnetic segments and to provide a smooth, low disk friction surface.

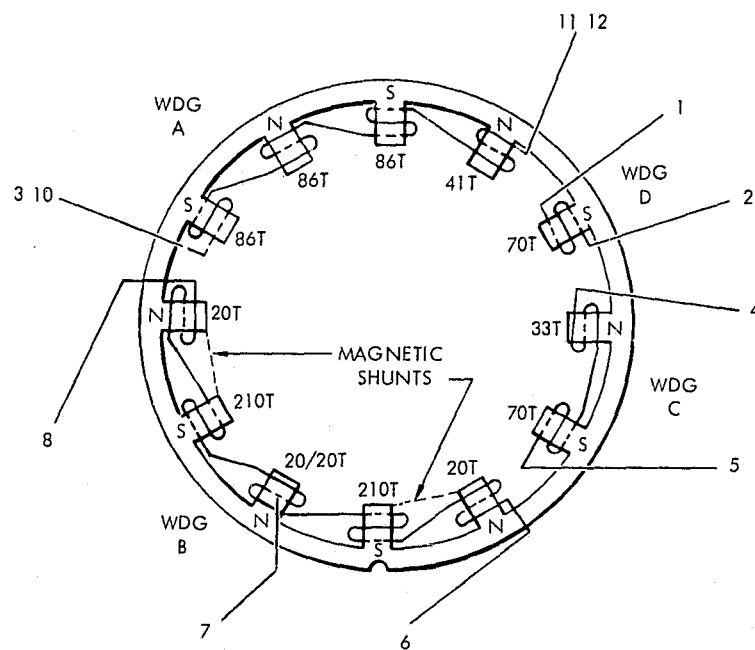
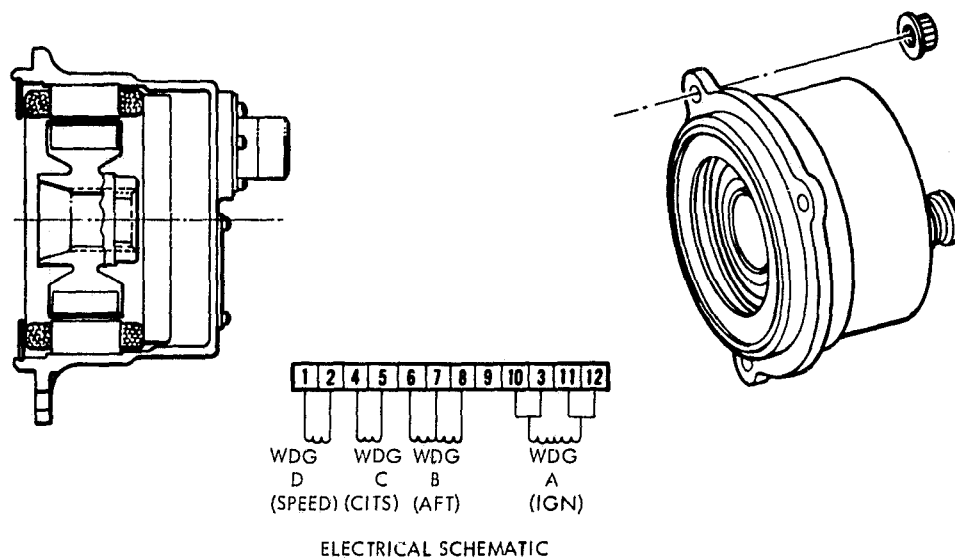


Figure 13-13. Alternating Current Generator.

Operation

The frequency of the sinusoidal wave form signal is used as an indication of core engine speed.

Design Features

Configuration 4-winding, 6-pole pair assembly

Rotor Speed 24,903 rpm (100%)
28,555 rpm transient

Frequency 6 cycles/rotor revolution
(2490 Hz at 100% speed)

Output:	<u>% Speed</u>	<u>Volts (rms)</u>	<u>Amps</u>
	10	5.0 min.	0.002
	100	82.5 max.	0
	100	50.0 min.	0.020
	115	95.0 max.	0
	115	0	6.5 max.

Rotor Dynamic Balance 7.06×10^{-6} Nm (0.001 ounce inch)

Air Gap 7.62×10^{-4} m (0.030 in.)

13.6.3 Fan Inlet Temperature (T2) Sensor

Purpose

The T2 sensor provides the engine control with an electrical signal representing the total temperature of the air entering the fan. This signal will be electrically compared with the T2 schedule for engine control purposes.

Description

The fan inlet temperature sensor shown in Figure 13-14 is identical to that used on the F101 engine. The sensor is a wire-wound resistance-type device mounted on and protruding through the front frame into the fan inlet air stream. The sensor consists of a sensing element and housing. The sensing element contains a platinum wire wound on a cylindrical platinum mandrel. The wires are insulated from each other and the mandrel by a ceramic insulant. The element is hermetically sealed in a capped platinum sheath and the connections are potted. The housing is a slotted airfoil which controls airflow so that the sensed temperature is that of the free stream. A series of small holes bleeds off the boundary layer and turns the stream, but not heavier particles, inward toward the sensing element. The boundary layer air is exhausted out the top. Some of the diverted air stream flows through the first slot and carries the lighter liquid contaminants. The remaining portion of the diverted flow goes through the second slot and around the sensing element.

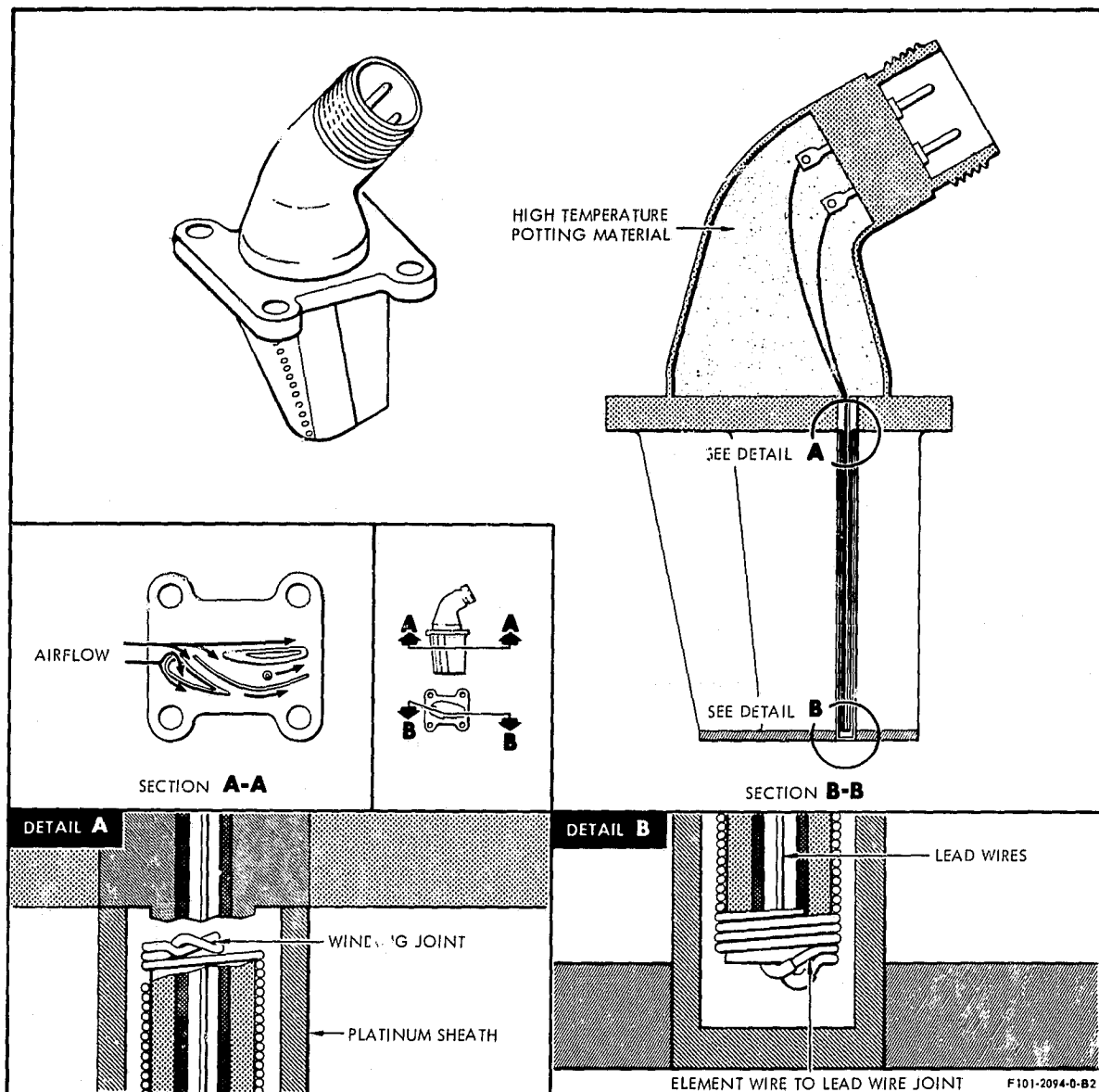


Figure 13-14. Fan Inlet Temperature (T_2) Sensor.

Operation

The T2 sensor operates on the principle that a temperature increase causes a corresponding increase in electrical resistance of the wound platinum wire. The sensing element has a large surface area in relation to its mass making it particularly suited to measuring a large representative air sample and providing rapid response to small changes in temperature.

Design Features

Temperature Range	-40 to 71.1° C	(-40 to 160° F)
Resistance Range		168 to 256 ohms
Excitation		12.5 ma dc (constant)
Accuracy	$\pm 1.11^{\circ}$ C	($\pm 2^{\circ}$ F) max.
Recovery Error		Less than 0.5% at Mach 0.4
Response Time (to 63.2% of final value)		Less than 5 seconds at 48.8 kg/sec/m ² at 10 pps/ft ² airflow

13.6.4 Absolute and Differential Pressure Sensors

Purpose

Fan inlet and discharge static pressures (PS11 and PS14) and total pressures (P2 and P14) are sensed with static pressure taps and total pressure probes installed in front of and behind the fan. A static pressure tap is installed downstream of the engine compressor to sense compressor discharge pressure (PS3). These pressure signals are routed to the engine digital control which houses the static pressure and total-minus-static pressure sensors. Electrical signals are generated in these sensors and used to schedule the engine control functions.

Description

The sensors are thin-film strain gage bridge transducers identical to those used in the F101 engine. A cross section of the sensor is shown in Figure 13-15. The sensors receive their electrical excitation from the control and change the ΔP and static pressure signals to electrical signals.

In the thin-film resistance strain gage bridge transducer [below 6.89×10^5 N/m² (100 psia)], the strain member is a cantilever beam which provides a metal substrate on which a ceramic film is deposited for electrical insulation. For higher pressures, a diaphragm is used instead of the cantilever beam. The four strain gage resistors are then vacuum deposited on the insulator. The resistors are electrically connected into a bridge circuit using film-deposited interconnecting leads.

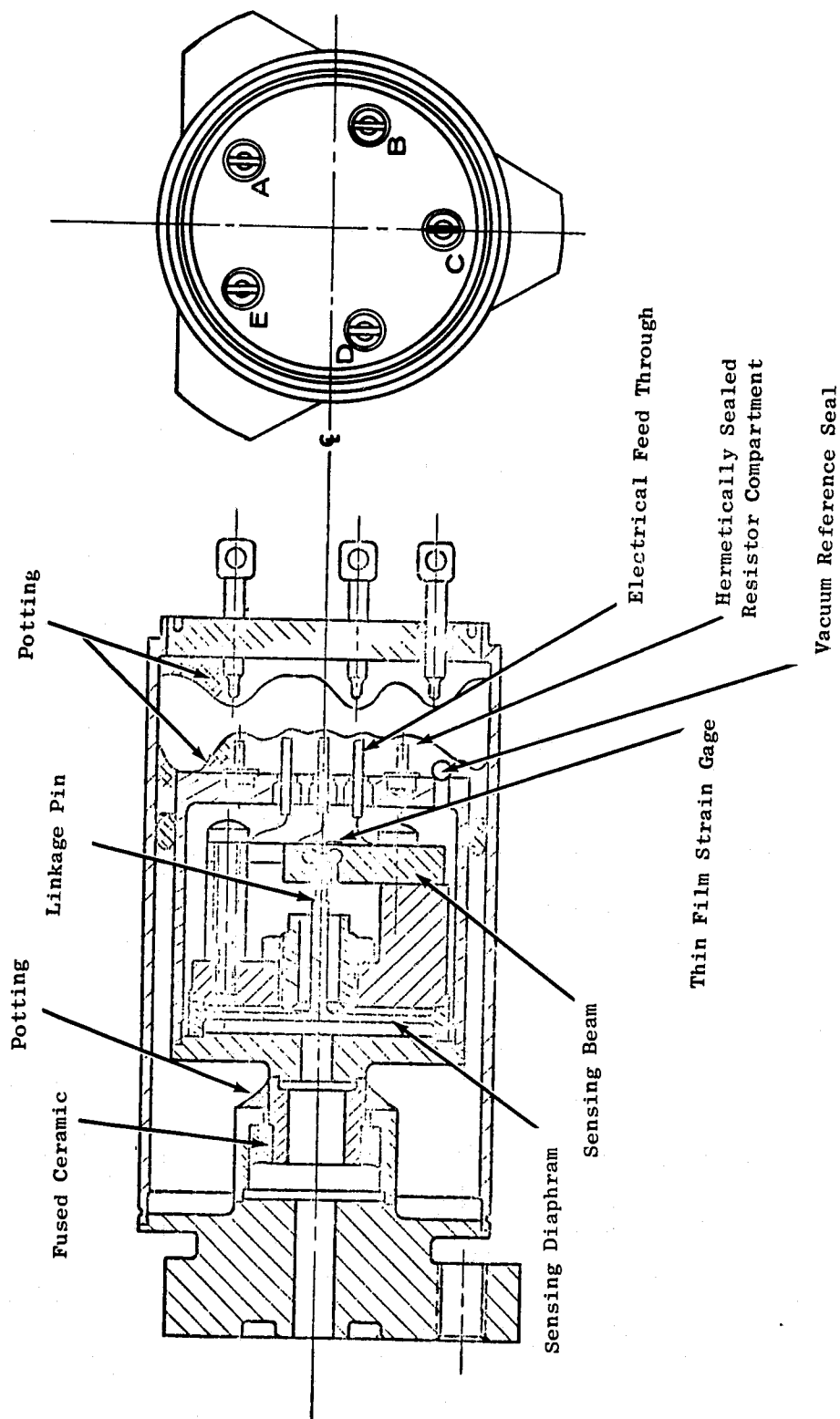


Figure 13-15. Pressure Sensor.

Overall accuracy such as $\pm 1\%$ of point or $\pm 1.72 \times 10^3 \text{ N/m}^2$ ($\pm 0.25 \text{ psia}$), which-
ever is greater, has been demonstrated for pressures to $2.07 \times 10^6 \text{ N/m}^2$ (300 psia)
over the temperature range of -53.9° to 121.1° C (-65° to 250° F). Response is
dependent on pressure level. For example, a $0-3.45 \times 10^5 \text{ N/m}^2$ (0-50 psia) trans-
ducer has an approximate natural frequency of 5,000 Hz while a $0-3.45 \times 10^6 \text{ N/m}^2$
(0-500 psia) transducer has an approximate natural frequency of 18,000 Hz.

For the F101 engine, these sensors (fan pressure ratio) provide a dc signal
within $\pm 1\%$ of $\Delta P/P_s$ point accuracy in ambient temperatures of -53.9° to 121.1° C
(-65° F to 250° F). The sensor is encased and potted in a stainless steel housing.

Operation

The sensors operate on the principle of a mechanical distortion producing
a change in electrical resistance across a strain gage and hence a change in
electrical current output from a bridge circuit. Referring to Figure 13-15,
pressure is ported to the sensing diaphragm which deflects and drives a
linkage pin against the sensing beam. The beam is shaped such that it bends
and causes "stretch" on the surface to which the strain gages are attached.

Design Features

Temperature:	-40 to 121.1° C	(-40 to 250° F)
Acceleration Loads:	3.048 m/sec^2	(10 G's)
Vibration:	12.19 m/sec^2	(40 G's) maximum

Pressures:

Fan Inlet Static (PS11)	6.89×10^3 to $1.38 \times 10^5 \text{ N/m}^2$	(1 to 20 psia)
Fan Inlet Total (P2)	6.89×10^3 to $1.31 \times 10^5 \text{ N/m}^2$	(1 to 19 psia)
Fan Discharge Static (PS14)	6.89×10^3 to $1.73 \times 10^5 \text{ N/m}^2$	(1 to 25 psia)
Fan Discharge Total (P14)	6.89×10^3 to $1.73 \times 10^5 \text{ N/m}^2$	(1 to 25 psia)
Compressor Discharge Static (PS3)	6.89×10^3 $1.90 \times 10^6 \text{ N/m}^2$	(1 to 275 psia)
Maximum Overload	20% of rated range through $3.45 \times 10^6 \text{ N/m}^2$ (500 psi)	
Nominal Bridge Resistance	350 ohms	
Excitation	10 VDC	

Full-Scale Output (open circuit)	3 mv/v nominal
Resolution	Infinitesimal
Nonlinearity	Less than $\pm 0.3\%$ FS (terminal)
Hysteresis	Less than $\pm 0.1\%$ FS
Zero Balance	Less than $\pm 2\%$ FS
Thermal Sensitive Shift	Less than $0.0028/^{\circ}\text{C}$ ($0.005/^{\circ}\text{F}$)
Thermal Zero Shift	Less than $0.0028/^{\circ}\text{C}$ ($0.005/^{\circ}\text{F}$)

13.6.5 Position Feedback Sensors

Purpose

Rotary and linear variable differential transformer transducers will be used to sense the position of various engine parts and components. These are:

	<u>Type</u>
Duct Nozzle A ₁₈ Actuators Position	LVDT
Throttle Lever Position	RVDT
Fuel Metering Valve Position	RVDT
Fan Blade Pitch Angle	LVDT

Description and Operation

The variable differential transformer translates the displacement of a magnetic core into an ac output voltage which is proportional to the displacement. Several different designs are used to obtain specific performance characteristics, but basically, these transducers are constructed of one primary coil and two secondary coils as shown in Figures 13-16.

An alternating current is fed through the primary winding. The magnetic core couples the primary and secondary coils by conducting the alternating field inside the coils. When the core is in center position, an equal portion of the core extends into each of the secondary coils and affects an equal coupling between the primary and each secondary coil. An alternating voltage of equal magnitude is induced in the secondary coils. With the secondary coils connected in series opposed as shown, the output is close to zero. As the probe is moved to either side, the coupling between the primary and one secondary coil is increased, while the coupling between the primary and the other secondary coil is decreased. A larger voltage is then induced in one secondary coil than in the other, and the output voltage will be the difference between the two voltages.

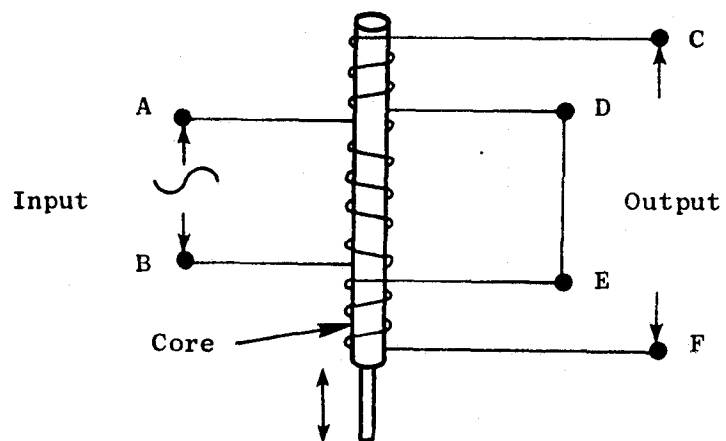


Figure 13-16. Variable Differential Transformer Schematic.

Design Features

Voltage	Constant 7.07 rms nom
Frequency	3000 ± 10 Hz
Wave Form	Sinusoidal
Harmonic Distortion	Less than 3%

Duct Nozzle A18 Actuator

The sensed position of the fan duct nozzle actuator (A18) which is proportional to fan duct nozzle area will be provided by the A18 actuator position transducer.

Frequency	3000 Hz nom.
Wave Form	Sinusoidal
Amplitude	Linearly proportional to the actuator stroke: 0 to 0.127 m (0 to 5 in.)
Null Voltage Position	6.35×10^{-2} m (2.5 in.)
Gain	0.08 VRMS/IN/VRMS Excitation ± 0.008 VRMS/IN/VRMS Excitation
Phase Shift from Excitation	0 ± 0.087 rad ($0^\circ \pm 5^\circ$) for in phase signal. 3.14 ± 0.087 rad ($180^\circ \pm 5^\circ$) for out of phase signal
Polarity	Out of phase with excitation at the retract position ref: 0 meters

Power Lever Position

The rotation of the throttle shaft input to the fuel control will be supplied by the throttle position transducer.

Frequency	3000 Hz nominal
Wave Form	Sinusoidal
Amplitude	Linearly proportional to throttle shaft rotation: 0 to 2.09 rad (0° to 120°)
Null Voltage Position	$3.49 \times 10^{-1} \pm 5.24 \times 10^{-2}$ rad ($20^\circ \pm 3^\circ$) throttle rotation

Gain	$0.3667 \text{ VRMS/rad/VRMS excitation}$ $\pm 0.0344 \text{ VRMS/rad/VRMS excitation}$ $(0.0064 \text{ VRMS/}^\circ \text{ rotation/VRMS}$ $\text{excitation} \pm 0.0006 \text{ VRMS/}^\circ \text{ rotation/}$ $\text{VRMS excitation})$
Phase Shift from Excitation	$0 \pm 0.087 \text{ rad } (0^\circ \pm 5^\circ)$ for in phase signal $3.14 \pm 0.087 \text{ rad}$ $(180^\circ \pm 5^\circ)$ for out of phase signal
Polarity	In phase with excitation above $3.49 \times 10^{-1} \text{ rad } (20^\circ)$ throttle rotation

Fuel Metering Valve Position

The position of the fuel metering valve is supplied by the metering valve position transducer on the fuel control.

Frequency	3000 Hz nominal
Wave Form	Sinusoidal
Amplitude	Linearly proportional to metering valve stroke: $0-2.29 \times 10^{-2} \text{ m}$ $(0-0.90 \text{ in.})$
Null Voltage Position	$2.29 \times 10^{-2} \text{ m } (0.90 \text{ in.})$ of stroke $-0+ 1.27 \times 10^{-3} \text{ m } (0.05 \text{ in.})$
Gain	$6.57 \text{ VRMS/m/VRMS excitation} \pm 0.79$ $\text{VRMS/m/VRMS excitation } (0.167 \text{ VRMS/}$ $\text{inch/VRMS excitation} \pm 0.02 \text{ VRMS/}$ $\text{inch/VRMS excitation})$
Phase Shift from Excitation	$0 \pm 8.73 \times 10^{-2} \text{ rad } (0^\circ \pm 5^\circ)$

Fan Blade Pitch Angle

The sensed angle of the fan pitch (β_F) will be provided by the fan blade angle transducer.

Frequency	3000 Hz nominal
Wave Form	Sinusoidal
Amplitude	Linearly proportional to the pitch angle: $0 \text{ to } 2.44 \text{ rad } (0^\circ \text{ to } 140^\circ)$
Null Voltage Position	$1.22 \text{ rad } (70^\circ)$

Gain	0.327 VRMS/rad β_F /VRMS excitation, + 0.0344 VRMS/rad β_F /VRMS excitation (0.0057 VRMS/ $^\circ\beta_F$ /VRMS excitation + 0.0006 VRMS/ β_F /VRMS excitation)
Phase Shift from Excitation	0 \pm 0.087 rad (0 $^\circ$ \pm 5 $^\circ$) for in phase signal 3.14 \pm 0.087 rad (180 $^\circ$ \pm 5 $^\circ$) for out of phase signal
Polarity	Out of phase with excitation at the retract position ref: 0 radians

13.7 ADVANCED TECHNOLOGY ELEMENTS

13.7.1 Inductive Connector

Description

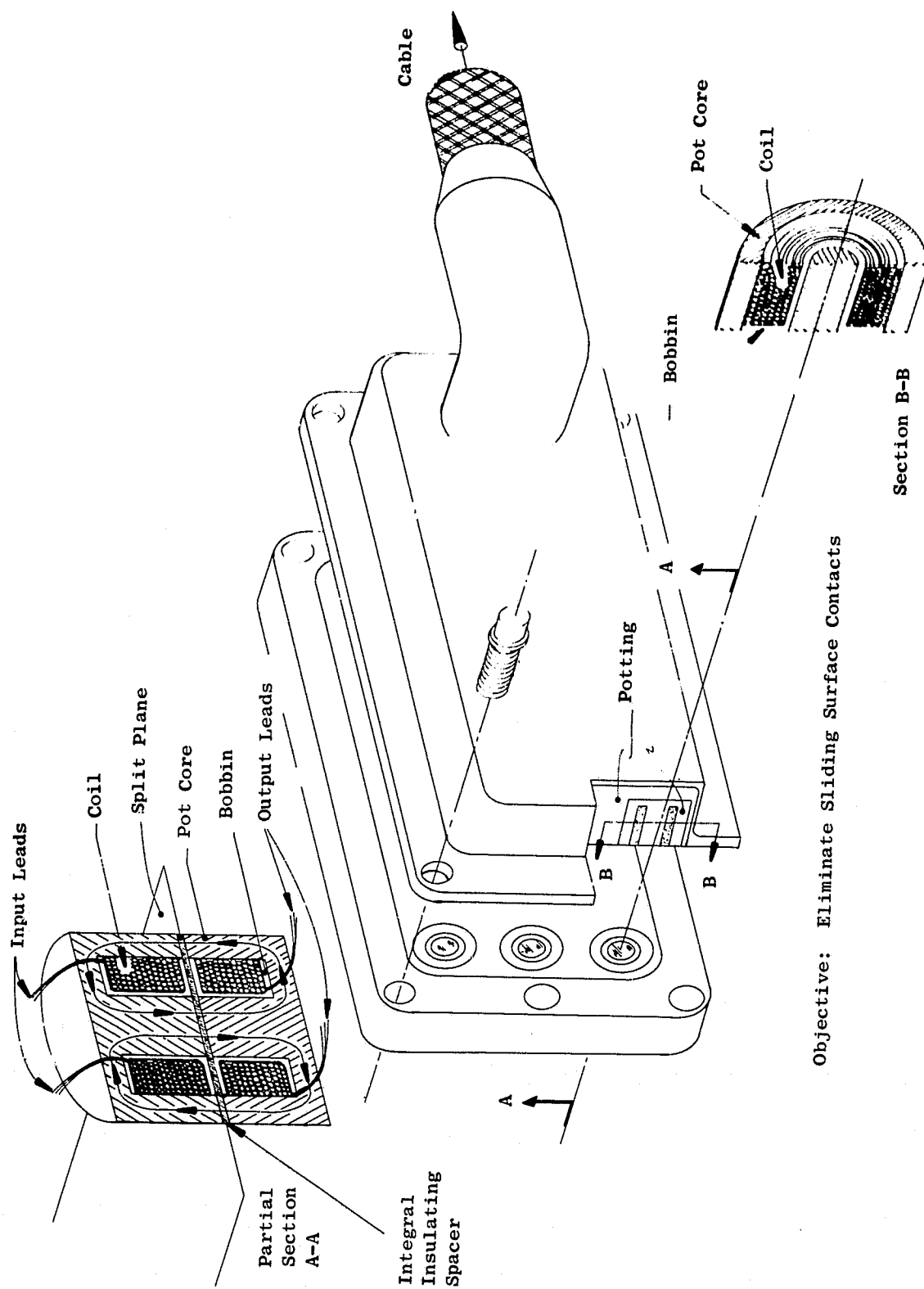
An inductive connector transmits electrical signals by transformer action rather than mechanical friction contacts. (See Figure 13-17). The connector consists of a multiplicity of inductively coupled sections or air gap transformers. Each half of the transformer consists of a coil housed in a pot core. The input into the first coil causes a magnetic field which encompasses both pot cores. The coil in the second pot core picks up the signal. There is a gap between the two pot cores and coils which will contain an insulating material. There is no metallic contact between the two transformer halves. The result is a clamped assembly having no pins, no requirement for wiping action, and no exposures directly to the elements. This type of connector is less subject to errors and damage in field assembly and disassembly, corrosion, open circuits, and grounds.

Development Status

The inductive connector is presently in the early development or bread-board stage. Some testing has been done and the results showed that the concept is feasible and promising. The present efforts are in the areas of minimizing size and material investigations. Early testing was done with 0.11 m (11 mm) diameter pot cores and the goal is to use 0.05 m (5 mm) diameter pot cores for signals such as those required for the magnetic shaft encoder. Present plans include having a bench demonstration model by the end of 1974.

Application on the QCSEE Engine

For a digital control system, most of the signals are ac or a frequency. This will become more so as other digital sensors and output devices are developed. One true digital sensor is the magnetic shaft encoder. The encoder is another advanced technology element so it is presently planned to use the inductive connector at the digital control end of the cable to the encoder.



Objective: Eliminate Sliding Surface Contacts

Figure 13-17. Inductive Connector.

13.7.2 High Reliability Electronic Module

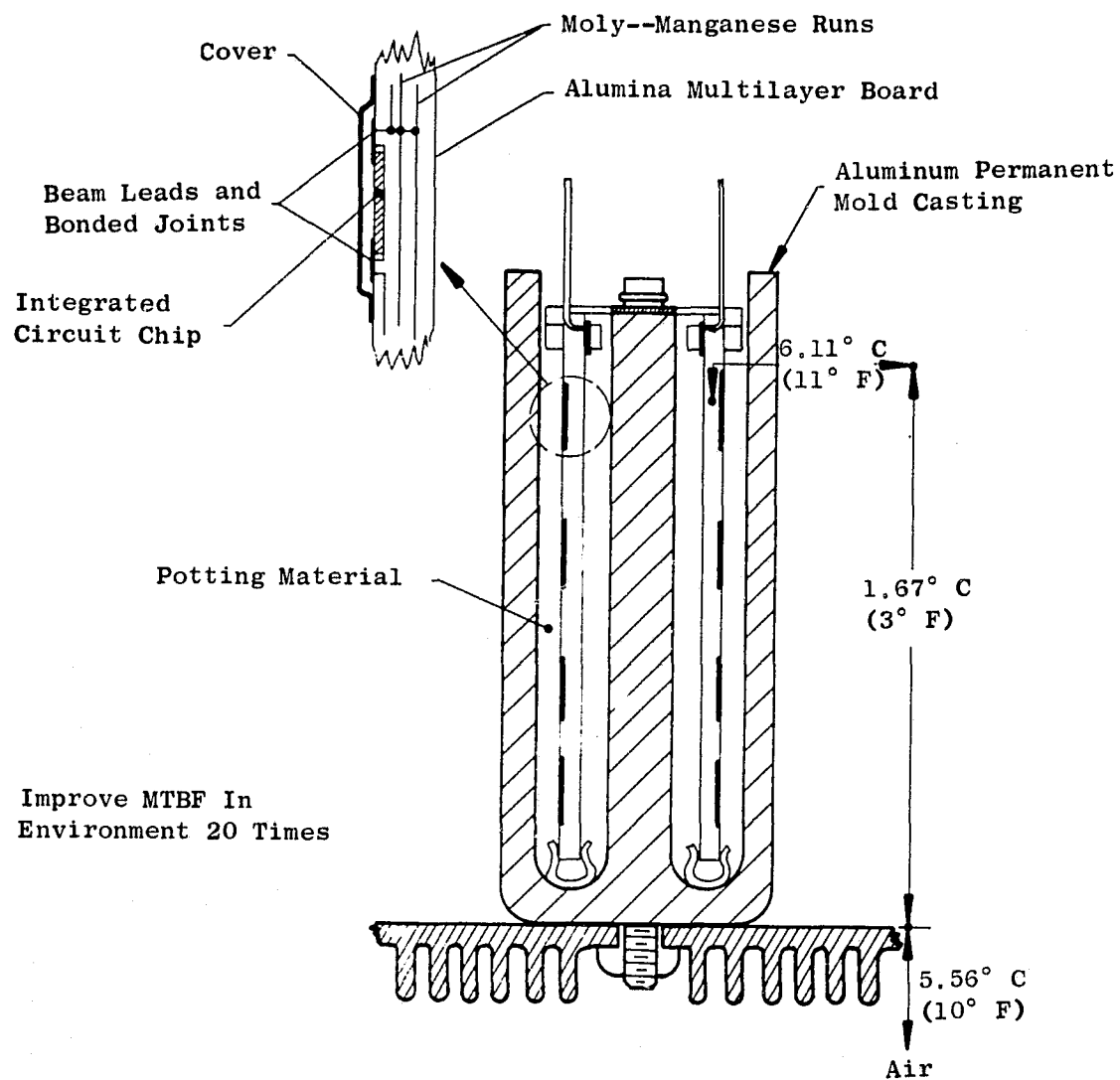
Description

Conventional digital control packaging involves the mounting of dual, inline packages to glass reinforced plastic multilayer boards. This approach has potential problems because the materials used have widely different coefficients of thermal expansion. A typical board assembly may consist of epoxy/glass or polyimide/glass laminates, tin-lead solders, Kovar leads, ceramic dual inline packages, and plastic conformal coatings. During temperature cycling over the range experienced on jet engines, the above combination of materials causes stresses which result in "opens" at electrical connections. This approach also typically requires eight connections in series between two integrated circuit chips on the same board and each has a potential failure rate.

Hybrid packaging, using large or medium scale integration, offers significant advantages for engine-mounted digital control packaging. Present hybrid packages use materials with much less difference in thermal expansion properties than the multilayer approach. A typical hybrid assembly uses an alumina board with gold runs, gold-tin solder, gold fly wires, and Kovar cans and covers. Expansion differences are significant and the potential stress problem with temperature cycling still exists. One important advantage with hybrid over multilayer board is that the number of connections between two integrated circuit chips is reduced from eight to four.

The goal of the high reliability electronic module effort is to improve the mechanical design to make the module especially suited for on-engine digital controls (see Figure 13-18). The major effort includes using materials of matched thermal expansion properties, improving heat transfer to reduce the temperature gradient between the electronics and the heat sink, and to make maximum use of large scale integrated circuits. Materials and interconnection approaches being considered are alumina boards with runs of moly-manganese, Kovar, or tungsten; bonded or welded electrical connections; beam leads; and tungsten heat sinks. To improve heat transfer, approaches being considered are:

1. Mount the chips to tungsten plates and in turn weld the tungsten plates to a tungsten heat sink which would conduct the heat to a cool chassis.
2. Bond the board to a low thermal expansion metal (or other material with good thermal conductivity) module can using a ceramic adhesive and use the module can wall to conduct the heat to the cooled chassis.
3. Reduce the height of the boards to shorten the heat path length.
4. Increase spacing between chips to decrease heat flux density (watts per square inch)
5. Use a thick alumina (or other ceramic with a high thermal conductivity) board and use it as the heat transfer path to the chassis.
6. Minimize the use and thickness of low thermal conductivity materials such as adhesives or potting compounds.



Objective : Improve MTBF In
Environment 20 Times

Figure 13-18. High Reliability Electronic Module.

The electronic industry is continuously developing more large-scale integrated (LSI) circuits and digital control components such as a central processor unit. Future digital controls will take advantage of these developments, and this high reliability module effort will give us the background to package LSI chips properly.

Development Status

The high reliability effort is presently in the preliminary design stage. The major design and development effort will occur during 1975.

Application on QCSEE Engine

The advanced hybrid technology will be applied to the program memory module. This module contains tested LSI chips and this allows meeting the goals of the program.

13.7.3 Fail-Fixed Servovalve

Description

A concept for a fail-fixed servovalve was defined early in 1972 (see Figure 13-19). The servovalve is shown in the zero current input condition and the jet pipe flow is directed toward the divider between the two receivers so that the pressures at the ends of the spool are essentially equal. Valve overlap allows for null shift and spool friction effects. The head and rod ports are blocked holding the servopiston fixed.

The jet pipe moves hard over to the right upon a step input of positive rated current. The jet pipe flow causes the spool to slew to the left until it hits the stop. During this stroke, a pulse of flow is ported to the rod end of the servopiston and, simultaneously, a pulse of flow is vented to return from the end of the servopiston. If the input is now switched to zero current, the jet pipe flow is again directed toward the divider between the two receivers. The spool is returned to the center position. During this stroke, a second pulse is added to the rod end of the servopiston while the head end is simultaneously vented. In other words, if the input is a series of square waves of current stepping from zero to positive rated current and back to zero, the servopiston will move to the left in small steps. The size of the step is determined by the velocity of the second-stage spool, the area of the ports, and the pressure difference. If the input current is in steps from zero to negative (opposite direction) rated current, and back to zero, the servopiston will move to the right in the same manner.

If the input frequency is much greater than the response capability, the servovalve performs as a proportional device. When the input current is from zero to rated, the spool goes to mid-stroke or maximum area, and allows a continuous flow to the servopiston. Pulse width modulation will cause the flow to be proportional to "on" time. In addition, pulse amplitude could also be varied as a function of a second parameter. The combination of width and amplitude modulation provides a flow proportional to the product. In other words, the valve provides a multiplying capability.

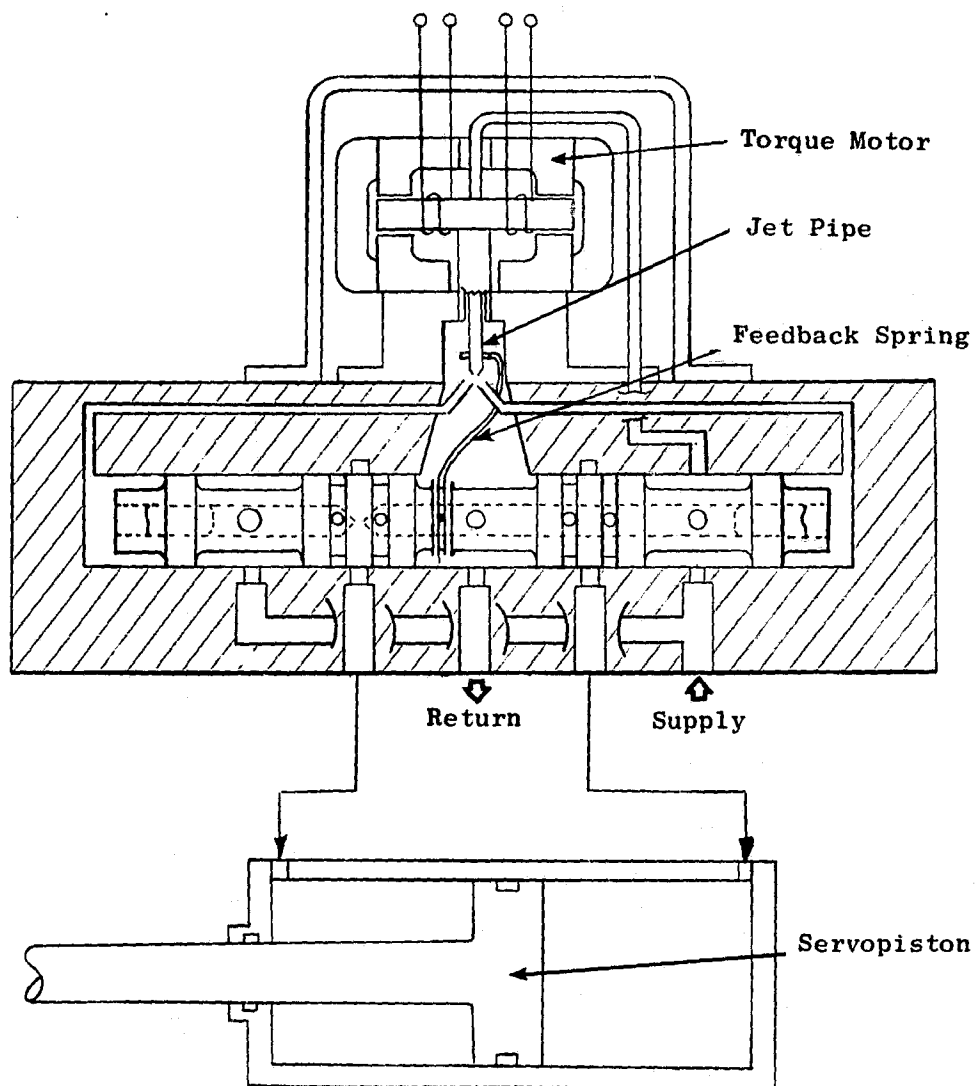


Figure 13-19. Fail-Fixed Servovalve Schematic.

This servovalve concept offers the following advantages or features for future advanced engine control systems.

1. The servopiston is essentially fixed upon loss of electrical signal or upon "hard over" signal in either direction. A creep rate, due to leakage, of less than 0.1% of full stroke per second is expected on applications such as fuel metering valves.
2. The input signal requirements are compatible with digital control techniques.
3. The servovalve is a versatile proportional device with "multiplier" capability.
4. The concept retains the desirable features of conventional servovalves so past experience and manufacturing techniques are applicable.
5. The servovalve can move a servopiston at a very slow rate without feedback. The flow to the piston can be blocked a large percentage of the time so it has the effect of a small orifice. A series of minute steps is acceptable in most servos because the percentage change can be tailored to meet requirements.

Development Status

A test block version of the fail-fixed servovalve was tested in 1973. A flight type version is presently being developed under AFAPL Contract No. F33615-74C-2007. At the present time we are waiting for quotes from two servovalve vendors for the design, fabrication, and design assurance testing. We expect to have servovalves for testing at GE by the first quarter of 1975.

Application on QCSEE Engine

The interface between the digital control and the hydromechanical control is an electrohydraulic servovalve. This servovalve modulates the fuel metering valve as directed by the digital control. A conventional servovalve is used on the F101 hydromechanical control. It is presently planned that a fail-fixed servovalve will be demonstrated on the engine in this application during the QCSEE program.

13.7.4 Magnetic Shaft Encoder

Description

Shaft encoders are used as digital position transducers. The basic types are contact, optical, and magnetic. The magnetic shaft encoders appear most feasible for jet engine control applications. This type has good resistance to hostile environments, fairly wide temperature operating range, and high reliability. Because frictional contacts are not used, service life is essentially determined by the bearings. Also, since there are no infrared or visible light sources to decay or fail, the magnetic sensors cannot be falsely triggered

by heat or rendered inoperable by dust, moisture, or oil mist. Totally immersed operation in most liquids is also feasible. Both incremental- and absolute-type magnetic shaft encoders are available. The absolute type is preferred for engine controls because the proper signal will still exist after an electrical power interruption.

A magnetic shaft encoder operates on the principle of discretely passing, or suppressing, a drive signal from input to output (see Figure 13-20). The input signal is presented to the input windings of bid sensing or read heads while observing the output winding on each head to determine whether the signal is or is not present. Logical ONE outputs appear only in the absence of discrete saturating magnetic fields located in the code disc. The ZERO signal condition results when the sensing head is in the immediate vicinity of a magnetic area in the code and the core is saturated by flux. The coded magnetic areas are located circumferentially in code tracks with a code track representing each bit of the output code word. Gray code is preferred because it requires fewer leads.

Development Status

Magnetic encoders with Gray code and with temperature capability to 204.4° C (400° F) are being developed under AFAPL Contract No. F33615-74-C-2007. Shaft encoders with Gray code and 121.1° C (250° F) have been ordered and these are expected by November 1974. These units will be used to develop the circuit for excitation and interrogation of the Gray code. Later this year, the 204.4° C (400° F) encoders will be ordered. These will be designed specifically for the on-engine environment.

Application on QCSEE Engine

The magnetic encoder will be used as a position transducer. Present plans are to use it for sensing fuel metering valve position. The existing sensor is a rotary variable differential transformer. An adapter will be required to mount the encoder because of the size difference. A layout study is planned to determine mounting requirements.

An alternate application is sensing fan nozzle position. In this application, the conventional sensor will be a linear variable differential transformer installed inside a hydraulic cylinder. The adapter will include a linear to rotary motion device and the encoder would be externally mounted to a hydraulic cylinder. A study is planned to determine feasibility and installation requirements. This study is needed because the fan nozzle doors are thin in the radial dimension.

13.8 VARIATIONS FOR FLIGHT ENGINES

One of the major changes which would be made in designing for a flight engine would be to reduce the complexity of the hydromechanical control. The F101 control being used on the demonstrator for reasons of economics and expediency has several features which would not be included on a QCSEE flight engine. In addition, certain functions of the hydromechanical control such as core stator vane control and accel/decel fuel flow limiting might be switched into the digital control.

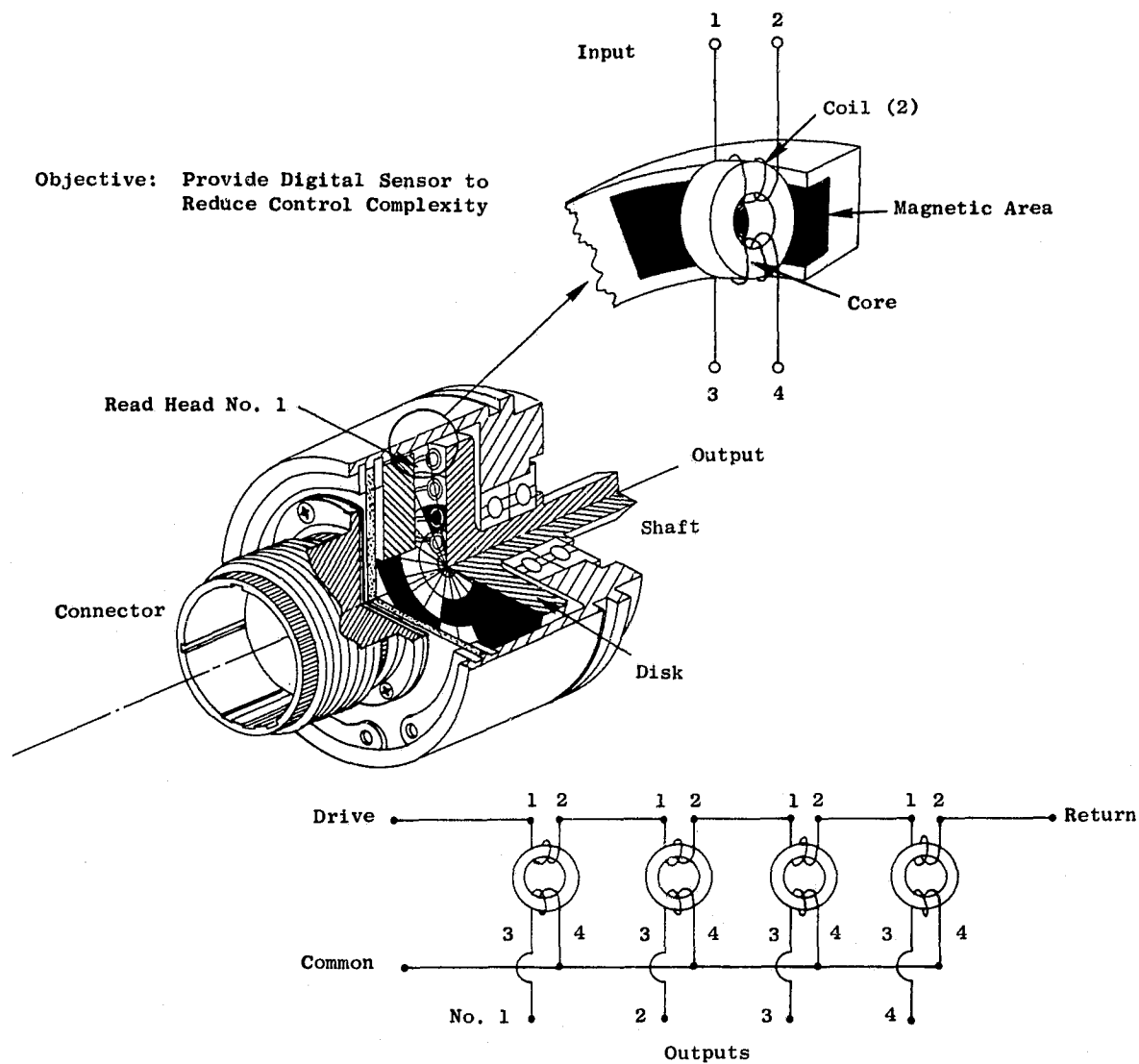


Figure 13-20. Magnetic Shaft Encoder.

Other changes would undoubtedly arise as a result of optimizing for a specific aircraft. Obviously it is not possible to identify such changes at this time but they would fall into the categories of control logic, component sizing, component packaging, and component arrangement.

Relative to component packaging, a major area that would change is the digital control. The demonstrator approach is to use polyimide two-sided circuit boards for the analog modules and the wire-wrapped digital boards. Only one digital module will use multilayer polyimide boards and one hybrid module with an alumina board will be demonstrated. The flight version of the digital control will use predominantly hybrid packaging and large-scale integrated circuits.

SECTION 14.0

NACELLE AERODYNAMICS DESIGN

14.1 SUMMARY

Preliminary nacelle aerodynamic flowpaths have been established for UTW and OTW experimental and flight propulsion systems. These designs integrate aerodynamic and acoustic requirements into high performance nacelle configurations which meet the overall objectives of the QCSEE program for the development of quiet powered lift engines for short haul transport aircraft. This section discusses the design status as of the PDR at NASA Lewis on June 25 and 26, 1974. The UTW and OTW propulsion systems are presented in light of the installation and cycle requirements. Differences between experimental and flight nacelles are also discussed. Component aerodynamic model test programs for new technology areas such as high throat mach number inlets and reverse flow inlets for UTW and OTW target reversers are in place to provide the necessary design information in these critical areas.

14.2 DESIGN REQUIREMENTS

The QCSEE UTW and OTW propulsion systems must be designed to meet the powered lift requirements and noise goals at takeoff and landing (approach, reversal) while providing high performance at altitude cruise conditions. Therefore, there are both internal and installation design requirements which must be considered in order to arrive at a balanced, high performance propulsion system. Important requirements for the QCSEE engines are discussed in the following section.

Installation

The UTW and OTW propulsion systems are to be representative of a four-engine aircraft installation having an unswept, moderately tapered wing planform. Since the wing flowfield for this design is essentially free of cross flows, engine nacelle and pylon design can be symmetrical about the vertical centerline. The propulsion systems are to be designed for low drag at 0.72 cruise Mach number. Engine installation must be such as to provide powered lift jet deflection angles of 30° for takeoff and 60° for landing approach. The inlet must be capable of operating without separation at 50° angle of attack at an aircraft speed of 41.18 m/sec (80 knots). 90° crosswind operation must be separation free up to 18 m/sec (35 knots).

Full-power reverser utilization is required down to 5.15 m/sec (10 knots) ground speed.

Propulsion Systems

The aerodynamic design of the QCSEE propulsion systems must integrate aero/acoustics requirements into a high performance nacelle configuration which meets engine cycle and installation needs.

The inlet is a hybrid design which utilizes high throat Mach number and acoustic treatment panels for fan noise suppression. The required throat Mach number for design level of suppression has been established at 0.79 for takeoff levels; no acoustic splitters are required.

The fan duct must accommodate extensive acoustic treatment on inner and outer duct walls and an acoustic splitter for the 609.6 m (2000 ft) runway experimental nacelle noise goals. Splitter length for the UTW nacelle must be 101.6 cm (40 in.) long; the OTW splitter must be 76.2 cm (30 in.) long. An average duct Mach number of 0.45 is required over the acoustic splitter region for noise suppression. The flight propulsion systems do not require acoustic splitters to meet 914.4 m (3000 ft) runway noise levels.

Separate flow concentric fan and core exhaust nozzles are used on the UTW engine, while a confluent (partially mixed) nozzle with a single-exit throat is used on the OTW engine. The exhaust nozzles must be variable to accommodate engine cycle area requirements in both cases. Table 14-I shows the degree of variability required for UTW and OTW propulsion systems.

Additional area variation capability is required to meet reverse thrust area needs. While not specific requirements, the UTW fan nozzle area flares open to 33,548 cm² (5200 in.²) for reverse flow entry, and the OTW blocker-type reverser must provide approximately 19,355 cm² (3000 in.²) effective area reverse flow turning losses. (Experimental scale model programs are in place to establish the real needs of these areas in reverse.)

UTW core nozzle effective area requirements are 3335 cm² (517 in.²) and 3226 cm² (500 in.²), respectively, for takeoff and cruise which can be provided by a fixed physical area of 3558 cm² (543 in.²); OTW core effective area at the mixing plane must be maintained at 3884 cm² (602 in.²) throughout the engine operating envelope.

In reverse, the UTW and OTW propulsion systems must provide a minimum of 35% of maximum forward thrust at static conditions.

Table 14-1. Propulsion System Exhaust Area Requirements.

Power Setting	UTW Effective Fan Nozzle Area	OTW Effective Combined Nozzle Area
Takeoff/Approach	15,626 cm ² (2422 in. ²)	17,490 cm ² (2711 in. ²)
Cruise	12,013 cm ² (1862 in. ²)	14,897 cm ² (2309 in. ²)

14.3 UTW NACELLE AERODYNAMIC DESIGN

The UTW experimental propulsion system nacelle aerodynamic design is shown on Figure 2-5; the flight propulsion system is shown on Figure 2-7. The nacelle designs shown on these figures reflect the integration of aerodynamic and acoustics requirements in the inlet, fan and core ducts, and nozzles, to provide a high performance propulsion system for QCSEE. This section discusses the important aerodynamic features of the nacelle designs, pointing out differences which exist between experimental and flight propulsion systems.

Inlet

The inlet contours for the UTW propulsion systems are shown in Figures 2-5 and 2-7. The internal contours for both configurations are identical.

Integration of the QCSEE inlet operating requirements results in some unusual design features relative to normal CTOL requirements. Figure 14-1 shows the throat Mach number levels that result during typical QCSEE and CTOL flight placards. Two points are significant:

1. The engine airflow schedule has been designed to provide constant corrected airflow from takeoff to cruise. This allows the inlet throat Mach number to be elevated at takeoff to facilitate fan noise suppression without the use of variable inlet geometry.
2. The QCSEE inlet has been sized to provide relatively higher throat Mach numbers at takeoff, compared to a conventional inlet.

In selecting the elevated design throat Mach number limit for QCSEE, the practical upper limit is dictated by consideration of a typical inlet recovery characteristic such as Figure 14-2. Large degradations in inlet recovery are encountered at one-dimensional throat Mach numbers on the order of 0.82, due to effects of radial throat velocity gradient and boundary layer growth along the inlet lip. Consequently, in order to provide margin for effects such as engine-to-engine flow variations, flow variation due to operational effects on engine tolerances, and inlet-to-inlet throat area variations, a practical upper design limit of 0.79 was selected for the QCSEE inlet throat Mach number.

The definition of the inlet internal lip contraction ratios needed to satisfy the QCSEE operational requirements was facilitated by consideration of separation boundaries expressed in terms of specific corrected airflow versus inlet angle of attack for several representative contraction ratios (Figure 14-3). The QCSEE maximum inlet upwash angles of approximately 50° at takeoff, 34° at approach, and 30° at flight idle are indicated at the corresponding specific flows. Due to the different operating conditions imposed on the inlet (i.e., angle of attack for the bottom lip and crosswind for the side lips), the inlet will have a symmetric throat and diffuser, but an asymmetric external lip shape, which is thickened locally for angle of attack (bottom) and crosswind (sides). The values indicated in Figure 14-4 for the local contraction ratio are those numbers selected prior to substantiation from the 30.48 cm (12 in.) inlet wind tunnel test program at NASA LeRC.

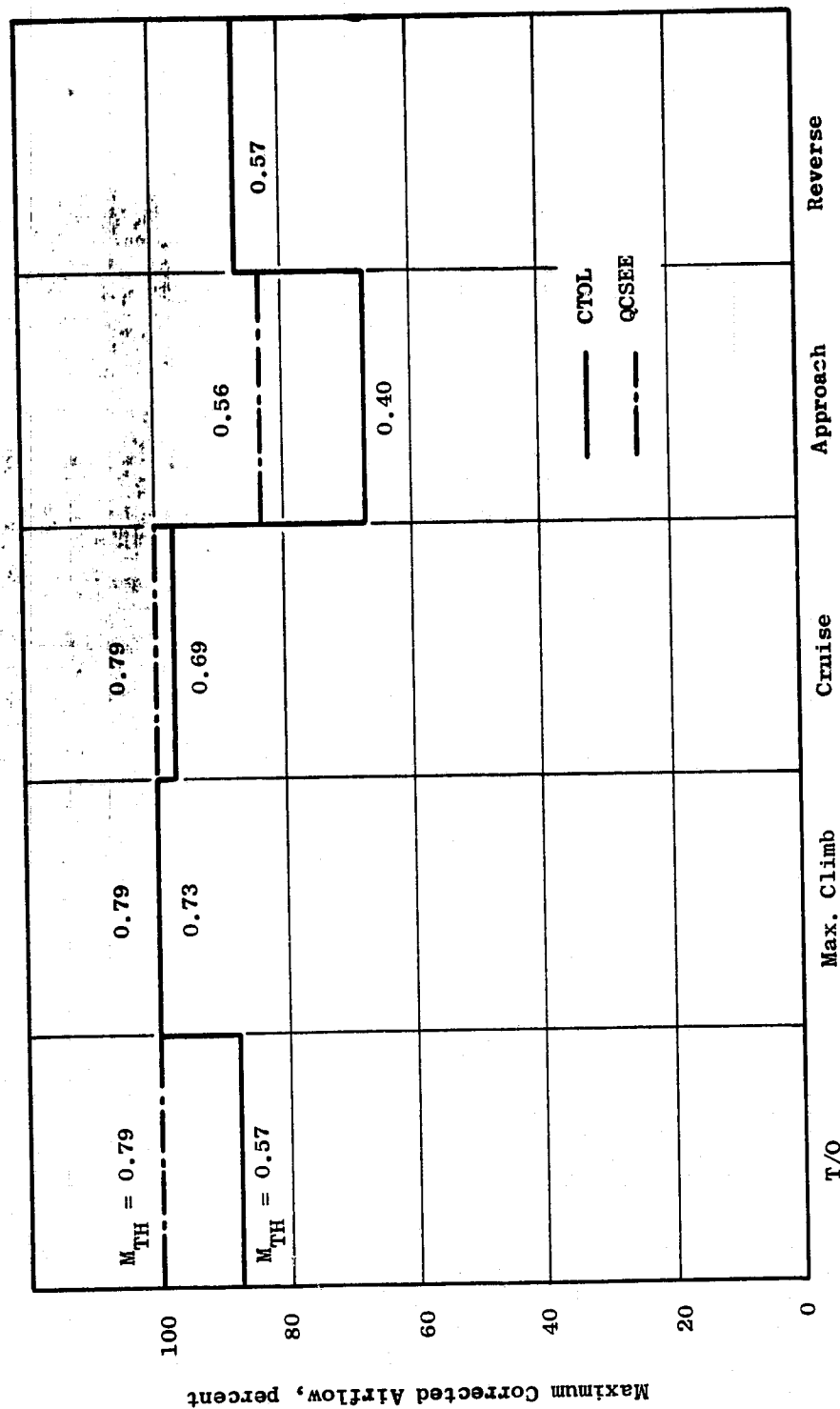


Figure 14-1. Flight Placard Airflow Characteristics for QCSEE and CTOL Aircraft.

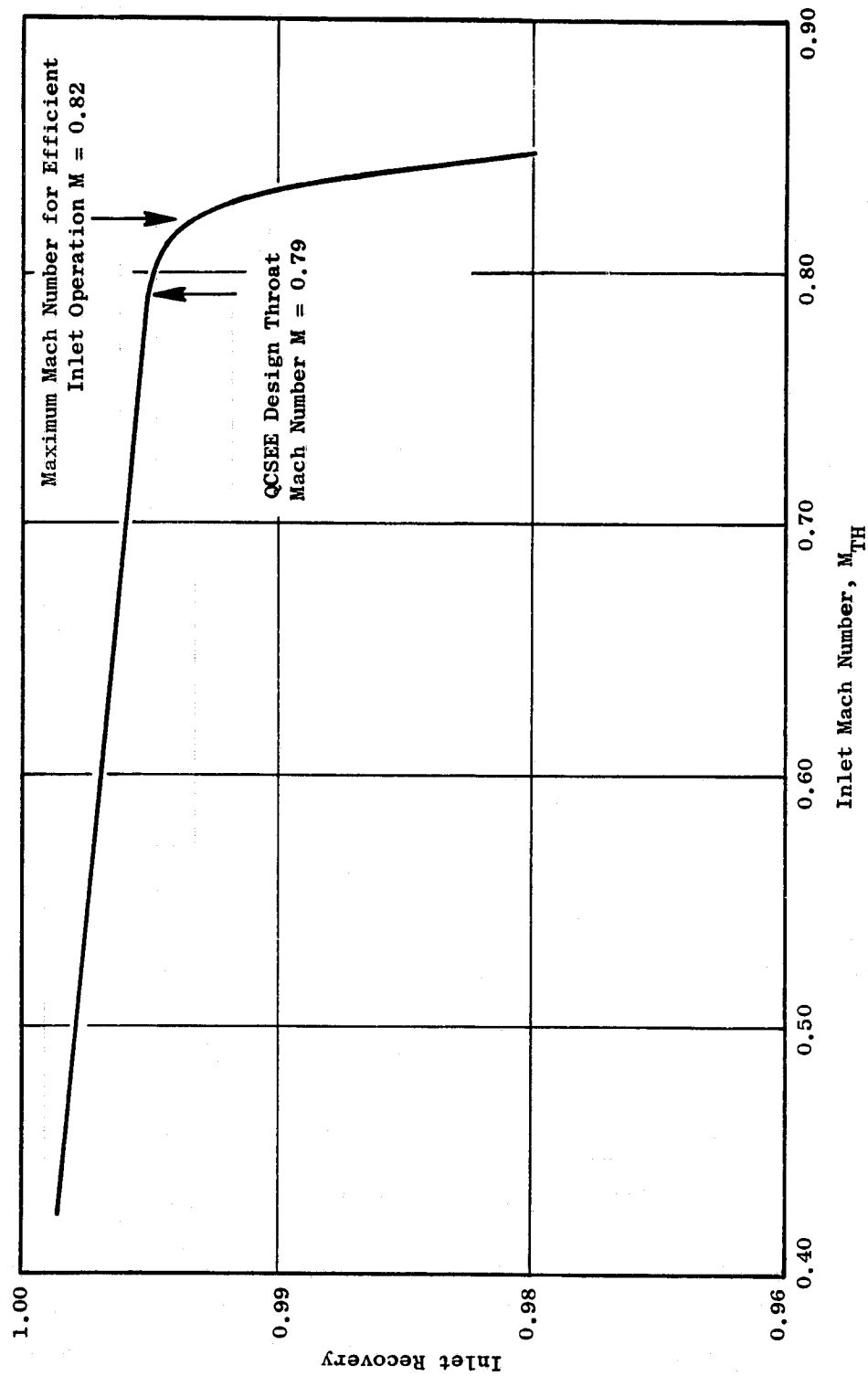


Figure 14-2. Inlet Throat Mach Number Selection.

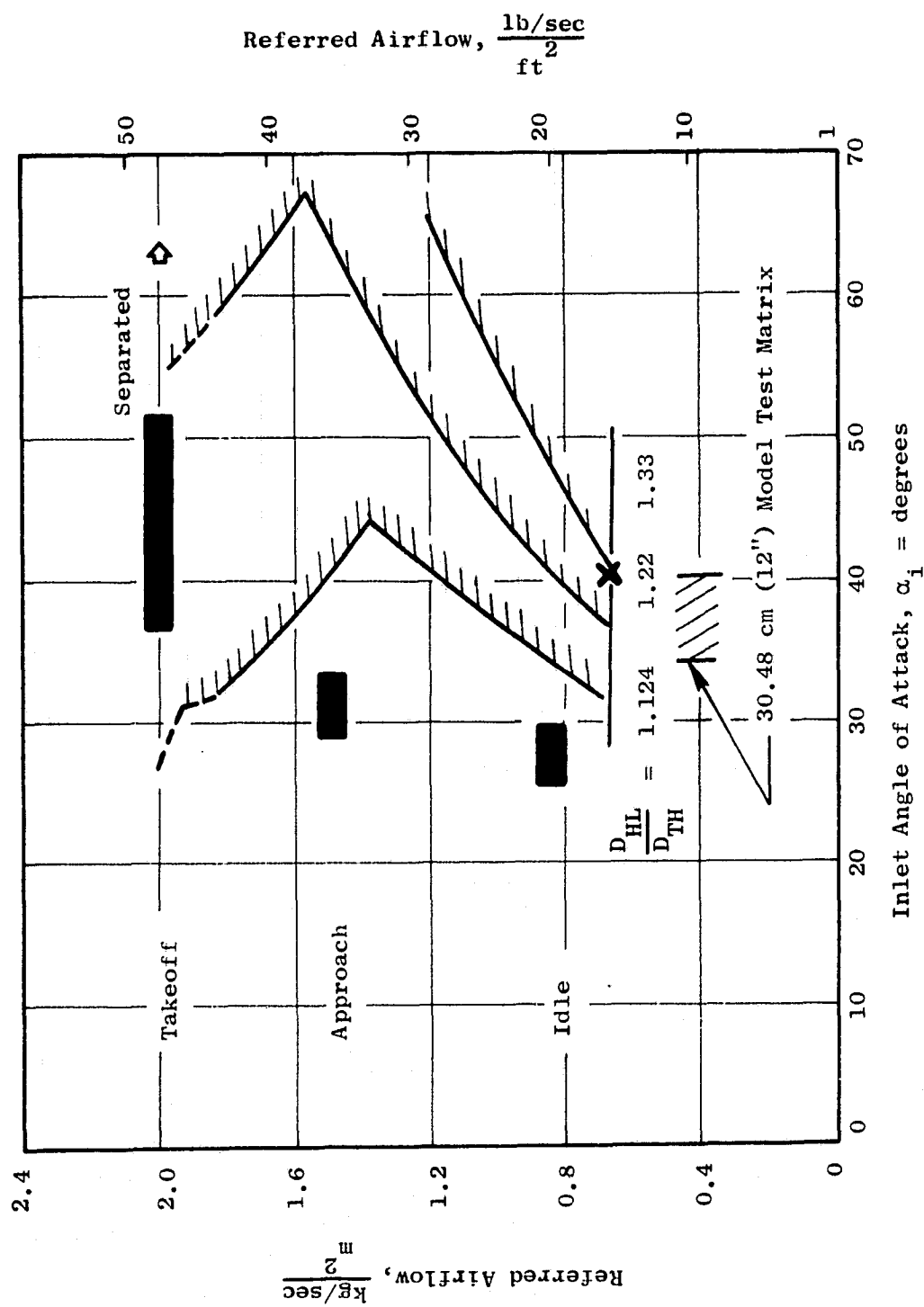
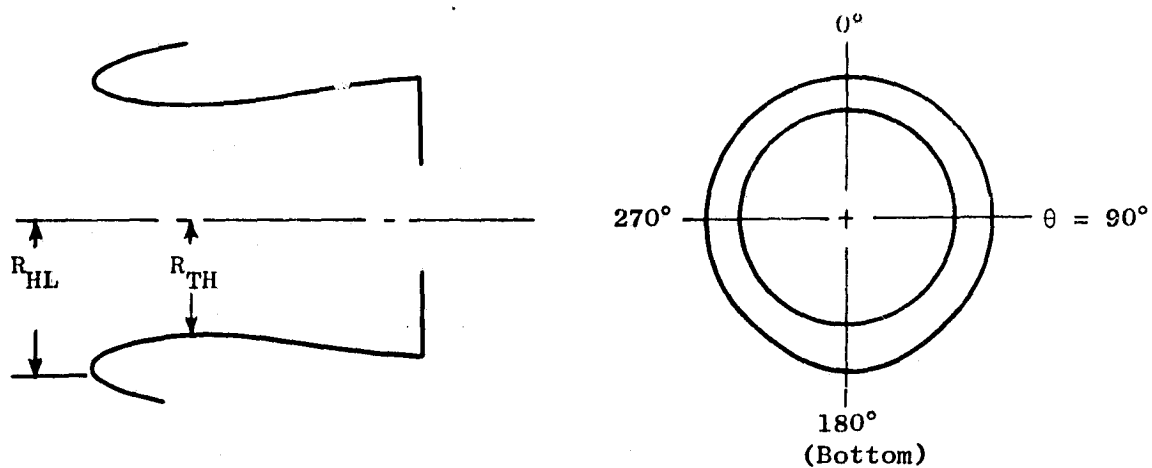


Figure 14-3. Definition of Inlet Contraction Ratio to Satisfy Operational Requirements.



- Increased Lip Thickness Applied Only Where Required

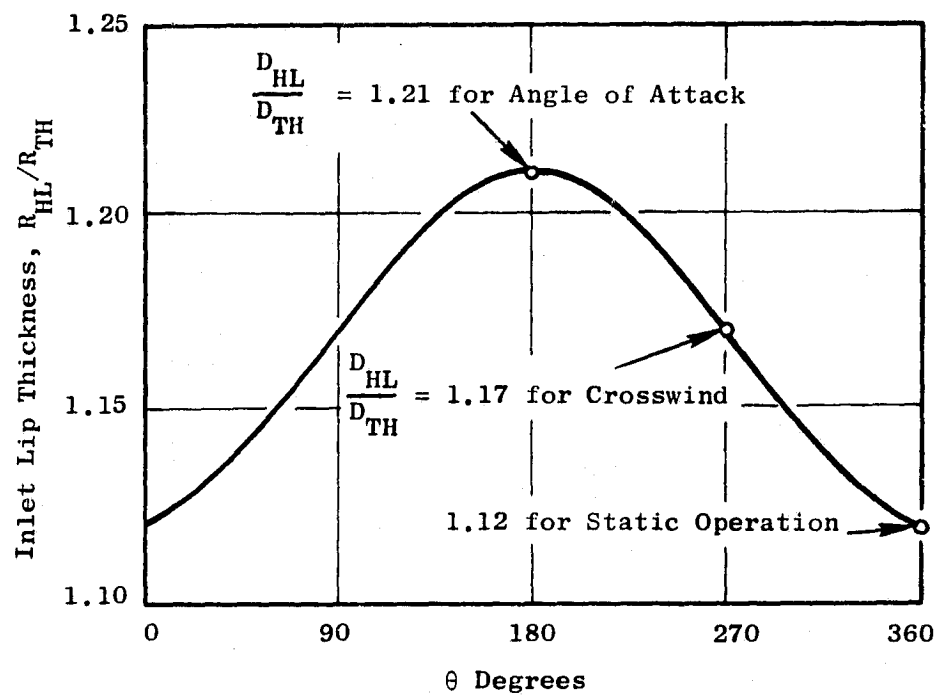


Figure 14-4. QCSEE Inlet Lip Design.

Selection of the external cowl contour was based upon dual consideration of low-speed and high-speed performance characteristics. The nose shape required for acceptable low-speed operation, where the combination of high inlet mass-flow ratio and high inlet flow incidence tends to produce a velocity peak on the internal surface, was determined by three-dimensional potential flow analysis of several external shape, diameter, and length ratio variations. Intent was to select a design that reduced the internal velocity peak, which could otherwise result in flow separation, and also satisfied the high speed design requirement. The cowl shape meeting these requirements with the highest diameter ratio, D_{HL}/D_{MAX} at a given length ratio, X/D_{MAX} , was selected to minimize Nacelle diameter. A D_{HL}/D_{MAX} of 0.905 with an X/D_{MAX} of 0.200 resulted as seen from Figure 14-5.

The assimilation of all the design requirements and design data results in the inlet preliminary design contained in Figure 14-6.

Fan Bypass Duct and Nozzle Design

The fan duct shown on Figures 2-5 and 2-7 is designed for extensive use of acoustic treatment on the inner and outer duct walls. A 101.6 cm (40 in.) long, 3.048 cm (1.2 in.) thick acoustic splitter is installed in the fan duct to meet 610 m (2000 ft) runway, 152.4 m (500 ft) sideline noise goals for the experimental engine. The duct geometry is sized to provide an average duct Mach number of 0.45 (see Figure 14-7) in the splitter region at takeoff power and results in a nacelle maximum diameter of 200.15 cm (78.8 in.). Also shown on Figure 14-7 are duct Mach number characteristics at cruise and the actuator fairing blockage effects. Similar characteristics for the reverse mode are shown on Figure 14-8. An evaluation of Mach number distribution in the inlet section in the reverse mode was not made because of the complexity of the fan flow field. Velocities in this region will be established from engine tests. The flight propulsion system, which is designed for 914 m (3000 ft) runway use requires no acoustic splitter; the fan duct is therefore, 17.78 cm (7 in.) shorter than the experimental nacelle because axial location of the nozzle hinge is no longer dictated by the splitter trailing edge position. Both the experimental and flight propulsion system nacelles employ a low leakage four-flap variable fan nozzle for maintaining area requirements between takeoff and cruise.

Nozzle flap length in both cases is 45.72 cm (18 in.). During thrust reversal, the nozzle flaps rotate outward to provide a flare inlet (exlet); flap angle in reverse is 28.5° with respect to engine centerline. The reverse flow inlet area at the flap trailing edge is approximately $33,548 \text{ cm}^2$ (5200 in.^2).

Nozzle geometry at the 0.72 Mach number cruise condition is characterized by an external boattail angle of 20° . This angle would normally be considered too high for a 0.8 Mach number cruise application, but for 0.72 Mach number, acceptable cruise drag is achieved. Fan flow inclination at the flap exit is 14 degrees inward at cruise to maintain attached flow on the core cowl section external to the fan nozzle. The core cowl angle itself is 13.5° relative to the engine centerline.

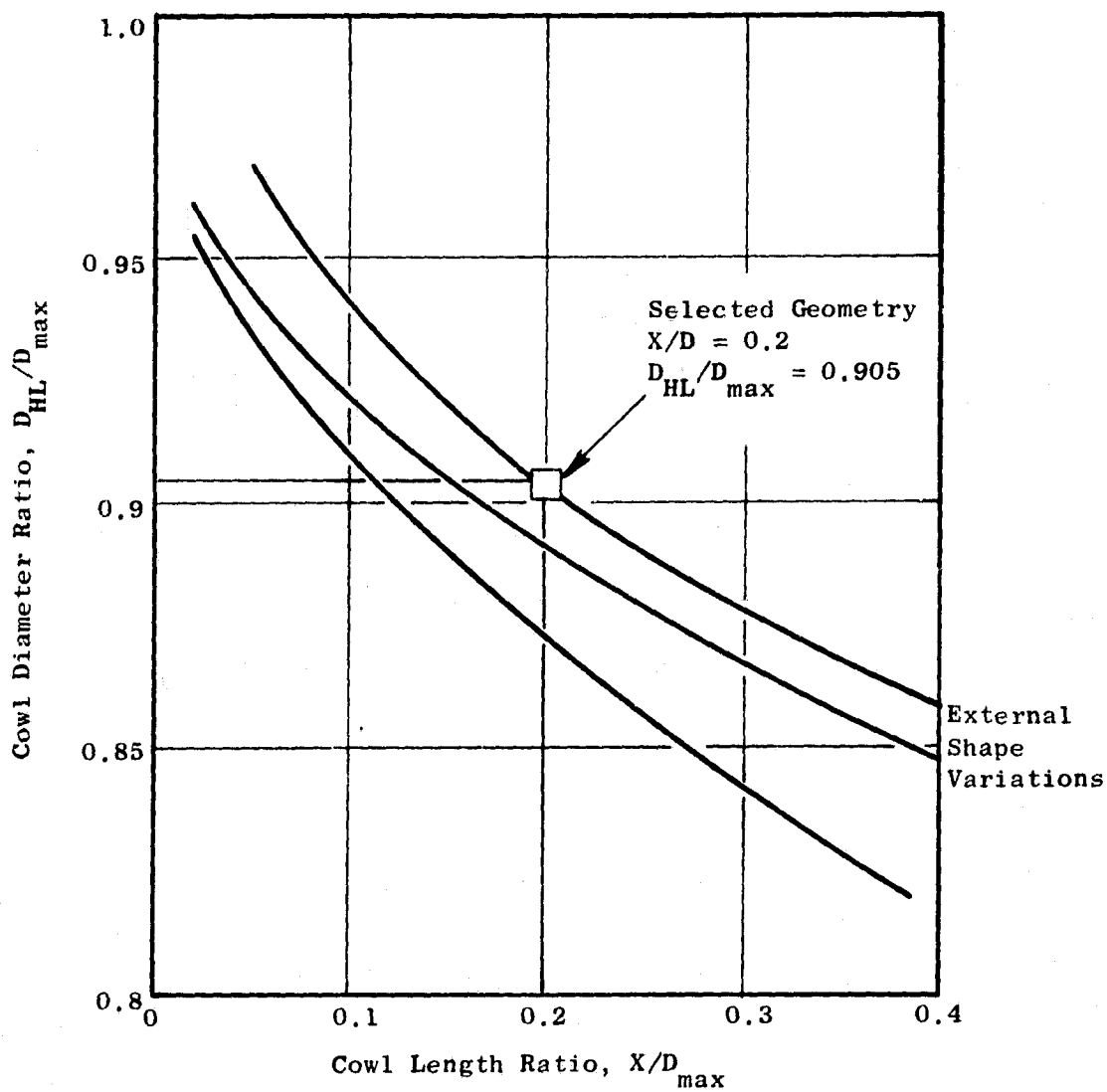


Figure 14-5. Cowl Geometries that Satisfy Low-Speed Nose Shape Requirements.

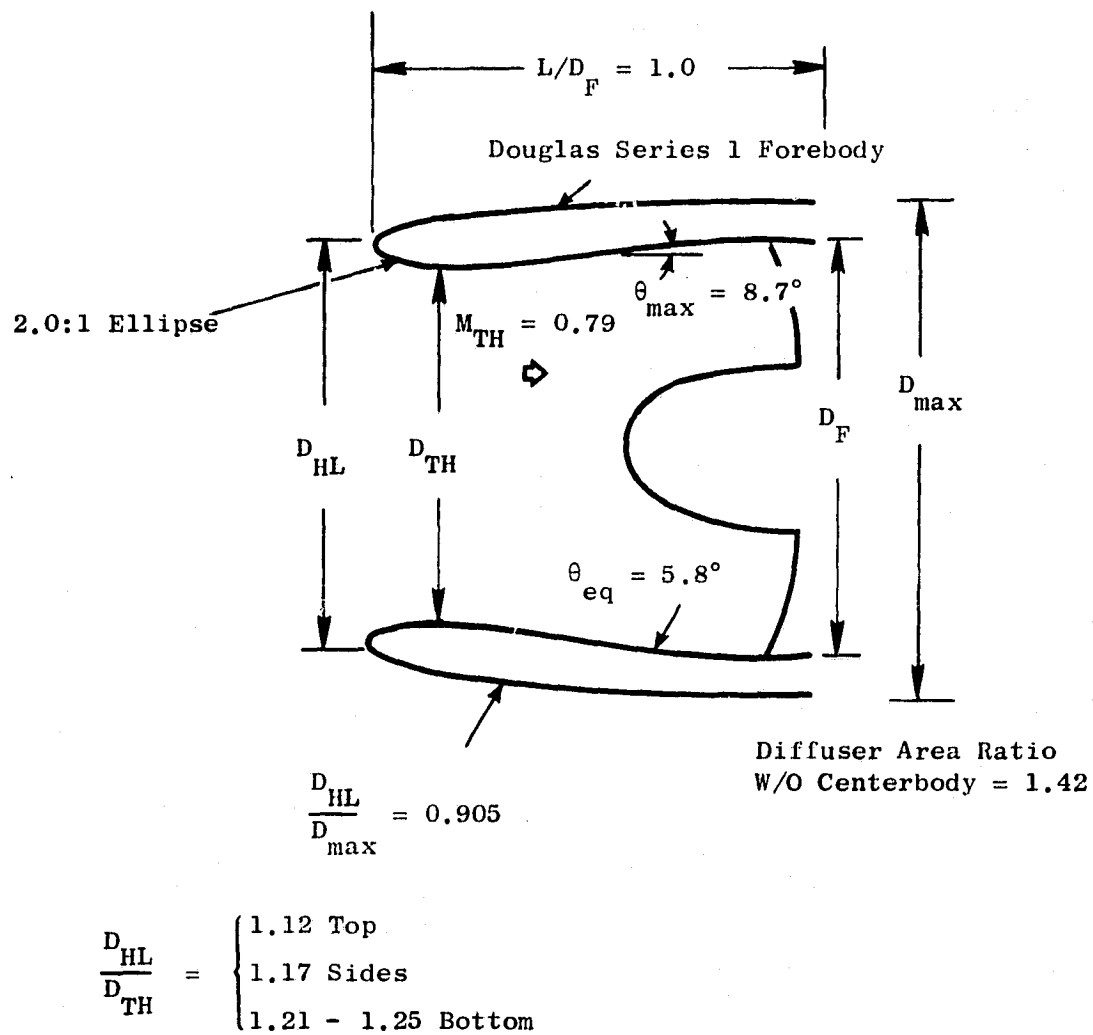


Figure 14-6. UTW and OTW Inlet.

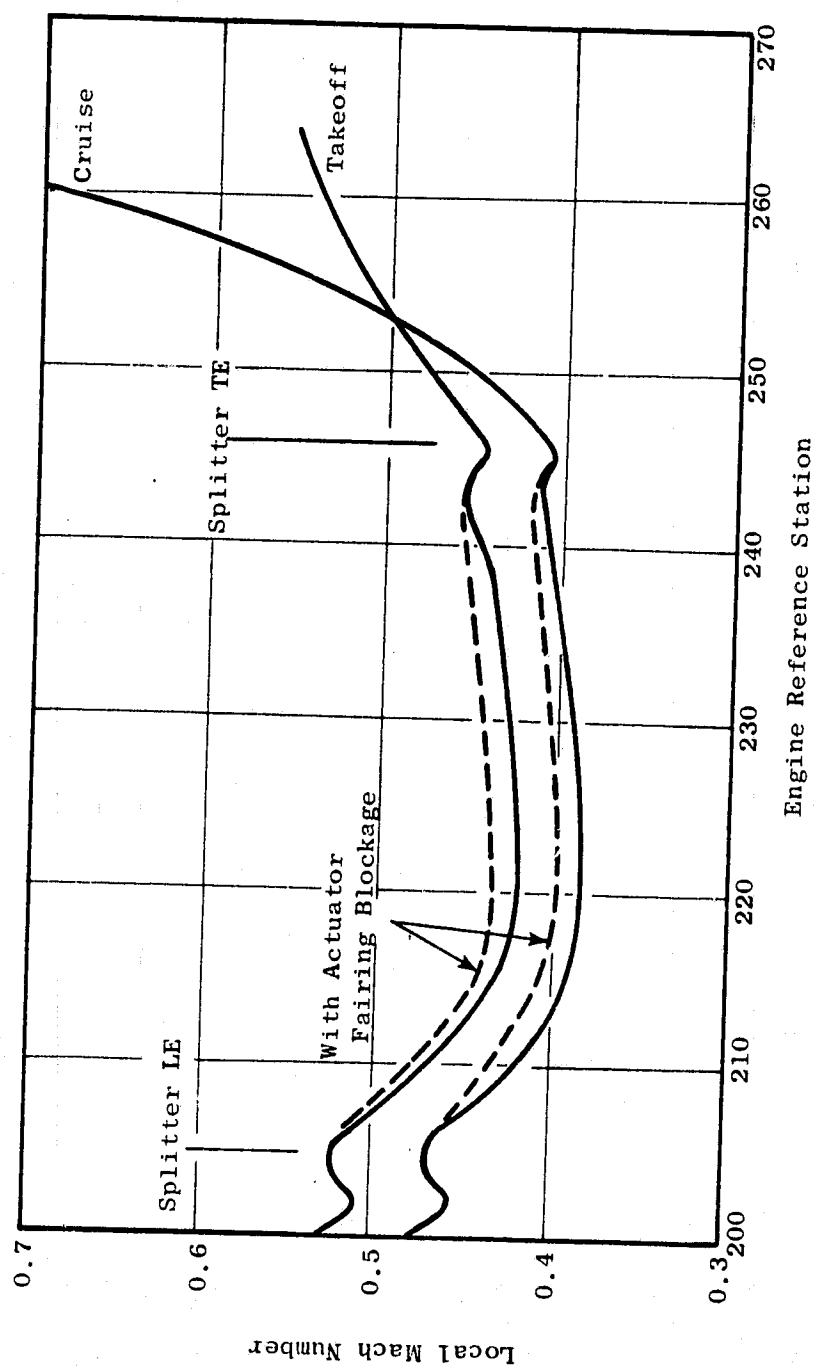


Figure 14-7. UTW Fan Duct Mach Number Distribution.

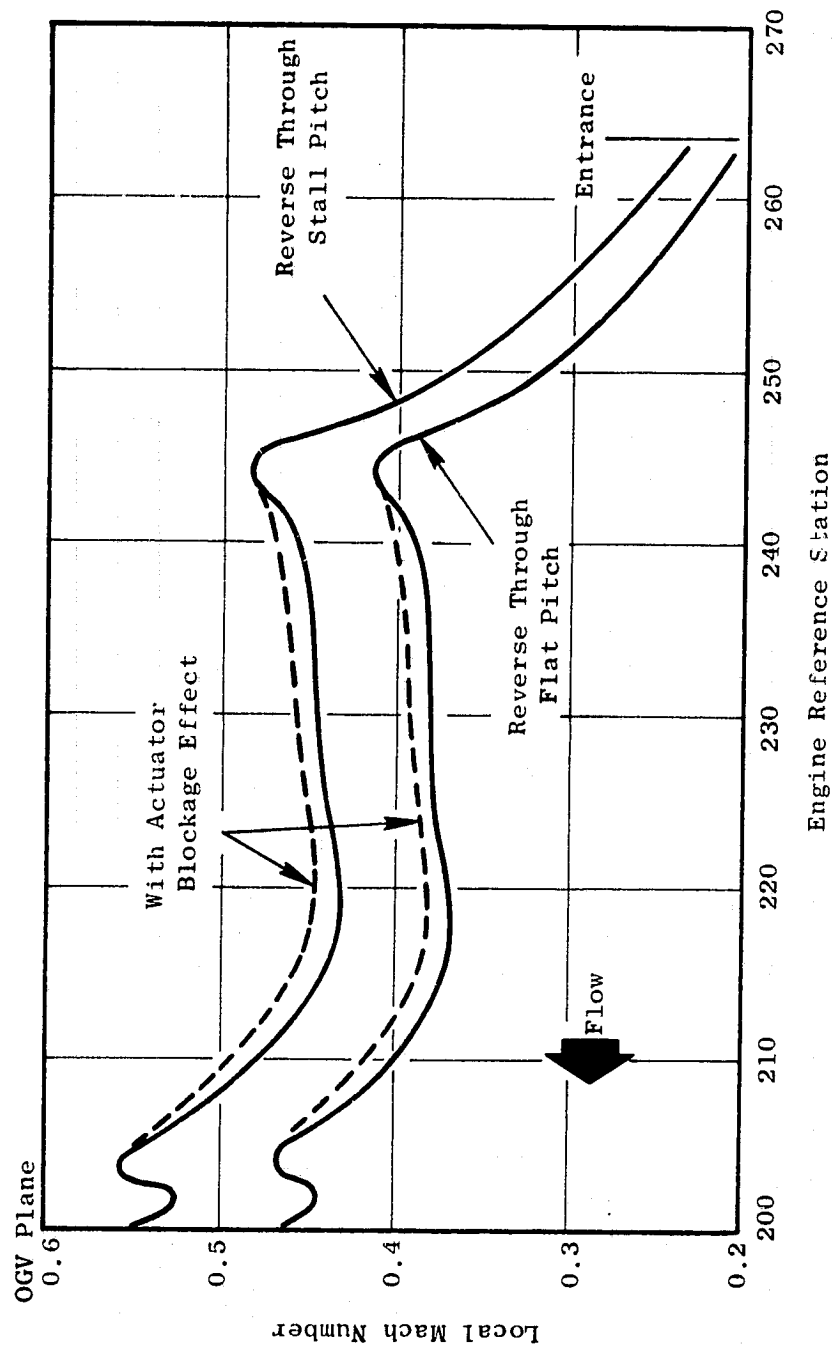


Figure 14-8. UTW Fan Duct Mach Number Distribution - Reverse Thrust/Flow Operation.

Core Nozzle Design

The core nozzle is an annular convergent nozzle having a fixed exit area of 3558 cm² (543 in.²). The nozzle duct length is established on the basis of acoustic treatment length requirements and the desired axial separation of fan and core nozzle exit planes to avoid hot core ingestion during thrust reverse. The aerodynamic flowpaths for the experimental and flight nacelles are identical (see Figures 2-5 and 2-7).

Pylon Design

The internal pylon is integrated into the fan OGV system, the nose being formed by a fan OGV housing the radial drive shaft. The pylon shape (thickness) from leading edge to maximum thickness, 40.64 cm (16 in.), over the turbine frame (station 248) has been determined by fan aerodynamic design considerations to eliminate fan back pressure in the pylon region. The internal (scrubbed by fan flow) pylon closes out with a 12° half angle boattail and extends slightly beyond the core nozzle exit plane.

The external pylon above the nacelle is 50.8 cm (20 in.) wide to accommodate the controls and accessories (C & A) packaging; the 50.8 cm (20 in.) width is blended into the internal pylon by undercutting along the C & A pylon and nacelle interface ahead of the fan nozzle exit plane. Refer to installation drawing shown on Figure 15-1.

The flight and experimental engine propulsion systems pylons are identical internally; however the experimental pylon is simplified to better fit the outdoor test facilities. The simplification does not affect the aerodynamic flow characteristics.

14.4 OTW NACELLE AERODYNAMIC DESIGN

The OTW nacelle aerodynamic design is shown on Figures 2-9 and 2-11. These two figures represent the experimental propulsion system configuration and the flight propulsion system, respectively. This section describes the important aerodynamic design elements of these systems and discusses differences between flight and experimental nacelles which result from special requirements for testing and mechanical design implementation for the experimental nacelle.

Inlet Design

The OTW propulsion system utilizes the same inlet as the UTW propulsion system. Since airflow level is the same for both engines and operational characteristics, cross wind and inlet angle of attack are nearly identical (except for small differences in angle of attack attributable to engine location with respect to wing flow field). Refer to Section 14.3 for inlet aerodynamic design details.

Fan Bypass Duct and Nozzle Design

The fan duct geometry used in the OTW nacelle is identical to that of the UTW propulsion system between the OGV exit plane (station 200) and the UTW flare nozzle hinge ring (station 246). Nacelle maximum diameter is 200.152 cm (78.8 in.) based on duct Mach number acoustics requirements. For the experimental engine propulsion system, a 76.2 cm (30 in.) long, 3.048 cm (1.2 in.) thick acoustic splitter is positioned within the fan duct. An average Mach number over the splitter region of 0.45 is maintained for acoustics needs. The duct is of sufficient length to accommodate required acoustic treatment on inner and outer walls. The flight nacelle meets acoustics goals [914.4 m (3000 ft) landing field length aircraft] without the splitter, and the duct Mach number in this region drops to about 0.4.

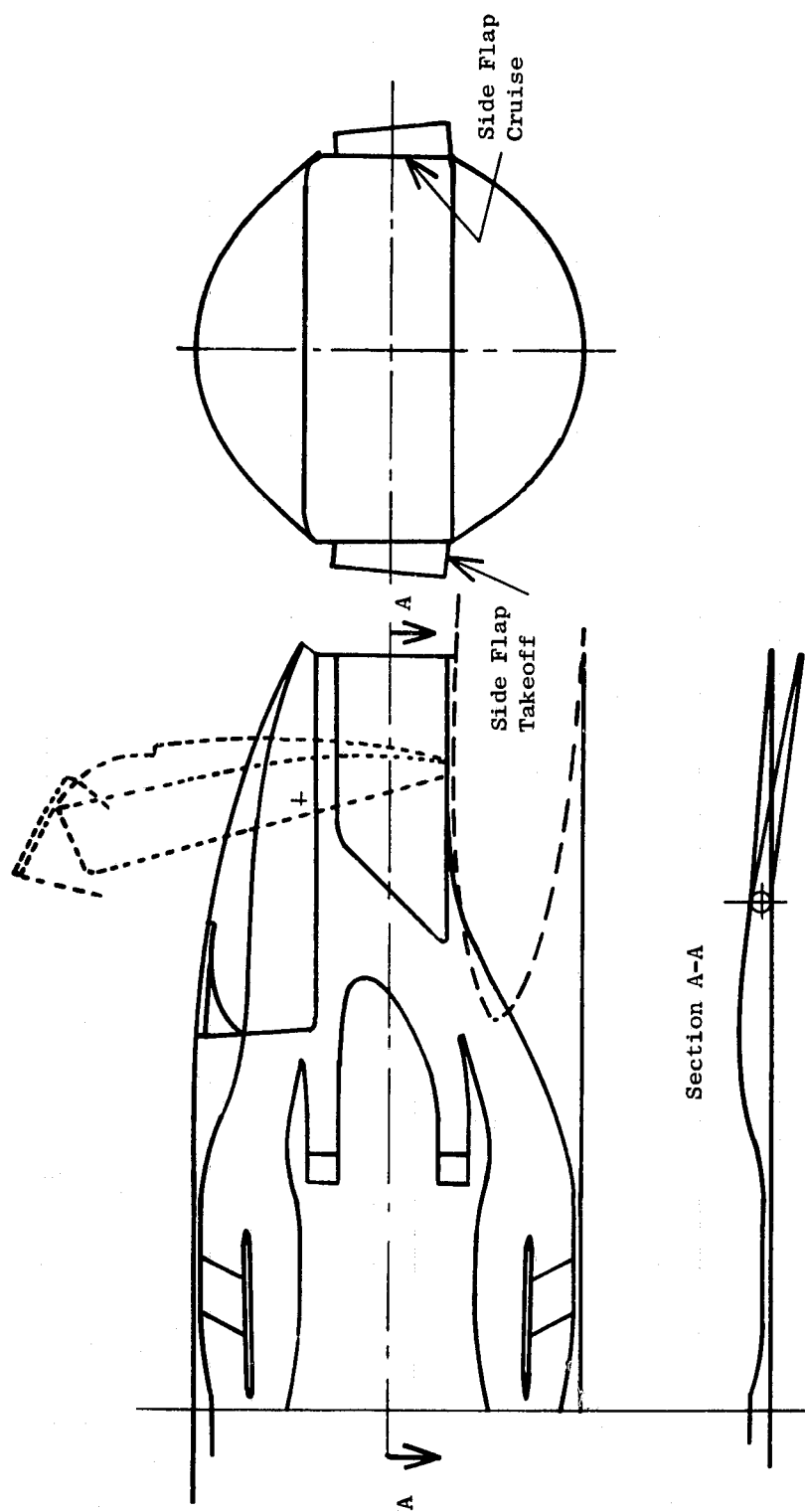
The fan duct inner and outer walls are circular in cross section with a transition to a "D"-shaped nozzle beginning in the vicinity of the LP turbine rear frame. The fan and core streams flow confluent through the aft duct and exit through a nozzle having an aspect ratio (width/height) = 3.07 at takeoff. The nozzle contains side flaps for exhaust area control and a blocker-door-type reverser. The exhaust system is schematically shown on Figure 14-9.

The overall duct and nozzle system length is increased 25.4 cm (10 in.) for the experimental engine to satisfy requirements for rotatability of the nozzle for Peebles (180° rotation) and NASA Lewis testing (90° rotation), and also to satisfy acoustic treatment requirements in the core nozzle. The plane of rotation has been established at station 254, 15.24 cm (6 in.) downstream of the turbine mounting system.

Important OTW nozzle geometric parameters are schematically shown on Figure 14-10. Proper selection of these parameters is required for obtaining the jet flap turning required at takeoff and approach flight condition without encountering large subsonic cruise drag losses.

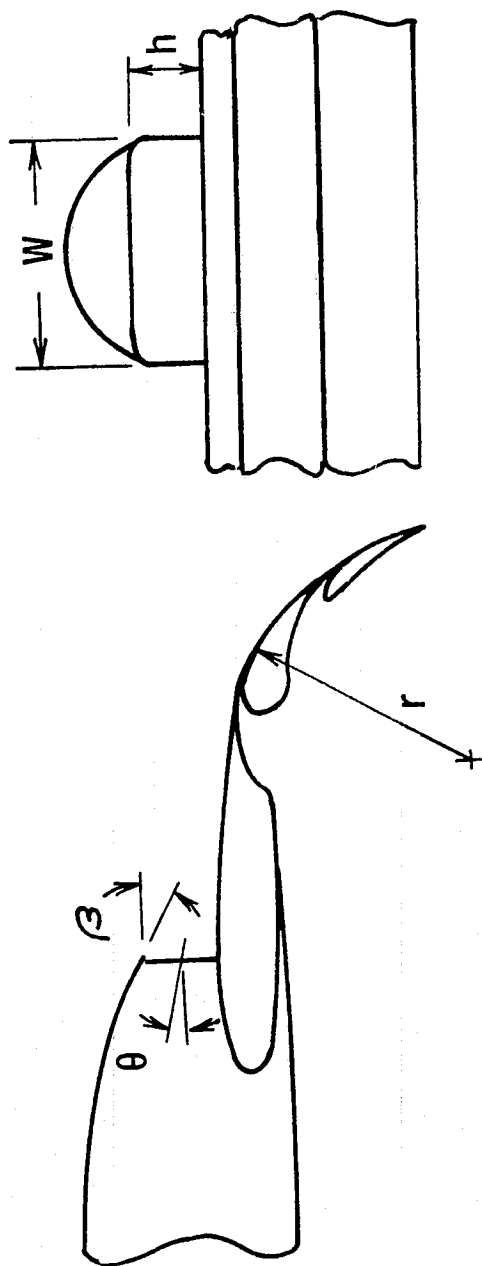
To achieve jet turning over flap systems having radius r , the jet exhaust must be spread out over the flap span. This spreading out causes the jet to thin down making it possible to negotiate the turn via coanda effect. The spreading is enhanced by the nozzle deflection angle (θ) and aspect ratio (width/height, w/h). These two parameters are interrelated such that any number of combinations would provide the desired jet turning for a flap of given radius. However, nozzles having large height/flap radius ratios also require large nozzle deflection angles, which in turn create steep boattail angles, β , (since θ is a function of β) and high cruise drag. Hence the OTW exhaust system must strike a balance between each of these parameters to ensure good-turning characteristics during powered lift flight and low drag at cruise.

In order to achieve maximum jet flow turning (60°) over the wing flaps at approach conditions a nozzle height/flap radius ratio of 0.3 has been selected. The exhaust flow is inclined downward toward the wing upper surface 13° 30' with respect to the engine centerline. This flow inclination angle results in a nacelle boattail angle of 28.5° at the top of the nozzle. Considering the low cruise Mach number 0.72 and the desirability of keeping wing geometry simple (free



Note: Side Door Concept - Boeing Input

Figure 14-9. QCSEE OTW Fan Duct and Nozzle System.



- Nozzle Deflection Angle, θ - Degrees
- Boattail Angle, β - Degrees
- Nozzle Aspect Ratio, Width/Height - W/h
- Nozzle Height/Flap Radius - h/r

Figure 14-10. OTW Exhaust System Parameters.

of extraneous deflector devices, for instance), the higher boattail angle and associated drag are an acceptable trade for a 0.72 cruise Mach number aircraft design. Flow spreading is further enhanced by the side flap area variation concept employed. These flaps, open at takeoff and approach power, make it possible to maintain airflow as high as possible for inlet Mach number control ($M_{throat} = 0.79$ at takeoff) for noise abatement. At cruise conditions, the side flaps close for area control and to minimize jet spreading for high cruise performance.

Core Nozzle Design

The core nozzle is designed to provide matched cycle conditions at the point of confluency with the fan flow. The core exit area is matched to the fan duct flow area at this point so that a stream static pressure balance is achieved. The core nozzle effective area is 3884 cm^2 (602 in.^2).

For the experimental propulsion system, the core nozzle is designed to utilize the UTW core nozzle centerbody. Core duct length is dictated by acoustic treatment requirements for the 610 m (2000 ft) runway noise goals. Wing skin temperature problems related to hot core exhaust scrubbing are eliminated by utilizing a steel plate simulated wing surface. The flight propulsion system core nozzle design is shorter, having a less severe noise problem [(914 m (3000 ft) runway)], hence less treatment length. Wing temperature problems are alleviated by canting the core nozzle and centerbody upward to provide a greater displacement of hot gases above the wing surface. This same concept is employed by the Boeing Company on the AMST aircraft program.

Thrust Reverser Design

Thrust reversal is accomplished by deployment of a fixed-pivot blocker door reverser stowed in the top of the OTW nozzle. The pivot point is located to position the blocker an appropriate distance aft of the emerging fan and core streams to avoid fan and core backpressuring. Final reverse flow direction is accomplished by an articulating lip at the top of the blocker door. The proper area is achieved by the formation of an aerodynamic throat across the lip of the reverser.

Pylon Design

The mounting system employed on the OTW flight propulsion system does not require a structural pylon as on the UTW configuration. However, a small accessories pylon positioned on the bottom of the engine cowl is employed for C & A packaging and drain systems. The aerodynamic blockage caused by the accessories pylon causes no real problem in meeting fan duct design objectives.

The OTW experimental propulsion system will employ the same pylon and engine mounting system used for UTW propulsion system. The pylon shape inside the fan duct is identical to the UTW system back to the pylon maximum thickness (station 248), beyond which point it closes out into a 15° (half angle) boattail inside the common exhaust nozzle. Aerodynamic cleanliness is achieved in the 90° and 180° nozzle rotation positions by appropriate side plate filler pieces which close out the pylon with the nozzle duct wall.

14.5 SUPPORTING DATA

Much of the high bypass ratio fan exhaust system design experience obtained from TF39, CF6, and Quiet Engine programs can be applied to the QCSEE engine propulsion systems. Experimental programs are in place for new technology areas critical to successful completion of the QCSEE contract. These programs include (1) inlet aerodynamic tests for high throat Mach number, high angle of attack capability required for meeting noise goals, and STOL aircraft takeoff and landing angles of attack respectively, (2) reverse flow inlet/exlet aerodynamic development tests, and (3) OTW nozzle and target reverser. Each of these programs is discussed in the following paragraphs.

UTW/OTW Inlet

The inlet development plan uses both 30.48 cm (12 in.) and 50.8 cm (20 in.) scale model inlet testing to arrive at the design for the boiler plate and composite inlets. The formulation of the inlet plan allows utilization of the 30.48 cm (12 in.) model test results in designing the 50.8 cm (20 in.) model test hardware.

The QCSEE contract requirement for the inlet must either meet or exceed the operational requirements of both the YC15 EBF and the YC14 OTW (Figure 14-11). The fixed demonstration points are an 18 m/sec (35 knot), 90° crosswind and a 50° angle of attack at the 41.18 m/sec (80 knots) conditions. The inlet must operate satisfactorily at these demonstration points over a range of airflows from idle thrust to maximum thrust.

Assimilation of the design requirements produced the test matrix described in Table 14-II. Execution of this matrix during June 1974 resulted in 583 data points from four inlet configurations. Figure 14-12 shows one of the inlet configurations installed in the NASA LeRC 2.74 m x 4.57 m (9 x 15 ft) wind tunnel.

Representative recovery data from the 30.48 cm (12 in.) scale model wind tunnel testing (14-13) indicates that it is possible to meet the design goals of 50° angle of attack with a 0.79 throat Mach number at the 41.18 m/sec (80 knots) takeoff and approach velocity. The excess angle of attack capability may be utilized as safety margin or to reduce the allowable inlet contraction ratio. The separation boundaries (Figure 14-14) for the inlet indicate a viable configuration between the 0.79 takeoff throat Mach number and the approach flight idle (minimum airflow) range of 0.38-0.46. Slight differences between the separation boundaries as indicated by the Kulite and steady-state measurements has been at least partially explained by calibration differences.

To assist in rapid assessment of data and test direction purposes, on-line indications of recovery and distortion were generated via Kulite high-response transducers programmed into an analog computer (Figure 14-15). Clear evidence of separation is manifested by the abrupt decrease in recovery and increase in distortion. Amplitude fluctuations in the above parameters occur since the Kulite/analog computer system provides real time, high frequency response calculations.

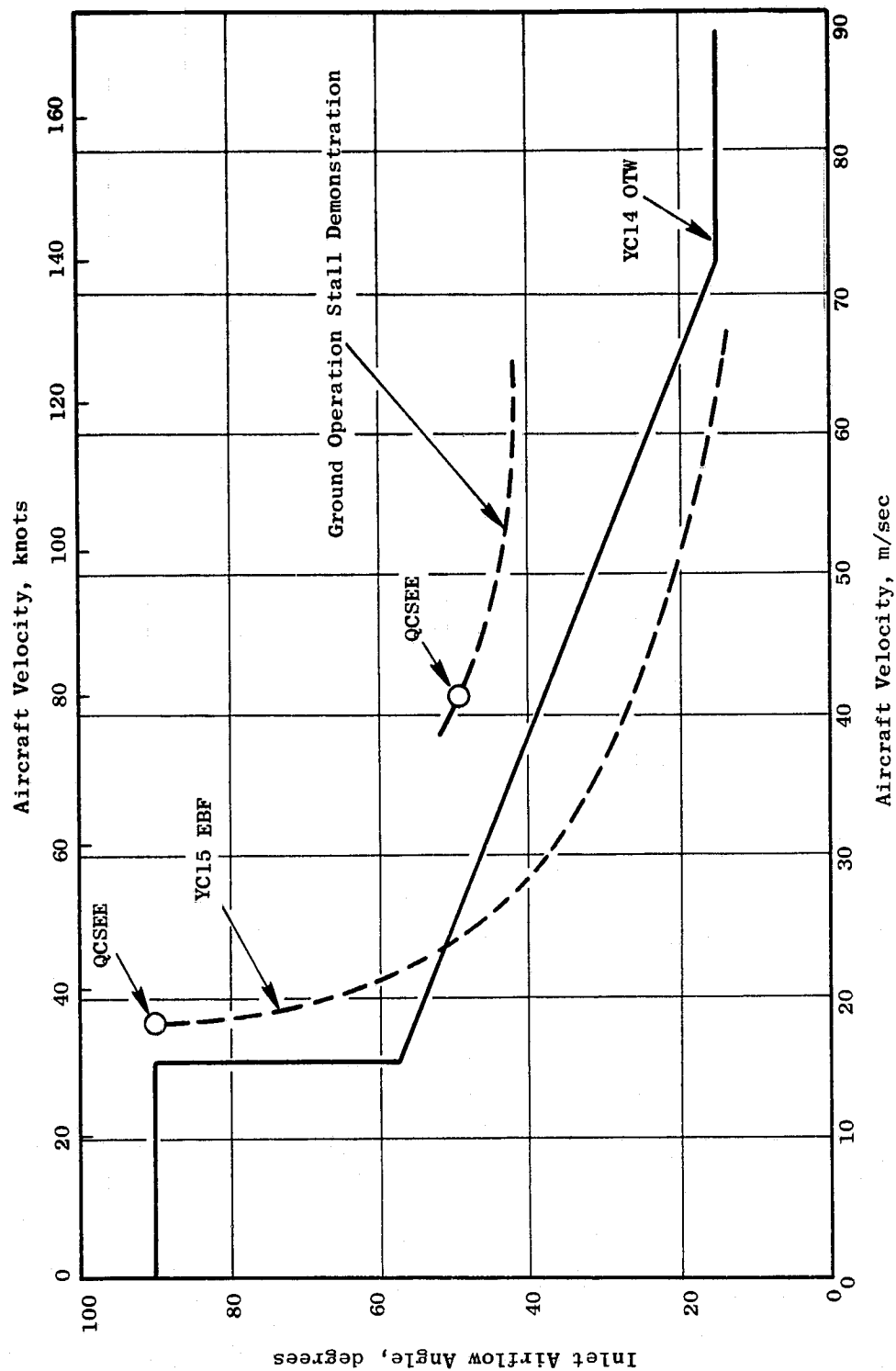


Figure 14-11. STOL Aircraft Design Envelope.

Table 14-II. 30.48 cm (12 in.) Inlet Test Matrix.

Model Variables

$\frac{D_{HL}}{D_{TH}}$	$\frac{D_{HL}}{D_{MAX}}$	$\frac{X}{D}$	External Forebody
1.17	0.905	0.2	DAC
1.21	0.905	0.2	Series 1
1.25	0.905	0.2	
1.21	0.935	0.175	NACA 1 - Series

Test Condition Variables

Angles of Attack

0°, 15°, 30°, 40°, 50°, Separation -5°, Separation +5°

Tunnel Velocities

Static, 18 m/sec (35 knots) x Wind, 41.18 m/sec (80 knots),
61.73 m/sec (120 knots)

Inlet Throat Mach Number

Flight Idle, 0.60, 0.70, 0.75, 0.79, 0.82, Max. Flow

Measurements

Inlet Wall Static, Inlet P_t , Selected Time Variant P_t & P_s

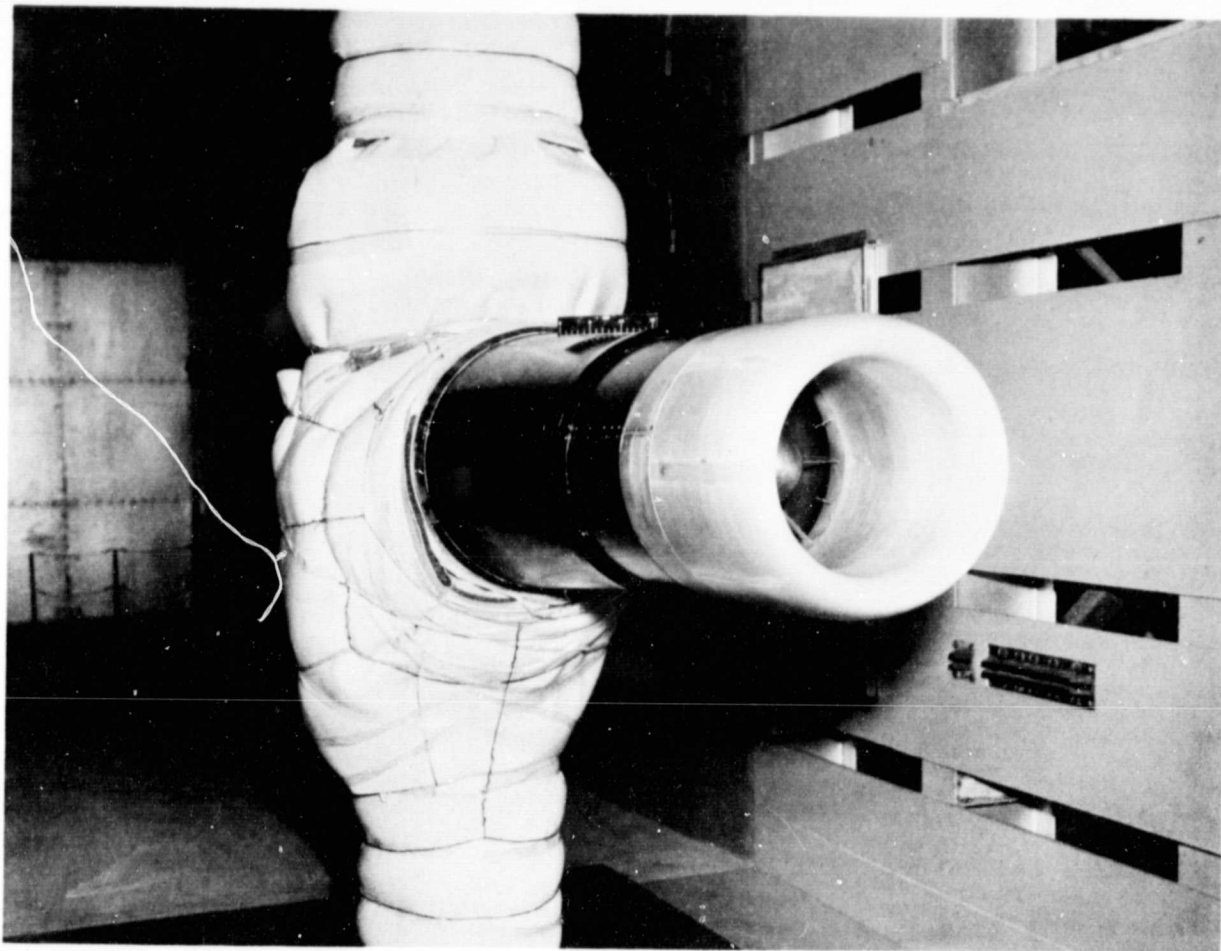


Figure 14-12. QCSEE 30.48 cm (12 in.) Inlet Model in NASA Lewis 2.74 x 4.57 m (9 x 15 ft) Wind Tunnel.

ORIGINAL PAGE IS
OF POOR QUALITY

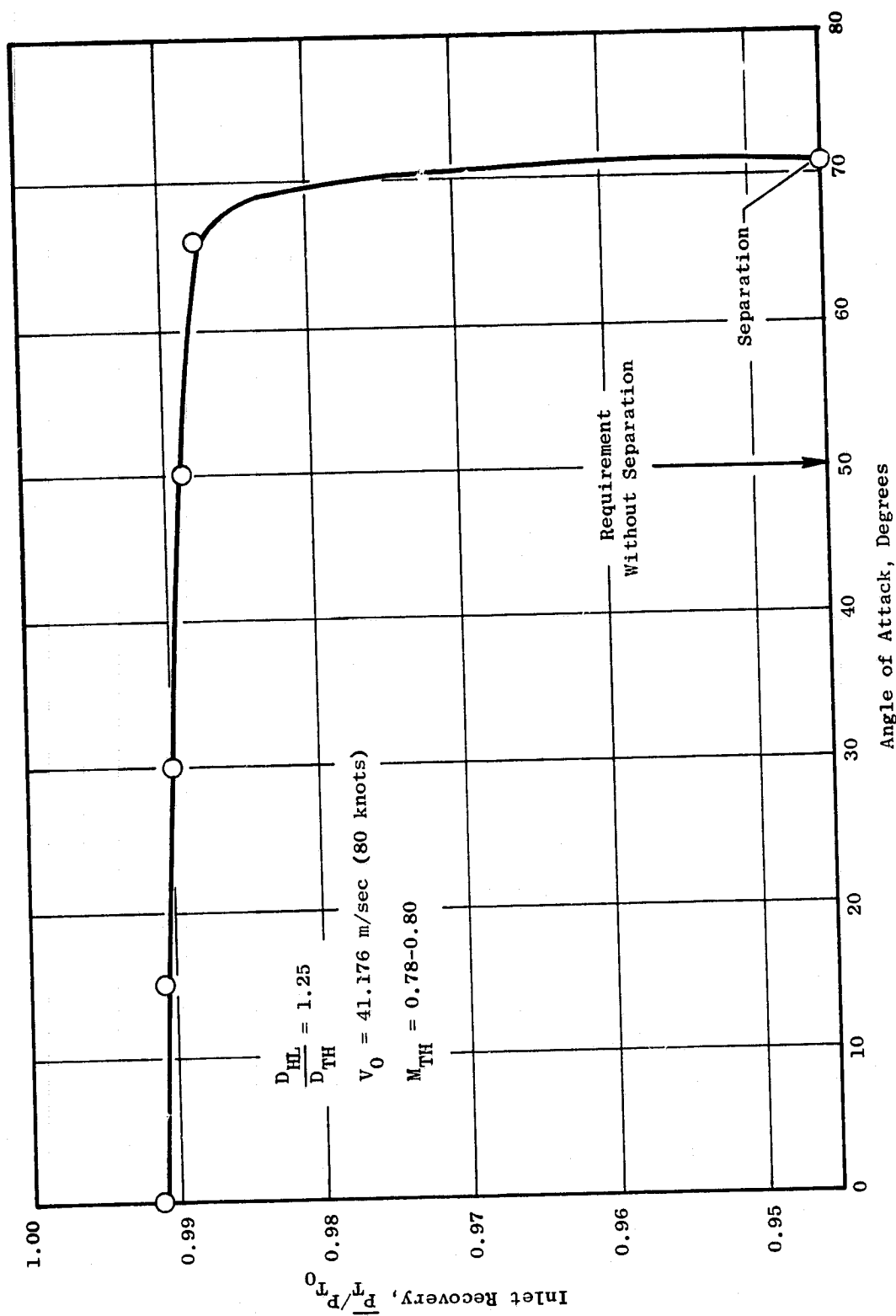


Figure 14-13. QCSEE 30.48 cm (12 in.) Inlet Test Results from NASA Lewis 2.74 x 4.57 m (9 x 15 ft) Wind Tunnel.

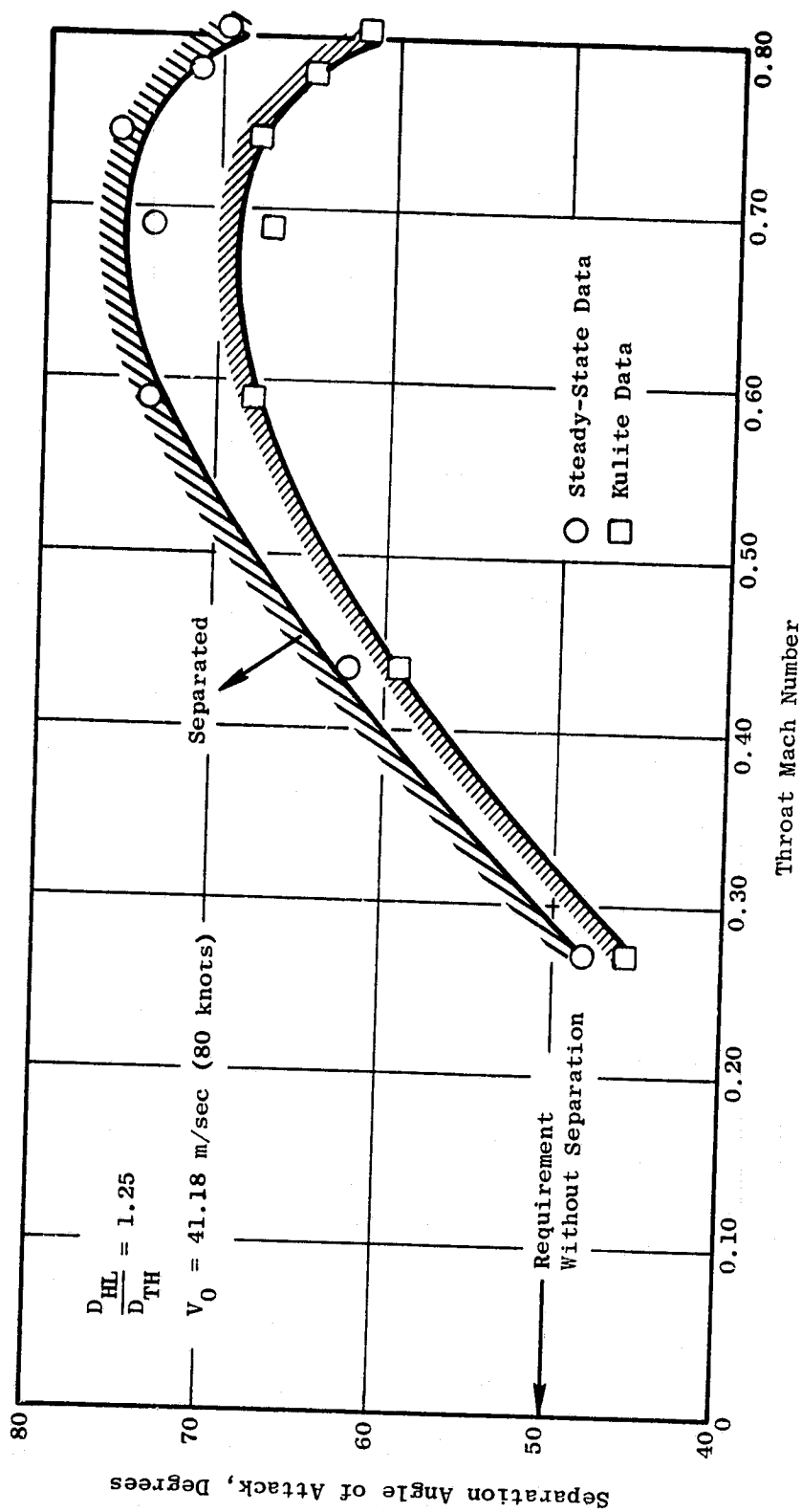


Figure 14-14. QCSEE 30.48 cm (12 in.) Inlet Test Results, NASA Lewis 2.74 x 4.57 m (9 x 15 ft) Wind Tunnel - Inlet Separation Boundaries.

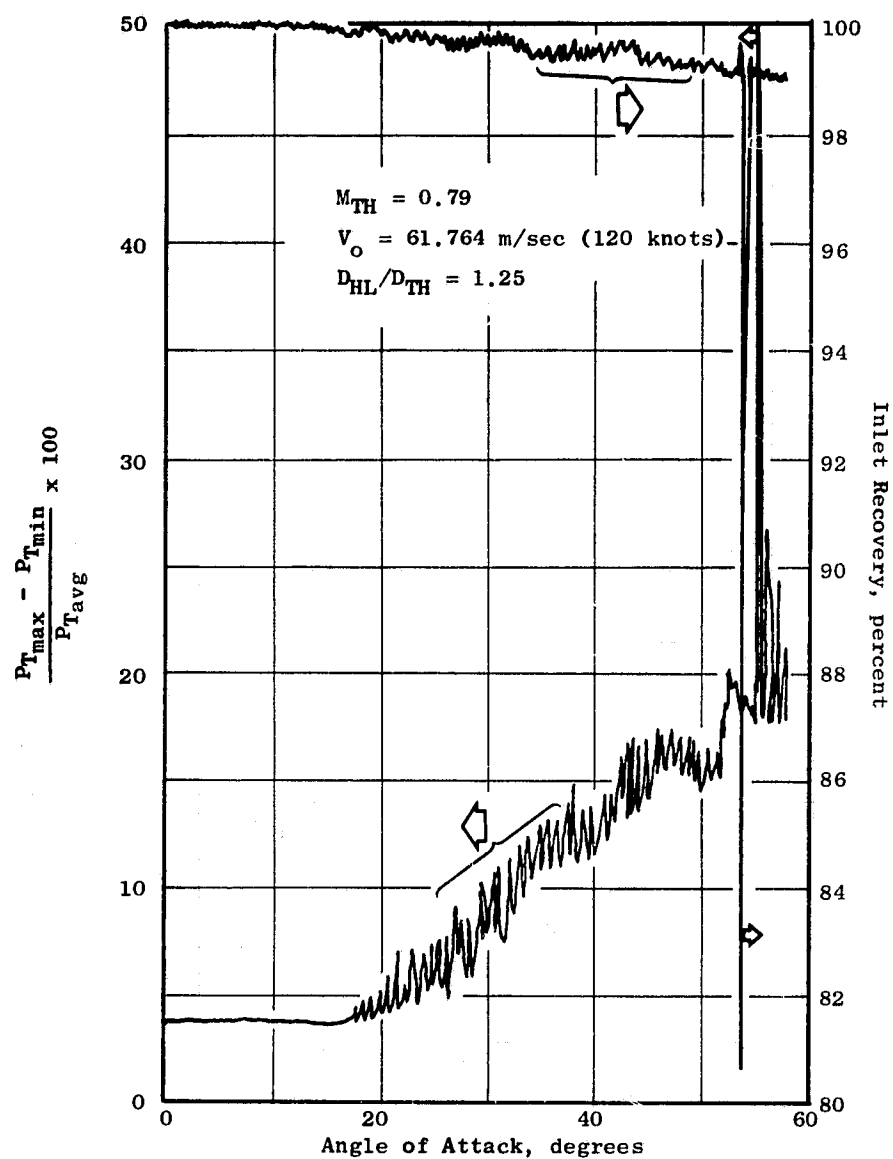


Figure 14-15. On Line Dynamic Transducer Results from NASA Lewis 2.74 x 4.57 m (9 x 15 ft) Wind Tunnel Tests.

At each throat Mach number setting, an angle of attack sweep was made from zero degrees to a point beyond inlet separation. Both steady-state and Kulite dynamic measurements were employed for this purpose. The steady-state indicators included lip wall static and diffuser exit total pressures in order to determine whether each separation originated at the lip or in the diffuser. From Figure 14-16, preliminary data at 41.18 m/sec (80 knots) show that the 1.21 and 1.25 contraction ratio designs provide unseparated inlet capabilities that are comparable and about 25° greater than the 1.17 contraction ratio in the 0.6-0.8 throat Mach number region. Thus, either of the former designs satisfies the 0.79 throat Mach/50° angle of attack requirement, with the 1.25 design being slightly better near the flight idle power setting (0.38-0.46 MTH as presently defined).

13.97 cm (5.5 in.) Exlet Aerodynamic Development Program

Figure 14-17 shows the QCSEE UTW scale model nacelle and exlet configuration installed on a 13.97 cm (5.5 in.) fan in the 2.74 m x 4.57 m (9'x 15') wind tunnel at NASA Lewis Research Center. This test program, scheduled for August 1974, will provide reverse mode airflow and exlet recovery characteristics expected of the QCSEE UTW propulsion system for a range of ground speeds between static and 66.91 m/sec (130 knots). Static pressure measurements on the flare internal and external surfaces and also on the fan inner flow path will be made for aerodynamic loading information and also for diagnostic information during data analysis. Dynamic instrumentation (two 4-element rakes) will also be used for unsteady flow analysis.

The test matrix shown on Figure 14-18 includes 11 flap length/flare angle combinations as shown. Mechanical constraints for a reasonable QCSEE configuration limited flare angle to 36° and flap length to 55.88 cm (22 in.). Reasonable exlet recovery dictates a lower boundary for area ratio of 1.4. Thus, within the above design constraints, the test matrix covers the region of interest using a typical "design-of-experiments" methodology.

Each of these configurations will be tested at four velocities, 0, 20.58, 41.18, and 66.91 m/sec (0, 40, 80, and 140 knots) including some 18 m/sec (35 knot) crosswind testing, and will simulate an exlet airflow range from 204 to 317 kg/sec (450 to 700 lb/sec) relative to full scale.

OTW Nozzle/Reverser Aerodynamic Development

A 20.32 cm (8 in.) diameter two-flow scale model test is planned for November-December 1974, at Fluidyne, to establish the aerodynamic flow path and performance for the OTW nozzle and thrust reverser. These tests will simulate the OTW nozzle configuration from approximately the LP turbine frame aft. Important takeoff mode internal performance information on fan and core flow matching characteristics at the core nozzle exit plane will be derived in addition to the usual nozzle flow and velocity coefficient data. These flow matching characteristics will provide a base line for reverse thrust analysis and selection of reverser blocker door axial position.

One of the important requirements of the OTW nozzle design is achievement of jet turning over the wing flap surface to provide powered lift during takeoff and

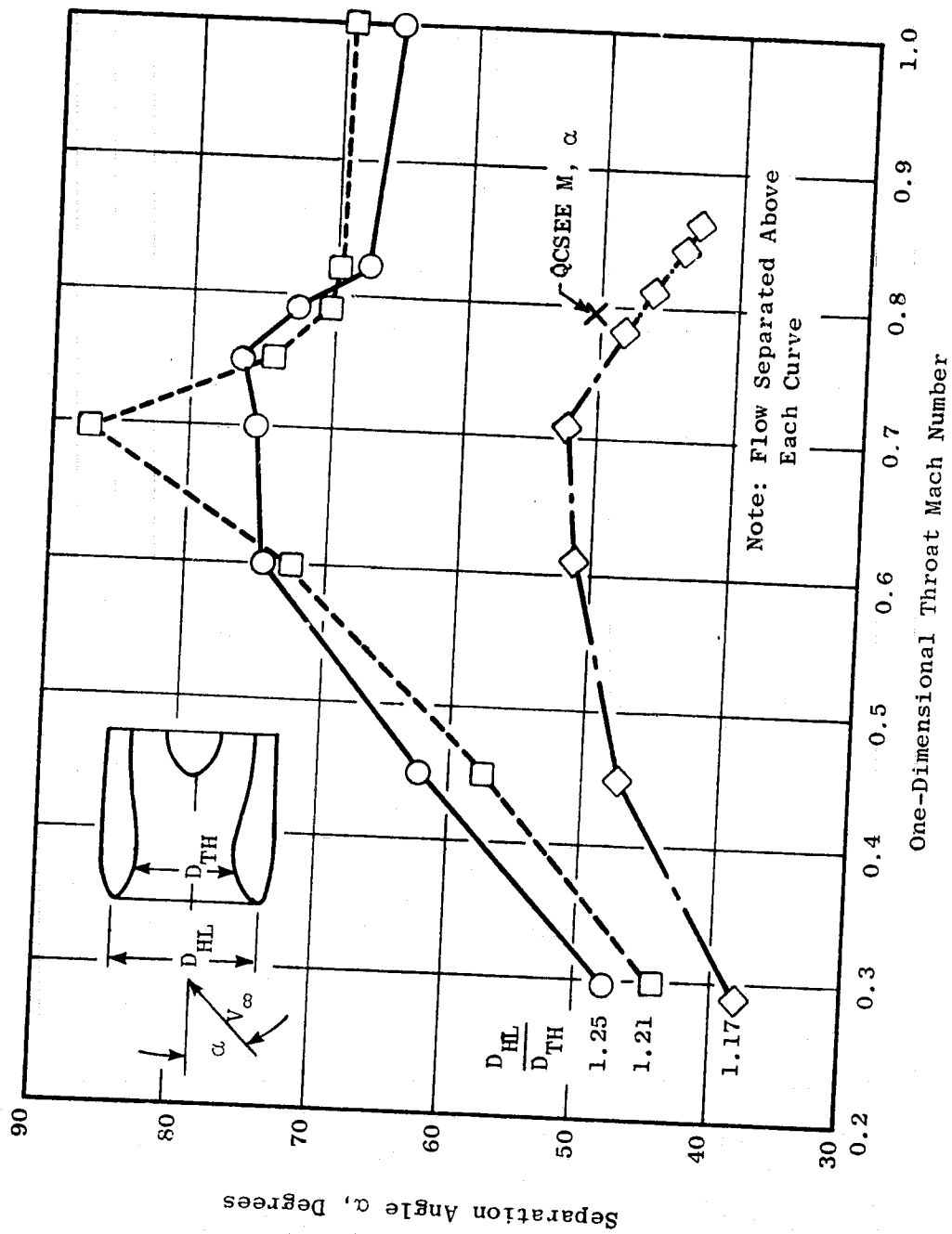


Figure 14-16. Inlet Flow Separation Bounds - $V_\infty = 41.18$ m/sec (80 knots) - Preliminary Data.

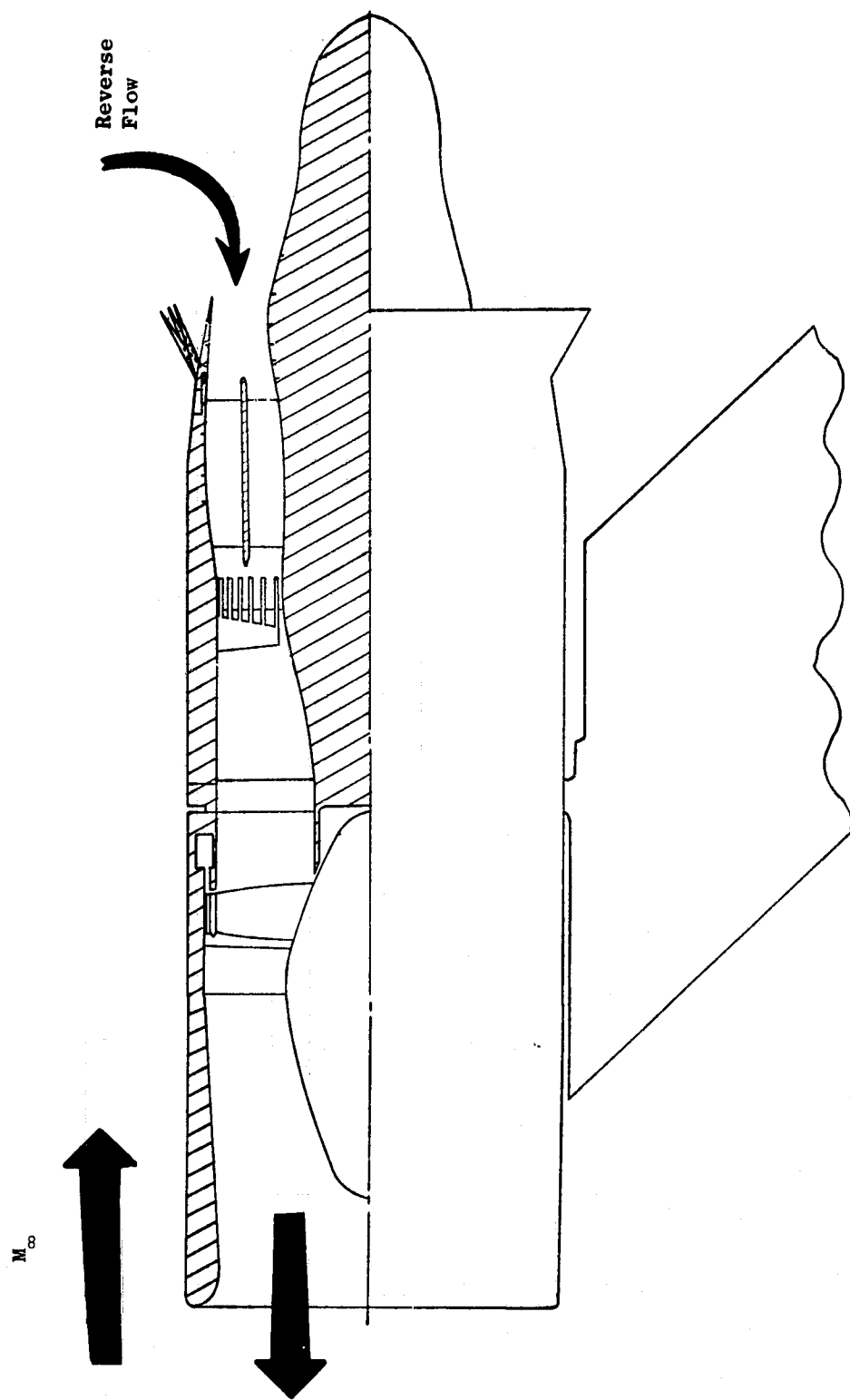


Figure 14-17. QCSEE 13.97 cm (5.5 in.) Exlet Model, Typical Tunnel Installation.

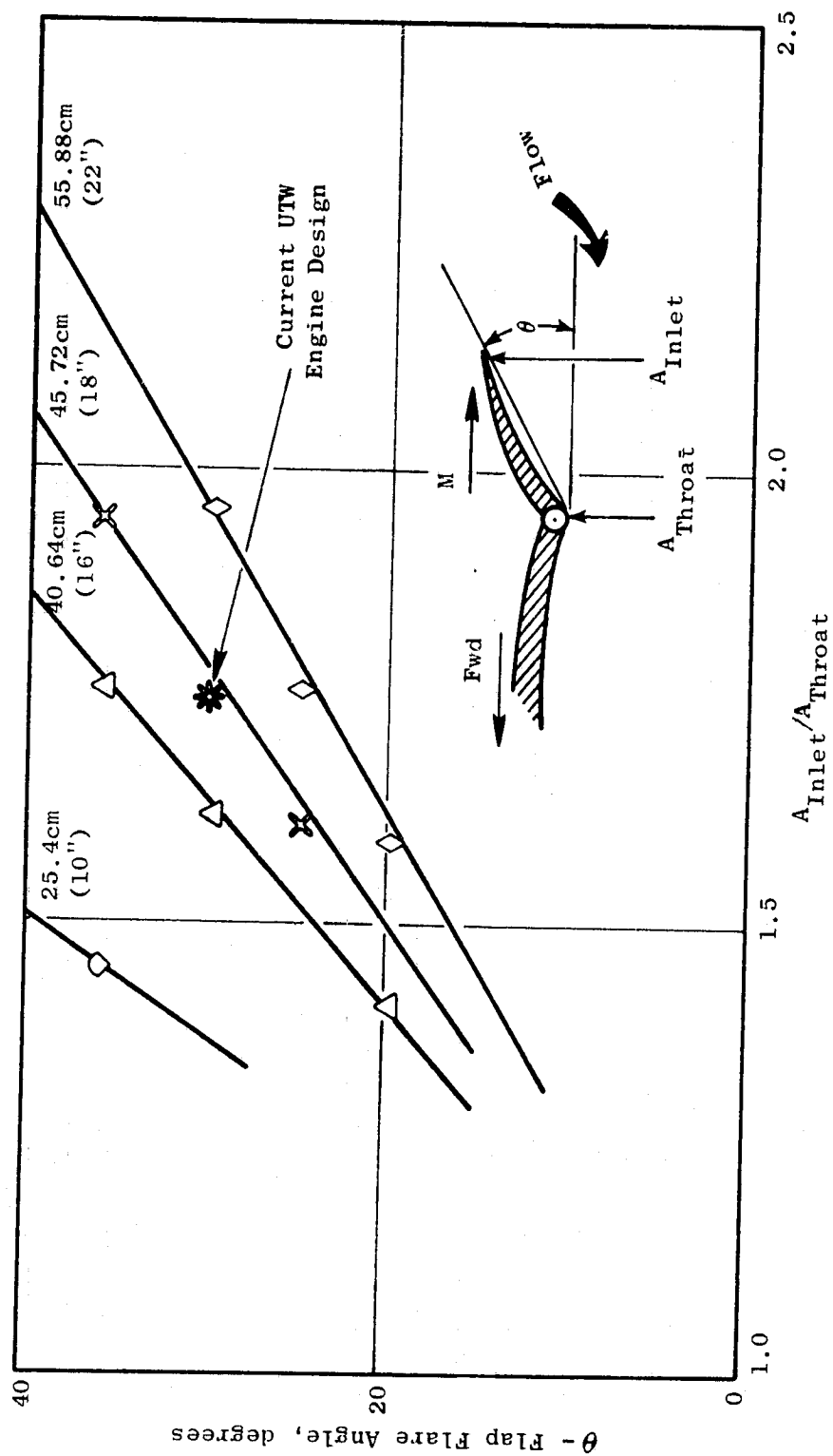


Figure 14-18. QCSEE Exlet Test Matrix.

approach. Some experimental results which show some of the critical parameters for jet turning are presented in Figure 14-19. This figure shows the relationship between jet flap turning angle (δ) and nozzle deflection angle (θ) for a range of nozzle height-to-flap radius ratios (h/r) between 0.3 and 0.66. The QCSEE OTW nozzle design status as of the PDR data (vertical line at $\theta = 13^\circ 30'$) indicates that the 60° of required turning at approach power can be met provided the nozzle height/flap radius ratio, h/r , = 0.3. The reference data was obtained from NASA Langley data as presented by J. Johnson in SAE Paper 740470, Dallas, Texas, April/May 1974.

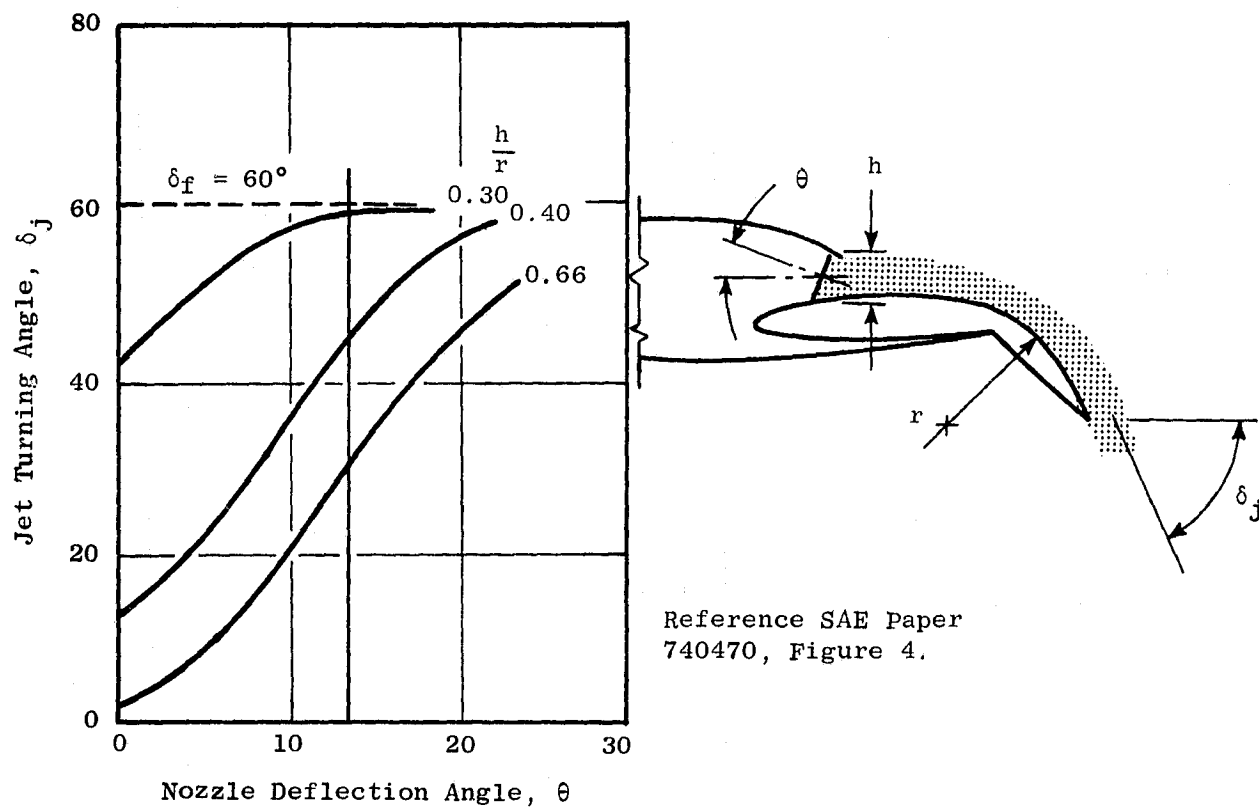


Figure 14-19. Effect of Nozzle Deflection on Turning Angle
(Reference: SAE Paper 740470, Figure 4).

SECTION 15.0

NACELLE MECHANICAL DESIGN

15.1 SUMMARY

15.1.1 UTW Flight Propulsion System

The "flight" Under-the-Wing propulsion system installation is shown in Figure 15-1 and 2-7. The nacelle maximum diameter is 198 cm (78.8 in.), and the overall length is 414 cm (163.0 in.) to the fan exhaust plane (engine station 256.5) and 535 cm (210.7 in.) to the tip of the core exhaust nozzle plug (engine station 304.2).

The short-haul aircraft using the UTW propulsion systems has high wings with externally blown flaps for powered lift (see Figure 17-2). This configuration results in a height to the bottom of the nacelle of approximately 3.05 m (10 ft). Therefore, a maintenance stand will be required to reach the engine accessories. A top-mounted accessory gearbox has been selected for the UTW installation because it yields several significant advantages in combination with the use of the integrated nacelle concept.

- Reduced Frontal Area - The top gearbox fits in the silhouette of the aircraft pylon and eliminates the bulge at bottom of the nacelle required for accessories mounted under the engine (reduced aerodynamic installation losses).
- Shorter Pipes and Wires - With accessories on top, the result is shortest "run" from the engine to the accessories and then on to the aircraft wing. On the DC-10/CF6 type installation, pipes have to be routed around the fan casing (reduced internal aerodynamic losses).
- Eliminates Bottom Pylon - Because there are no bottom accessories, no bottom pylon is required (reduced internal aerodynamic losses).
- Permits Integrated Engine/Nacelle Structure - The high Mach inlet reduces required throat area (smaller diameter throat), with the throat to highlight diameter ratio required for good crosswind flow capability. The highlight to maximum diameter ratio consistent with aircraft Mach number requirements permits nacelle thickness and maximum diameter to be kept to a minimum. This results in combining the fan cowl (nacelle component) into the fan frame structure, and completes the integration of nacelle and engine structure.
- The nacelle component eliminated reduces cost and weight. The resulting thin walls, 8.9 to 10.2 cm (3.5 to 4.0 in.), uniformly around the nacelle, compared to 25.4 to 50.8 cm (10 to 20 in.) thickness on the DC-10/CF6, is ideal for composite construction.

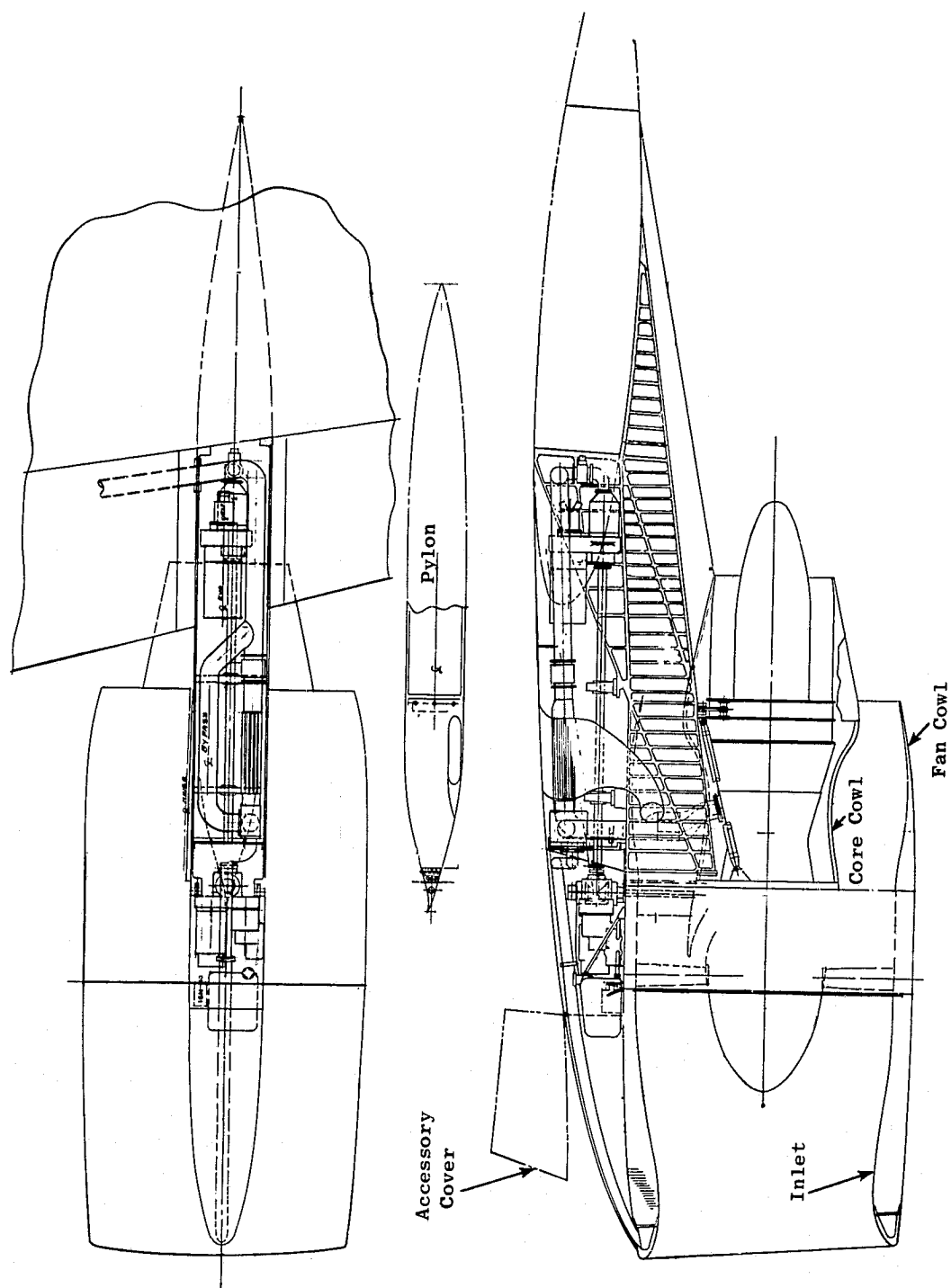


Figure 15-1. Under the Wing Flight Propulsion System.

The accessory cover (see Figure 15-1) for the top gearbox rotates forward and is supported from the inlet. This permits direct access to install or remove any component and allows visual inspection of accessories and piping while the engine is operating.

Since the time of the original QCSEE proposal several changes have been made to the flight propulsion system:

- Nacelle maximum diameter increased to 2 m (78.8 in.), due to fan tip diameter increase, required inlet geometry, and reduced Mach number in the fan exhaust duct.
- Hinged accessory cover - discussed above
- Changed to flare nozzle on fan exhaust in place of inflatable nozzle and exlet door, to facilitate area modulation.
- Fuel/Oil Heat Exchanger replaces the large air/oil exchanger.
- Front engine mount has been moved to the core cowl cavity to provide improved access to the accessories and gearbox.
- Hinged inlet was eliminated based on recommendations from Douglas and American Airlines.
- Acoustic splitter in fan duct deleted since it is not required to meet noise objective with 914 m (3000 ft) take-off.

15.1.2 QTW Flight Propulsion System

The flight Over-the-Wing propulsion system installation is shown in Figure 15-2 and 2-11. The nacelle maximum diameter is also 2 m (78.8 in.) and the overall length is 667 cm (262.8 in.) to the edge of the confluent flow exhaust nozzle (engine station 356.4). This is 133 cm (52.2 in.) longer than the UTW nacelle.

The short-haul OTW aircraft has a high wing (see Figure 17-9). Bottom of nacelle is approximately 4.6 m (15 ft) off ground. A maintenance stand is required. For many of the same reasons stated for mounting the UTW accessories on top of the nacelle, the OTW accessories and gearbox are on the bottom of the nacelle:

- Reduced frontal area - no top pylon is required.
- Shorter pipes and wires - services follow direct line to wing
- Eliminates top pylon
- Permits integration of engine and nacelle structure with "hybrid" (High Mach) inlet

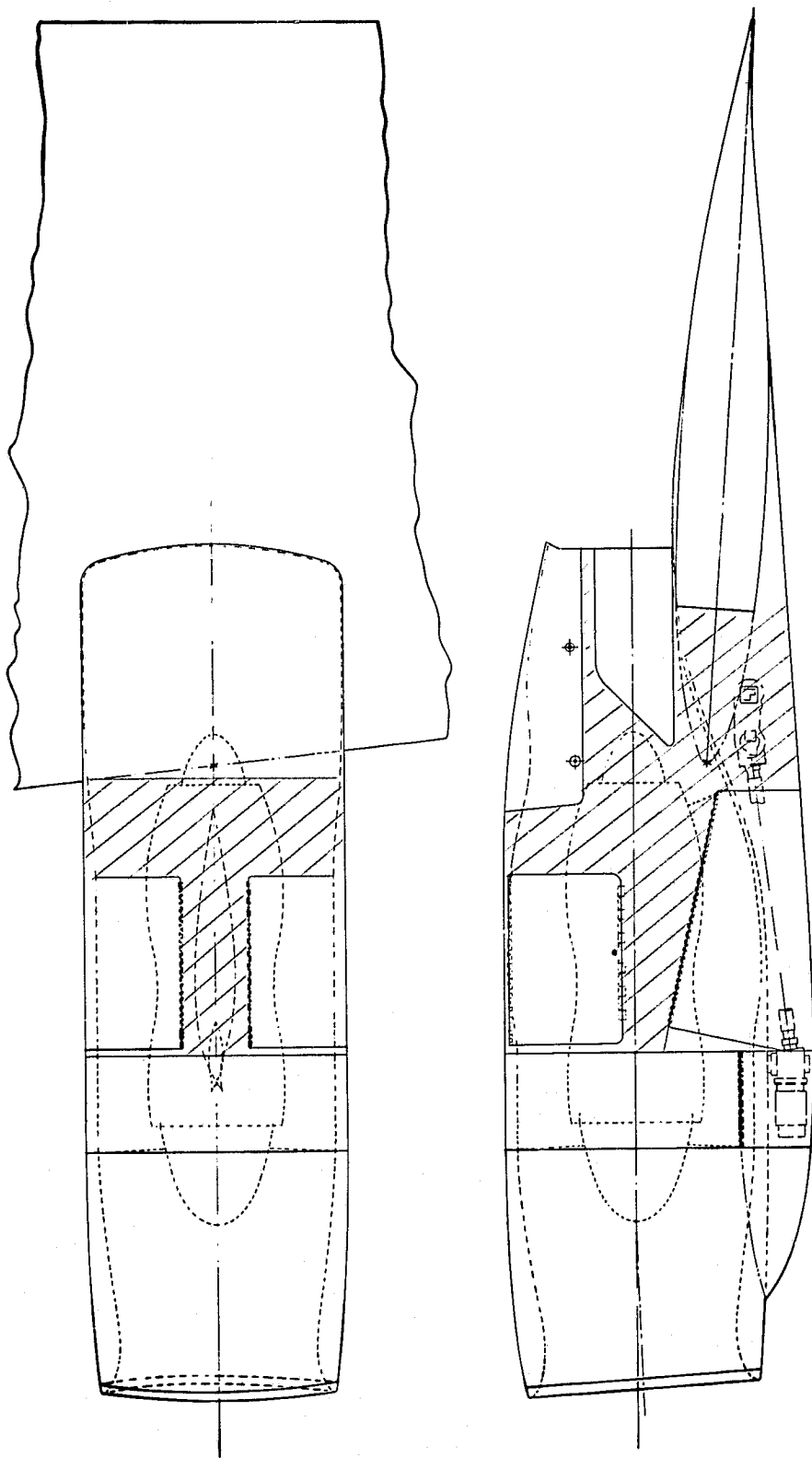


Figure 15-2. Over the Wing Flight Propulsion System.

ORIGINAL PAGE IS
OF POOR QUALITY

Since the original QCSEE proposal, major effort on the OTW engine has been the definition of good aerodynamic/mechanical internal and external flow lines. The present configuration is shown in Figure 15-3. Flight OTW propulsion system changes during the preliminary design include:

- Side doors for required exhaust nozzle area control and flow spreading over the wing.
- Nacelle maximum diameter increased to 2 m (78.8 in.) - reasons same as UTW
- Fuel/oil heat exchangers replace large air/oil exchangers
- Hinged inlet eliminated
- Acoustic splitter in fan duct deleted with 914 m (3000 ft) runaway

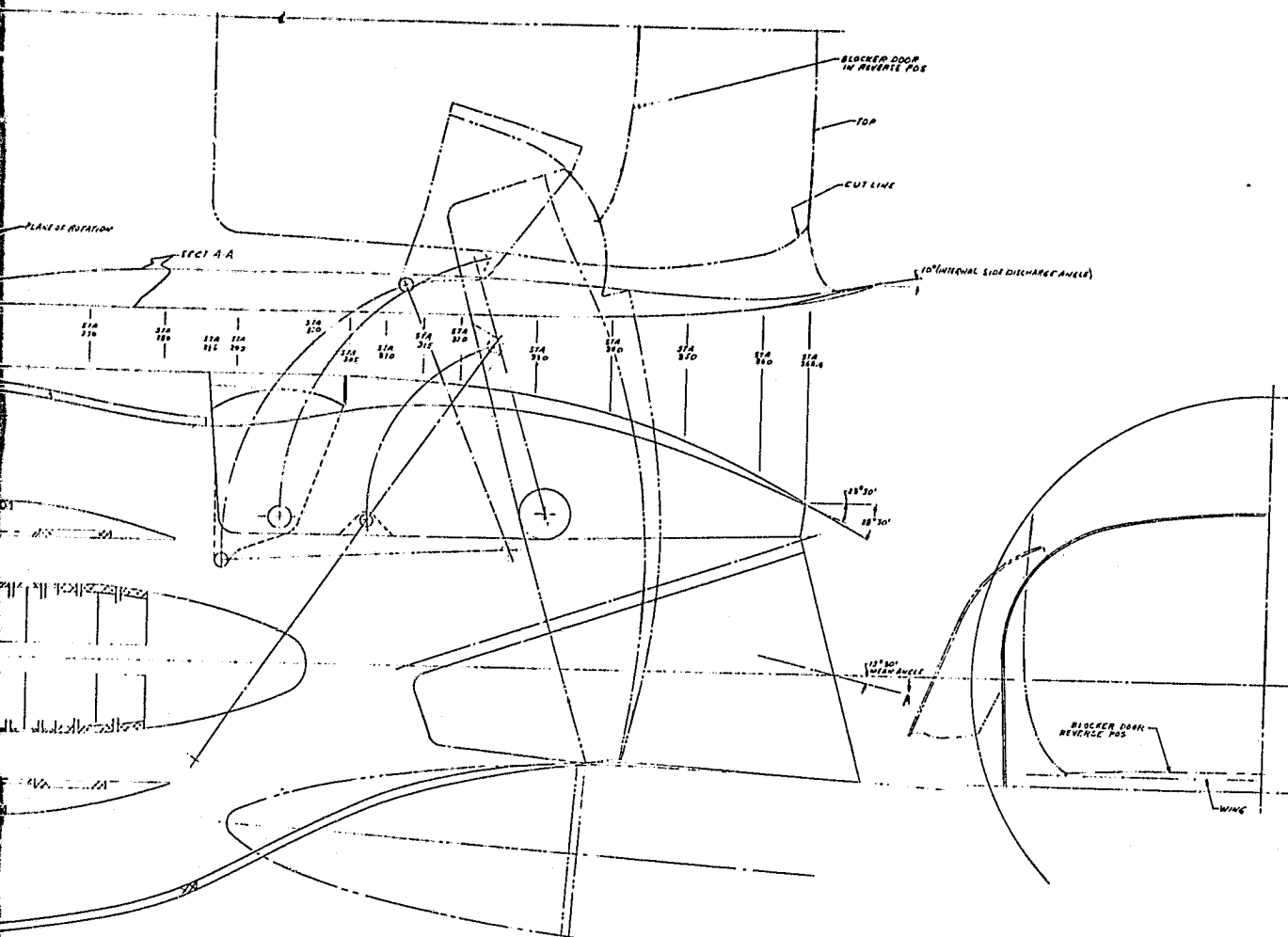
15.1.3 UTW Experimental Propulsion System

The Under-the-Wing experimental propulsion system is shown in Figure 2-5. The nacelle maximum diameter is the same as in the flight installation; however, the overall length is 17.8 cm (7 in.) greater to house the 101.8 cm (40 in.) long fan exhaust splitter required to meet acoustic objectives with a 610 m (2000 ft) runway. The overall length is 432 cm (170.0 in.) to the fan exhaust plane (engine station 264) and 553 cm (217.7 in.) to the core nozzle tip (engine station 311.2).

Initial testing of the UTW system in the second quarter of 1976 will incorporate the boiler plate nacelle. Internal flow lines will be the same as the flight system with the 17.8 cm (7 in.) extension. The external lines will be approximately 8.9 cm (3.5 in.) on the radius larger than the flight configuration. This is required for the structure to support the replaceable acoustic panels. There will be two complete sets of treated panels for noise suppression and one set of "hard-walls" for the base line noise run. Acoustic fan exhaust splitters will be replaceable. All boiler plate nacelle hardware is supported from the test stand to prevent overloading of the composite fan frame. Primary component attachment joints will be the same as in the flight configuration to assure normal flange air and noise leakage. Secondary joints will be provided to "break" the load path between the engine and the test-stand-mounted boiler plate components (i.e., normal engine thrust and other operating loads will be carried through the main engine mounts to the test stand).

Upon completion of initial testing, the required acoustic treatment will be selected and the composite nacelle components constructed. In these parts, the acoustic treatment is an integral part of the nacelle structure. This UTW propulsion system, after initial testing at Peebles, will be shipped to NASA in mid-1977.

The conceptual design of the experimental engine nacelle components and installation were presented at the preliminary design review. The actual facility and hardware design will take place during the latter part of 1974 and



3. OTW Flow Paths.

ORIGINAL PAGE IS
OF POOR QUALITY

499

C-3

2 FOLDOUT FRAME

the preliminary design will be reviewed with NASA in the first quarter of 1975 prior to hardware construction. During this period close coordination with NASA will be required to assure that the experimental propulsion system installation is compatible with NASA facilities.

15.1.4 OTW Experimental Propulsion System

The Over-the-Wing experimental propulsion system shown in Figure 2-9 will have a nacelle maximum diameter of approximately 2.18 m (86 in.) with the boiler plate components. The inlets and fan cowls through the flar nozzle hinge will be the same hardware that was used on the initial UTW system tests. An additional set of acoustic panels will be procured that are tailored to the OTW system noise requirements.

The nacelle length of the OTW experimental propulsion system will be approximately 25.4 cm (10 in.) longer than the flight installation to give concentric circular sections aft of the rear main mount to establish a plane of rotation prior to the transition into the "D"-shaped exhaust system. Except for the OTW exhaust system and target reverser, which require a special support system, the installation of the two propulsion systems will be the same.

This propulsion system, complete with boiler plate nacelle components, will be shipped to NASA late in 1977.

15.2 Design Requirements

Components will be designed consistent with the requirements specified in Section 2.0. All items refer to both OTW and UTW flight and experimental system designs unless otherwise stated.

General

- Flight weight hardware will meet the specified weight object. Deviation from flight weight status will be tabulated on all components to establish a logical step-by-step progression from scale weight to projected flight weight.
- Minimum safety factor of 3 for plastic/composite components and 1.5 for metal components for all "limit" load conditions as described in Section 2.0.
- Flight weight composite nacelle components will include sound suppression treatment as an integral part of the system structure.
- Composite components will withstand an ultimate load equivalent to the loss of 5 adjacent composite fan blade airfoils. Metal components will withstand an ultimate load equivalent to the loss of 2.5 adjacent composite fan blades.

- All components will meet life/mission requirement as stated in Section 2.0.

Inlet

- Design for experimental engine inlets will be compatible with anti-icing system requirements, but no anti-icing system components will be included. (Note: Adder to be included in determining flight weight.)
- One piece, 6.28 radians (360°) structure with quick connect and disconnect type fasteners. Experimental engine composite design will not include forward extension at external pylon/accessory cover. (Note: Adder to be included for determining flight weight.)
- Boiler plate hardware will be supported from the facility; composite hardware will be supported from the engine.

Fan Exhaust

- Fan nozzle actuation system is to be submerged within the nacelle wall with required bulges faired internally on the composite nacelle and external fairings if required on the boiler plate cowling (UTW only).
- No cowl power opening devices are included for either flight or boiler plate propulsion system hardware.
- Flare nozzle must be capable of meeting the system requirement of 35% thrust reversal from maximum forward thrust in 1.5 seconds and from full reverse thrust position to takeoff power in 1.5 seconds.
- Aft cowl to fan frame attachment will be quick disconnect type similar to DC-10/CF6 design.
- UTW experimental engine 17.8 cm (7 in.) longer than flight system to accommodate 102 cm (40 in.) long sound suppression splitter required to meet noise objective with 610 m (2000 ft) runaway. (UTW only - Note: Added section and splitter to be subtracted in determining flight weight.)
- "Boiler plate" fan exhaust ducts are common to both OTW and UTW systems to the plane of the flare nozzle hinge.
- Flare nozzle and target reverser must be sealed against leakage in all forward thrust conditions.
- Flare nozzle and target reverser will assume an operable forward thrust position on actuation system failure.
- Flare nozzle and target reverser must be capable of withstanding inadvertent deployment to the reverse thrust position under the following operating conditions:

- At speeds up to 154 m/sec (300 knots) from 0 to 3048 m (10,000 ft) altitude at cruise power without damage.
- At speeds up to 193 m/sec (375 knots) above 3048 m (10,000 ft) altitude at maximum power without separation from the aircraft.
- Boiler plate cowling and OTW target reverser will be mounted from facility. All composite hardware will be mounted from the engine.
- OTW exhaust nozzle and target reverser must be capable of rotation for testing with a wing in the vertical or horizontal position. Internal pylon fairing trailing edge requires modification to fit nozzle contour in each position.

Maintainability

- Engines must be capable of removal from aircraft wing and facility:
 - Without disconnecting engine-to-engine configuration hardware and engine components (except for facility-mounted components and connecting hardware on experimental engine).
 - Vertically downward (after uncoupling facility mounted components on experimental engines).
 - Without disassembly of fan exhaust cowl doors and UTW flare nozzle. OTW target reverser and exhaust nozzle section on experimental engine must be moved aft prior to engine vertical removal.
- Propulsion systems must be trimmable on the test stand.
- Access will be provided to boroscope ports without removal of engine components or disconnecting any configuration hardware.
- Engine accessories shall be located for easy inspection and maintenance.
- Accessory cover will be hinged from the inlet on the flight configurations and removable from the experimental propulsion systems.

15.3 Material Selection

Flight Nacelles

The major portion of the composite nacelle, with exception of the core cowl, operates at very modest temperatures, less than 355° K (180° F), permitting use of a wide variety of composite materials. The primary composite material selected for these areas consists of a woven Kevlar 49 fabric impregnated with a laminating adhesive system. This material exhibits lightweight, good tensile

strength, moderate stiffness, and excellent impact strength. Its major drawback is its poor compressive strength, therefore, in areas requiring higher compressive capabilities, woven glass cloth is substituted for the Kevlar. The use of Kevlar cloth in conjunction with an epoxy laminating adhesive provides a system that is easy to handle and does not require an additional adhesive layer when cured on a honeycomb core. The material provides good fillets to the core and is easy to work with, even when making perforated acoustic panels. The exact matrix system has not yet been chosen but a material screening test program has narrowed the choice down to Ferro CE9000, Ferro CE9040, and Narmco 8517. Based on the test data obtained to date, the material system will be limited to uses at temperatures less than 394° K (250° F). Typical properties obtained at 394° K (250° F) are 27.6×10^6 N/cm² (4000 psi) interlaminar shear and 138×10^6 N/cm² (20,000 psi) edgewise compression [68.9×10^6 N/cm² (10,000 psi) was used for the analysis which was done prior to these tests].

Where it is necessary or desirable to use glass instead of the Kevlar fiber, the standard 7781 weave "E" glass will be used. It will be impregnated with the same matrix system as finally selected for use with the Kevlar. In some cases, it may even be necessary to use graphite fibers. In this case, the selected system will be the same Type AS fiber in Hercule's 3501 resin system that is used in the fan frame. This material has 449.8° K (350° F) capability and is a candidate for application to at least the outer skin of the core cowl doors. Depending on the temperature environment in this area, a polyimide resin system may be required. This system has not been selected but a leading candidate would be Kerimid 601.

Erosion protection on the inner flow surfaces of the nacelle will be provided by a sprayed-on urethane coating similar to that currently used on the DC-10/CF6 installation. The exterior surfaces will be protected either by a good quality epoxy aircraft paint or by a film material such as "Tedlar."

The honeycomb core material will be various cell sizes and densities of Hexcel's corrosion resistant 5052 aluminum core. The core in the acoustically treated panels will be slotted to provide drainage.

Secondary bonding will be accomplished using metal bond 328 adhesive.

A number of thermal protective systems are currently under consideration for use on the inner face of the core cowl to provide a flame barrier but no selection has been made at this time.

15.4 UTW Composite Nacelle Design

The UTW experimental propulsion system as delivered to NASA in mid-1977 will include flight weight composite nacelle hardware mechanically coupled to the engine. This section deals with the description of these components.

15.4.1 Inlet

The QCSEE UTW inlet, shown in Figure 15-4, is designed as a flight weight, acoustic composite structure with integral sound treatment. The internal and external flow paths were determined by aerodynamic considerations while the thickness of the inner honeycomb sandwich well was based on acoustical considerations.

The basic structural elements of the inlet design are shown in Figure 15-5a. The main body is composed of inner and outer honeycomb sandwich walls separated by circumferential stiffeners. The skins of these walls are all 0.0635 cm (0.025 in.) thick Kevlar 49. The inner skin of the inner wall is perforated with hole configurations that suit the acoustical requirements of the inlet. The inner wall thickness (honeycomb depth) is also tailored to acoustical requirements. The outer wall thickness is 2.54 cm (1 in.) to provide adequate stiffness. Honeycomb is made of 0.00635 cm (0.0025 in.) thick aluminum utilizing a 0.9525 cm (0.375 in.) cell size. This results in a honeycomb bare crush strength of $1.86 \times 10^6 \text{ N/cm}^2$ (270 psi) and density of 59.27 kg/m^3 (3.7 lb/ft^3). Stiffeners are segmented and are constructed of 0.127 cm (0.050 in.) thick aluminum sheet with flanged weight reduction cutouts and with composite (Kevlar) flanges to provide bonded attachment to the walls.

The leading edge of the inlet is all metal (aluminum for the experimental engine, titanium for the flight engine) for resistance to foreign object damage and erosion and for anti-icing provisions. This section is removable (by unbolting) from the main body. The outer skin of the leading edge is 0.1016 cm (0.040 in.) thick aluminum sheet and is stiffened by a corrugated 0.0813 cm (0.032 in.) thick backup sheet. The corrugated backup sheet also provides possible passages for anti-icing airflow. This arrangement has the advantages of isolating the anti-icing air from the composite materials and of containing the flow for effective heat transfer and minimum air usage. However, anti-icing is not a part of the QCSEE program and will not be demonstrated on the experimental engine.

The aft end of the inlet attaches to the forward end of fan frame by means of 16 rotary latches. Each of these latches is operated by turning a flush receptical 3.1416 radians (180°) with a 0.635 cm (0.250 in.) square drive wrench. A pressure and acoustical seal is achieved at this joint by means of a thick (in the radial direction) elastomer gasket.

Original design concepts for the inlet considered full-depth honeycomb filler as shown in Figure 15-5b. While this approach is advantageous over existing state-of-the-art design, it is not as efficient as the double sandwich wall construction of the selected design described above. The latter design also has the advantage of easier access to internal piping or wiring. Aluminum skins for the main body of the inlet were also considered. A substantial weight penalty is associated with this system. Calculated weights of various design approaches are compared in Table 15-I.

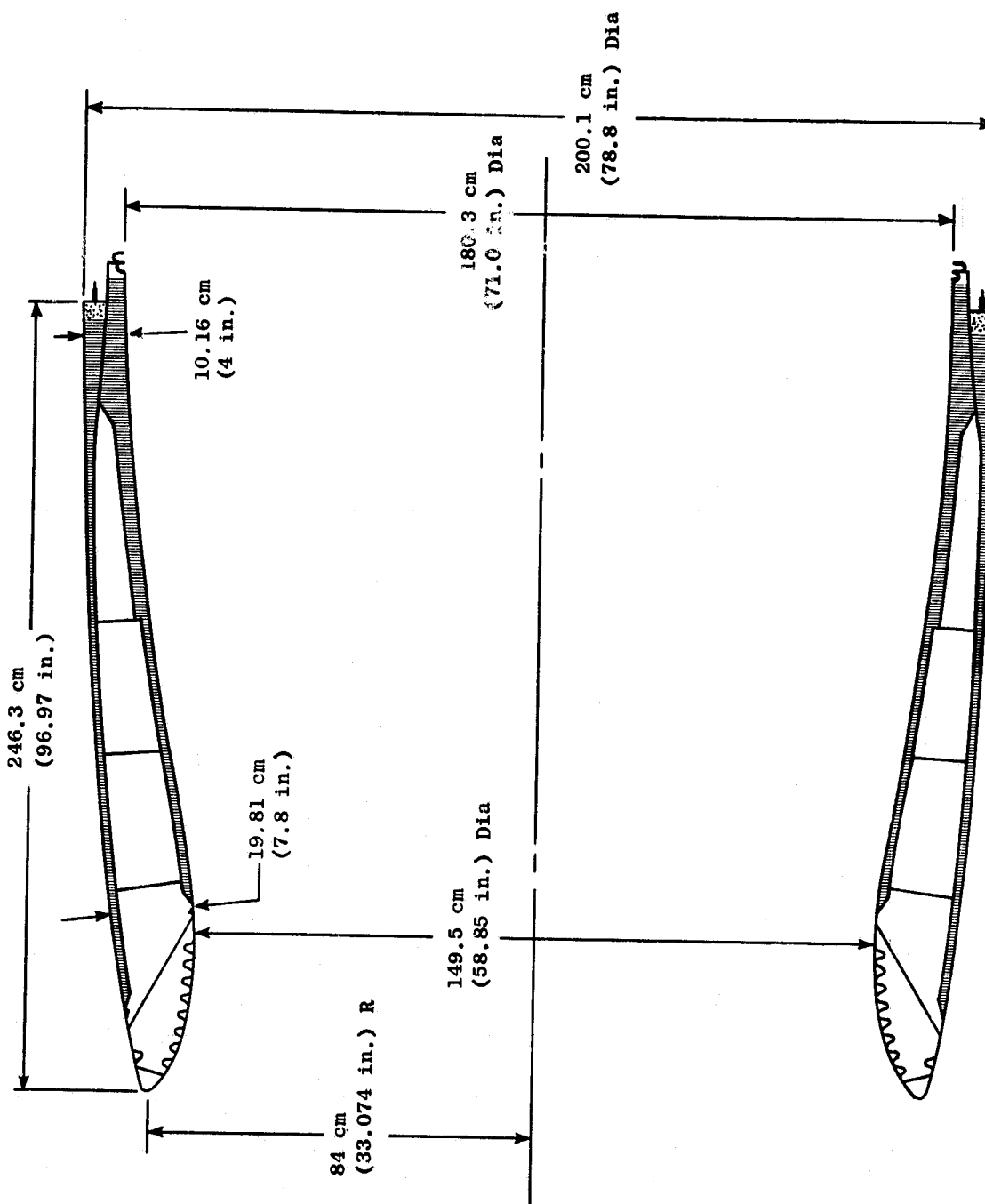
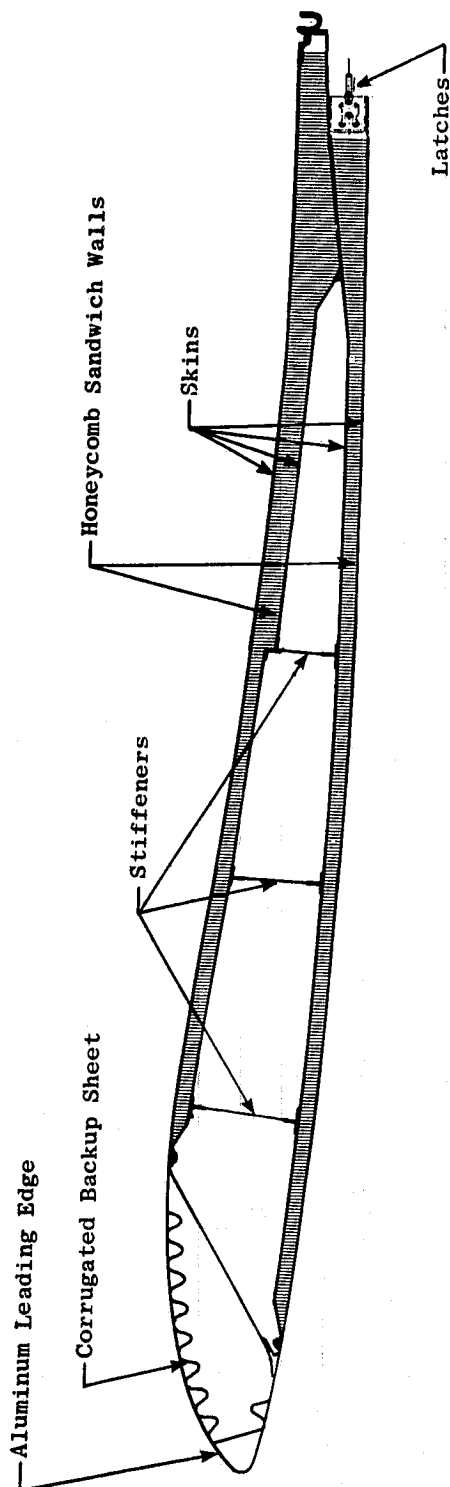
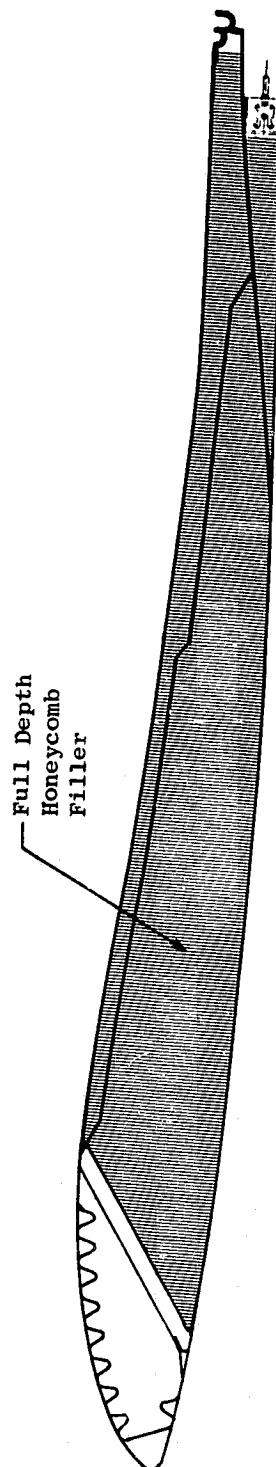


Figure 15-4. QCSEE Inlet Physical Properties.



a. Honeycomb Sandwich Design.



b. Full-Depth Honeycomb Design.

Figure 15-5. UTW Inlet Design.

Table 15-I. Inlet Weight Comparison.

Design	Weight		Δ Wt.	
	kg	(lb)	kg	(lb)
1. Selected QCSEE inlet design	132	(290.9)	-	
2. Same as No. 1 except with full-depth honeycomb.	169.2	(373.1)	37.3	(82.2)
3. Same as No. 1 except with aluminum skins	167.5	(369.2)	35.5	(78.3)
4. CF6-6 or -50 scaled to QCSEE size	217.3	(479.0)	85.3	(188.1)

Aerodynamic loading of the inlet is far more significant than inertia loading. The primary cause for this is the large transverse loads produced by the inlet as it turns the entering engine air flow during any flight condition in which the direction of the free stream air is not parallel to the inlet axis. In contrast, the lightweight structure of the inlet produces rather low inertia loads. From Douglas Aircraft Company analysis, the most severe aerodynamic loads occur during a 3 g stall, sea level, at a flight Mach number of 0.4, and maximum continuous engine power, as shown in Table 15-II. For preliminary design analysis, the loads resulting from this condition were combined with the most severe additive inertia loads caused by dynamic landing (inertia load factors were also from Douglas Aircraft Company analysis). In addition, compressive hoop loads were considered for the sea level static takeoff power operating condition. Resistance to local load application during maintenance, such as a man standing on the inlet, was also considered.

Using the above loads, a preliminary structural analysis of the inlet was performed. Direct stresses due to the applied moment and shear and axial loads are shown in Table 15-III.

Critical buckling loads were calculated and are summarized in Table 15-IV. The inlet is subjected to two types of buckling loads. These are:

- Overall beam bending caused by the loads previously discussed.
- Compressive loop loading resulting from internal wall static pressures at lower levels than the external pressure.

Pressure data from inlet model testing indicates that minimum internal wall static pressure occurs at or near the inlet throat during sea level static, maximum power operation. Under these circumstances a maximum compressive load of $5.9 \times 10^4 \text{ N/m}^2$ (8.5 psi) is generated. This maximum load is rather localized at the throat, but for conservative preliminary design purposes it was assumed that the cavity between the inlet walls might be vented to throat inner wall

Table 15-II. Estimated Forces and Moments on QCSEE Inlet Cowl Based on Potential-Flow Theory, Left-Hand Cowl.

Flight Condition	Altitude (ft)	Freestream			Power Setting	Engine Inlet			Inlet Cowl Loads				
		M _o	α _F (Deg)	β _F (Deg)		M _I	α _c (Deg)	β _c (Deg)	Forces (lbs)			Moments (in.-lbs)	
									F _x	F _y	F _z	M _y	M _z
Abrupt Roll	18,150	0.751	0.8	-3.9	MCT	0.789	1.5	-3.9	-1406	3103.5	681	15,275	170,639
Max Speed	S.L.	0.605	0	0	MCT	0.789	0.4	0	-136	0	-172	-36,119	0
3g Pull-up @ Max q	S.L.	0.605	5.9	0	MCT	0.789	9.0	0	-897	0	8266	461,611	0
3g Stall	S.L.	0.40	12.5	0	MCT	0.789	18.4	0	-1153	0	8345	555,488	0
-1g @ Max q	S.L.	0.528	-3.9	0	MCT	0.789	-4.9	0	220	0	-4160	-273,274	0
Max β _q	S.L.	0.559	0.5	6.0	MCT	0.789	1.2	6.0	-68	-5076	548	11,324	-305,407
Static, Takeoff Thrust	S.L.	0	0	0	TO	0.789	0	0	-5410	0	142	10,097	0
Static, Takeoff Thrust 35 kt XWIND	S.L.	0.053	0	90	TO	0.789	0	90	-7695	-1523	94	10,922	-160,943

Forces and moments based on ambient pressures

Bulkhead forces and moments not included in above table

*Limiting load condition

The analysis adjusted the moment loads shown above to the proposed latching station which is 17.8 cm (7 in.) aft of the station applicable to the above moments.

Most severe additive dynamic landing inertia loads were added to above loads (these loads have little significance).

Table 15-III. Stresses From Shear, Moment, and Axial Loads.

Load Conditions	Allowable Loads		Actual Loads		F/S
	N/m ²	(psi)	N/m ²	(psi)	
Max. Axial Tension	482.6 x 10 ⁶	(70,000)	18.97 x 10 ⁶	(2752)	25.4
Max. Axial Compression	68.9 x 10 ⁶	(10,000)	17.3 x 10 ⁶	(2507)	4.0
Max. Vertical Shear	68.9 x 10 ⁶	(10,000)	2.39 x 10 ⁶	(347)	28.3

static pressure (this would probably not occur unless the throat inner wall was damaged). In this case the entire outer wall of the inlet would need to withstand the compressive load generated by the low static pressure at the throat. Therefore, both the composite outer sandwich wall of the main body and the stiffened aluminum sheet outer wall of the leading edge were checked for buckling resistance relative to this load. Since the outer wall buckling analysis is applicable for a tube stiffened at intervals, the overall structure without additional stiffening was also checked. In considering the inner wall it was assumed that the cavity between walls might alternately be vented to external pressure. In this case the inner wall would need to withstand the overall pressure difference. The load would vary axially, depending on internal static wall pressure. No analysis was made for the composite sandwich wall, since the diameter is smaller than for the outer wall and the pressure load is lower except at the throat. However, the short unstiffened aluminum wall at the throat (aft) end of the leading edge structure was checked and found to need the additional thickness afforded by extension of the 0.032 stiffener material aft to the bolted joint. This was the only buckling consideration that appeared to have significance. Since the inlet cross section is thicker at the bottom than the top, the outer wall is not a surface of revolution. The preliminary buckling analysis described above was not modified on this account. The factors of safety indicated by the analysis were so large, however, that it is believed the outer wall eccentricity can be tolerated. This will be verified later by further analysis.

The sensitivity of the composite sandwich wall to local loads was investigated by calculating the deflection due to a local area being stressed to the material allowable as shown in Figure 15-6. The overall vertical deflection of the inlet under the applied loads was 0.16 cm (0.063 in.).

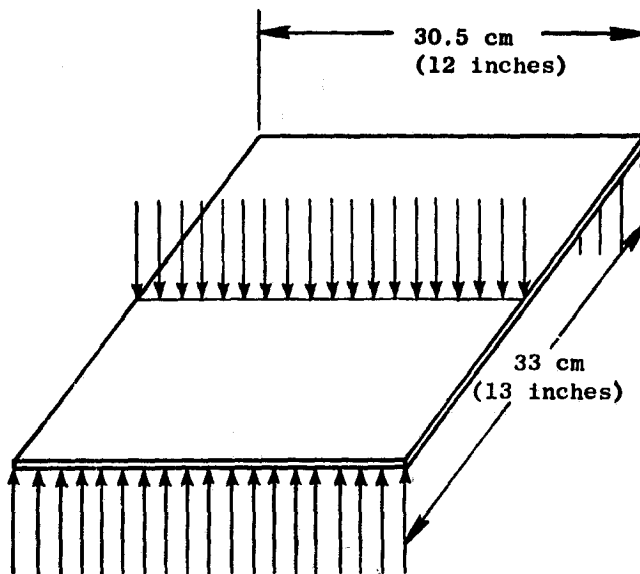
The stiffener flanges were designed to prevent the bearing load between the stiffener flange and sandwich wall from exceeding 2.48×10^6 N/m² (360 psi). This resulted in a flange width of 1.55 cm (0.61 inches). Assuming a 137.9×10^6 N/m² (20,000 psi) flange bending stress allowable resulted in a flange thickness of 0.1778 cm (0.07 inches).

Latch loads were calculated for all 16 latches engaged and for one critical latch disengaged. These loads are shown in Table 15-V.

Table 15-IV. Critical Buckling Loads.

Buckling from Bending					
Load Conditions	Critical Moment		Actual Max. Moment		F/S
	Joules	(in-lb)	Joules	(in-lb)	
Moment on Outer Skins	4,556,670	(40,329,928)	69,307	(613,423)	65.7
Buckling from Compressive Hoop Load					
Loads Conditions	Critical Pressure		Actual Pressure		F/S
	N/m^2	(psi)	N/m^2	(psi)	
Pressure Supported by Single Sandwich Wall (2 skins) Between Stiffeners 33.04 cm (13 in.) Apart	1.5×10^6	(223)	58.6×10^3	(8.5)	26.2
Pressure Supported by Overall Wall Structure	2.75×10^6	(399)	58.6×10^3	(8.5)	46.9
Pressure Supported by Single Outer Aluminum Nose Wall 40.64 cm (16 in.) Long with Stiffening Corrugations	3.5×10^6	(509)	58.6×10^3	(8.5)	59.9
Pressure Supported by Single Inner Aluminum Nose Wall Aft of Corrugation with Corrugation Sheet Extended to Form Doubler: 6.35 cm (2.5 in.) Long x 0.183 cm (0.072 in) O/A Thk	0.162×10^6	(23.47)	58.6×10^3	(8.5)	2.76

<u>Load</u>	<u>Deflection</u>
(923 lb) 4106 N	0.16 cm
(76.9 lb/in)	(0.063 in.)
134.6 N/cm	



Single Sandwich Wall
Supporting Local Load at
Center of 33 cm (13 inches)
(Stiffener Spacing) Simple
Beam Distributed Over 30.5
cm (12 inches) Circumferential
Distance. Compressive Load
Limited to 6900 N/cm^2 to
(10,000 psi)

Figure 15-6. Sensitivity of Composite Wall to Local Loads.

Table 15-V. Latch Loads.					
Latch Condition	Ultimate Strength		Maximum Load		F/S
	Newton	(lb)	Newton	(lb)	
All Latches Latched	28,804	(6475)	9617	(2162)	3.00
One Latch Unlatched	28,804	(6475)	10,738	(2414)	2.68

As can be seen from the above preliminary analysis, the inlet is not highly stressed. The skin gages selected were estimated minimum gages required for load impact at handling.

15.4.2 Fan Bypass Duct and Fan Nozzle Design

The fan bypass duct and fan nozzle constitute the outer nacelle section aft of the fan frame (see Figure 15-7). Mounted inside the bypass duct is a single-ring acoustic splitter. These components are designed to take full advantage of the latest advanced type of composite materials in order to provide a light-weight, thin profile nacelle suitable for advanced air transports.

Fan Bypass Duct

The fan bypass duct is designed as right and left hand sections split on the vertical center line (see Figure 15-8). Each section is attached at its upper edge to the aircraft pylon structure by means of a piano-type hinge. The sections are fastened to each other along the bottom vertical center line split by a series of cowl latches. This allows the duct to be opened for accessibility to the core cowl, and thereby to the core engine. The duct forward "close-out" ring contains a circumferential, inward facing tongue which engages a corresponding groove in the fan frame when the duct sections are closed and latched (see Figure 15-9). The tongue and groove are tapered on the forward side (with corresponding axial free play in the piano hinge) to aid in the engagement when closing the duct. The aft surface of the joint is vertical for transmittal of the duct axial loads into the fan frame and hence through the engine mounts into the pylon.

The duct is of a sandwich-type construction with Kevlar 49 face sheets and aluminum honeycomb core with stiffening rings and members where required. The sound suppression treatment is totally integrated in that the sound suppression honeycomb and perforated face sheets are fully structural. The inner face sheet provides a continuation of the outer wall of the fan exhaust duct and the outer face sheet forms the outer surface of the nacelle. The minimum thickness of the duct is predicted on the acoustical design requirements. Located within the outer confines of the duct are the six fan nozzle actuators (three per side). As the actuator diameter exceeds the nacelle thickness, the actuators are covered by streamlined fairings on the internal duct surface. It was decided

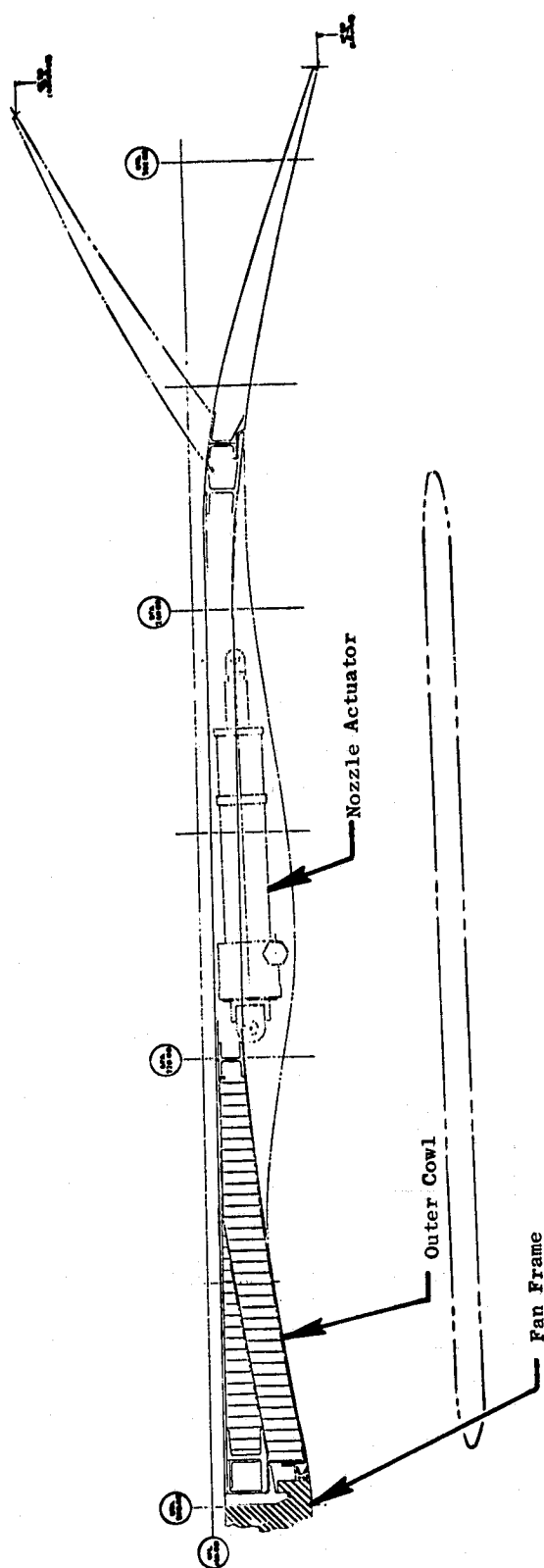


Figure 15-7. Outer Cowl Cross Section.

ORIGINAL PAGE IS
OF POOR QUALITY

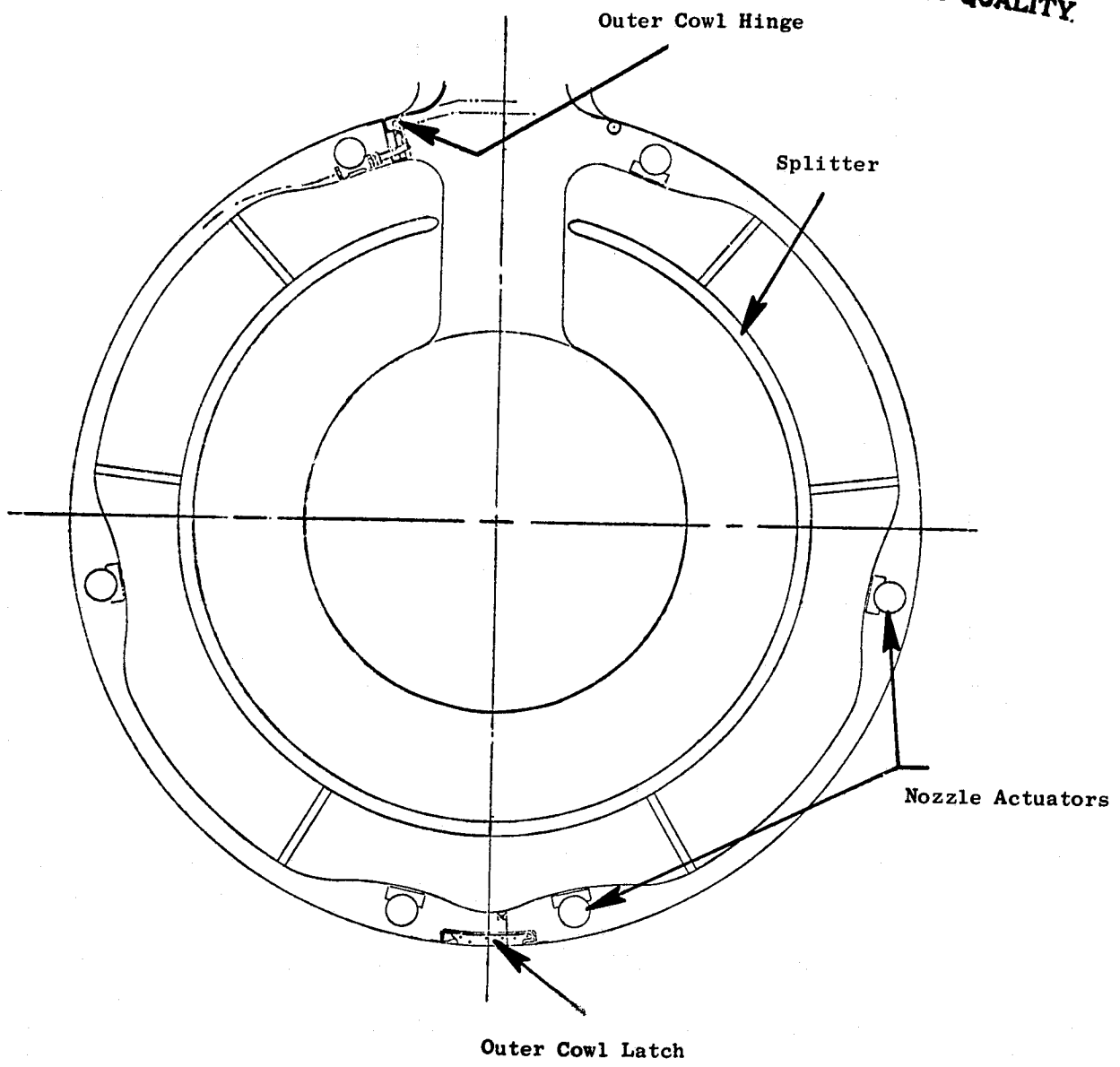


Figure 15-8. UTW Nacelle Cross Section.

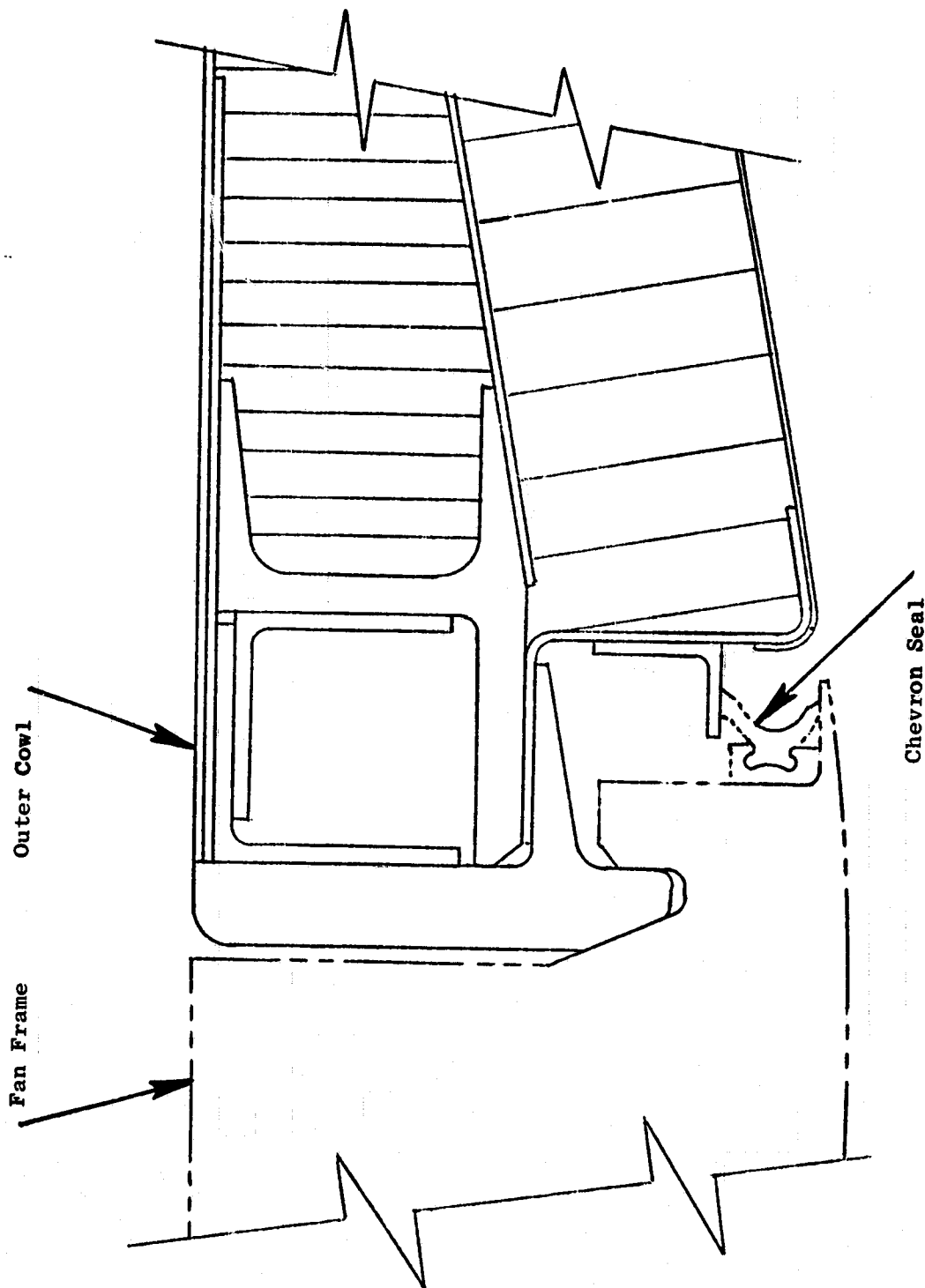


Figure 15-9. Fan Frame/Outer Cowl Joint.

to fair on this surface rather than the external surface because of flow Mach numbers. This approach reduces drag loss and provides a smooth outer nacelle surface. The actuator cavities are formed by a circumferential ring forward of the actuators and by side members which bridge this ring and the aft close-out ring. These members are also the edge close-outs for the honeycomb structure. Built into the side members are the support tracks for the rod end clevises of the actuators. These tracks transfer the radial component of the nozzle flap link load into the adjacent sandwich structure, and guide the actuator rod end/link joints by means of rollers engaged in the tracks. This allows the links to pass through the aft close-out ring without interference. The forward ends of the actuators are mounted in clevises with circumferential pins and slight side clearances. This allows the actuator to rotate slightly as the nozzle is translated. The actuators are mounted at a shallow angle to the engine center line in order to maintain a minimum fairing envelope and to confine the fairing to one flow surface. The hydraulic fluid lines, and the seal drain lines are also submerged within the structure of the bypass duct. These lines will be built-in and will terminate at connector fittings at the actuator cavity side members. As hydraulic leakage in service generally occurs at connections, these will be readily accessible for installation and maintenance by means of access covers at each of the actuator cavities. These covers will be held in place by mechanical fasteners.

The piano hinge will be built into the upper edge close-out and will be continuous from the forward close-out ring to the aft close-out ring. The loads are relatively small as can be seen in Table 15-VI.

The bottom latch system, shown in Figure 15-10, will have Hartwell King latches at the hard points (forward, mid, and aft rings) and rotary type latches between. While discussions have been held with the Hartwell Company concerning the development of latches suitable for mounting into advanced composite structure without additional housings, the timing of this program necessitates the use of existing latch configurations with the attendant nacelle design modifications. With the duct closed and latched, the internal pressure loads will be resisted by hoop tension stresses, the hinge forces being reacted by the pylon support structure.

The duct will be sealed against gas and noise leakage along the hinge and latch joints and around the forward flange (Ref. Figures 15-9 and 15-11). The gas leakage will be controlled by a chevron-type elastomer seal of the type presently used on the DC-10/CF6 engine nacelle installation. The acoustic leakage barrier will consist of sound absorbent material such as Scots Felt in the joints, compressed at assembly by cowl closing. Since the forward tongue and groove joint will have good line contact between the structural components, no sound absorbent material will be included in this joint.

Fan Nozzle

The fan exhaust nozzle is a fully modulating variable-flap type capable of not only providing various areas for forward thrust, but also of a flaring outwards to provide increased area for inlet flow to the variable-pitch

Table 15-VI. Fan Duct Hinge/Skin Stresses.

Flight Condition	ΔP Max		Hoop Load		Hinge Pin Brg. Stress		Hinge Pin Shear Stress		Skin Circumferential Stress		Skin Axial Stress	
	N/cm ²	psi	N/cm	lb/in	N/cm ²	psi	N/cm ²	psi	N/cm ²	psi	N/cm ²	psi
M = 0.3 @ SL, 100%	1.1	(1.60)	700.6	(62)	214	(310)	386	(560)	949	(1375) (T)	476	(690) (T)
M = 0.8 @ 9.1 km (30 K), MCR	2.7	(3.85)	1684	(149)	549	(795)	932	(1350)	2277	(3300) (T)	1139	(1650) (T)
M = 0.9 @ 6.1 km (20 K), MCR	4.8	(7.00)	3062	(271)	997	(1445)	1690	(2450)	4140	(6000) (T)	2077	(3000) (T)
M = 0.225 @ SL, RT	-2.5	(-3.60)	-1571	(-139)	511	(740)	869	(1260)	2139	(3100) (C)	1070	(1550) (C)

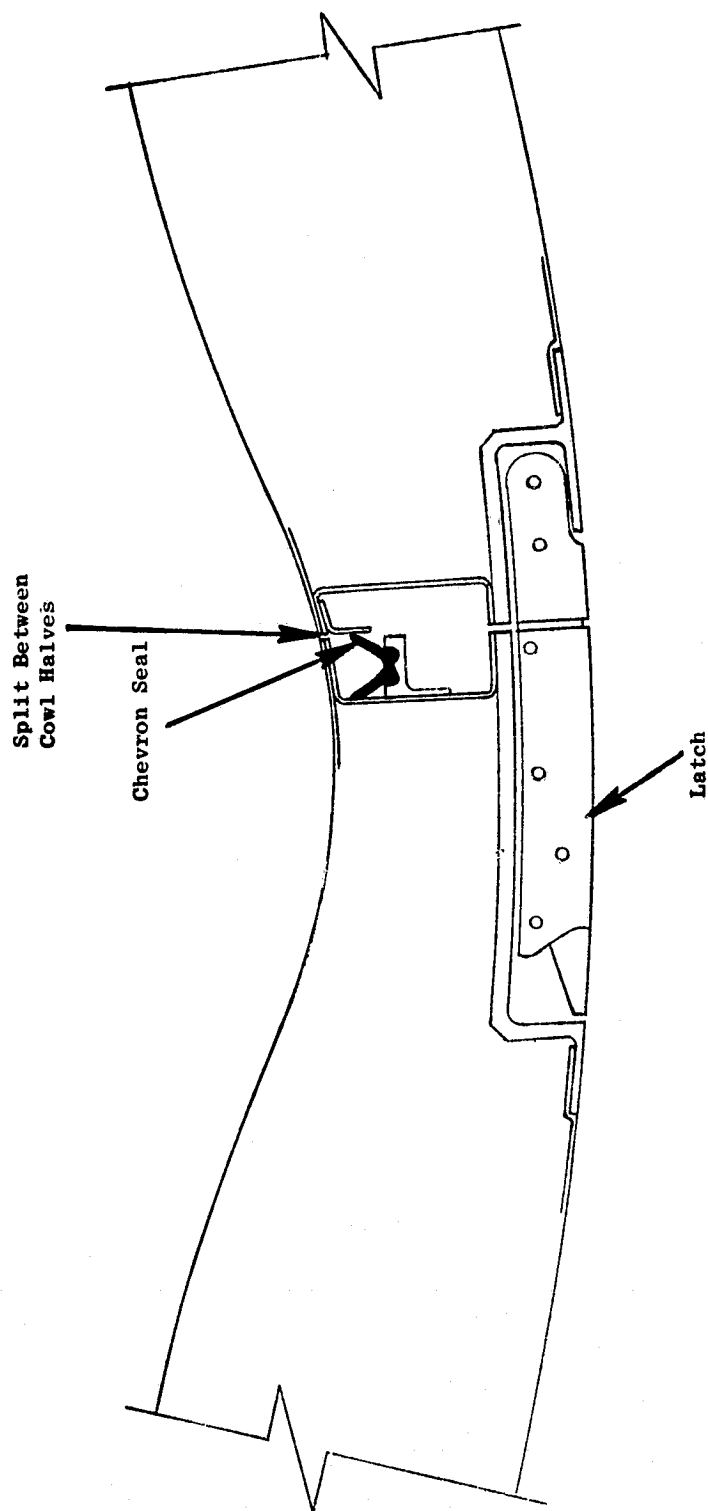


Figure 15-10. Outer Cowl Lower Latch and Seal.

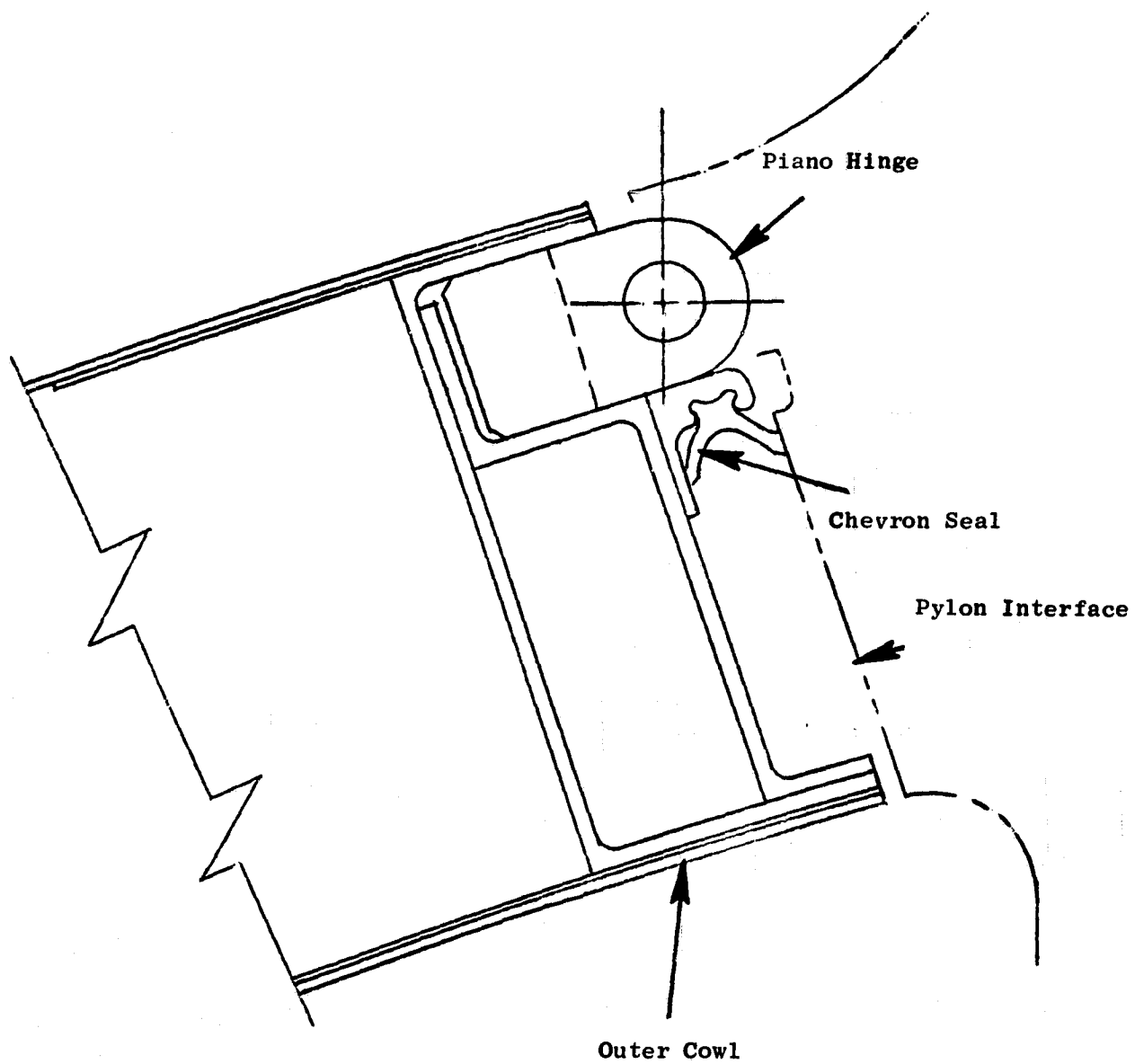


Figure 15-11. Outer Cowl Hinge and Seal.

fan in the reverse mode (see Figures 15-12 and 15-13). This design was chosen on the basis of cost/weight/performance trade studies of several means of providing the required inlet area in reverse mode.

The nozzle consists of four hinged flaps each 45.72 cm (18 in.) long and 1.396 radians (80°) wide. Two each of these flaps will be mounted to the aft close-out ring of each duct section by hinges located 15.24 cm (6 in.) each side of the flap center line along the flap forward edge close-out. The flaps are designed such that they can be translated from an angle of about 0.227 radians (13°) down toward the engine center line to an angle outward of approximately 0.523 radians (30°). From the minimum nozzle area position (cruise) to an intermediate position, giving a nozzle area somewhat greater than that required for takeoff thrust, a tongue-and-groove-type seal between the flaps will be fully engaged. Throughout this same motion, a sliding-type seal on the inner, forward lip of the flap forward close-out will be in contact so that the nozzle flaps will always be sealed during normal forward thrust engine operation. Sealing is not required during reverse thrust, therefore, the seals begin to disengage as the maximum nozzle area for forward thrust is exceeded. In the maximum reverse thrust position only a short length of seal is still engaged. Retaining some engagement in all cases will ensure a smooth reengagement of the seal when translating the flaps from the reverse to the forward thrust position.

The means for opening the flaps will be a linkage connection between the hydraulic actuators and the forward corners of each flap. The mid-actuator in each half section will be joined to both flaps mounted on that section by a double linkage (see Figure 15-13). This keeps the number of actuators to a minimum (6) and synchronizes the movement of adjacent flaps. Location of the hinges towards the center of the flaps, and the actuating linkage outboard ensures that during rotation of the flap, only a small section of the flap will rotate into the mounting ring, eliminating cut outs to permit passage of the flaps. This also permits the actuation linkage system to be completely submerged within the duct envelope, and reduces the link passage through the duct aft close-out ring. The construction of the flap is similar to the rest of the duct, being a composite bonded assembly with Kevlar 49 skins and 5052 aluminum honeycomb core. The sound suppression treatment is integral with the structure.

A preliminary load study based on varying the number of flaps was conducted to arrive at the optimum number for the QCSEE design requirements. This study showed large changes in actuation load and stroke with small changes in the number of flaps (see Figure 15-14). A two-flap system with a small actuation load but long stroke, would have resulted in an actuation system which exceeded the physical envelope of the nacelle. Also, the hinge ring radial loads imposed by the flap hinges would be 52% greater than those imposed by the four-flap system. The six-flap system, while it has a short actuation stroke of 3.556 cm (1.4 in.), has an actuation load which would impose excessive local loads on the nacelle structure. Also, a much larger actuator would have to be provided with its attendant bulge in the fan duct, increasing the flow Mach number and noise level. The four-flap system offered the best compromise. The loads and stroke were such as to allow the use of existing actuators (J79 nozzle hydraulic actuators) for the demonstrator nacelle. The loads imposed on the structure are also low enough to be carried by the nacelle structure without excessive stresses and deflections.

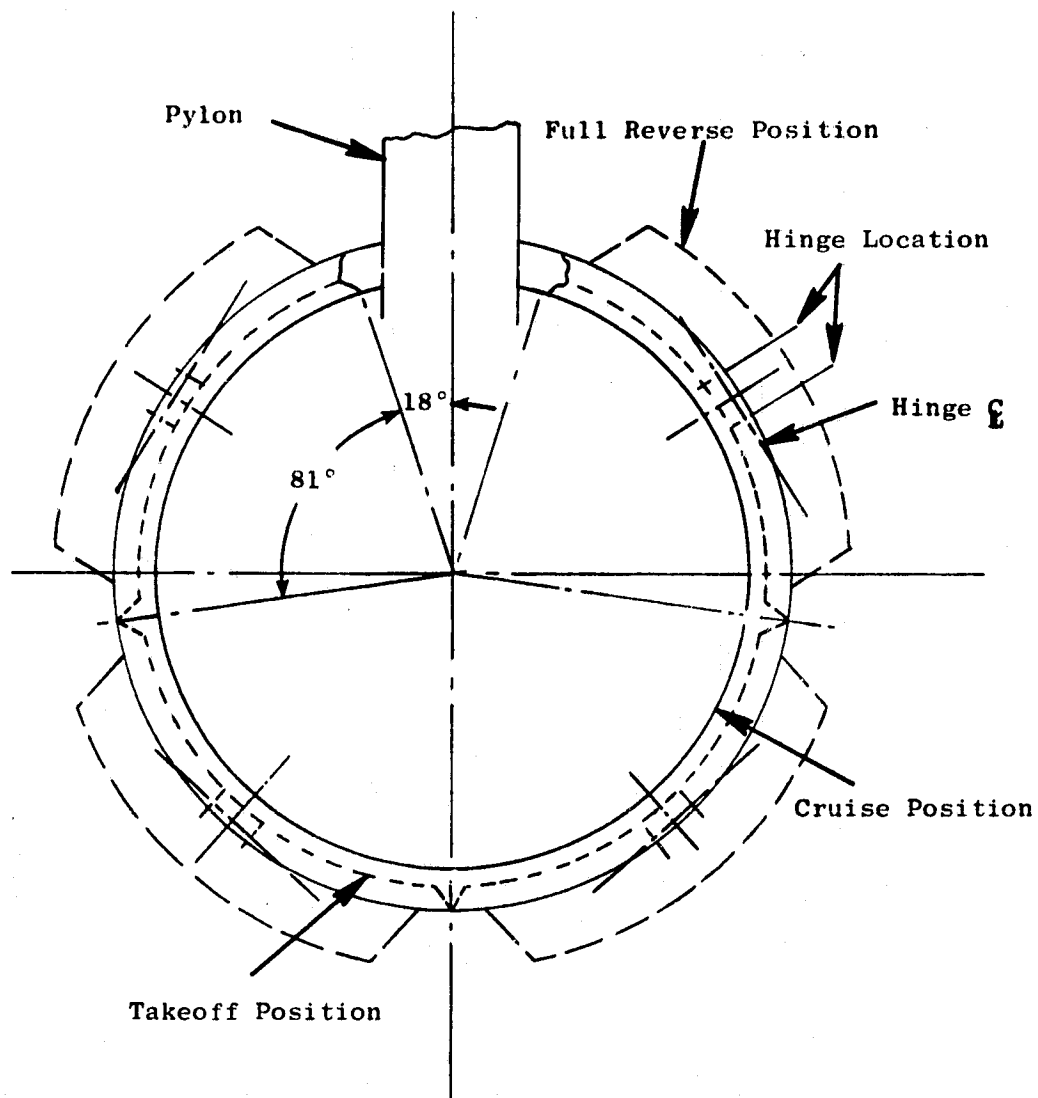


Figure 15-12. Flare Nozzle Flap Schematic.

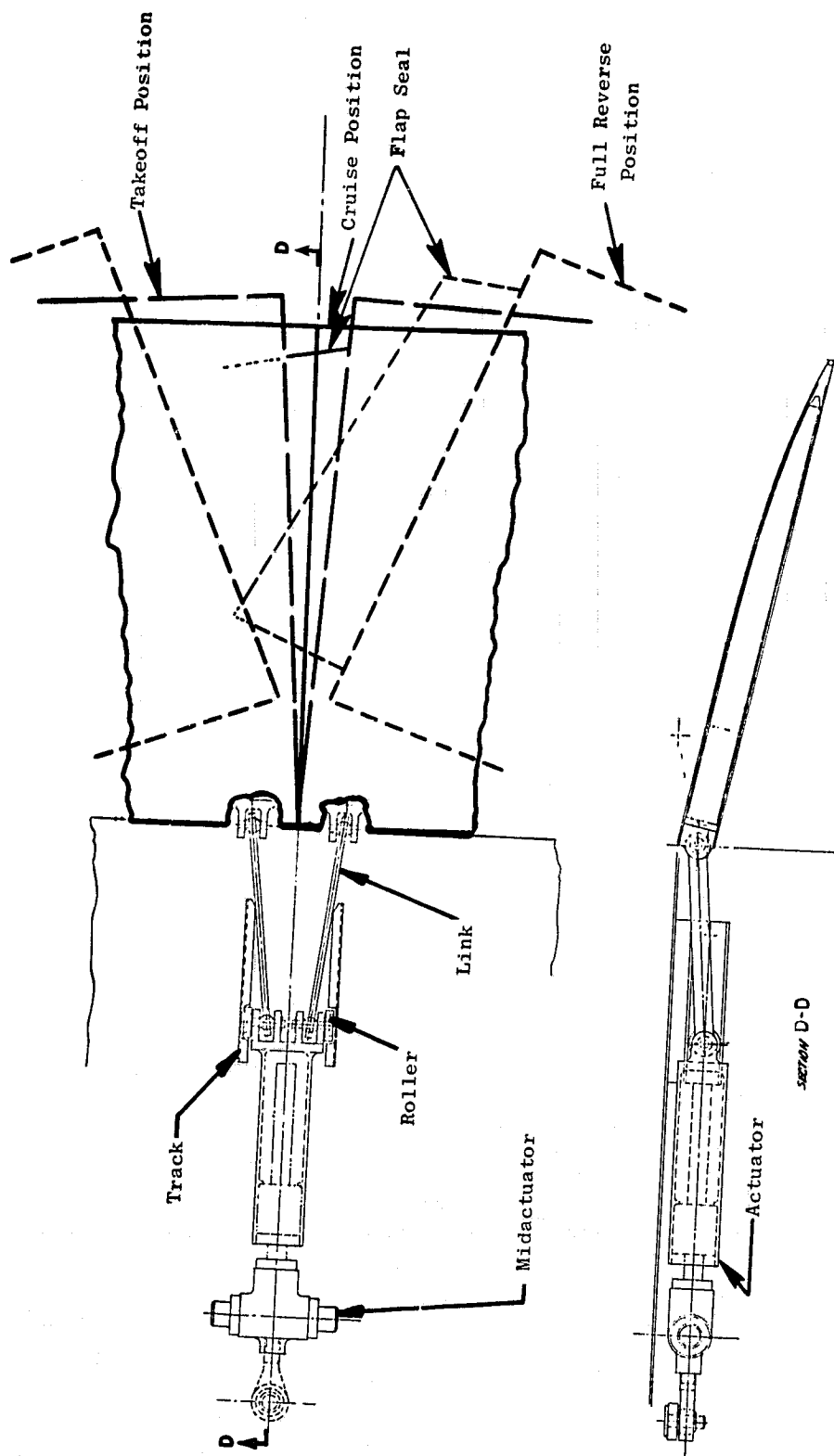


Figure 15-13. Variable Flap Nozzle.

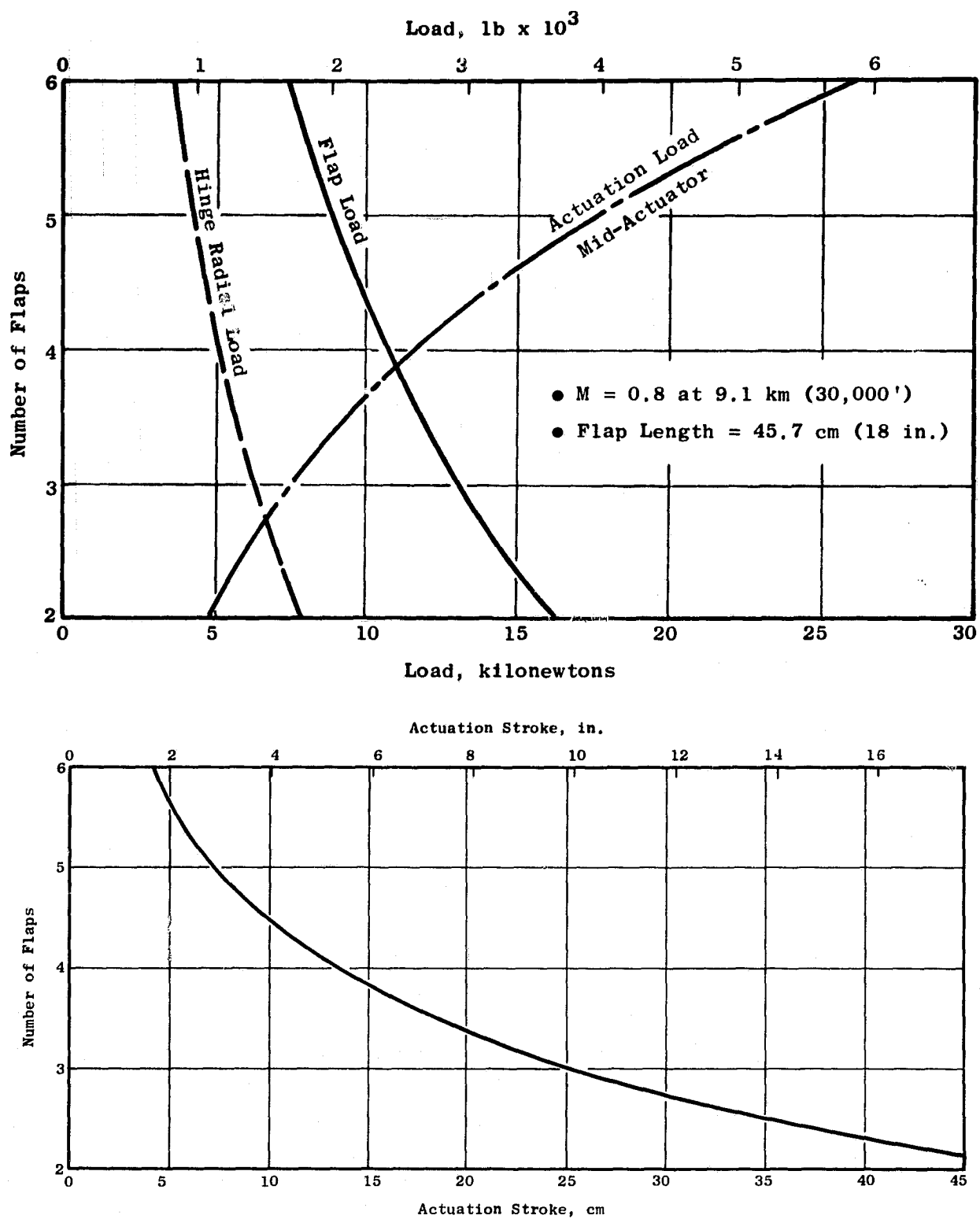


Figure 15-14. Flare Nozzle Flap Tradeoff Study.

An aerodynamic study determined that the most desirable flap length was about 45.72 cm (18 in.) which resulted in a flap open angle of 0.523 radians (30°). A 0.523 radian (30°) reverse thrust flap angle appears to be the practical limit mechanically in order to maintain the linkage system within the envelope limits of the duct aft close-out ring and also to preclude door lip interference with the hinges and supporting structure in the maximum reverse thrust position. The load study showed that the actuation and hinge load changes were small in the flap length range from 40.6 cm (16 in.) to 50.8 cm (20 in.), see Figure 15-15, so a flap length of 45.7 cm (18 in.) was permissible from a mechanical stand point; therefore, this length was chosen.

Acoustic Splitter

The splitter (Figure 15-16) can be considered as the only nonstructural component in the nacelle, since its only purpose is to provide additional sound suppression treatment, and the only loads it transmits is its own aerodynamic and inertia forces. The demonstrator nacelle splitter is presently contemplated to be two semiannular rings each mounted on the outer fan duct halves by three struts (see Figure 15-17). This ring will be 3.05 (1.2 in.) thick and 101.6 cm (40 in.) long in the sound treatment area with aerodynamically faired leading and trailing edges. In order to prevent cross flow, the upper axial close-out supports a formed elastomer seal which will match with and seat against the pylon side wall. The lower axial joint where the two ring halves come together will be of the tongue and groove type (see Figure 15-18). This lower joint will stabilize the ring ends as well as prevent cross flow. Three struts were chosen as this is the minimum number which will provide a stable support against overturning moments. These struts will be of a minimum cross section for low drag losses and therefore will not contain sound suppression treatment.

15.4.3 Core Cowl Design

The core cowl doors define the inner boundary of the fan air flowpath from the fan frame to the core nozzle. They are also used as sound attenuators. Maintenance access to the core engine is also provided.

Temperature considerations are of primary importance in determining cowl door construction materials and configuration. The inner surfaces of the doors are exposed to radiant and convective heat from engine casings and may be insulated from cooling effects of the fan air stream if conventional honeycomb sandwich walls are used. This condition is somewhat alleviated by allowing a relatively small quantity of fan air to flow between the outside of the engine casing and the inner surface of the cowl doors. It is believed that this arrangement will satisfactorily control temperatures during most engine operating conditions so that the use of low-cost, lightweight composite materials will be allowable. However, widely differing thermal situations may be set up by operating conditions such as reverse thrust, ground idle, and post shutdown. The latter condition may cause the highest normal temperatures in the cowl door structure. Heat transfer analysis has been started to establish severity of the problem and to identify the best solution. In addition, the core cowl

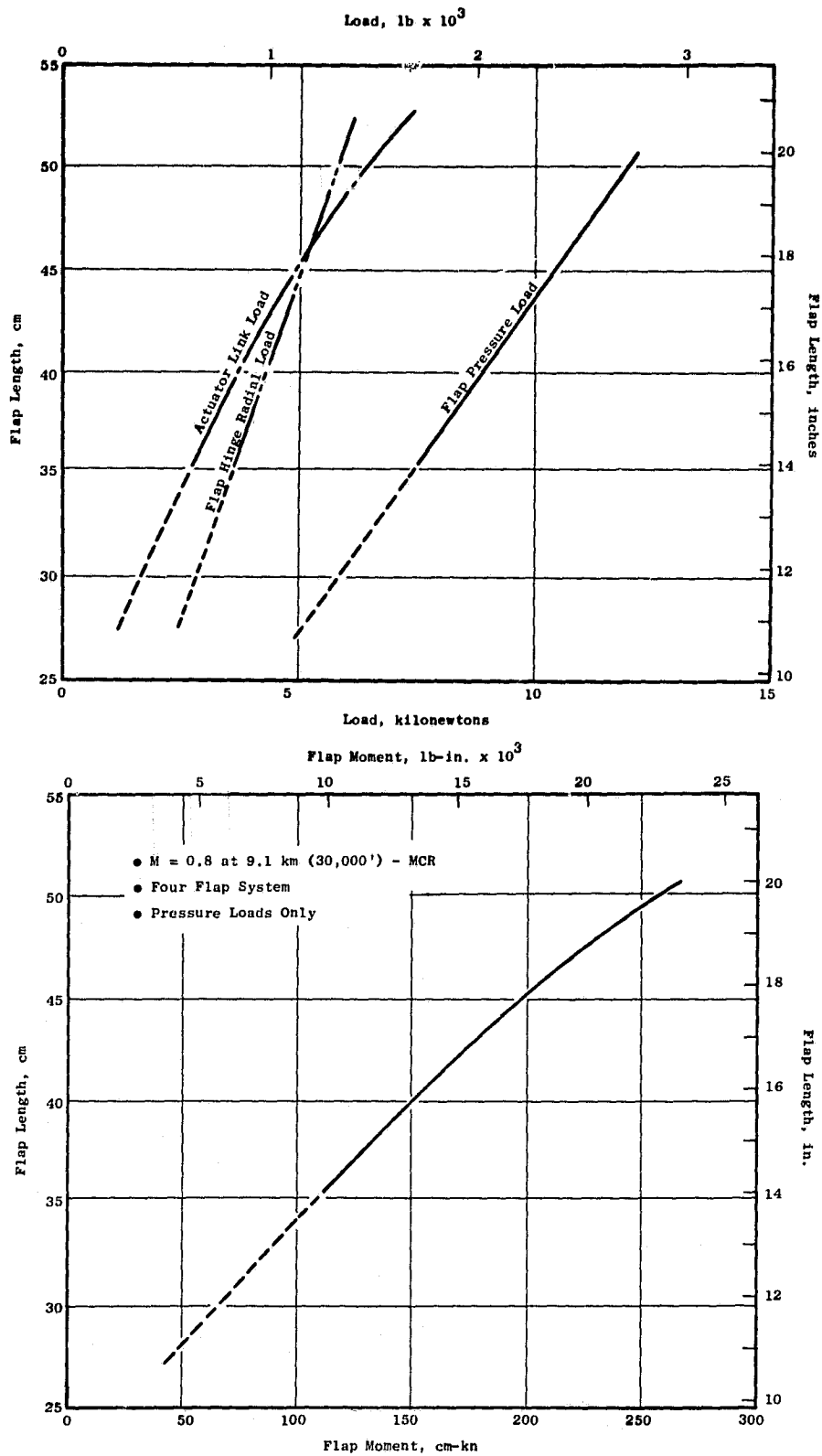


Figure 15-15. Nozzle Flap Loads Vs. Flap Length.

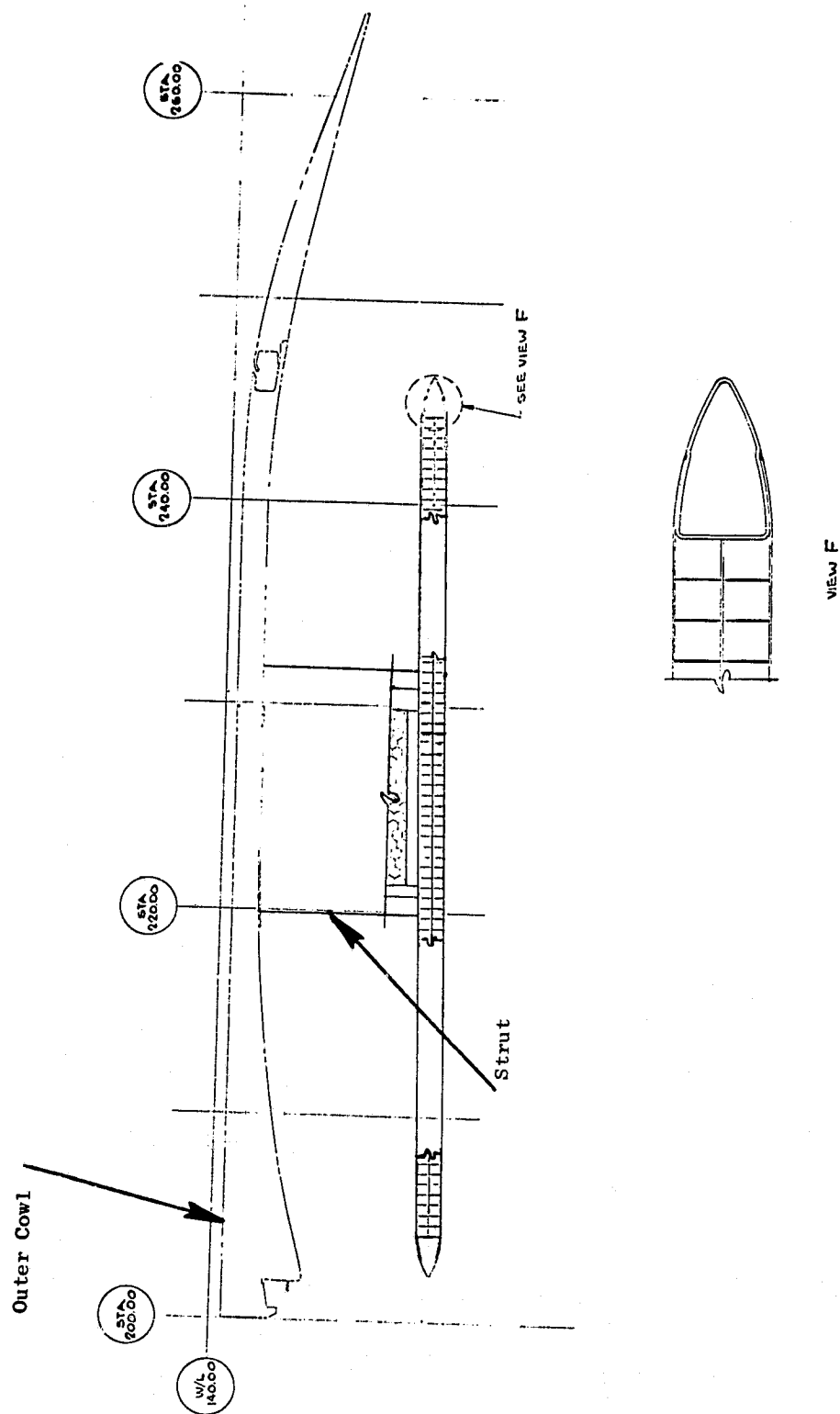


Figure 15-16. Splitter Cross Section.

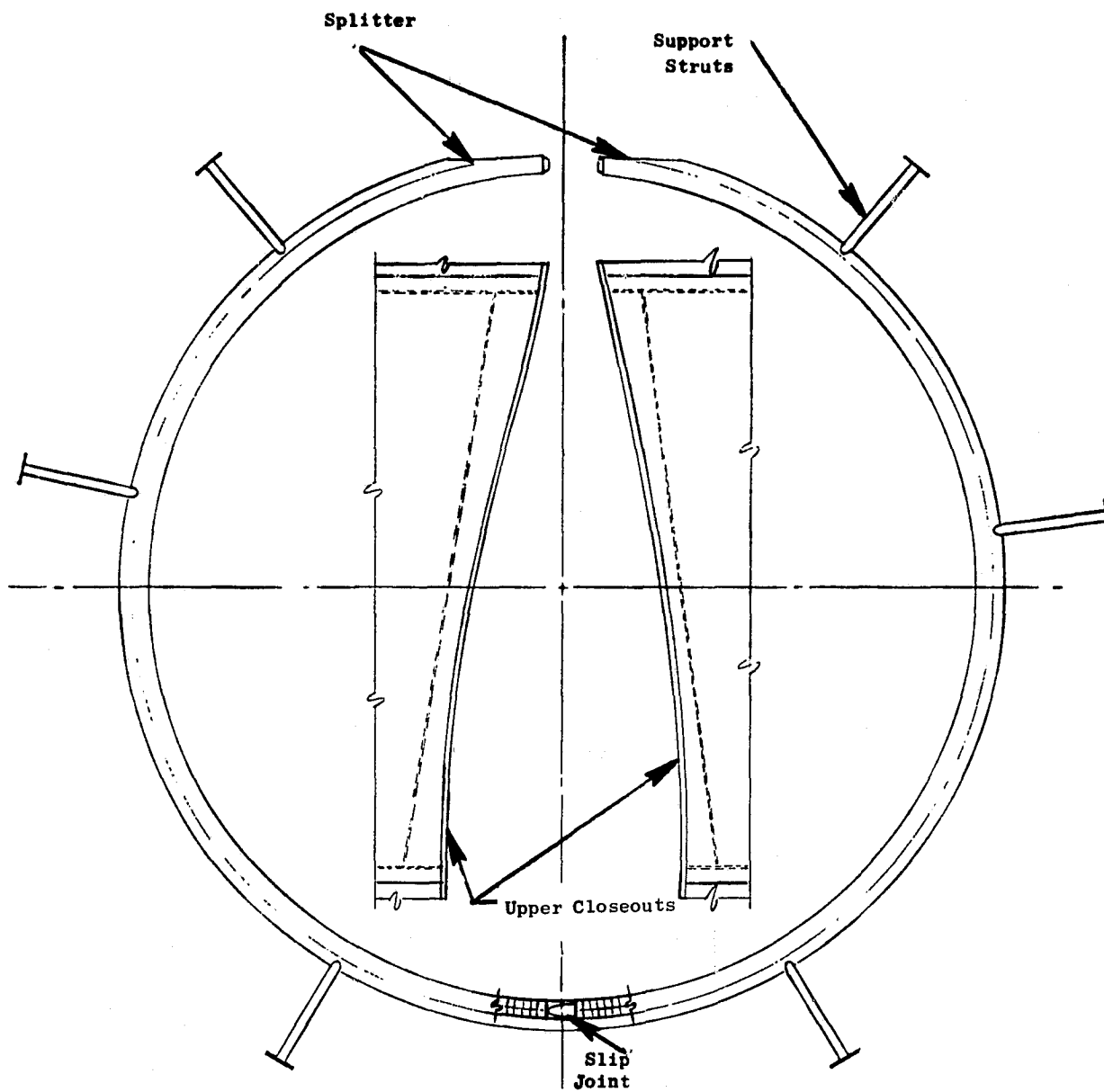
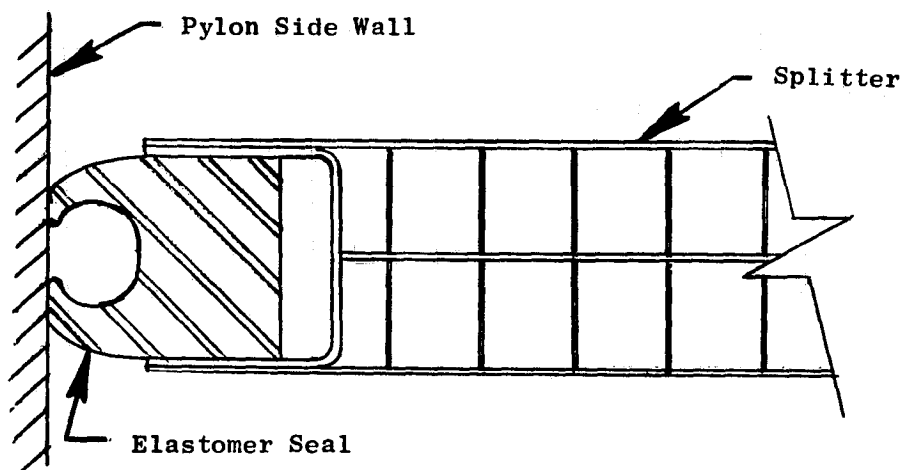
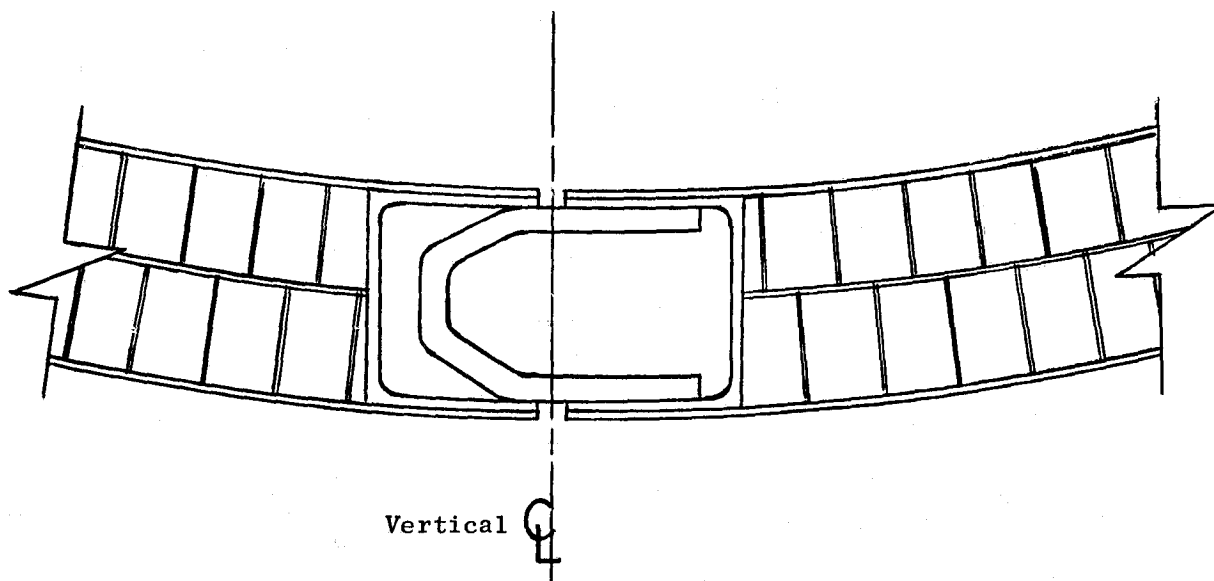


Figure 15-17. Splitter End View.



● Upper Splitter/Pylon Joint



● Splitter Halves Bottom Joint

Figure 15-18. Splitter Joints.

doors must also act as a firewall capable of withstanding 1367° K (2000° F) for 15 minutes. This function can be provided by a number of different coatings and protective systems applied to the inner facing of the doors. These methods and concepts are currently being evaluated as to effectiveness, weight, and cost.

As currently conceived, the cowl doors will consist of a composite sandwich structure. The resin system has not yet been selected pending completion of the heat transfer study. The dual, nearly semicylindrical doors are hinged at the top adjacent to the pylon to swing outward 0.785 radians (45°) for access to the core engine. They are latched at the bottom with flush latches. At the forward end, the doors hook into the aft flange of a short nonhinging section of the cowl that is bolted to the fan frame. This short section cannot be part of the cowl doors because the cowl doors must clear the fan frame outer casing aft flange when they are swung outward. The short section is needed, however, to allow clearance for removal of a core compressor casing half without separation of the fan frame. The short section is axially split for this reason. The aft end of the cowl doors have a slip (axial) fit with the core nozzle structure to accommodate axial differential thermal expansion. Cooling and ventilating air ports will be provided at the forward and aft end of the core engine cavity under the doors in accordance with requirements indicated by the heat transfer analysis.

It was assumed that the pressure in the engine space under the cowl doors is essentially ambient by virtue of venting to the flowpath near the aft end of the cavity downstream of the fan nozzle. This produces a compressive hoop load during most flight conditions. The estimated maximum compressive pressure difference is $39.6 \times 10^3 \text{ N/m}^2$ (5.75 psi). This causes a negative hoop load of approximately 201.4 N/cm (115 lb/in.).

Because of the core cowl and engine contours, it is not practical to provide a continuous axial hinge line without local discontinuities in flowpath. The selected axial hinge line involves a maximum gap of 71.1 cm (28 in.) between hinges in the expected flight version of the engine. Hoop loads between the hinges were assumed to be supported by the edge of the door acting as a beam with a distributed load (the hoop loads) supported at the hinges. Analysis indicated that it would be feasible to design the door edge to support the loads on this basis.

The cowl door contour is also such that one or more hinges must be located at a shorter distance from the engine center line than the cowl wall. This means that the wall hoop load line of action does not pass through the hinge center. This introduces a torsional load to the door structure. Analysis indicates that this torsional load may be resisted without unreasonable design compromise.

15.4.4 Core Nozzle Design

The preliminary mechanical design activity was limited to conceptual designs that include one nonflight- and two flight-type designs. The main objectives of

the study were to establish the core nozzle interface requirements and to determine the available envelope for acoustic treatment. The method and sequence of assembly were also studied and the design layouts were used in the preliminary weight analysis.

The nonflight UTW exhaust nozzle is shown in Figure 15-19. The design consists of a spool-type, load-carrying structure with a separate, interchangeable acoustic treatment assembly that could easily be replaced without the disassembly of the turbine flange connection. This construction permits interchange of the acoustic treatment.

The assembly procedure to be used for the nonflight design is as follows:

1. Bolt the inner plug spool to the turbine frame flange.
2. Slide the acoustic treatment assembly over the spool.
3. Bolt the rear cone to the inner spool to mechanically lock the acoustic assembly in place.

The outer core nozzle is assembled in a similar manner as follows:

1. Bolt the outer spool section to the turbine flange.
2. Slide the acoustic treatment into the spool section.
3. Bolt the outer core nozzle fairing to the aft spool flange, mechanically locking the acoustic treatment in place.

A streamlined strut is shown in the study to provide an aerodynamic flow path around the oil-in, oil-drain, and balance piston air lines. Not shown are instrumentation pads or ports for pressure, temperature, and acoustic measurements that are required for development testing.

For the flight-type UTW engine, a stacked acoustic treatment core nozzle, as shown in Figure 15-20, and a side branch resonator-type core nozzle, as shown in Figure 15-21, were designed based on the latest sound suppression test data.

In the flight-type design, the acoustic treatment is welded into the structure and is an integral part of the load carrying structure. This is essential to achieve an efficient, lightweight core nozzle design.

The assembly of the inner core plug in the flight weight design is facilitated by the reorientation of the inner turbine frame/core nozzle flange from a radial to an axial configuration. The inner core plug flange can then be slid over the turbine frame flange and bolted together with countersunk bolts to form a smooth inlet flow path without the use of a cover plate. The integral outer core nozzle assembly is then bolted to the turbine frame flange which is easily accessible.

15.4.5 Mounting System

The UTW experimental and flight engines use the same type mounting system. Figure 15-22 shows a typical engine change unit or neutral engine system. The change unit will include the inlet and accessory cover, the engine accessories and piping, the thrust links and rear mount, and the basic engine and core exhaust system.

- No disassembly of "engine-to-engine" piping is required on engine removal
- Thrust links and rear mount, which are aircraft system hardware, remain with engine to limit the mount system disconnect points to two.
- Fan and core cowl doors remain "on-the-wing"
- Disconnect points include:
 - Mount System - 2 places (4 to 7 Bolts)
 - Bleed air pipe
 - Power shaft to aircraft accessories
 - Anti-icing air tube
 - Aircraft-to-engine services - pipes, lines, cables, wires, etc.

The mounting system is shown in further detail in Figure 15-23. Thrust is taken at the front frame at two points to minimize core bending due to thrust, and thereby to improve rotor to stator clearance control. Vertical and side loads are simply supported. The mount schematic shows vertical, side, and thrust loads taken at the front mount plane on the aft ring of the fan frame and vertical, side, and torque loads taken at the rear mount plane on the outer ring of the turbine frame.

The rear engine mount and thrust link assembly in Figure 15-24 shows a three link arrangement similar to that used on the DC-10/CF6 mount system. Uni-balls at the ends of each of the links permit axial movement for differential thermal growth between the engine and the support structure. The thrust links fit into a double clevis at the rear mount adaptor center pin. This arrangement provides minimum vertical reactions due to the mount load. An alternate arrangement of the thrust links coming into the forward mount fitting will also be studied.

When mounted as described, the engine and its mounting structure will withstand the flight maneuver forces described in Figure 2-2. The precession rates used are consistent with CF6 and GE19 requirements:

One Radian/second in either pitch or yaw combined with the maximum resultant vertical, fore or aft, and angular acceleration loads (in the shaded area of the diagram) at zero to maximum thrust combined with normal cycle pressure and thermal loads.

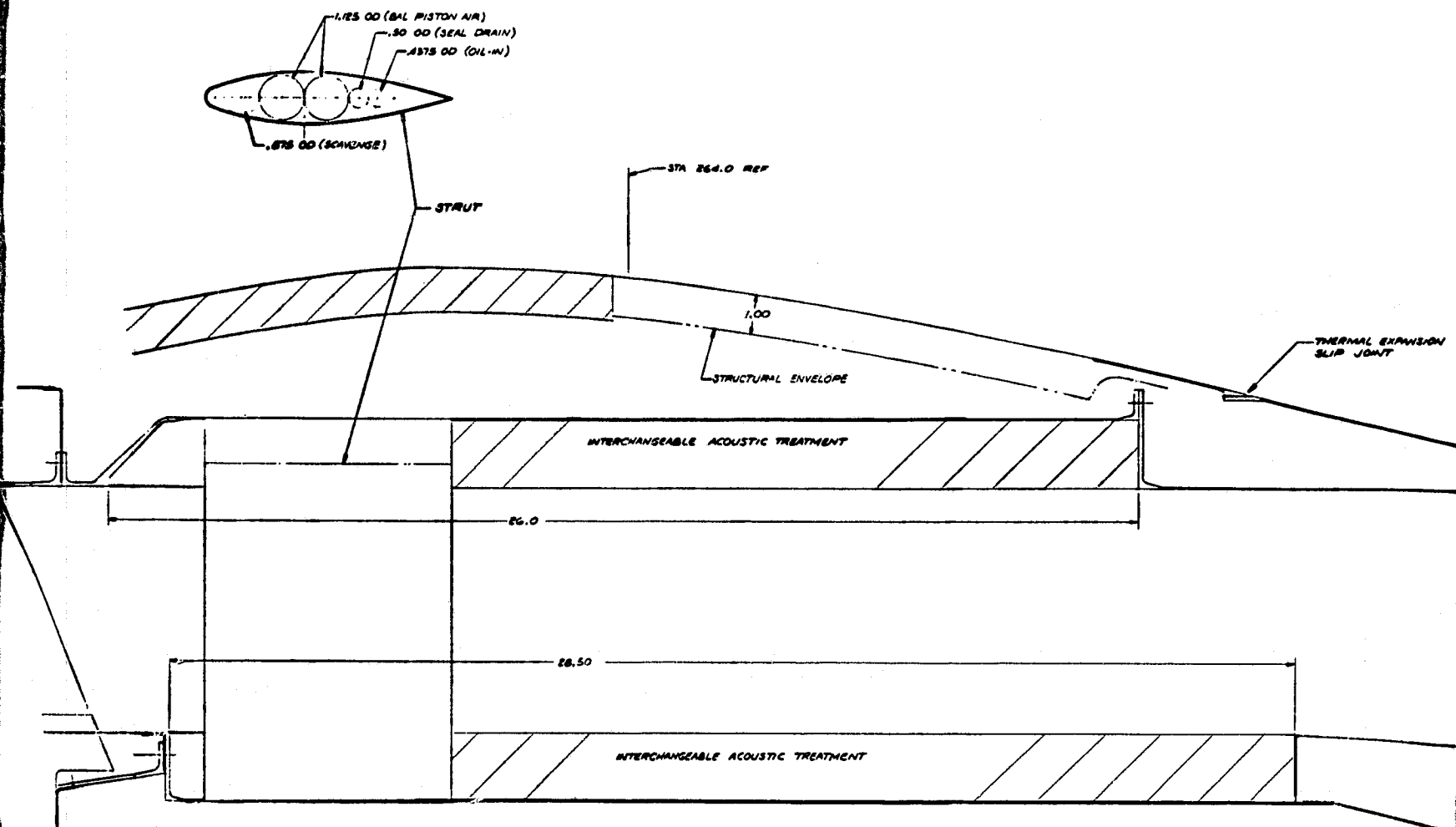


Figure 15-19. Core Exhaust Nozzle, UTW Experiment

/ FOLDOUT FRAME

ORIGINAL PAGE IS
OF POOR QUALITY



ust Nozzle, UTW Experimental Engine.

533

2 FOLDOUT FRAME

ORIGINAL PAGE IS
OF POOR QUALITY

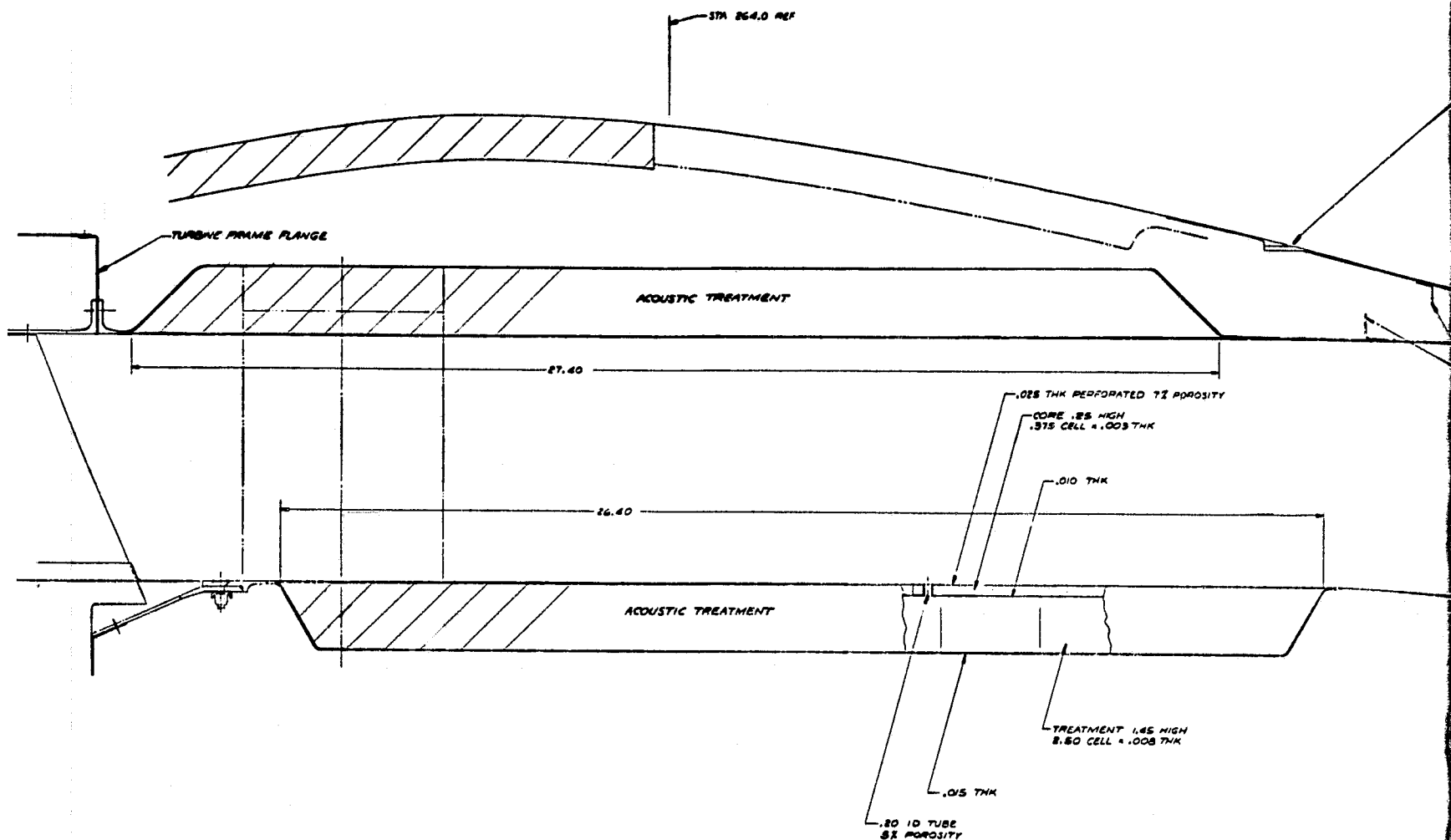
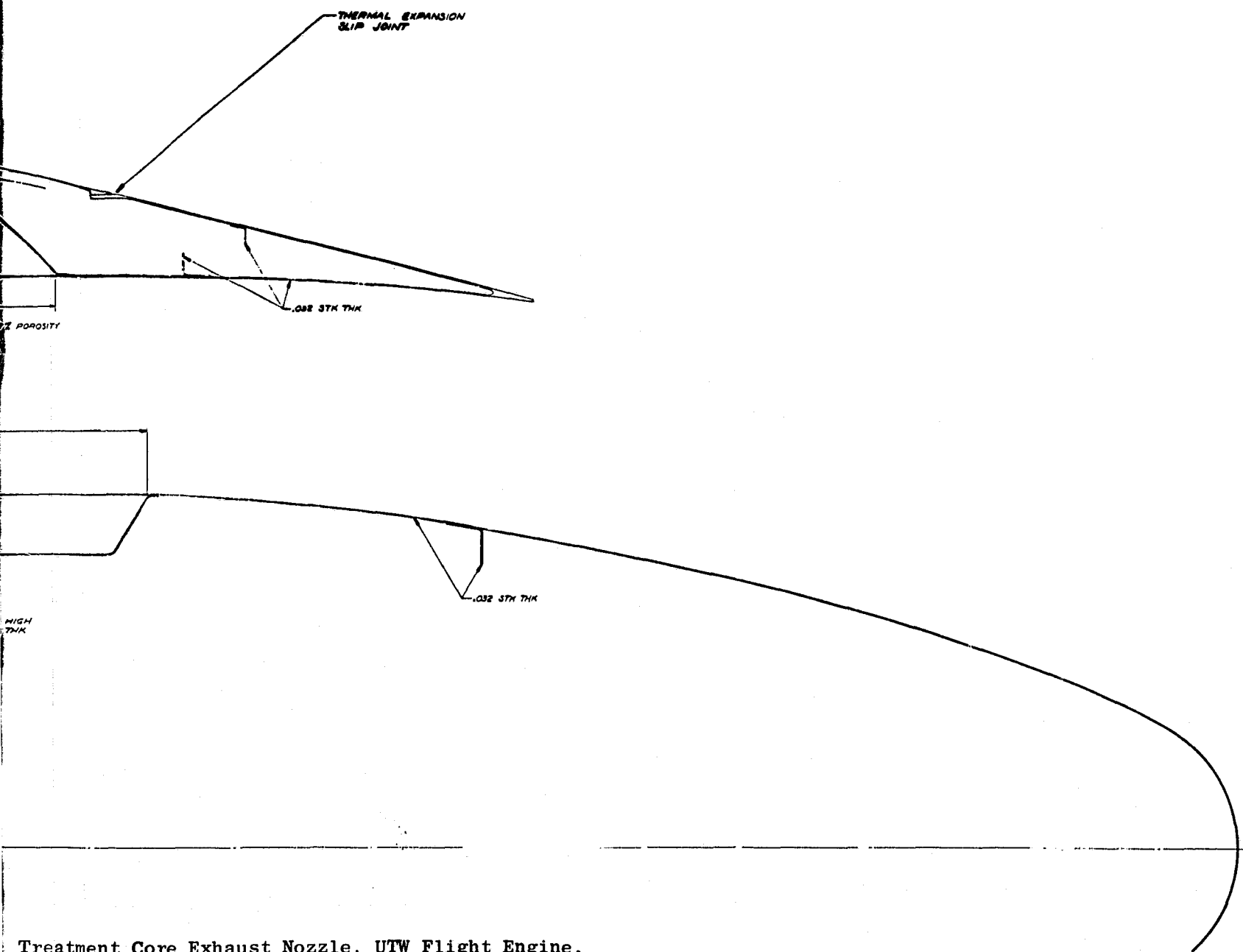


Figure 15-20. Stacked Acoustic Treatment Core Exhaust

/ FOLDOUT FRAME

534

ORIGINAL PAGE IS
OF POOR QUALITY



Treatment Core Exhaust Nozzle, UTW Flight Engine.

2 FOLDOUT FRAME

ORIGINAL PAGE IS
OF POOR QUALITY.

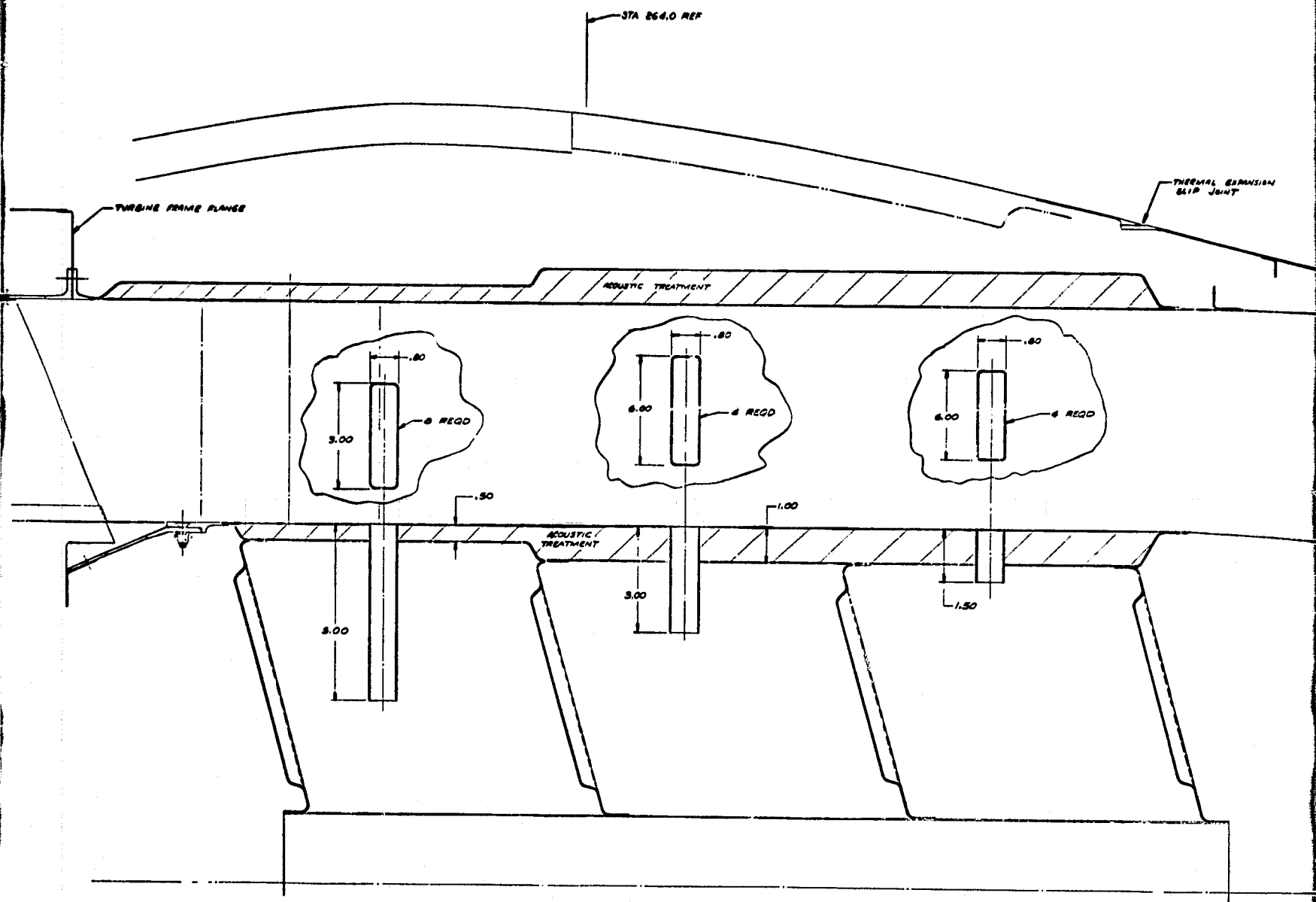
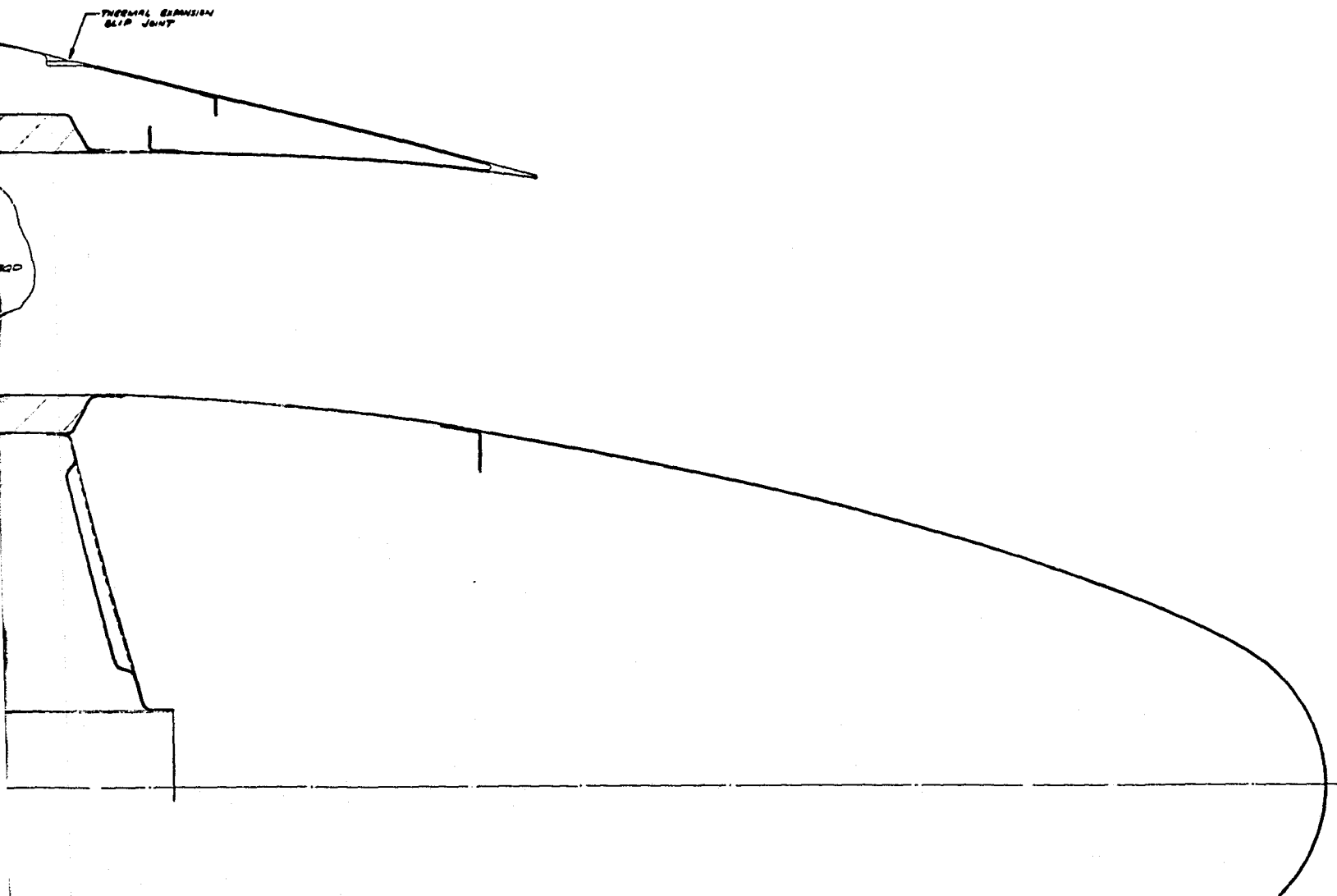


Figure 15-21. Side Branch Resonator Type Core Exhaust

ORIGINAL PAGE IS
OF POOR QUALITY

/ FOLDOUT FRAME



r Type Core Exhaust Nozzle, UTW Flight Engine.

ORIGINAL PAGE IS
OF POOR QUALITY

535

2 FOLDOUT FRAME

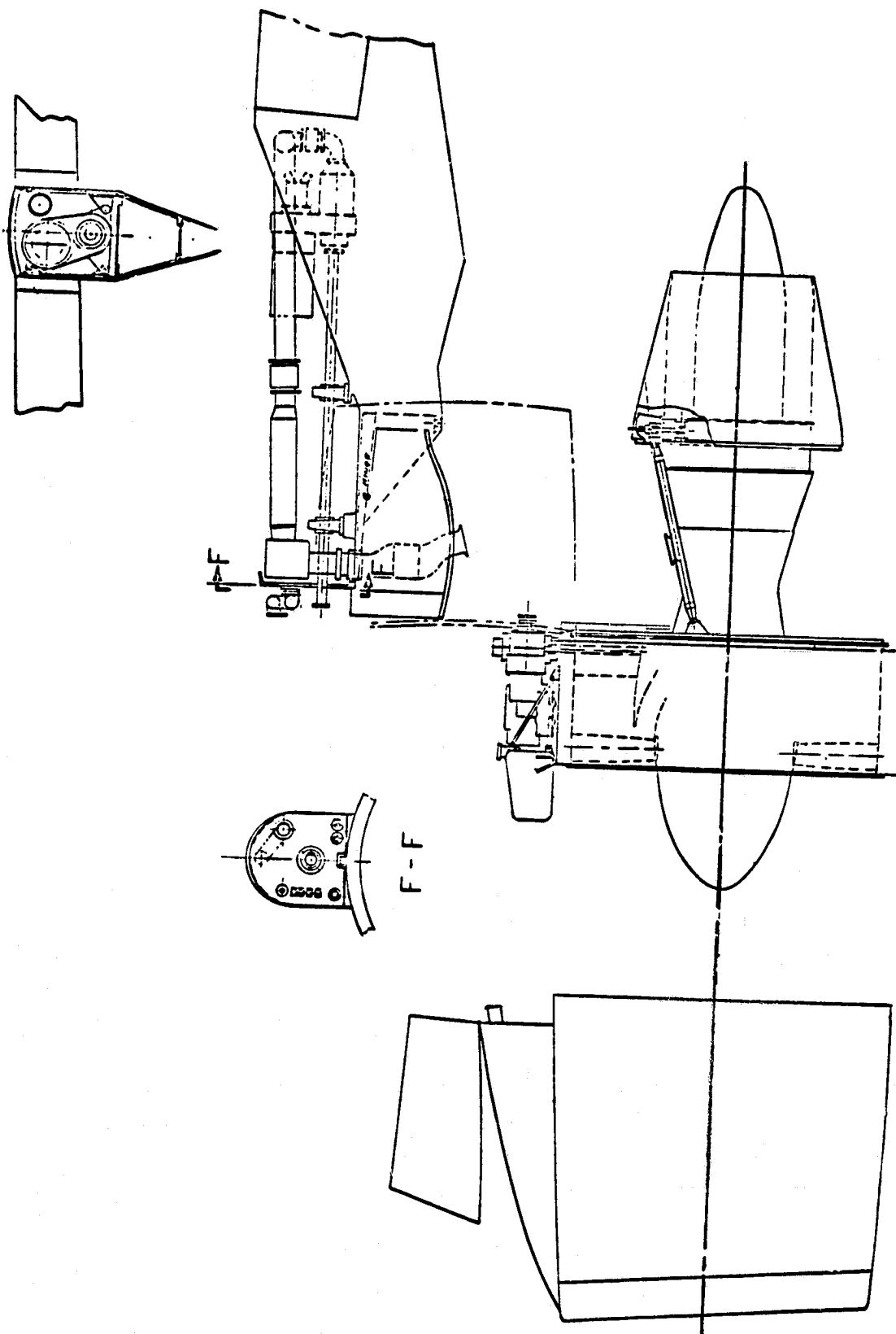


Figure 15-22. Engine Change Unit.

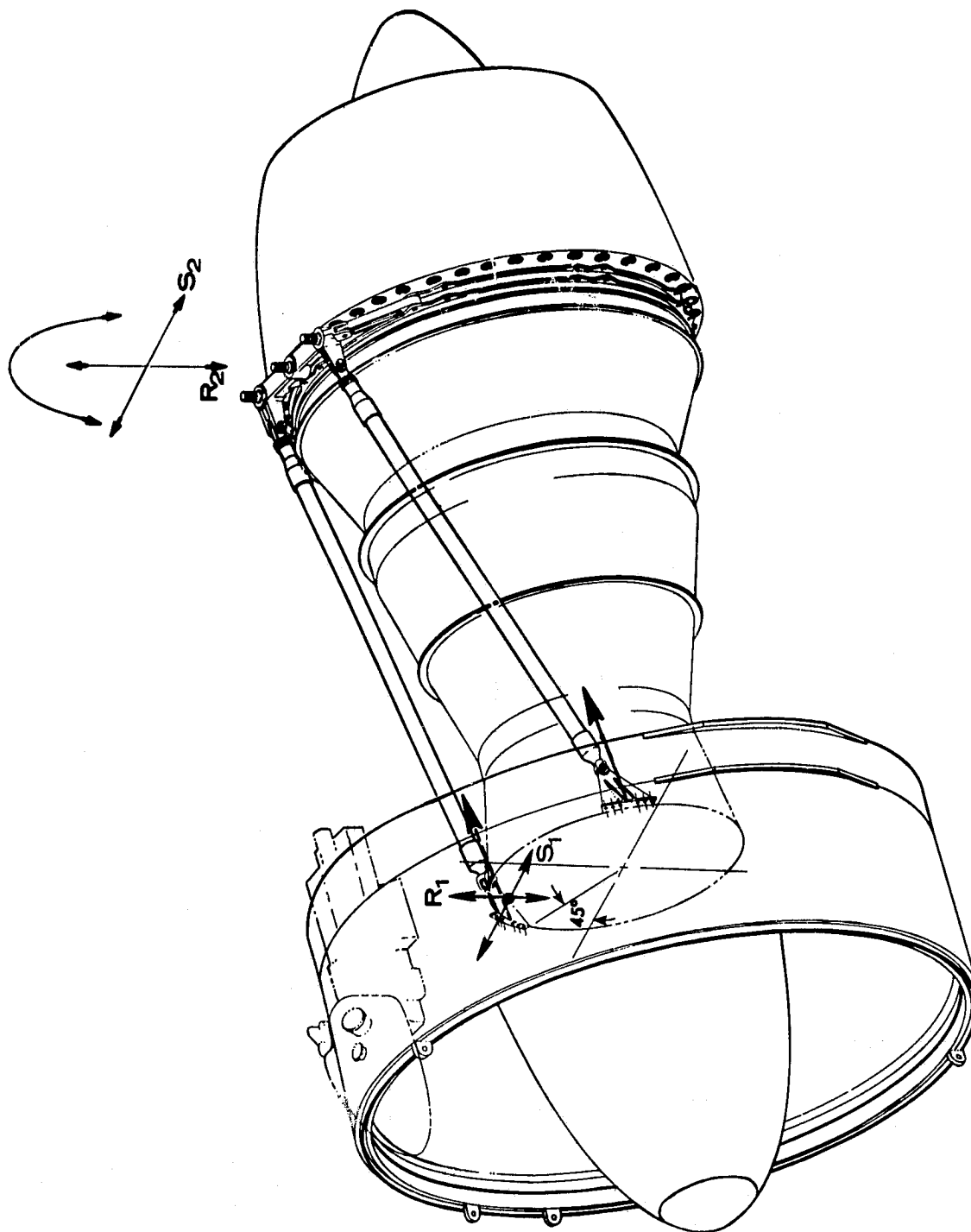


Figure 15-23. Mounting System used for UTW and OTW Experimental Engines and UTW Flight Engine.

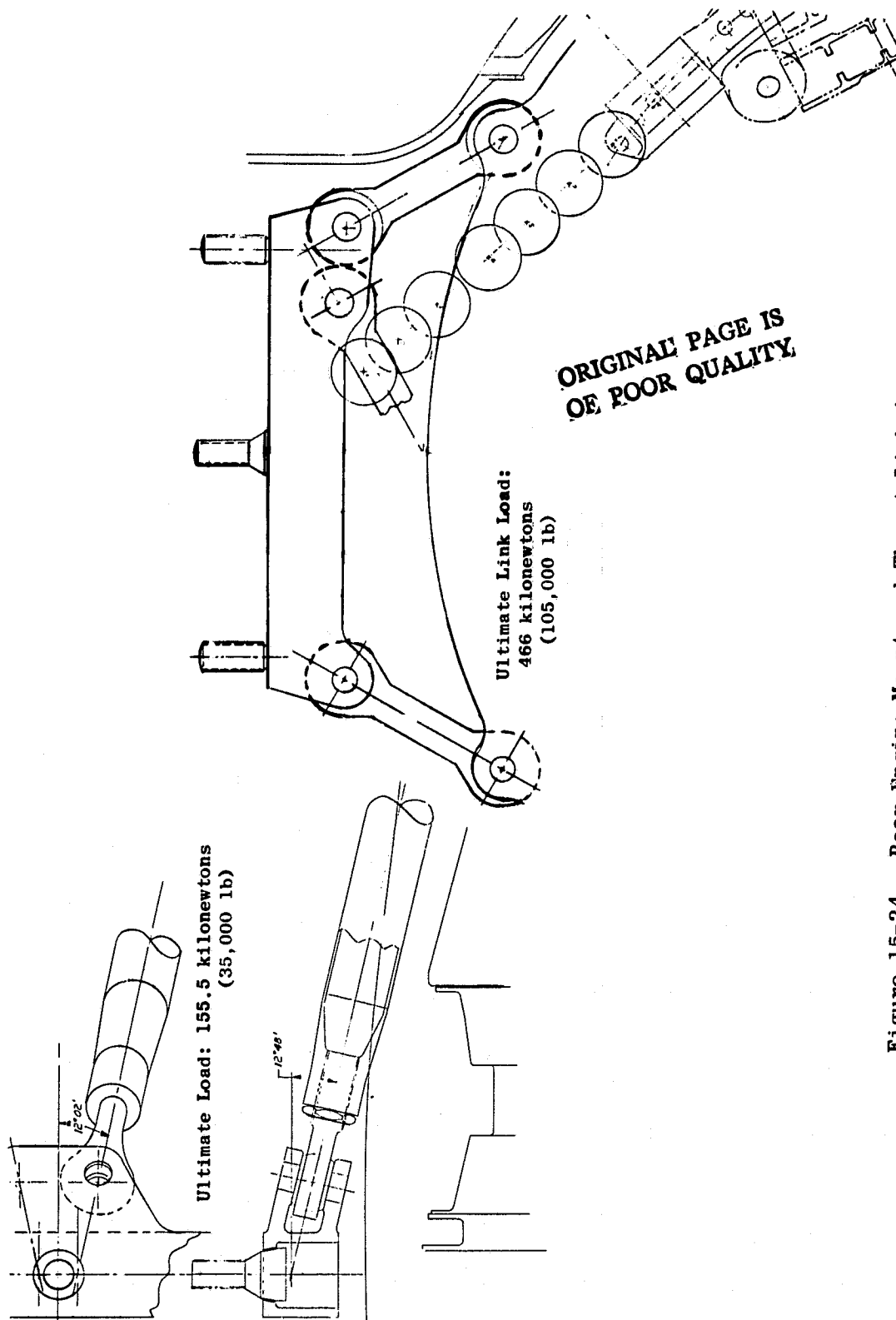


Figure 15-24. Rear Engine Mount and Thrust Link Assembly.

Except as noted, all loads are applied at the engine center of gravity. QCSEE propulsion system weight, including all engine mounted equipment such as the inlet, fan exhaust cowls, thrust reverser and accessories, will be used to determine mount loads.

Forward thrust load for design purposes is 81,400 N (18,300 lb) for the UTW system.

Load notations are defined in Figure 15-25.

A summary of typical mount reactions for unit maneuvers and "blade-out" loads is shown in Table 15-VII.

15.4.6 Engine System Dynamics

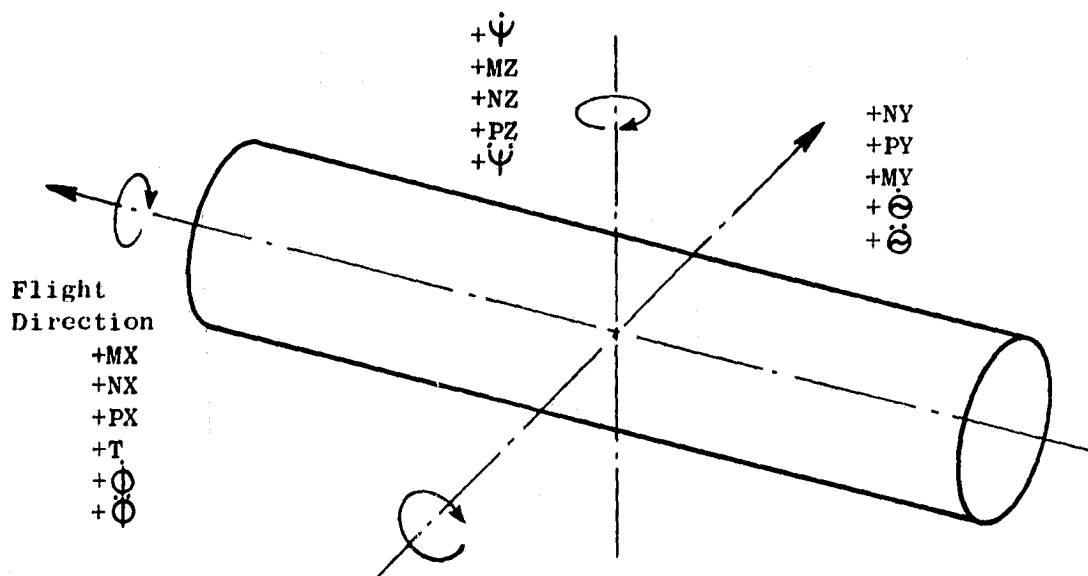
The preliminary engine vibration response analysis for the UTW engine was carried out using General Electric's VAST computer program. This program performs a linear elastic analysis of an axisymmetric structure. Figure 15-26 shows a schematic of the analytical model. Structural shells and cones are shown as solid lines, and their appropriate stiffnesses are calculated from the equation of elasticity. Bearings and frames are shown as springs, and their stiffnesses are obtained from past experience, coupled with other proven analytical techniques. Critical speeds are calculated assuming no damping, and then an estimate of the actual deflections is made at that speed by including damping coefficients along with possible unbalance locations on the rotor system. The results from these calculations are shown in the following tables.

In Table 15-VIII are presented the basic engine weights and inertias of principal components for the UTW Configuration No. 1 (experimental engine minus inlet and fan exhaust system weight).

Table 15-IX presents the system critical speeds, excluding mount modes, for the UTW Configuration No. 1. The speed range for which critical speeds were calculated was 1000 rpm to 5000 rpm.

Table 15-X presents the system critical speeds, excluding mount modes, for the UTW Configuration No. 1. The speed range for which criticals were calculated was 1000 rpm to 9000 rpm.

Table 15-XI presents the system critical speeds, excluding mount modes, for the UTW Configuration No. 1. The speed range for which critical speeds were calculated was 1000 to 15000 rpm.



Right Hand Rule for Forces, Moments, and Maneuvers

Nomenclature

- NZ - Weight Acting Down
- NY - Weight Acting Right Side
- NX - Weight Acting Forward
- T - Engine Thrust/Drag
- $\dot{\Phi}$ - Angular Pitch Velocity (rad/sec)
- $\ddot{\Phi}$ - Angular Pitch Acceleration (rad/sec²)
- $\dot{\Psi}$ - Angular Yaw Velocity (rad/sec)
- $\ddot{\Psi}$ - Angular Yaw Acceleration (rad/sec²)
- $\dot{\Phi}$ - Angular Roll Velocity (rad/sec)
- $\ddot{\Phi}$ - Angular Roll Acceleration (rad/sec²)
- PZ - Vertical Force
- PY - Side Force
- MZ - Moment About Vertical
- MY - Moment About Side
- MX - Moment About Engine Axis (Torque)

Figure 15-25. Load Locations.

Table 15-VII. UTW Experimental Propulsion System Mount Loads with Composite Nacelle.

Maneuver	R ₁	S ₁	R _{2L}	R _{2R}	S ₂
N 1G Down (1b)	+ 14,680 + (3300)		+ 3200 + (720)	+ 3200 + (720)	- - -
N 1G Side (1b)	- - -	+ 14,680 + (3300)	+ 38,475 + (8650)	+ 16,460 + (3700)	38,180 + (8583)
N 1 \odot Pitch Velocity (1b)	- - -	+ 17,125 + (3850)	+ 8320 + (1870)	+ 4450 + (1000)	+22,020 + (4950)
N 1 ψ YAW Velocity (1b)	+ 17,125 + (3850)	- - -	+ 9785 + (2200)	+ 9785 + (2200)	- - -
N 1 \odot Pitch Accel. (1b)	+ 180 + (40)	- - -	+ 110 + (25)	+ 110 + (25)	- - -
N 1 ψ YAW Accel. (1b)	- - -	+ 180 + (40)	+ 90 + (20)	+ 45 + (10)	+ 220 + (50)
N 1000 Lb Thrust (1b)	- 1110 - (250)	- - -	+ 1110 + (250)	+ 1110 + (250)	- - -
N 1 Blade Out (1) (1b) Composite Blade	+ 210,670 + (47,360)	+ 210,670 + (47,360)	+ 188,700 + (42,420)	+ 133,320 + (29,970)	+ 95,950 + (21,570)
(1) Vertical And Side Loads Do Not Act Simultaneously					

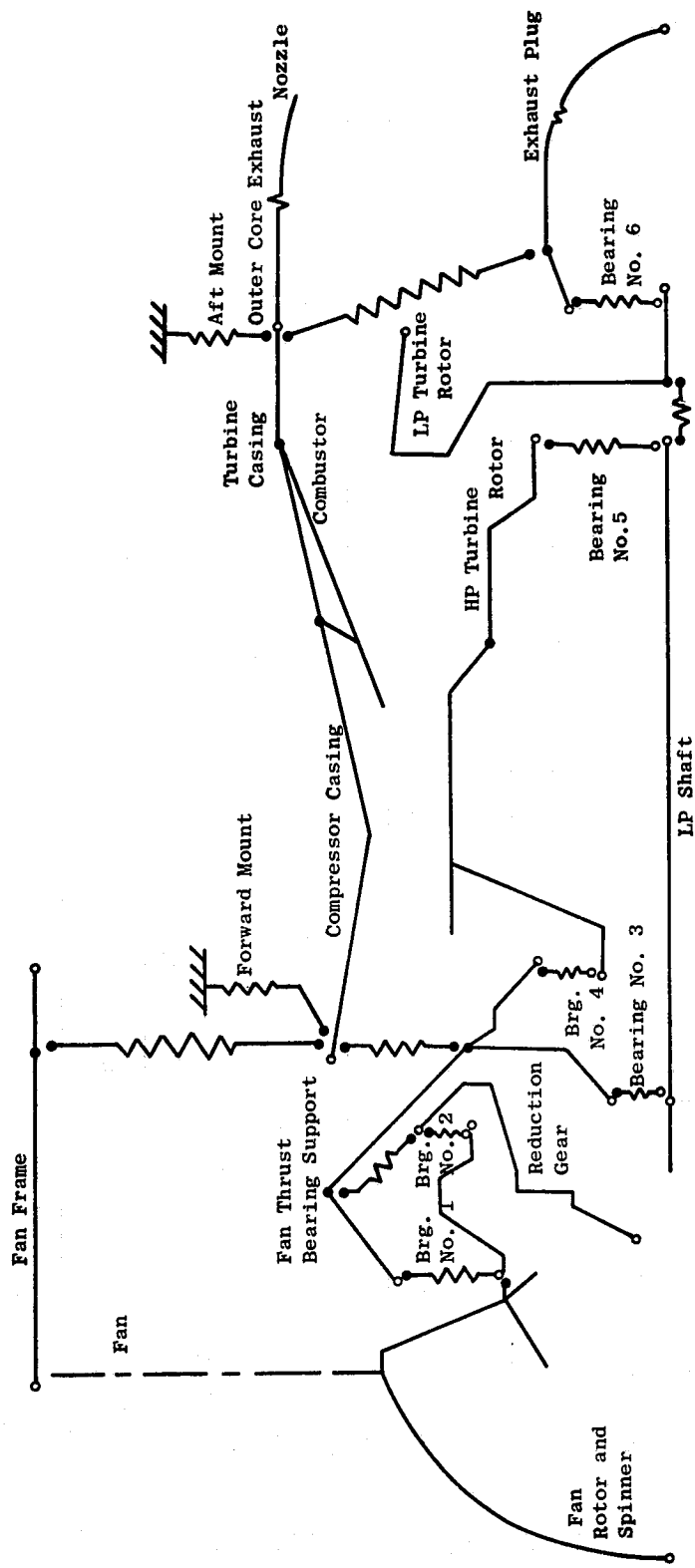


Figure 15-26. QCSEE Vibration Model, Configuration No. 1 (Typical UTW and OTW).

Table 15-VIII. Basic Engine Weight and Moment Data,
UTW Configuration No. 1.

Overall Engine

- Total weight - 1806 kg (3982 lb.)
- Transverse moment of inertia about C.G. $1.68 \times 10^7 \text{ kg-cm}^2$ ($5.73 \times 10^6 \text{ lb-in}^2$)
- C.G. location 48 cm (18.9 in.) aft of fwd. mount plane
- Distance between mounts 123 cm (48.5 in.)

<u>Rotors</u>	<u>Weight</u>		<u>Polar Moment</u>	
	<u>kg</u>	<u>(lb)</u>	<u>kg-cm²</u>	<u>(lb-in²)</u>
Fan (including V.P. Actuation System)	237	(523)	258,200	88,245
Lp	105	(232)	41,940	14,332
HP	193	(425)	68,250	23,322

Table 15-IX. System Critical Speeds, Maximum Response
Due to Fan Rotor.

<u>Mode Description</u>	<u>Fan Speed,</u>		<u>Response⁽¹⁾</u>
	<u>rpm</u>	<u>cm</u>	
LP Rotor Bending	2332	0.0013	(0.5)
Turbine Frame & Exhaust Plug	2748	0.025	(10)
Core Casing	3677	0.018	(7)

(1) Single amplitude response at point of maximum deflection,
in mils, for 100 gm-in. unbalance at fan centerline.

Table 15-X. System Critical Speeds, Maximum Response
Due to LP Turbine Rotor.

<u>Mode Description</u>	<u>LPT Speed,</u>		<u>Response⁽¹⁾</u>
	<u>rpm</u>	<u>cm</u>	
Fan Rotor & Compressor Case	2517	0.013	(5)
Turbine Frame & Exhaust Plug	3168	0.028	(11)
Fan Rotor & Fan Frame	4146	0.008	(3)
HP and LP Rotors	6092	0.041	(16)
Core Casing	8287	0.005	(2)

(1) Single amplitude response at point of maximum deflection,
in mils, for 100 gm-in. unbalance in LP turbine.

Table 15-XI. System Critical Speeds, Maximum Response Due to HP Rotor.

Mode Description	HP Rotor Speed, rpm	Response ⁽¹⁾			
		Unbalance At Compr. Stg. 1		Unbalance At HPT	
		cm	(mils)	cm	(mils)
Fan Rotor & Exhaust Plug	2564	0.020	(8)	0.020	(8)
Fan Rotor & Exhaust Plug	3236	0.013	(5)	0.020	(8)
Fan Frame & Core Case Bending	4166	0.005	(2)	0.005	(2)
LP & HP Rotors	5534	0.005	(2)	0.122	(48)
Core Casing	8029	0.023	(9)	0.002	(1)
LP Rotor	9861	0.033	(13)	0.046	(18)
Fan Rotor & Fan Frame	10099	0.028	(11)	0.008	(.3)
LP & HP Rotors	13587	0.097	38	0.002	(1)
(1) Single amplitude response at point of maximum deflection, in mils, for 100 gm-in unbalance at indicated location.					

The results of the VAST computer analysis show that no rotor flexural criticals exist in the engine operating range for any of the rotors. The most significant critical occurs at 5534 rpm and indicates an estimated response of 0.122 cm (48 mils) for 100 gm-in. unbalance in the HP turbine. However, since a substantial portion of the bending energy is absorbed by the frames, this critical is not considered hazardous assuming that standard rotor balancing procedures are followed at HP rotor assembly.

15.4.7 Accessories

The accessory arrangement, for the UTW experimental propulsion system will be similar to the arrangement planned for the UTW flight system (Figure 15-27) with many of the same maintenance features. To reduce cost, experimental engine components in the accessory area are "off-the-shelf" items.

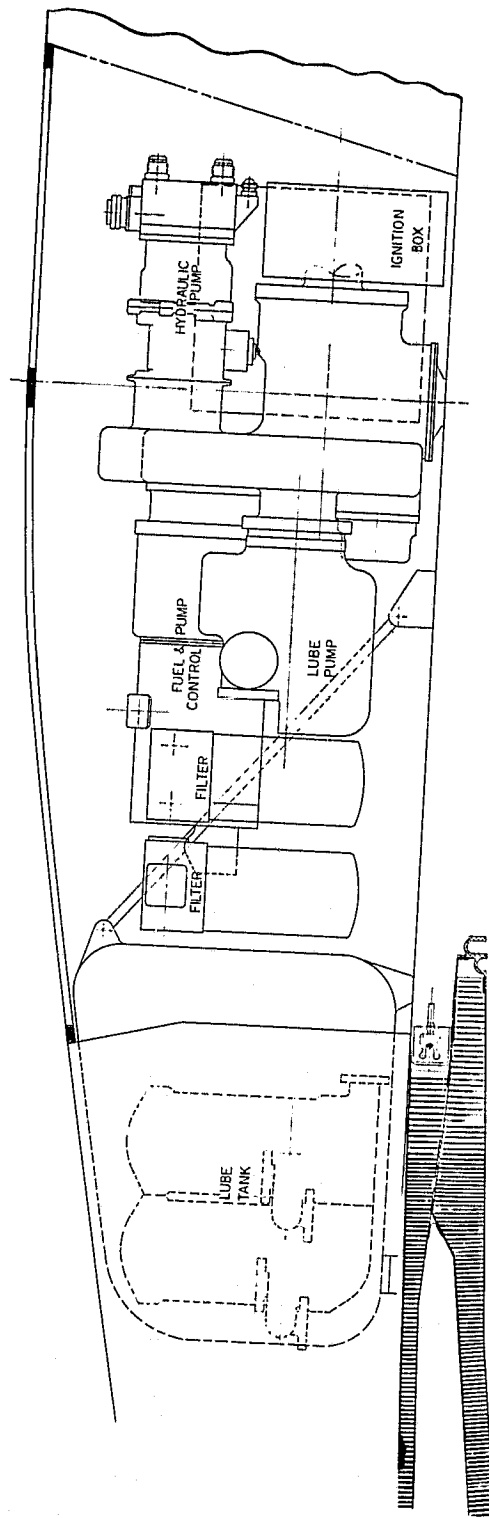


Figure 15-27. UTW Experimental Engine Accessories.

- Main Fuel Pump and Control - Modified F101
- Fuel Shutoff Valve - Nonflight design
- Fuel/Oil Coolers from the CF6
- Lube Tank from the TF39
- Lube Filters from the CF6
- Air/Oil Separator
- Lube and Hydraulic Pumps
- Magnetic Chip Detectors from the F101
- Alternator from the F101
- Digital Control - non flight weight design
- Ignition Box from F101
- Control Cables
- Anti-Icing Valve (Not included on experimental engine)
- Power Take-off (PTO)

The above items optimized to meet flight system requirements will be mounted on the outer casing of the fan frame in the accessory area. Location of components will permit removal of the inlet without removing or uncoupling any of the engine fluid systems. Removal of the engine vertically will be possible without removing or uncoupling engine to engine piping. The experimental engine gearbox is a "boiler plate" component using gears and bearings from the F101 gearbox.

Opening fan and core cowl doors will provide access to the core engine mounted equipment:

- Fuel Manifold, Valves and Tubes from the F101
- Stator Actuators from the F101
- Scavenge Pump
- Ignitors
- Instrumentation
- Speed Sensors
- Vib Sensors
- Fire Detection and Extinguishing

The scavenge pump with its own inlet gearbox and radial drive is on the bottom of the engine to provide a gravity drain lube system.

The UTW flight system will include the following items not planned for the experimental engine.

- Flight Weight Gearbox
- Double Wall Fuel Piping and Manifold
- Improved replaceability of Fuel Injection Tubes
- Flight Radial Drive for Scavenge Pump
- "Hard-wall" titanium piping in place of soft hardware coupling F101 engine plumbing with accessories

15.5 UTW AND OTW BOILER PLATE NACELLE DESIGN

This section deals with the conceptual design of the "boiler-plate" nacelle hardware for the initial testing of the UTW propulsion system and the total OTW propulsion system as it will be shipped to NASA in 1977. All boiler-plate nacelle hardware used initially for the UTW will be part of the OTW propulsion system assembly. The preliminary design review of the boiler-plate nacelle and facility hardware for the UTW system has been scheduled for March of 1975 and the preliminary review of the OTW system will be in August of 1975.

15.5.1 Inlet

Planned testing of the UTW and OTW engines will require two boiler-plate inlet configurations. A bellmouth inlet will be utilized for aerodynamic engine mapping and baseline acoustic evaluation. A hybrid configuration featuring elevated throat Mach number and multiple acoustic suppression designs will be employed for the flight-type aero and acoustic evaluations. Both inlets will be mechanically decoupled from the engine (Figure 15-28). The boiler plate nacelle components are decoupled to prevent overload of the composite fan frame flanges due to excessive engine motion/vibration. A typical decoupled or "load-break" joint is shown in Figure 15-28 (View A). The air seal is provided by a closed-cell foam, such as Scott-Felt, bonded to one-half of the flange and pressed against the other. The acoustic seal is provided by a lead foil in a vinyl cover. By nullifying the acoustic and air leakage through these extra joints, the boiler plate, test, systems can best represent the final composite propulsion system assembly. A typical inlet to test stand mounting system at the Peebles test site is shown in Figure 15-29.

The bellmouth inlet package consists of a fiberglass/honeycomb bellmouth and cylindrical or conical casings that satisfy the aerodynamic requirements for a low Mach number inlet (Figure 15-30).

The hybrid inlet package (see Figure 15-30, bottom) includes a fiberglass/honeycomb lip and a structural shell that provides the attachment bosses for two interchangeable sets of acoustic treatment and one matched set of hardwall panels for initial UTW system testing. One additional set of acoustic panels will be procured specifically for OTW testing. Acoustic configurations will provide three treatment thicknesses in accordance with the current acoustic design philosophy. A typical acoustic panel fabrication will consist of an aluminum perforated face plate stretch formed to the correct contour and bonded to a honeycomb/single degree of freedom panel which in turn is bonded to an aluminum or fiberglass backing sheet.

For the OTW system testing, additional hardware will be procured for the inlet to simulate an external flowpath. These external flow lines will not, however, be identical to a true flight-type configuration. The inclusion of removable acoustic panels will necessitate the usage of a larger outer cowl diameter [maximum diameter approximately 218 cm (86 in.)].

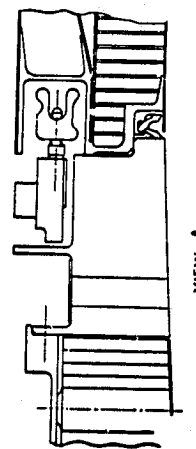
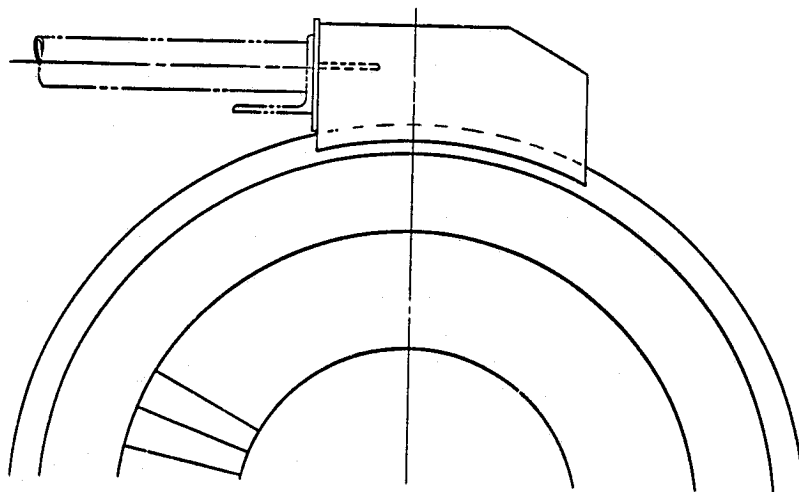
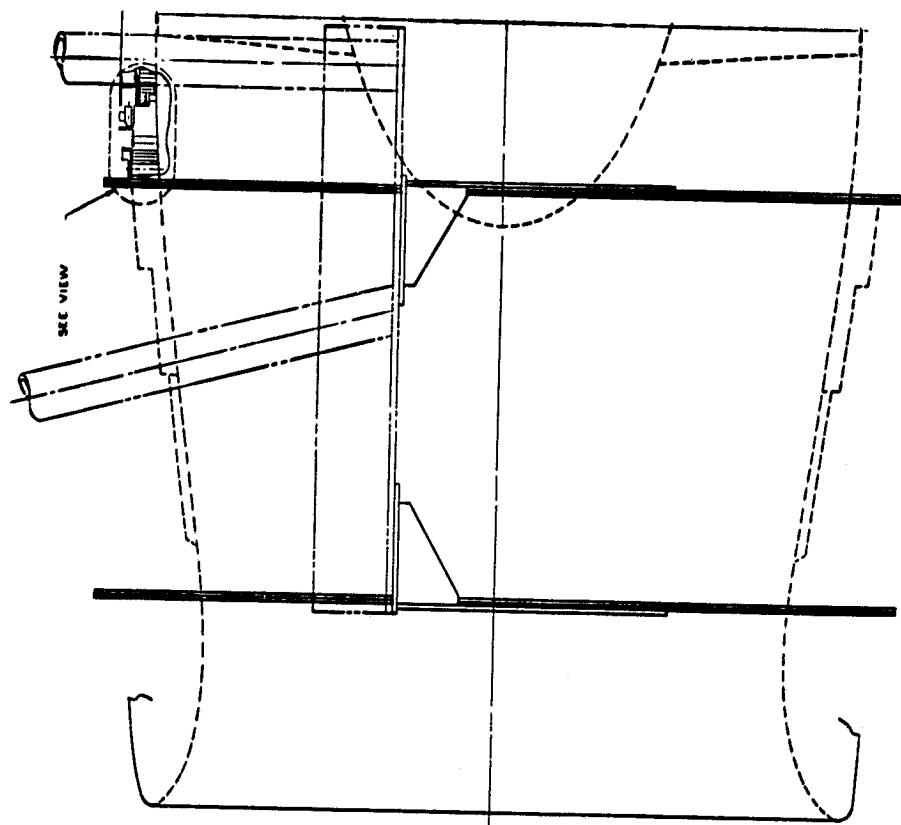


Figure 15-28. Inlet Configuration.

ORIGINAL PAGE IS
OF POOR QUALITY

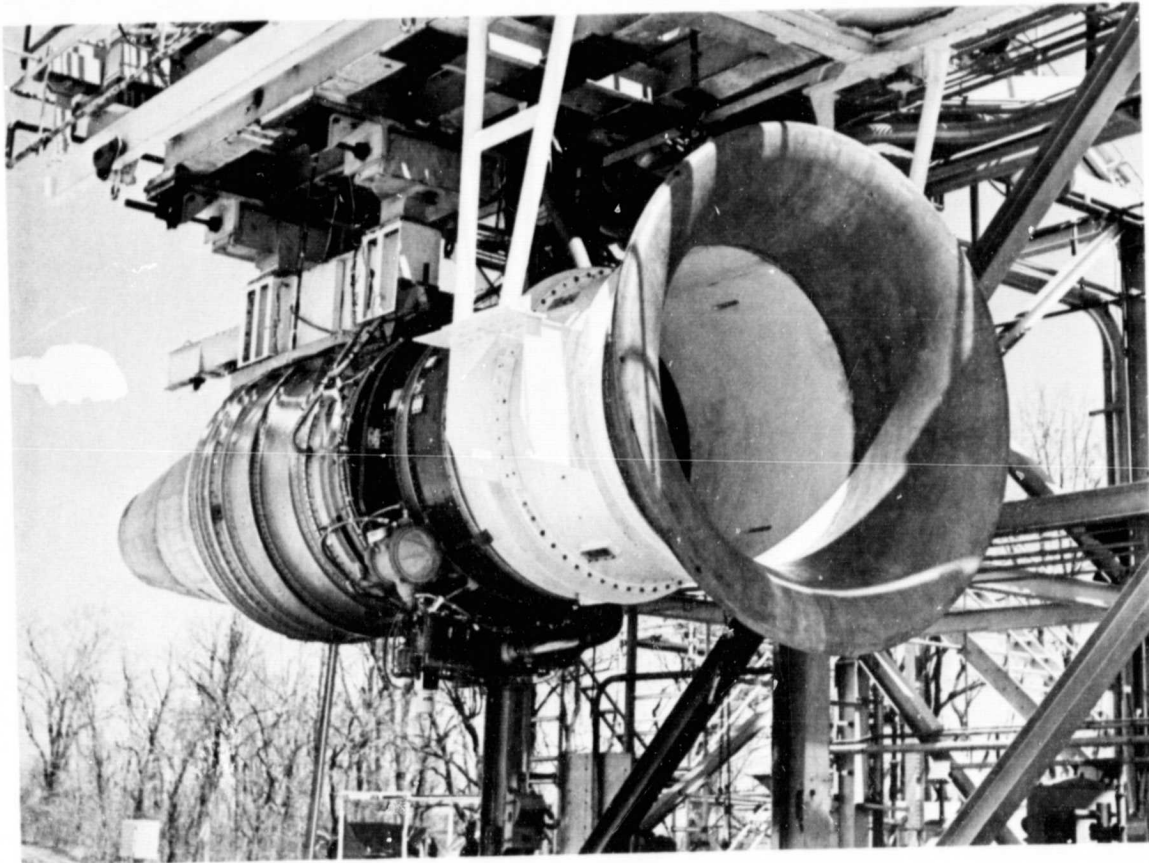
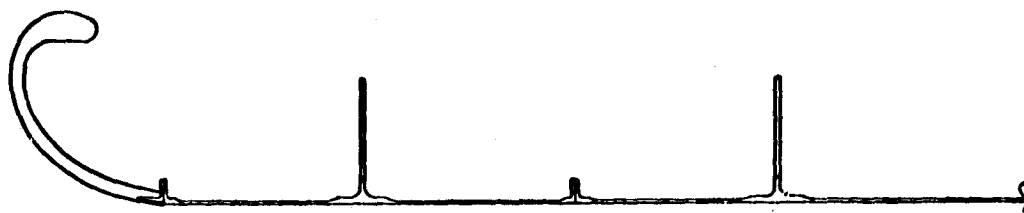


Figure 15-29. Inlet Mounted on Test Stand at Peebles Proving Grounds.

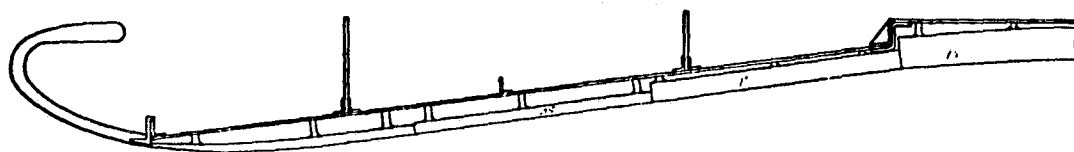


Bellmouth

Baseline

- M 0.45
- No Suppression

Rotate for Crosswind Effects



Flight Contour

ROTOR SA

Hybrid Inlet

- M 0.79
- One Set Hardwalls
- Two Sets Acoustic Treatment
- Three Panel Designs

Figure 15-30. Boiler Plate Inlets.

15.5.2 Fan Bypass Duct

The UTW fan bypass duct is a fabricated structural shell that provides the attachment capability for two interchangeable sets of acoustic treatment and one matched set of hardwall panels. Two single-ring splitters will be procured to match the two acoustic configurations. They will be supported by the duct through six airfoil-shaped aero/mechanical struts. Core cowl access is accommodated by the hinged door construction of the outer ducting. The doors are supported from the facility through a beam internal to the pylon. (see Figure 15-31). The duct/fan frame interface is a typical Marman-type joint.

The variable UTW fan nozzle will be designed and procured as a component of the composite nacelle assembly and will be utilized in both the composite and boilerplate nacelle configurations. It is fully operable and attaches as an assembly to the fan duct.

The OTW bypass duct is comprised of the UTW duct structural shell with one new set of acoustic panels and one acoustically treated, single-ring splitter. Since the UTW nozzle will be removed at Station 246, new structure and panels will be procured from this station aft to the thrust reverser. Fairings will provide smooth aerodynamic, external flowlines from the inlet to the thrust reverser.

15.5.3 Core Cowl

The UTW core cowl embodies the same design philosophy established for the fan duct. It is a fabricated structural shell that supports two sets of interchangeable acoustic panels and one set of hardwall panels. It has a forward interface (Marman-type joint) with the fan frame and an aft interfacing slip joint with the core nozzle. Access to the compressor and turbine is provided by the hinged door construction of the core ducting which is supported by the facility beam extending down within the pylon (see Figure 15-32).

The core cowl assembly between the fan frame and station 246 will also use the UTW boiler-plate core cowl structure and a new set of acoustic panels. From station 246 aft to the slip joint at the core nozzle both new acoustic panels and new structure will be the differences between OTW and UTW flowpaths.

15.5.4 Core Nozzle

The mechanical design activity in the OTW core exhaust nozzle was limited to one nonflight conceptual design as shown in Figure 15-33 with interchangeable acoustic treatment. The layout was made primarily to show the latest flow path and to define the envelope available for acoustic treatment.

The design is similar to the UTW as described in Section 15.5.4. The flight-type OTW core nozzle design would also be similar to that previously described for the UTW flight design with either the stacked core or side branch resonator acoustic treatment design as determined from scheduled sound suppression tests.

15.5.5 Pylon - Boiler Plate and Composite

The pylon/box-beam assembly is the primary structural support system for the fan exhaust duct assembly. The beam is a welded fabrication that extends from the overhead facility structure to the engine core through the pylon. It is pinned to the facility structure at its aft end and soft mounted in rubber bushings at its forward end. The aft, pinned joint of the beam support system will be designed to relieve the composite fan frame of a portion of the load of supporting the boiler plate nacelle (see Figure 15-34). All thrust loads applied to the fan ducting are transmitted to the engine mounts through the fan frame. Aerodynamic contour of the pylon is provided by a nonstructural fairing bolted to the structural beam.

Two pylon/box-beam assemblies will be procured. The configurations will be identical for both the UTW and OTW experimental engines.

15.5.6 OTW Target Thrust Reverser

The OTW nacelle assembly will include a target-type, thrust reverser. The reverser assembly will be decoupled from the engine, as discussed in Section 15.5.1, with separate mounts to the test facility (Figure 15-35) similar to the inlet support system previously shown in Figure 15-29. Due to the uncertainty of the aerodynamic requirements, there has been minimal preliminary mechanical design effort in this area. The flight assembly will require a variable area exhaust nozzle. The boiler plate nacelle will achieve the desired areas by adjustable, rotating side doors or fixed position, interchangeable hardware. Cost, complexity, and maintainability will determine the final configuration selection.

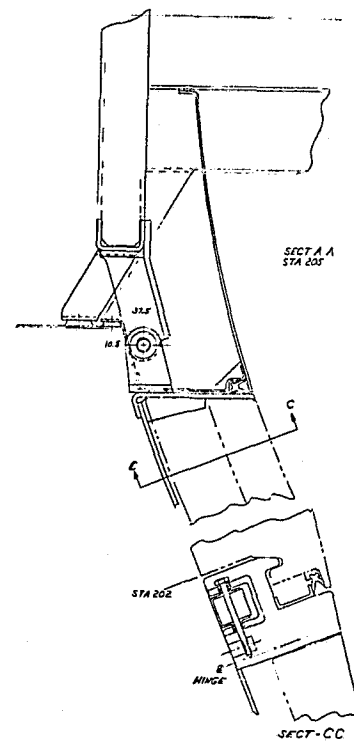
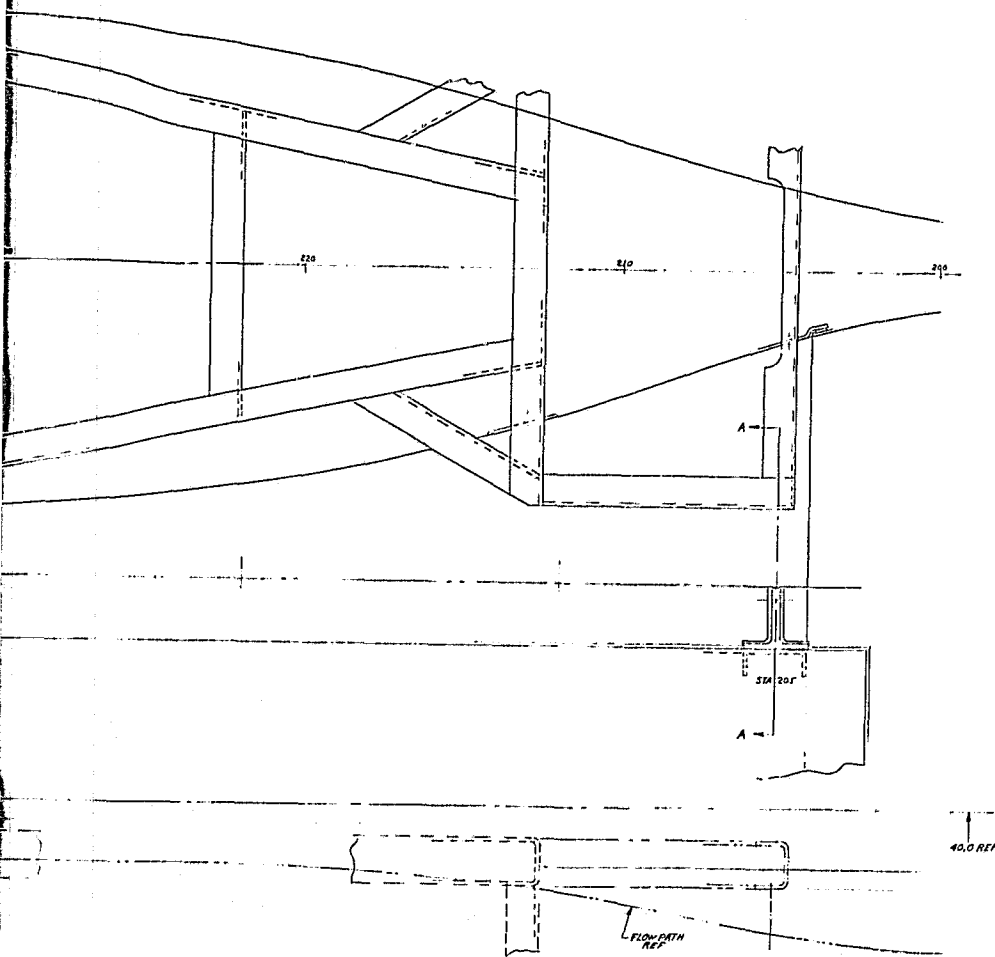
15.5.7 OTW Containment Ring

Special hardware is required for containment of the large metal blades on the OTW fan rotor. This will be provided as shown in Figure 15-36. The composite fan frame common to both the OTW and UTW has a casing diameter of 200 cm (78.8 in.). The containment ring mounts to the boilerplate inlet rear flange, and its weight is supported through the inlet test stand mounts. The outer surface of the boiler plate nacelle covers the containment ring at the 218 cm (86 inch) diameter position, Figure 15-36.

15.5.8 OTW Mounting System

The OTW experimental engine mounting system is identical to the UTW mounting system described in Section 15.4.5.

The OTW flight mounting system will be developed to be compatible with this unique installation. Figure 15-37 shows a concept of an engine change unit. The unit would include the inlet, engine accessories, and PTO shaft to the aircraft accessories, bottom pylon, and the basic engine with the core exhaust system.

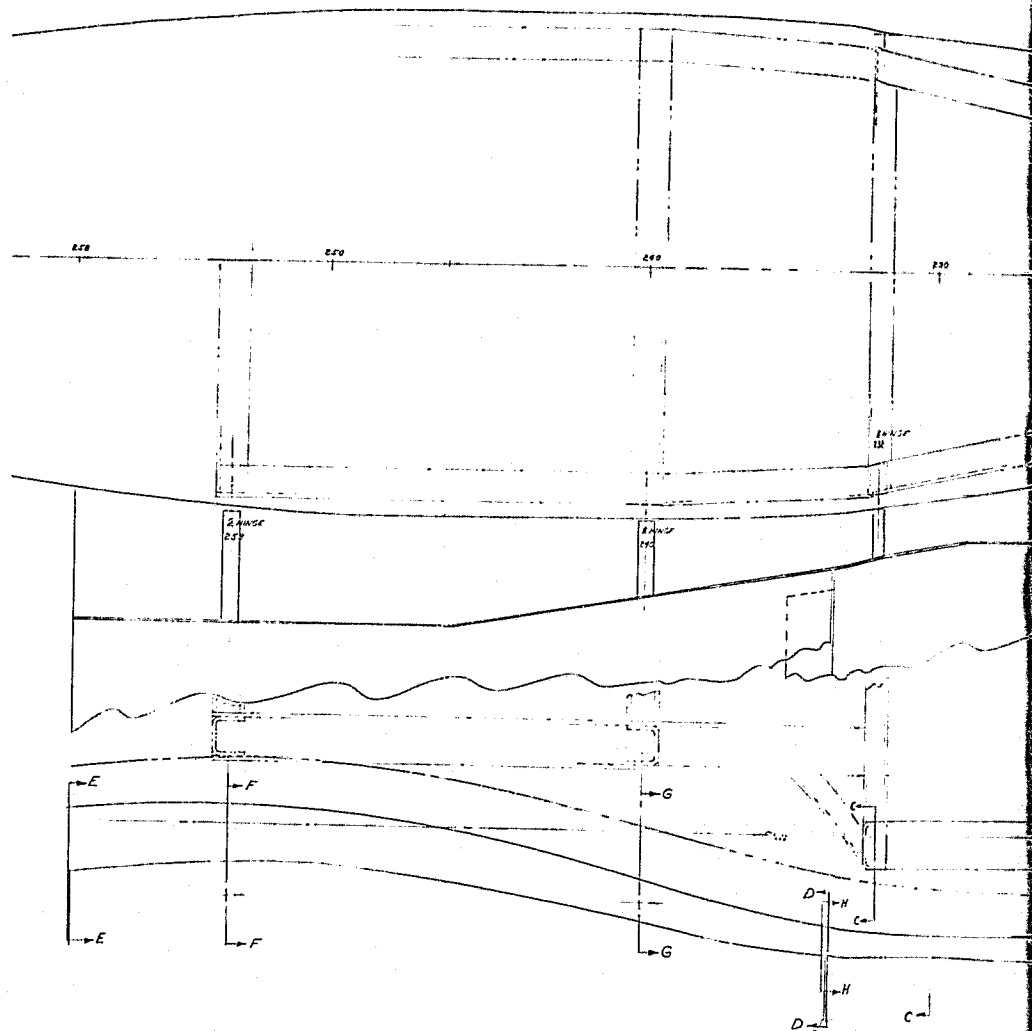
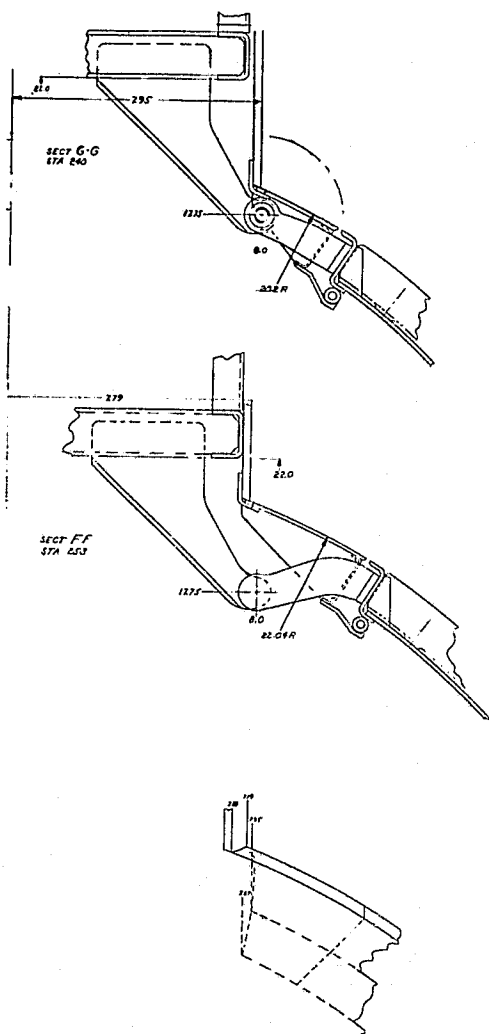
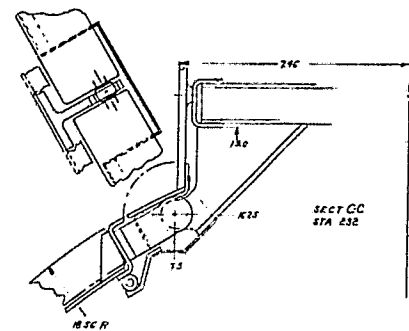
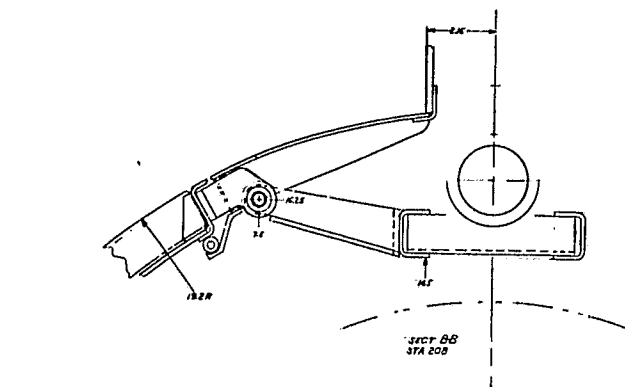


Fan Cowl Door Attachment.

2 FOLDOUT FRAME

555

ORIGINAL PAGE IS
OF POOR QUALITY

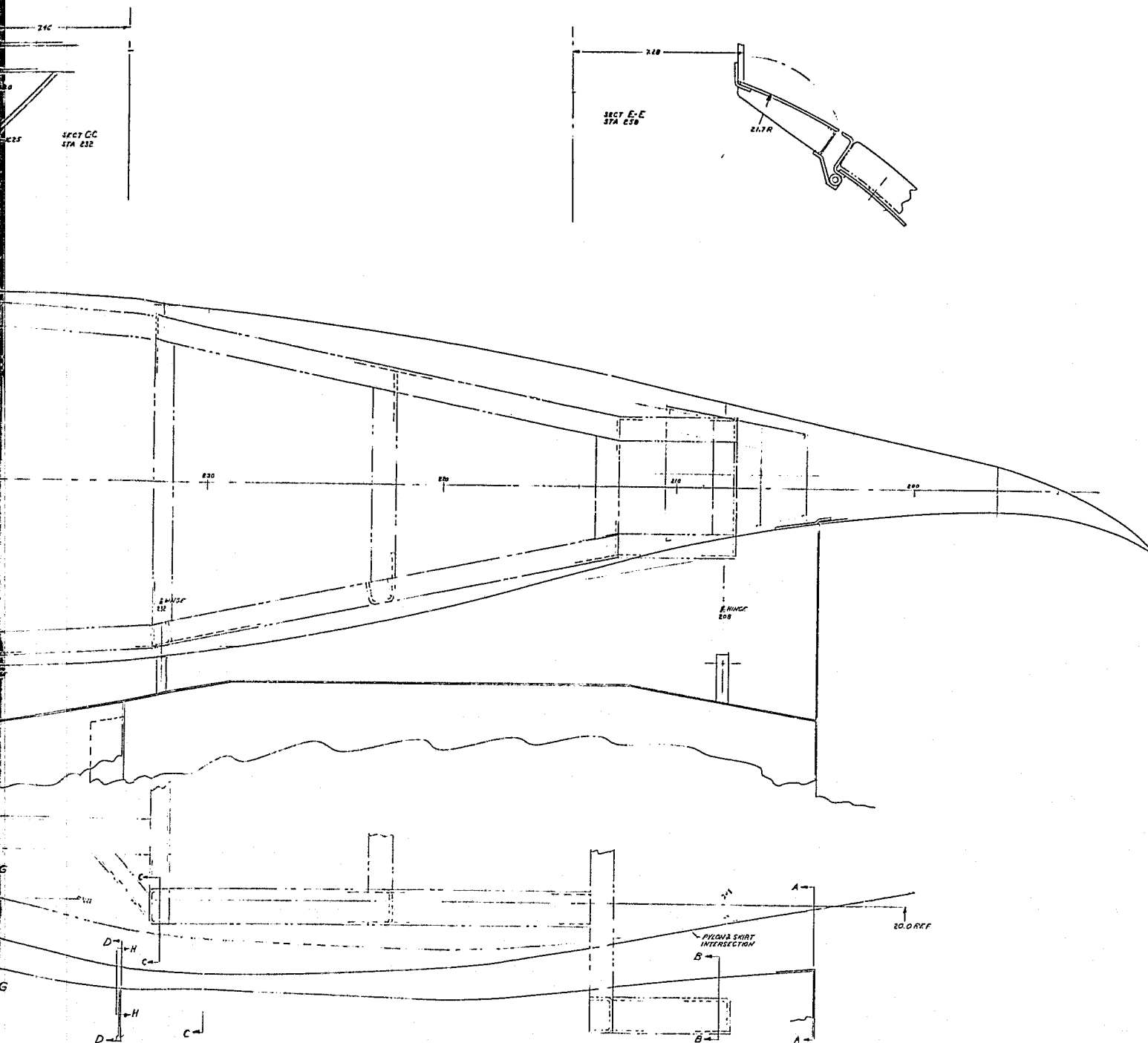


FOLDOUT FRAME

556

Figure 15-32. Fan Core Cowl Door At

ORIGINAL PAGE IS
OF POOR QUALITY



2. Fan Core Cowl Door Attachment.

2 HOLDOUT FRAME

ORIGINAL PAGE IS
OF POOR QUALITY

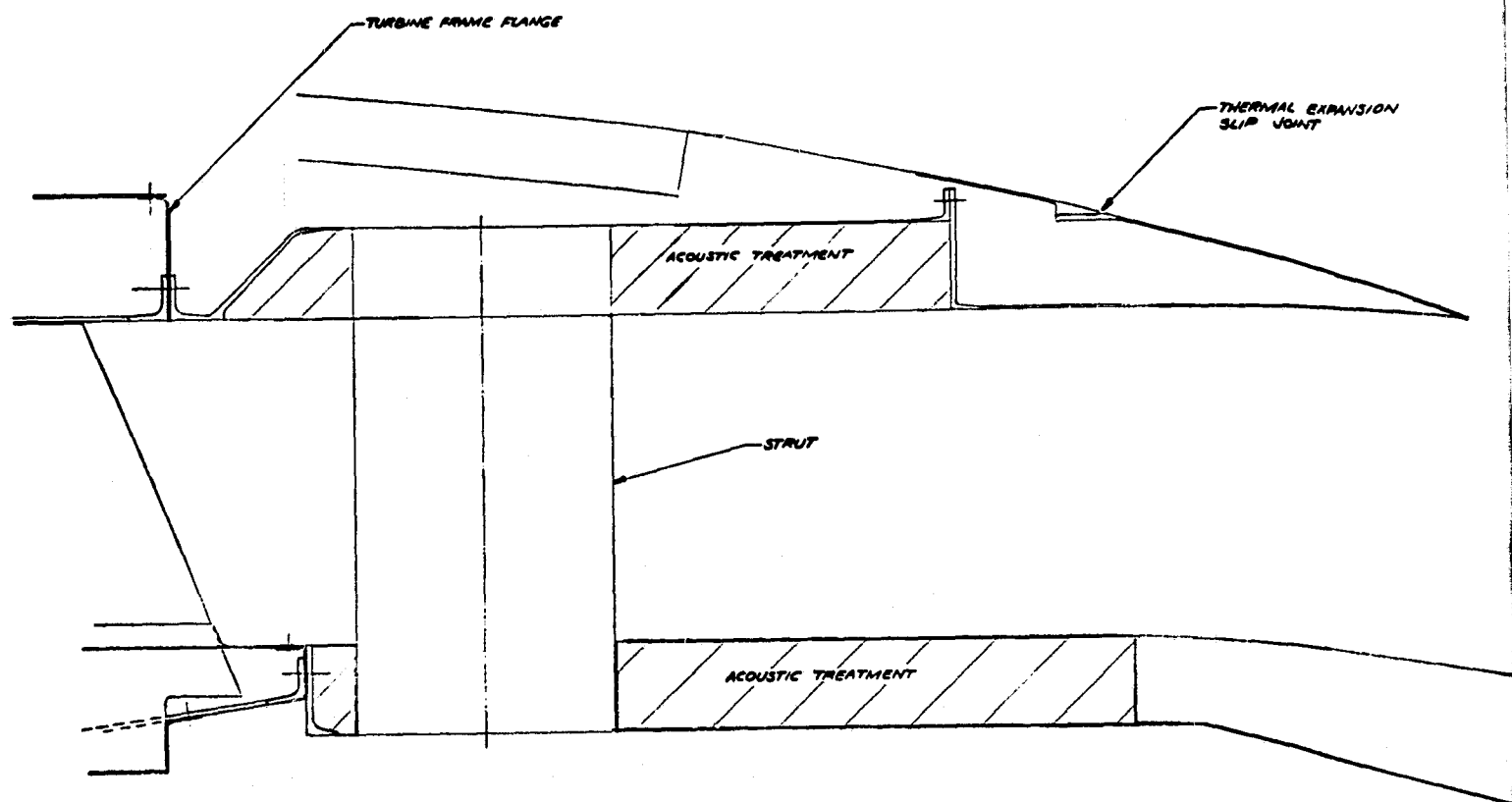
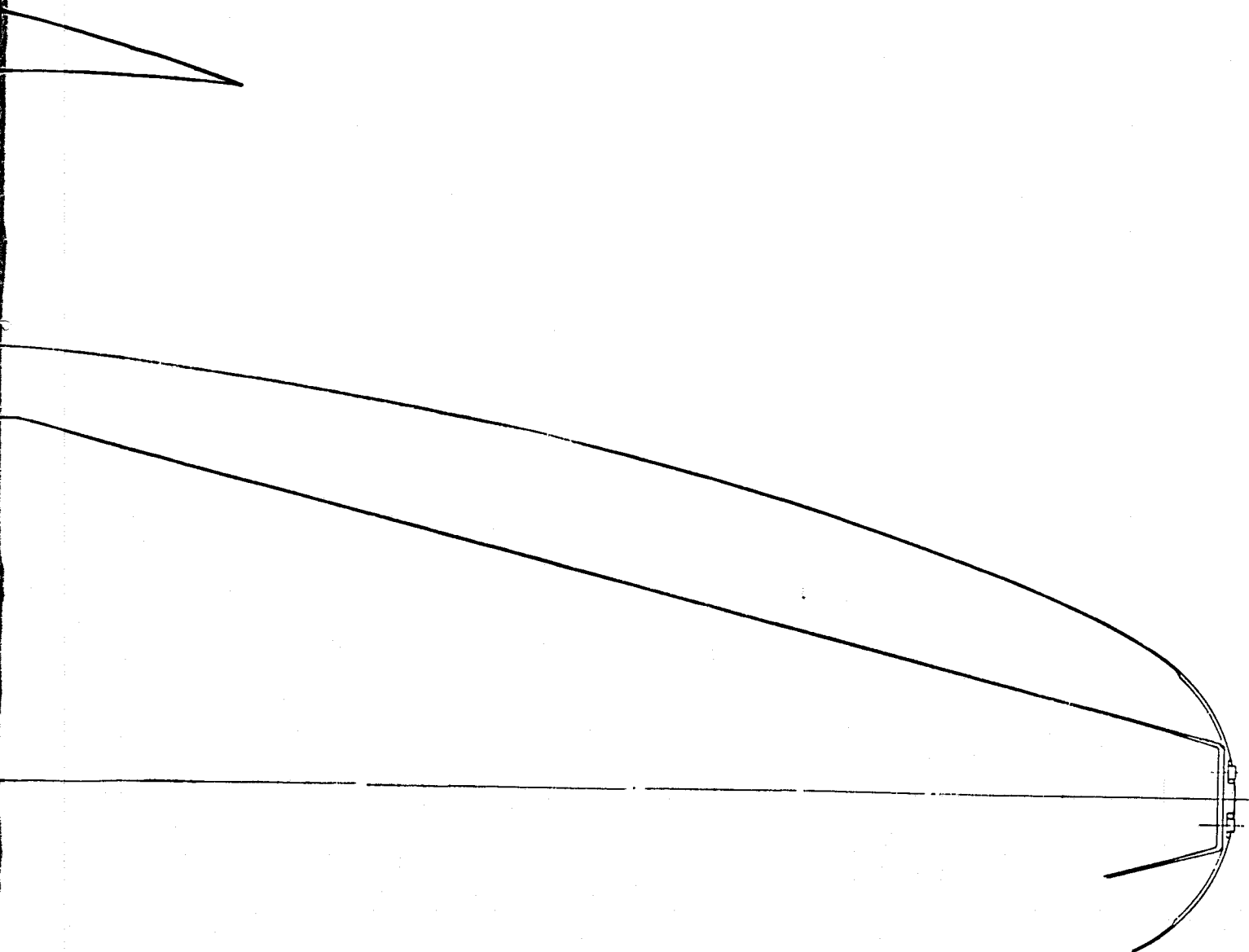


Figure 15-33. OTW Experimental Core

/ FOLDOUT FRAME

ORIGINAL PAGE IS
OF POOR QUALITY

THERMAL EXPANSION
SLIP JOINT

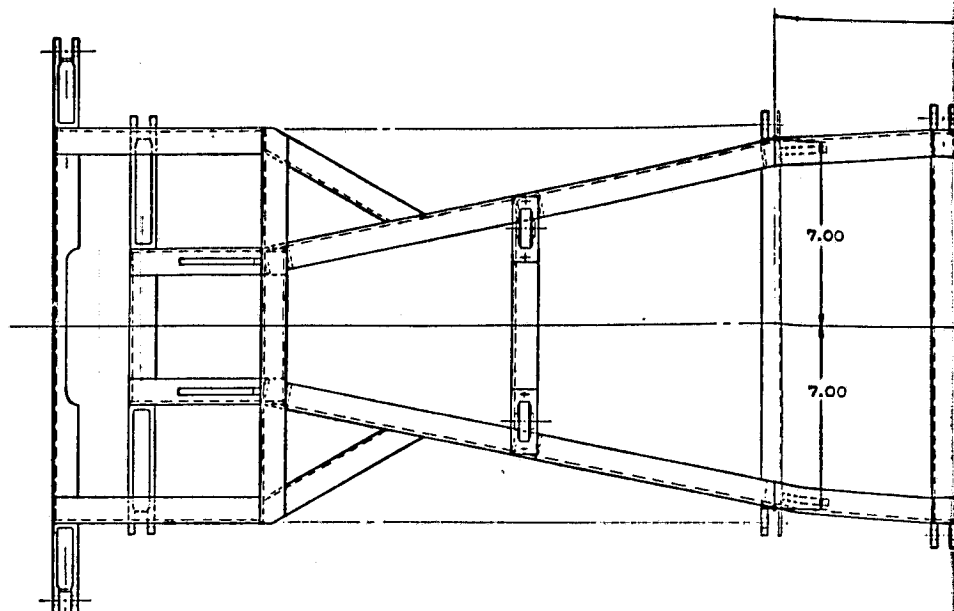
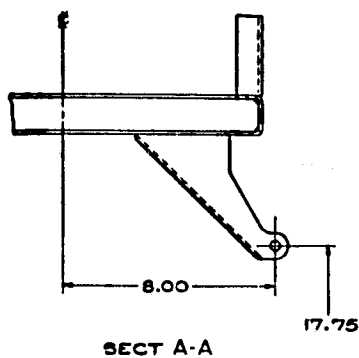


OTW Experimental Core Exhaust.

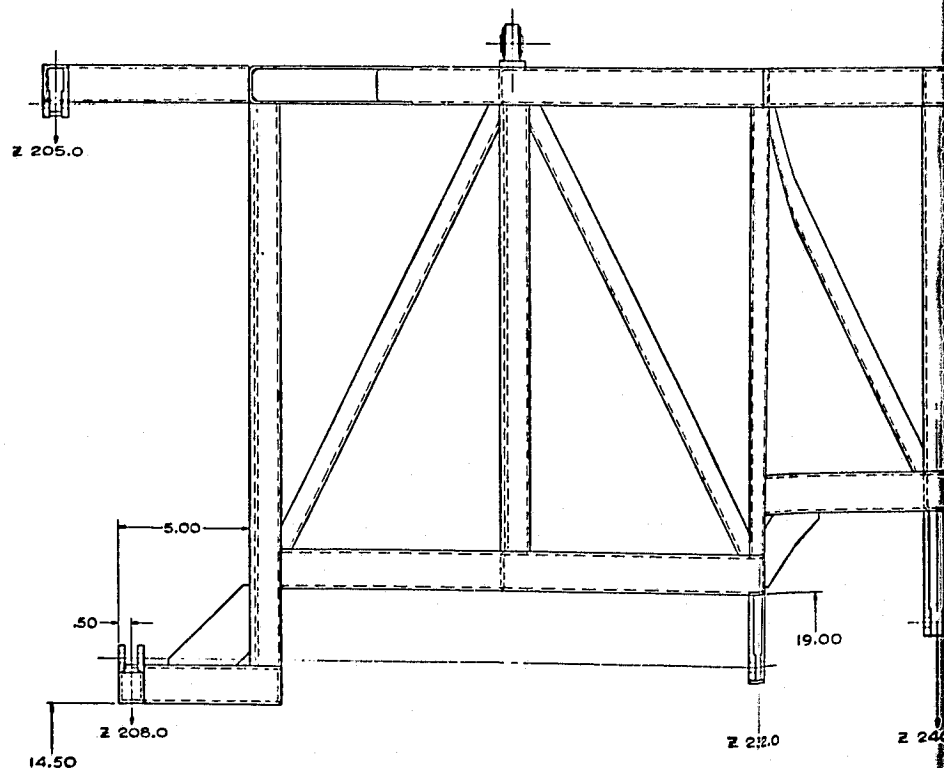
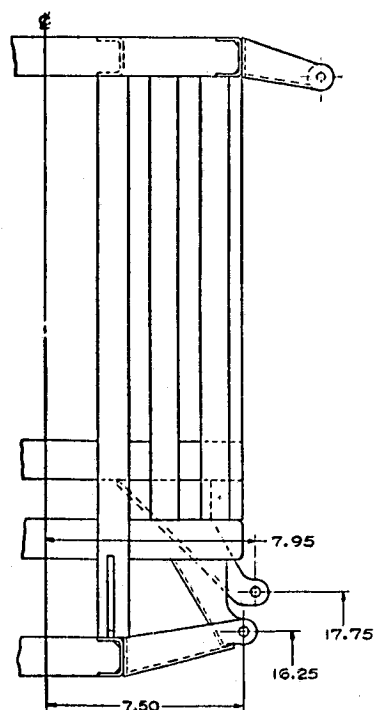
2 FOLDOUT FRAME

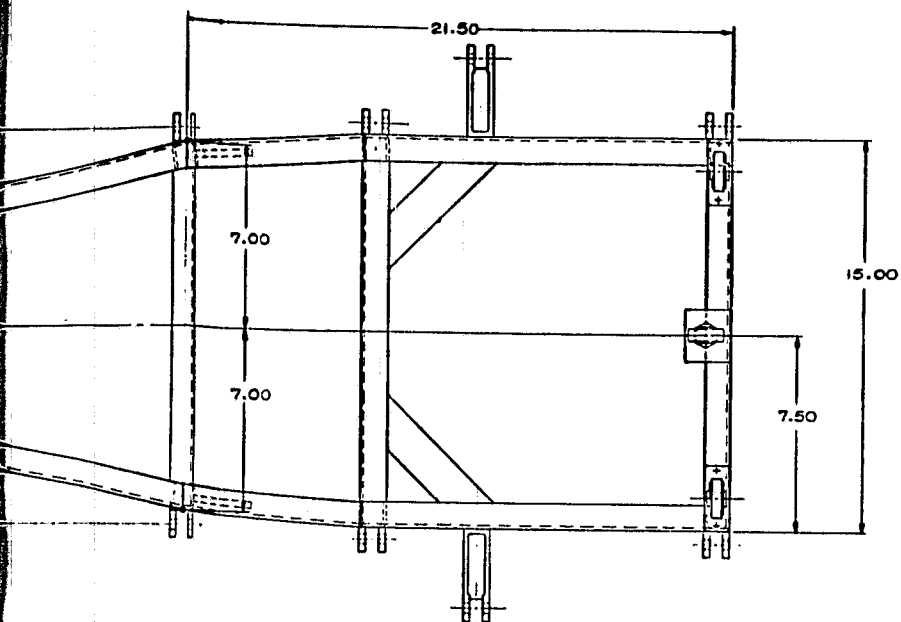
557

ORIGINAL PAGE IS
OF POOR QUALITY
ORIGINAL PAGE IS
OF POOR QUALITY

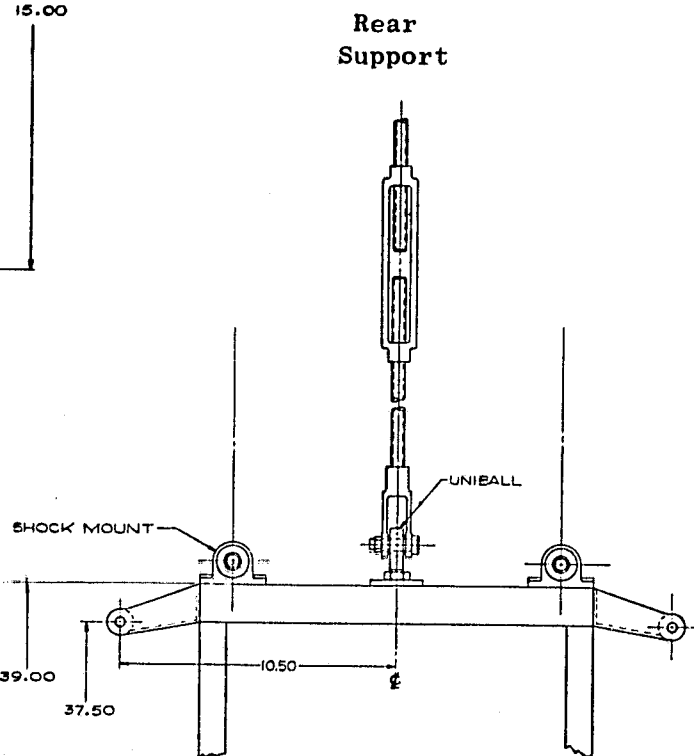
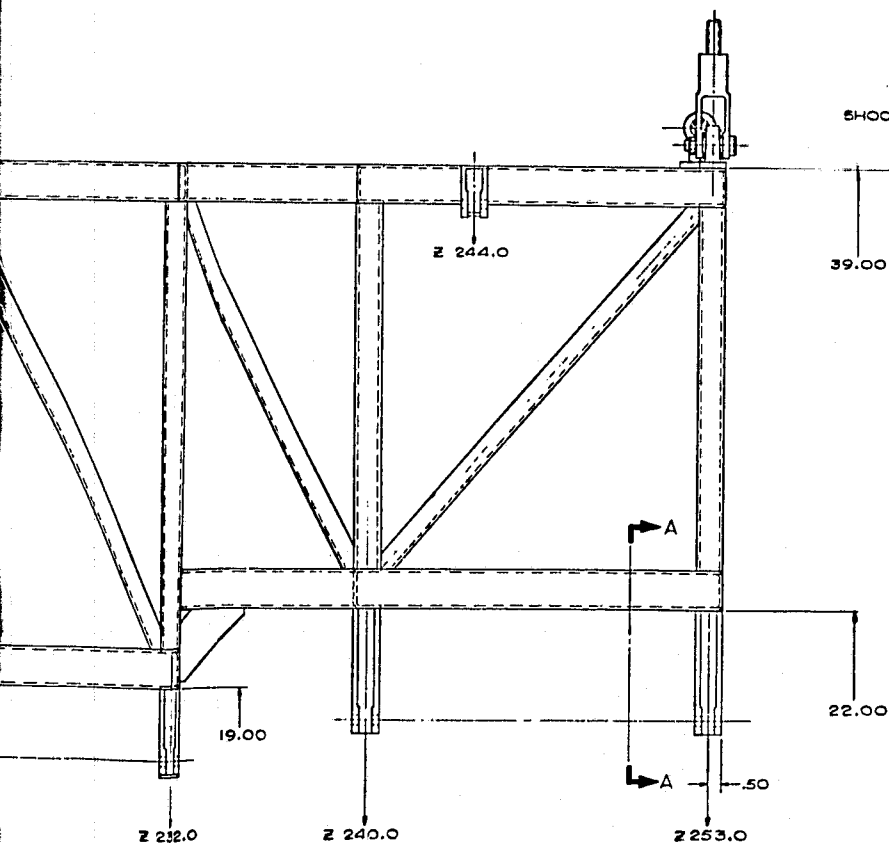


Shock Mounts





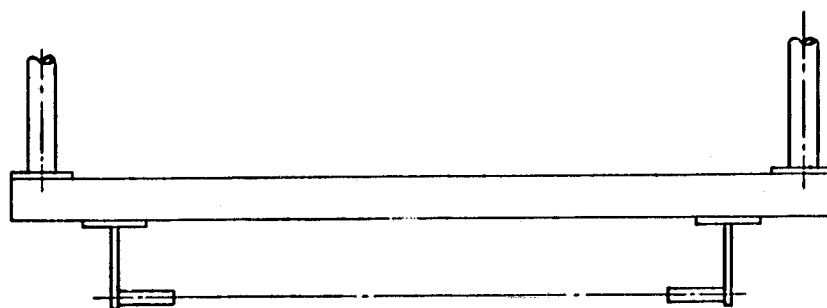
Shock Mounts



2 FOLDOUT FRAME

Figure 15-34. Facility Pylon.

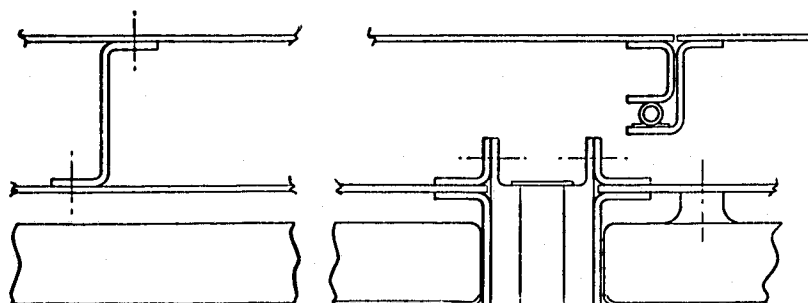
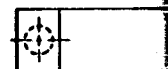
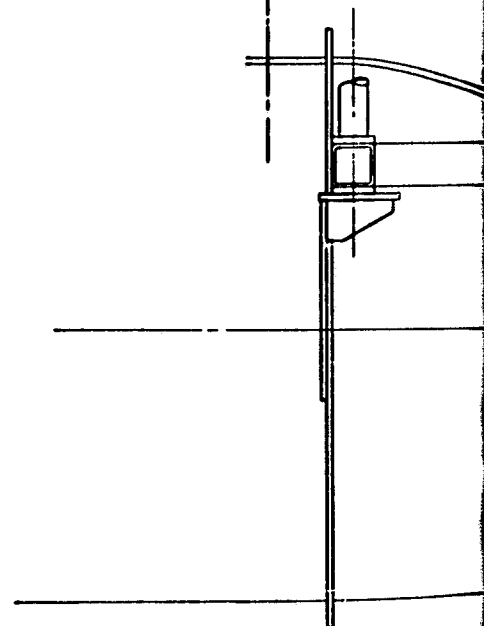
ORIGINAL PAGE IS
OF POOR QUALITY
ORIGINAL PAGE IS
OF POOR QUALITY



SECT A-A

- Boiler Plated
 - "D" Nozzle
 - Target Reverser
- Rotates for Test with:
 - Vertical Wing
 - EBF, Up or Down

STA 24600



STA 24600

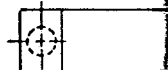


Figure 15-35. OTW Thrust Reverser Assembly

FOLDOUT FRAME

ORIGINAL PAGE IS
OF POOR QUALITY

WING EXTENSION
UNDEFINED

OTW Thrust Reverser Assembly.

2 FOLDOUT FRAME

ORIGINAL PAGE IS
OF POOR QUALITY

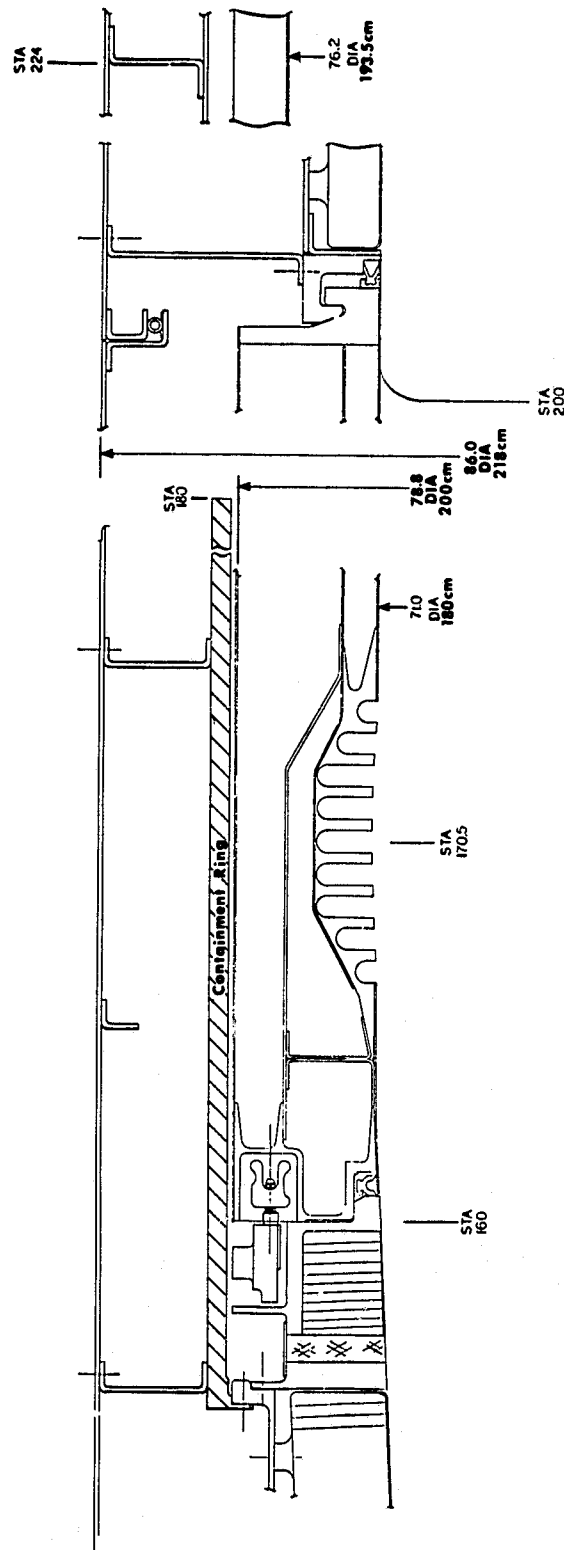


Figure 15-36. OTW Containment Ring.

ORIGINAL PAGE IS
OF POOR QUALITY

PRECEDING PAGE BLANK NOT FILMED

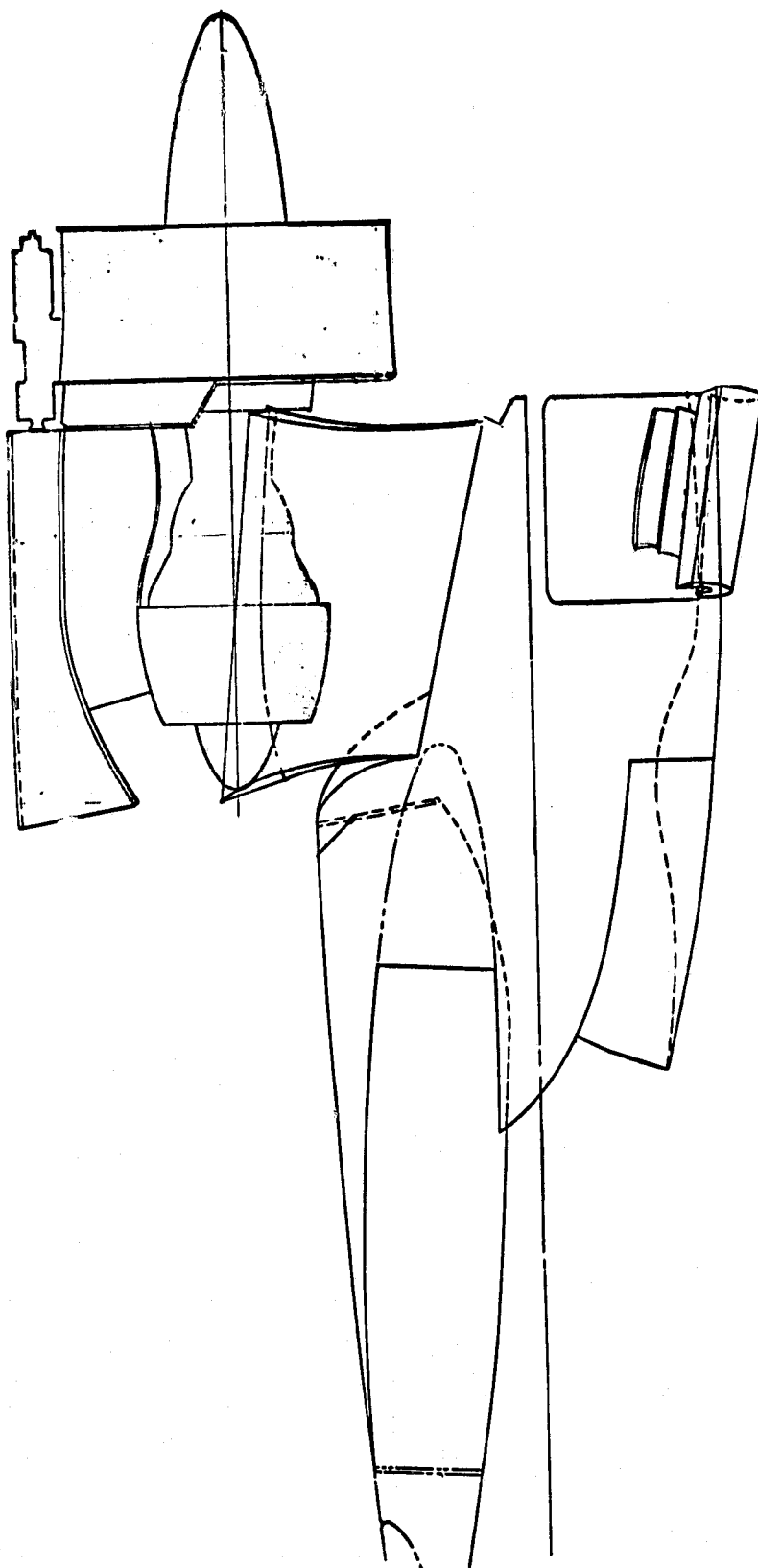


Figure 15-37. OTW Engine Change Unit.

With this arrangement the engine change unit can be removed vertically downward.

- Fan and core cowl doors remain "on-the-wing"
- Engine-to-engine piping is not disassembled
- Disconnect points include:
 - Mount System (4 places - 4 Bolts or Pins)
 - Bleed Air Pipe
 - Powershaft at aircraft accessory gearbox
 - Anti-icing air tube
 - Aircraft-to-engine service pipes, lines, cables, and wires

The flight-type mounting structure, shown in Figure 15-38, can be an integral part of the wing. The forward section is for the engine mounts; the aft section provides the mounts for the target reverser. Note that thrust is taken at the fan frame outer casing at two points on the horizontal center line. These mounts also take vertical load. The top mount takes side load. Vertical loads are simply supported and side loads are cantilevered from the front mount plane. This is a standard-type mount system - with two thrust mounts, either side or vertical, loads must be cantilevered to have a determinate (not redundant) mount system. Usually side reactions are cantilevered because required load conditions are smaller in that direction.

The mount schematic shows vertical, side, thrust, and torque loads taken at the front mount plane and vertical load only taken at the rear mount plane on the outer ring of the turbine frame.

The mount design requirements are the same as described in Section 15.4.5. Both mount systems are designed for "flight" propulsion system loading conditions. The weight including all engine mounted equipment will be used for determining mount loads.

Forward thrust load for design purposes is 93,400 N (21,000 lb) for the OTW system. Load notations are the same as shown in Figure 15-25. A summary of typical mount reactions for unit maneuver and "blade out" loads are shown in Table 15-XII. These loads are for a flight propulsion system with composite fan blades. The experimental engine is designed to loads described in Table 15-VII for both UTW and OTW installations.

15.5.9 OTW Engine System Dynamics

The preliminary engine vibration response analysis for the OTW engine was carried out using General Electric's VAST computer program. This program performs a linear elastic analysis of an axisymmetric structure. Figure 15-26 shows a schematic of the analytical model. Structural shells and cones are shown as solid lines, and their appropriate stiffnesses are calculated from the equation of elasticity. Bearings and frames are shown as springs, and their

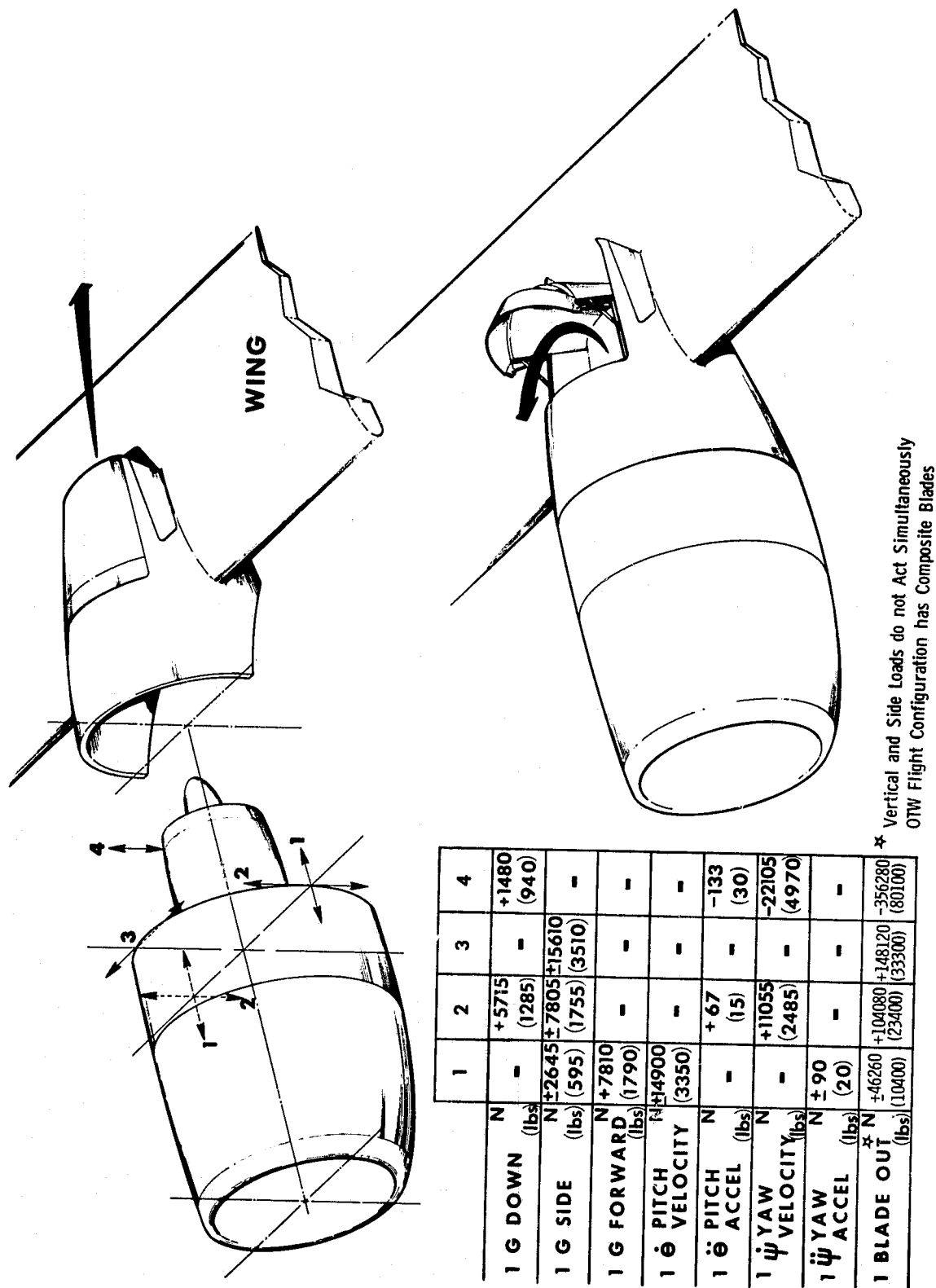


Figure 15-38. OTW Flight Type Mounting System.

Table 15-XII. OTW Flight Engine Mount Reaction Loads.

	R ₁	T ₁	R ₂	R ₃	T ₃	R ₄
1G Down N (1b)	+5716 +(1285)	-	-	+5716 +(1285)	-	+4181 +(940)
1G Side N (1b)	+7806 +(1755)	-	+15612 +(3510)	-7806 -1755	-	-
1000# Thrust N (1b)		+2224 +(500)	-	-	+2224 +(500)	-
1° Pitch N 1° Velocity (1b)	-	+14900 +(3350)	-	-	-14900 -(3350)	-
1° Pitch N 1° Accel (1b)	+67 +(15)	-	-	+67 +(15)	-	-133 -(30)
1° Yaw N 1° Velocity (1b)	+11053 +(2485)	-	-	+11053 +(2485)	-	-22105 -(4970)
1° Yaw N 1° Accel (1b)	-	-90 -20	-	-	-90 -20	-
1 Blade Out *N (1b)	-104080 -23400	+46260 +10400	+148120 +33,300	-104080 -23400	-46260 -10400	356280 80,100

*Vertical and side loads do not act simultaneously
 •OTW "Flight" configuration has composite blades

stiffnesses are obtained from past experience, coupled with other proven analytical techniques. Critical speeds are calculated assuming no damping, and then an estimate of the actual deflections is made at that speed by including damping coefficients along with possible unbalance locations on the rotor system. The results from these calculations are shown in the following tables.

Table 15-XIII presents the basic engine weights and inertias of principal components for the OTW Configuration No. 1.

Table 15-XIII. Basic Engine Weight and Moment Data, OTW Configuration No. 1.

Overall Engine

- Total weight 1776kg (3916 lb).
- Transverse moment of inertia about C.G. $1.39 \times 10^7 \text{ kg-cm}^2$ ($4.75 \times 10^6 \text{ lb-in.}^2$)
- C.G. location - 13.3 in. aft of forward mount plane
- Distance between mounts 123 cm (51.22 in.)

<u>Rotors</u>	<u>Weight</u>		<u>Polar Moment</u>	
	<u>Kg</u>	<u>(lb)</u>	<u>Kg-cm²</u>	<u>(lb-in.²)</u>
Fan	300	(661)	531,100	(181,483)
LP	105	(232)	41,940	(14,332)
HP	193	(425)	68,250	(23,322)

Table 15-XIV presents the system critical speeds, excluding mount modes, for the OTW Configuration No. 1. The speed range for which critical speeds were calculated was 1000 rpm to 5000 rpm.

Table 15-XIV. System Critical Speeds, Maximum Response Due to Fan Rotor.

<u>Mode Description</u>	<u>Fan Speed, rpm</u>	<u>Response⁽¹⁾</u>	
		<u>cm</u>	<u>(mils)</u>
LP Rotor Bending	2483	0.001	0.5
Turbine Frame & Exhaust Plug	3294	0.033	13
Core Casing & Turbine Frame	4230	0.018	7

(1) Single Amplitude response at point of maximum deflection, in mils, for 100 gm-in. unbalance at fan centerline.

Table 15-XV presents the system critical speeds, excluding mount modes, for the OTW Configuration No. 1. The speed range for which criticals were calculated was 1000 to 9000 rpm.

Table 15-XV. System Critical Speeds, Maximum Response Due to LP Turbine Rotor.			
Mode Description	LPT Speed, rpm	Response ⁽¹⁾	
		cm	(mils)
Fan Rotor & Compressor Case	2160	0.005	(2)
Turbine Frame & Exhaust Plug	3542	0.025	(10)
Fan Frame & Turbine Frame	4554	0.033	(13)
HP and LP Rotors	6998	0.008	(3)
Core Casing	8234	0.001	(0.4)
⁽¹⁾ Single Amplitude response at point of maximum deflection, in mils, for 100 gm-in unbalance in the LP turbine.			

Table 15-XVI presents the system critical speeds, excluding mount modes, for the OTW Configuration No. 1. The speed range for which criticals were calculated was 1000 to 15,000 rpm.

Table XVI. System Critical Speeds, Maximum Response Due to HP Rotor.					
Mode Description	HP Rotor Speed rpm	Response ⁽¹⁾			
		Unbalance At Comp. Stg. 1		Unbalance at HPT	
		cm	mils	cm	mils
Fan Rotor & Fan Frame	2296	0.010	(4)	0.001	(0.3)
Turbine Frame & Exhaust Plug	3561	0.013	(5)	0.030	(12)
PT & HP Rotors, Casing Bending	4471	0.013	(5)	0.033	(13)
LP & HP Rotors	6202	0.030	(12)	0.096	(38)
Fan Rotor & Fan Frame	8450	0.005	(2)	0.0005	(0.2)
LP Rotor & Casing	9899	0.091	(36)	0.028	(11)
LP Rotor & Casing	10061	0.033	(13)	0.020	(8)
LP & HP Rotors	13547	0.104	(41)	0.003	(1)
⁽¹⁾ Single amplitude response at point of maximum deflection, in mils, for 100 gm-in. unbalance at indicated location.					

As shown for the UTW system (Section 15.4.6), the most significant response is due to HP turbine rotor unbalance. This is not considered hazardous with rotor balance at assembly.

15.5.10 Accessories

The accessory arrangement for the OTW experimental engine will be the same as described in Section 15.4.7 with the exception that the hydraulic pump will be deleted, since the OTW experimental engine will have a movable (not actuated) target reverser and area control side flaps.

The flight arrangement will have bottom-mounted accessories with a CF6-type gearbox configuration. For this arrangement the lube scavenge pump is mounted on the main gearbox in the accessory area. All other components are positioned as indicated in Section 15.4.7.

SECTION 16.0

WEIGHT

QCSEE propulsion system weight status at the conclusion of the preliminary design phase is presented in the following paragraphs. Analyses of the individual components indicate that the goal thrust-to-weight ratios will be met by both the UTW and OTW propulsion systems.

Weight tables contain projected weights of the flight propulsion systems based on design weight of the flight-type components, and equivalent flight weight of the nonflight components. Estimated weights of the experimental engines are also shown, with brief explanatory notes to indicate differences from the flight engine configurations. Because of the many nonflight design nacelle components, there is no contract goal for the experimental installed propulsion system weights. Therefore, no attempt has been made to monitor the weights of boiler plate components.

16.1 UTW ENGINE

Weight breakdowns of the experimental and flight UTW engine components are presented in Table 16-I. The flight engine total weight of 1338 kg (2943 lb) meets the goal uninstalled thrust-to-weight ratio of 6.2 with 81,400 N (18,300 lb) thrust.

16.2 UTW PROPULSION SYSTEM

Weight summaries of the installed experimental and flight UTW propulsion systems are presented in Table 61-II. The flight system total installed weight of 1920 kg (4015 lb) meets the goal installed thrust-to-weight ratio of 4.3 with 77,400 N (17,400 lb) installed thrust.

16.3 OTW ENGINE

Weight breakdowns of the experimental and flight OTW engine components are presented in Table 16-I. The flight engine total weight of 1275 kg (2814 lb) meets the goal uninstalled thrust-to-weight ratio of 7.4 with 93,500 N (21,000 lb) thrust.

16.4 OTW PROPULSION SYSTEM

Weight summaries of the installed experimental and flight OTW propulsion systems are presented in Table 16-III. The flight system total installed weight of 1780 kg (3931 lb) results in an installed thrust-to-weight ratio of 5.1 with 90,300 N (20,300 lb) installed thrust. This value does not include the nacelle supporting structure (normally an aircraft responsibility), but exceeds the contract goal of 4.7. If 160 kg (353 lb) is allowed for this structure (GE estimate), the installed thrust-to-weight ratio would be 4.7. Further aircraft integration studies are required to refine the estimate of the structure.

Table 16-1. Engine Detail Weight Breakdown.

July 26, 1974

	UTW				OTW			
	<u>Experimental</u>		<u>Flight</u>		<u>Experimental</u>		<u>Flight</u>	
	<u>kg</u>	<u>(lb)</u>	<u>kg</u>	<u>(lb)</u>	<u>kg</u>	<u>(lb)</u>	<u>kg</u>	<u>(lb)</u>
F101	442	974	425	936	442	974	425	936 ⁽¹⁾
F101 LP Turbine	117	259	117	259	117	259	117	259
F101 LP Shaft	<u>27</u>	<u>60</u>	<u>27</u>	<u>60</u>	<u>27</u>	<u>60</u>	<u>27</u>	<u>60</u>
<u>F101 Core and LPT Total</u>	587	1293	569	1255	587	1293	569	1255
Fan Blades	42	92	42	92	124	273 ⁽²⁾	41	90
Disk and Blade Support	78	171	78	171	100	220 ⁽²⁾	64	142
Fan Shaft	32	70 ⁽³⁾	23	50	32	70 ⁽³⁾	23	50
Spinner	<u>22</u>	<u>48</u>	<u>22</u>	<u>48</u>	<u>22</u>	<u>48</u>	<u>22</u>	<u>48</u>
<u>Fan Total</u>	173	381	164	361	275	606	147	325
<u>Reduction Gear</u> (Curtiss-Wright Est.)	96	211 ⁽⁴⁾	77	170	94	208 ⁽⁴⁾	77	170
Fan Frame Composite Structure	120	265	120	265	120	265	120	265
Casing and Flanges	48	106	48	106	48	106	48	106
Sump and Shield	3	6	3	6	3	6	3	6
Containment	21	46	21	46	21	46	21	46
Core OGV's	<u>17</u>	<u>37</u>	<u>17</u>	<u>37</u>	<u>17</u>	<u>37</u>	<u>17</u>	<u>37</u>
<u>Fan Frame Total</u>	209	460	209	460	209	460	209	460
<u>Turbine Frame Total</u>	80	177 ⁽⁵⁾	48	105	80	177 ⁽⁵⁾	48	105

(1) Commercialized core, modified for lower pressure, lower temperature QCSEE engines

(2) Titanium versus composite blades

(3) Steel versus titanium shaft

(4) Steel versus titanium star carrier

(5) Modified F101 frame versus new design

Table 16-1. Engine Detail Weight Breakdown (Concluded).

	UTW				OTW			
	<u>Experimental</u>		<u>Flight</u>		<u>Experimental</u>		<u>Flight</u>	
	<u>kg</u>	<u>(lb)</u>	<u>kg</u>	<u>(lb)</u>	<u>kg</u>	<u>(lb)</u>	<u>kg</u>	<u>(lb)</u>
Bearing Supports	37	81 ⁽⁶⁾	29	64	37	81	29	64
Bearings, Sumps and Seals	81	179 ⁽⁷⁾	60	133	81	179 ⁽⁷⁾	60	133
Accessory Gearbox	<u>56</u>	<u>124⁽⁸⁾</u>	<u>38</u>	<u>83</u>	<u>56</u>	<u>124⁽⁸⁾</u>	<u>38</u>	<u>83</u>
<u>Bearings, Sumps and Drives Total</u>	174	384	127	280	174	384	127	280
Fuel System	31	68 ⁽⁹⁾	22	48	31	68 ⁽⁹⁾	22	48
Elect System	32	70 ⁽¹⁰⁾	26	58	32	70 ⁽¹⁰⁾	26	58
Lube and Scav. Syst.	20	43	20	43	20	43	20	43
Oil Tank	15	32 ⁽¹¹⁾	10	22	15	32 ⁽¹¹⁾	10	22
V.P. Mechanism	42	93	42	93	-	-	-	-
Piping and Wiring	<u>36</u>	<u>80⁽¹²⁾</u>	<u>22</u>	<u>48</u>	<u>36</u>	<u>80⁽¹²⁾</u>	<u>22</u>	<u>48</u>
<u>C&A Total</u>	175	386	142	312	133	293	99	219
Total Engine Weight	<u>1493</u>	<u>3292</u>	<u>1335</u>	<u>2943</u>	<u>1552</u>	<u>3421</u>	<u>1276</u>	<u>2814</u>
Uninstalled Thrust	81400	18300	81400	18300	43500	21000	93500	21000
	N	(lb)	N	(lb)	N	(lb)	N	(lb)
Uninstalled Thrust/Weight		-		6.2		-		7.4

(6) Steel versus Titanium

(7) CF6 No. 1 bearing and available hardware versus optimized design

(8) Fab steel gearcase versus cast aluminum

(9) F101 hydromechanical back-up control

(10) Nonflight packaging

(11) TF39 lube tank

(12) Steel versus titanium piping and flex tubing

Table 16-II. UTW Propulsion System Weight Status.

	<u>Experimental</u>		<u>Flight</u>	
	kg	(lb)	kg	(lb)
Inlet	138	305	138	305
Fanduct and Splitter	123	272	109	241
Flare Nozzle	26	57	26	57
Core Cowl	47	103	44	98
Core Exhaust	*	*	60	132
Mounts	*	*	10	23
Hydraulic System	*	*	6	14
Nozzle Control	*	*	26	57
Fire Det. and Ext.	*	*	25	56
Instrumentation	*	*	11	25
Drains and Vents	*	*	5	13
Inlet Anti-Icing	*	*	13	28
Oil Cooler	12	27	11	24
Total Installation			486	1072
Engine			<u>1335</u>	<u>2943</u>
Propulsion System			1821	4015
Thrust/Weight (Installed)			4.3	4.3
Fn/Wt (Installed) Goal			4.3	4.3

*Boiler Plate Component

Table 16-III. OTW Propulsion System Weight Status.

	<u>Experimental</u>		<u>Flight</u>	
	<u>kg</u>	<u>(lb)</u>	<u>kg</u>	<u>(lb)</u>
Inlet	*	*	138	305
Fanduct and Splitter	*	*	109	241
Core Cowl	*	*	44	98
Core Exhaust	*	*	51	113
Mounts	*	*	7	15
Target Reverser	*	*	78	171
Hydraulic System	*	*	6	14
Reverser and Nozzle Control	*	*	26	57
Fire Det. and Ext.	*	*	25	56
Instrumentation	*	*	11	25
Drains and Vents	*	*	5	12
Inlet Anti-Icing	*	*	13	28
Oiler Cooler	12	27	<u>11</u>	<u>24</u>
Total Installation			528	1159
Engine			<u>1280</u>	<u>2822</u>
Propulsion System			1806	3981
Thrust/Weight (Installed)			5.1	5.1
Pylon Structure			160	353
Fn/Wt (Including Pylon Struct)			4.7	4.7
Fn/Wt (Installed) Goal			4.7	4.7

* Boiler Plate Component.

SECTION 17.0

AIRCRAFT SYSTEM STUDIES

17.1 SUMMARY

During the QCSEE preliminary design phase, the aircraft system studies defined the operational model or mission scenario upon which the baseline UTW and OTW aircraft could be designed. Through the team effort of American Airlines, Douglas, Boeing, and GE, a set of common economic ground rules were established with latitude permitted, where reasonable, to reflect individual aircraft manufacturing background. With baseline aircraft defined by Boeing for the OTW and Douglas for the UTW, DOC calculations were made. Aircraft sizes are the result of using the flight configurations of the QCSEE engines. No attempt has been made to directly compare UTW vs. OTW aircraft since it is not the intent of the QCSEE program to decide the merit of the aircraft designs.

17.2 STUDY OBJECTIVE

The objectives of the aircraft system studies are to:

1. Provide design guidance for the OTW and UTW experimental-and flight-type engine designs which are the final product of the QCSEE contract.
2. Provide inputs for the test planning of the hardware, both component as well as the experimental engines.
3. Based on the experimental engine test results, provide flight, economic, and acoustic performance of commercial short-haul OTW and UTW aircraft.
4. Provide various trade studies such as DOC versus noise footprint areas.

Overall, then, it is the purpose of the Task 10 effort to "keep alive" the flight engine configurations with updating information as the four year experimental program progresses.

17.3 MISSION SCENARIO

The operational scenario for short-haul transportation in the 1980 and beyond time period is projected to include the spread of congestion at more of the major hub airports and the inability to obtain the large land areas necessary for conventional airports. The environmental impact of aircraft in terms of noise and pollution suggest severe restrictions will be encountered in siting new airports and in the initiation or expansion of commercial service to existing smaller airports. In order to meet these transportation requirements, shorter takeoff and landing aircraft which have greatly reduced noise and pollution levels will be required. Continued growth in the short-haul transportation market is projected based on population and demographic trends. The reduced availability of automotive gasoline had a strong positive effect on the number of passengers carried during the recent energy crisis and any recurrence should

have similar positive influences. Projected costs for aviation fuels will place heavy demands on engine and aircraft performance features which reduce the quantity of fuel required per passenger seat mile. These factors establish the baseline for a tentative aircraft operational scenario for use in the QCSEE propulsion system trade studies.

Figure 17-1 shows a typical short-haul aircraft's route network for the 1980 time period. The average trip distance is approximately 462 kilometers (250 nmi) with longest leg close to the design range point for a typical STOL aircraft. Table 17-I lists the major aircraft acoustic goals and aircraft independent variables of size, aircraft design stage length, extended range capability, and design field length. Table 17-II lists the dependent design characteristics and objectives for a typical advanced short-haul STOL aircraft. Selection of flight speed on short-haul flights within the suggested range is not projected to be as critical as the economic impact of the projected cost of fuel and results in the requirements to optimize the aircraft to achieve maximum available seat miles per unit of fuel consumed. The cruise altitudes suggested are those actually used today in the short-haul flight market. While they may not represent optimums they do reflect the effect of air traffic system in the congested area of the Northeast corridor. The wing loading value listed was selected on the basis of passenger ride qualities. Uninstalled takeoff thrust to aircraft gross weight ratio is a representative level for an aircraft that meets the requirements set forth previously in Table 17-I.

Table 17-1. QCSEE Preliminary Aircraft System Definition.

Independent Variables

- 95 EPNdB, 152 m (500 ft) sideline during takeoff and approach
- 100 PNdB, 152 m (500 ft) sideline with reverser at 35% takeoff thrust
- Passenger size 150-170
- Design stage length, 926 km (500 mi)
 1390 km (750 mi) increased field length
- Design field length, 914 m (3000 ft) @ 32° C (90° F) sea level

The field length, approach, and climb out gradients are associated with achieving the noise objectives set forth for the program. Engine response characteristics have been established on the basis of aircraft handling qualities. The remaining design objectives are those desired to provide a widely useable aircraft in commercial service. Table 17-III shows the distribution by segment range of total number of departures flown by a typical trunk airline. Immediately below is shown the average city pair demand by number of passengers per day and the percentage of departures that fall in each category. These data suggest the strong need to ensure that the aircraft is properly sized to meet the short-haul market. The aircraft must not be too large as to be uneconomic from a load factor

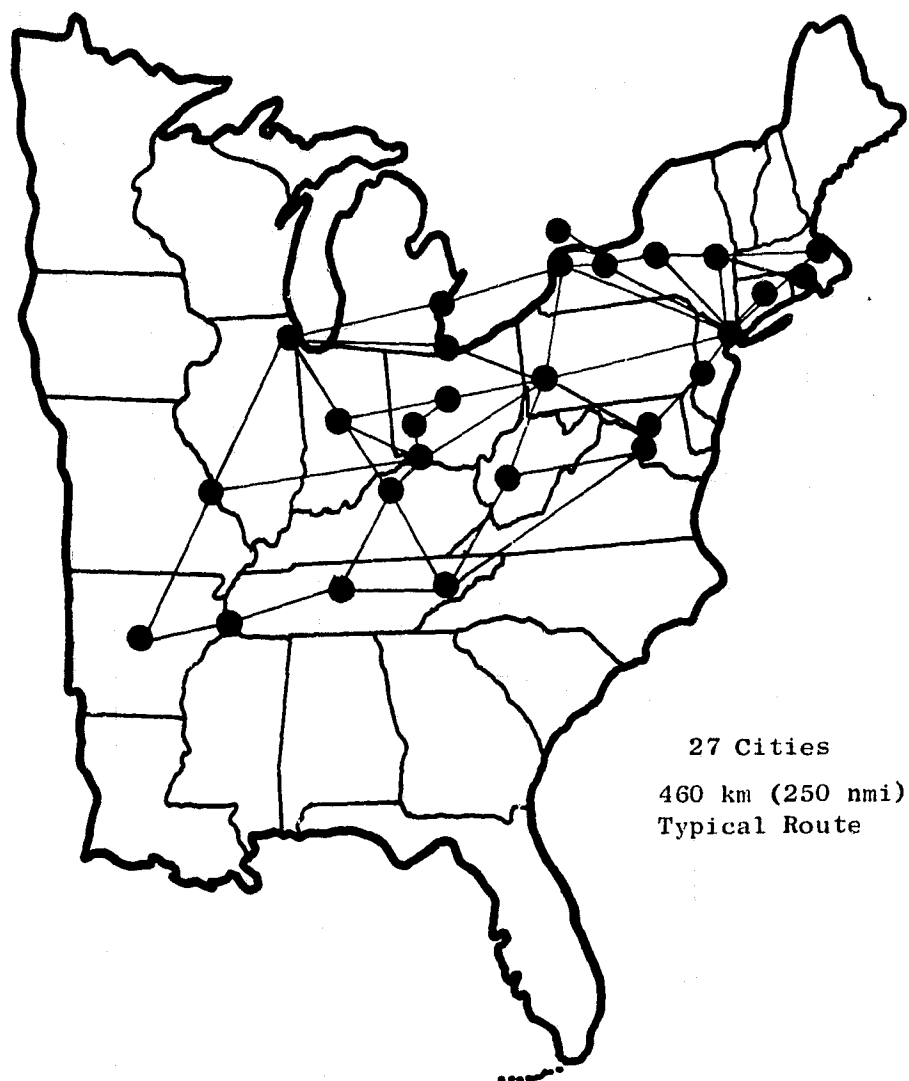


Figure 17-1. Short-Haul Network.

Table 17-II. QCSEE Preliminary Aircraft System Definition.

Dependent Variables

- Aircraft Mach number [fallout from 914 (3000 ft) balanced field length and maximized ASM/100,000 gallon fuel]
- Cruise altitude 6.9-8.25 km (21-25 kft)
- Wing loading 450 kg/m² (100 lb/ft²)
- 51.4 m/sec (100 kts) initial climb-out 100% thrust, 20° Flaps, 12.5° Path
- 51.4 m/sec (100 kts) approach 65% thrust, 50° Flaps, 6° Path
- Uninstalled T/GW of A/C 0.5
- Field length calculation QCSEE A/C study rules
- Engine Response Per section 2.2.4 and 2.2.7
- Thrust Reverser 35% Takeoff thrust from touchdown to 5.2 m/sec (10 kts)
- Bleed and hp Will evaluate
- Engine duty cycle 0.67 Flight hr. per cycle
- Upwash & crosswind Per Table 3-II
- Engine operating envelope Per Figure 2-1
- Accessory replacement 45 min. (30 min. goal)
- Wing cross section at engine To be provided for 914 m (3000 ft) runway
- Four engines 80,300-89,000 N
(18,000-20,000 lb) uninstalled thrust/engine
- Wing span 32.8 m (108 ft)

Table 17-III. Typical Trunk Airline Departures.

Segment Range	km (nmi)	0-370 (0-200)	372-926 (201-500)	928-1852 (501-1000)	1852-2770 (1000-1500)	2772-4620 (1501-2500)	4622-6500 (2501-3500)
% of Total Departures		15.8	39.3	25.0	6.4	11.5	1.4
Cumulative %		15.8	55.1	80.1	86.5	98.0	99.4
Average Daily City Pair Demand		0-100	101-200	201-300	301-400	401-500	501-600
% of Total Departure		32.7	18.1	18.6	4.3	5.3	7.9
Cumulative %		32.7	50.8	69.4	73.7	79.0	86.9

standpoint or to reduce the frequency of service to an unacceptably low level. These factors were used along with others in selecting the passenger load size for a typical advanced short-haul propulsive lift aircraft.

17.4 PRELIMINARY DOC GROUND RULES

The design of the QCSEE propulsion system must consider the impact of the various propulsion system features on aircraft operating costs and economics. Short-haul flight profitability is much more sensitive to delays, cancellations, out-of-service costs, indirect operating expenses and direct operating expense variations than are long-haul operations. The usual tools for economic assessment, such as the ATA method for determining direct operating cost of turbine powered aircraft, are too crude for technological guidance. In an effort to improve the usefulness of such tools both Boeing and Douglas have readjusted their cost equations in an attempt to more truly reflect short-haul economics. This area will receive additional attention. In addition, the propulsion system economic method suggested in NASA CR1344645 will be evaluated for possible use with suitable modification to assess the different cost/benefits for specific design trade studies undertaken under the QCSEE Program. Table 17-IV provides the preliminary data for the preliminary economic studies undertaken by Boeing and Douglas.

17.5 UTW AIRCRAFT CHARACTERISTICS

The primary design requirement for the baseline aircraft is to carry 150 passengers 926 km (500 nmi) from a 914 m (3000 ft) length field. The general arrangement of the Douglas Aircraft Company (DAC) UTW aircraft design which meets these requirements is shown in Figure 17-2.

Four variable pitch fan QCSEE engines of 81,400 N (18,300 lb) rated thrust are mounted on the 140 m² (1507 ft²) wing. The aspect ratio 9 wing utilizes a supercritical airfoil section and has approximately 0.08 radian (5°) of sweep at the quarter chord. This low wing sweep limits cruise Mach number to about 0.75, but this is ample for the short stage lengths on which the aircraft will be operated. A 25 % chord, double-slotted flap in conjunction with full-span leading-edge devices, provide high-lift performance. Spoilers are used for direct lift control in the approach mode. The high-lift system does not require engine bleed.

The engines are located inboard to reduce engine-out asymmetric effects. The location of the outboard engine at 50% of the wing semispan allows sufficient spacing to avoid significant interference drag penalties. Figure 17-3 defines the location of the engine relative to the wing-flap system at the inboard pylon station. The takeoff and landing flap positions and supercritical airfoil section are visible. The displacement of the engine relative to the wing leading edge and wing reference plane are based on DAC low and high speed wind tunnel test experience.

In order to reduce the dependence of the aircraft on ground support equipment, airstairs have been included in the design. They are located at the left side entrance doors at each end of the passenger compartment. In excess of 57 m³ (2000 ft³) of cargo volume is available in forward and aft under-floor compartments.

Table 17-IV. Preliminary Data for Economic Studies.

Number of Engines	4
Aircraft Passenger Capacity	150
Number of Crew/Cabin Attendants	2/4
Average Load Factor (%)	55-65
Average Stage Length, km (nmi)	926 (500)
Flight Time	TBD
Block Time	TBD
Block Fuel	TBD
Fuel Cost (cents/gal)	30
Insurance Rate (% AC Cost)	2 (DAC 1%)
Labor Rate (\$/hr)	7.20
Utilization (hr/yr)	2555
Airframe Maintenance (Labor & Material)	TBD
Engine Maintenance (Labor & Material)	Per GE
Fly-away Cost	TBD
Airframe Cost	TBD
Total Engine Cost	TBD
Airframe Spares Factor (% of AC Cost)	6
Engine Spares Factor (% of Engine/AC)	30
Residual Value (% of AC Cost)	2 (DAC 10%)
Depreciation Period (Yrs)	14 (DAC 15 yrs)
Base Year	1974
UTW Engine System Price (Average over 1500 Units)	\$1.26M
UTW Engine Price	1.03M
OTW Engine System Price	1.3M
OTW Engine Price	0.997M

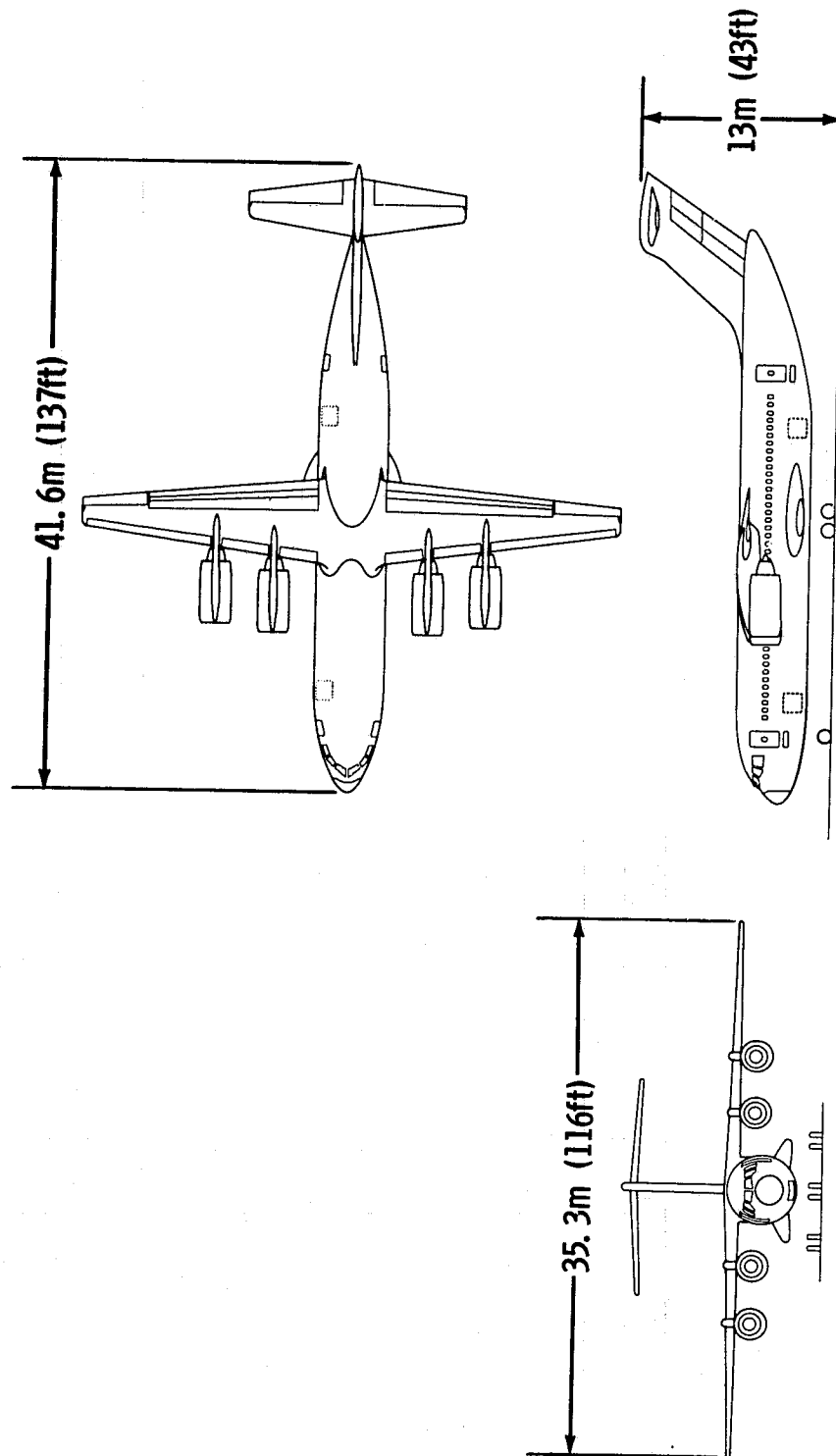
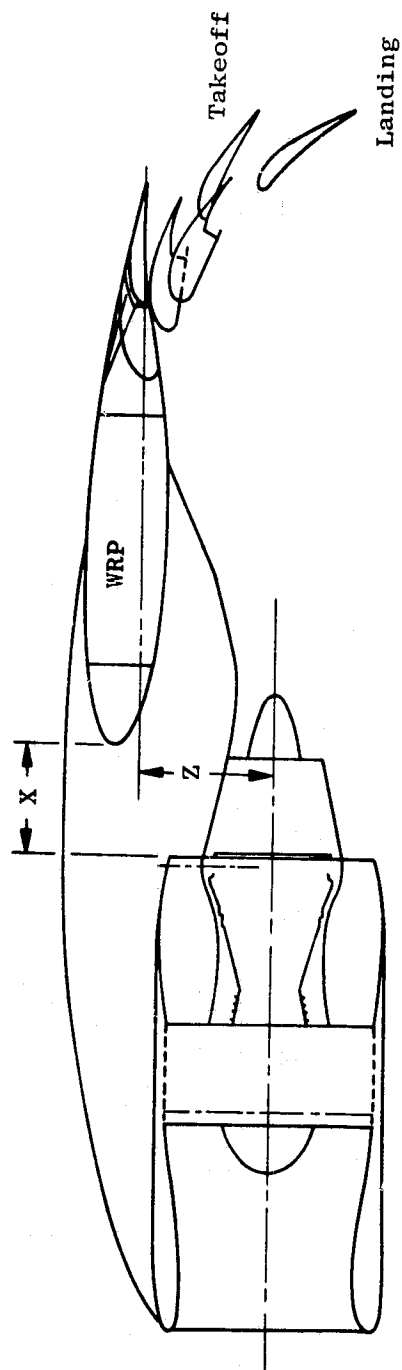


Figure 17-2. QCSEE Baseline UTW Aircraft.



- $X/C = 0.20$
- $Z/C = 0.24$
- No Engine Tilt Relative to WRP

Figure 17-3. Engine/Flap Relationship, Inboard Station.

The 4.5 m (189 in.) diameter wide-body fuselage is designed to accommodate 150 passengers in a double aisle, six abreast, single class seating arrangement with 0.86 m (34 in.) pitch. Seat size is similar to that in a DC-9, approximately 2.54 cm (1 in.) wider per passenger than DC-8 or B707/727/737 seats. An aisle width of 0.51 m (20 in.) was chosen, consistent with current wide-body airplanes to minimize passenger loading and unloading times. The arrangement of the passenger compartment is shown in Figure 17-4. Overhead baggage compartments are like those in current wide-body aircraft, and coat racks are located near the exits. Due to the short stage lengths over which the aircraft will be operated, there are no provisions for hot meal service galleys; however, buffet-coffee bars are located at each end of the passenger compartment.

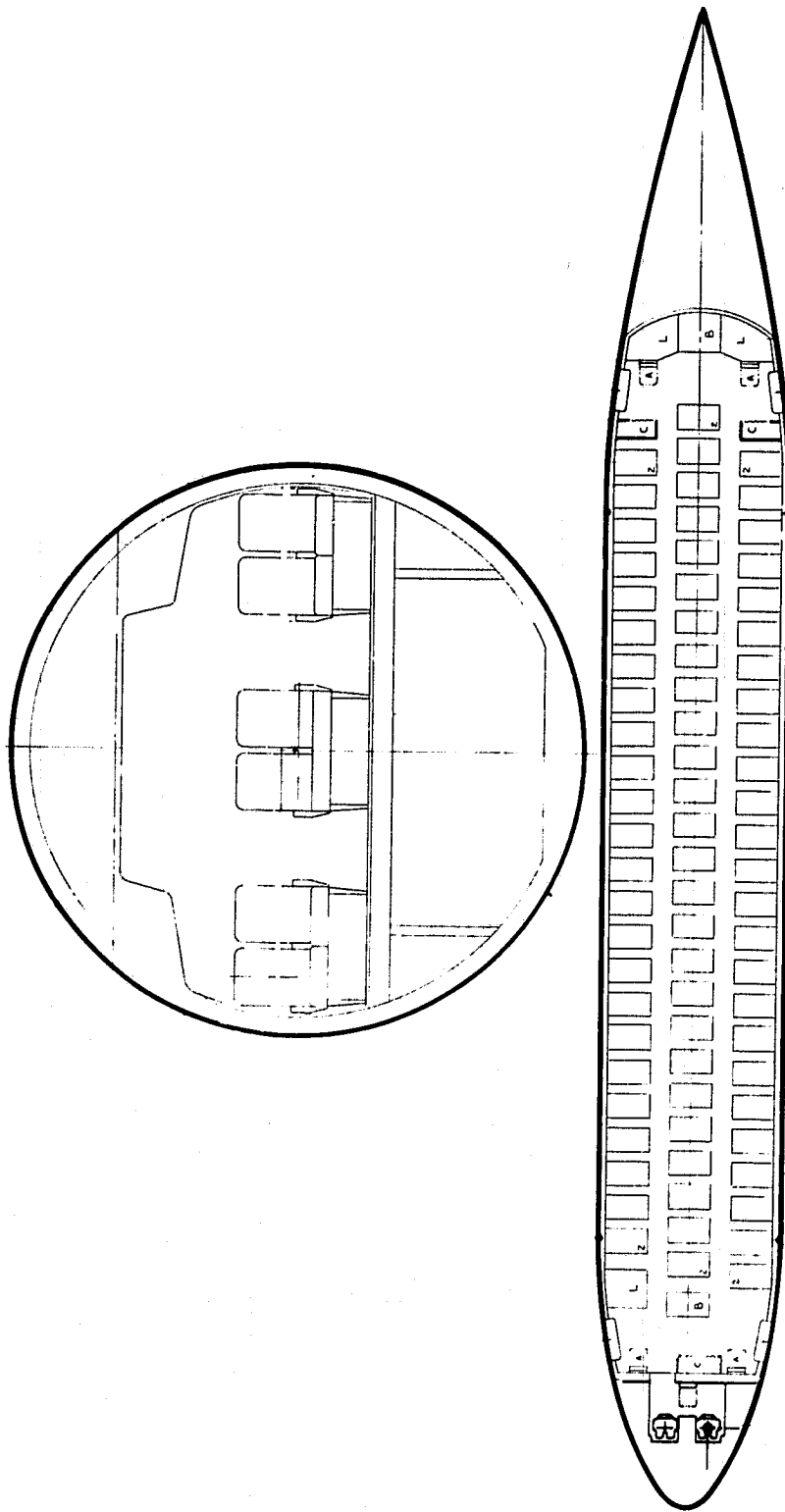
The cockpit area is arranged for operation with two crew members, but jump seats are provided for an optional third crewman and for an observer. The third crewman's seat is positioned midway between the pilots' seats behind the center pedestal so that he can reach all center pedestal controls including throttles and could monitor systems on the overhead panel. In addition, he could assist in check list procedures and provide a third pair of eyes for avoidance of mid-air collisions. The observer's seat position is suitable for observing all crew procedures as would be required by a check pilot.

The parametric aircraft sizing process involves calculating takeoff and landing performance to determine wing loading (W/S) and thrust-to-weight ratio (T/W) combinations that meet the 914 m (3000 ft) field length requirement. Aircraft that meet the payload-range requirement are then sized for each of these W/S and T/W combinations. The design point is then selected, usually on the basis of minimum direct operating cost (DOC).

The mission profile used for aircraft sizing is shown in Figure 17-5. A digital computer program calculates the mission time history by numerical integration of the flight path. A constant cruise Mach number of 0.70 at 9450 m (31,000 ft) was selected based on requirements submitted by American Airlines. The profile accounts for the 129 m/sec (250 knot) speed limit below 3050 m (10,000 ft) altitude and a cabin pressurization rate limited descent. Fuel reserves include provision for a 185 m (100 nmi) diversion to alternate plus 45 minutes hold at long-range cruise speed. Mission performance was calculated for standard day conditions.

The sizing chart for the baseline aircraft, shown in Figure 17-6, consists of plots of direct operating cost, gross weight, rated thrust per engine and uninstalled thrust-to-weight ratio as a function of wing loading. The plot of T/W vs W/S shows lines of constant 914 m (3000 ft) takeoff and 914 m (3000 ft) landing field length. Takeoff and landing performance were calculated for sea level 32° C (90° F) conditions.

The aircraft was sized on the basis of minimum DOC and gross weight. This occurs at the W/S and T/W where takeoff and landing field length are both equal to 914 m (3000 ft); $W/S = 450 \text{ kg/m}^2$ (100 lb/ft²) and $T/W = 0.486$. The resulting required engine size is 81,400 N (18,300 lb) uninstalled.



150 Passengers - 6 Abreast - DC9 Tourist Seats - 34 Pitch

Figure 17-4. 150 Passenger Interior Arrangement.

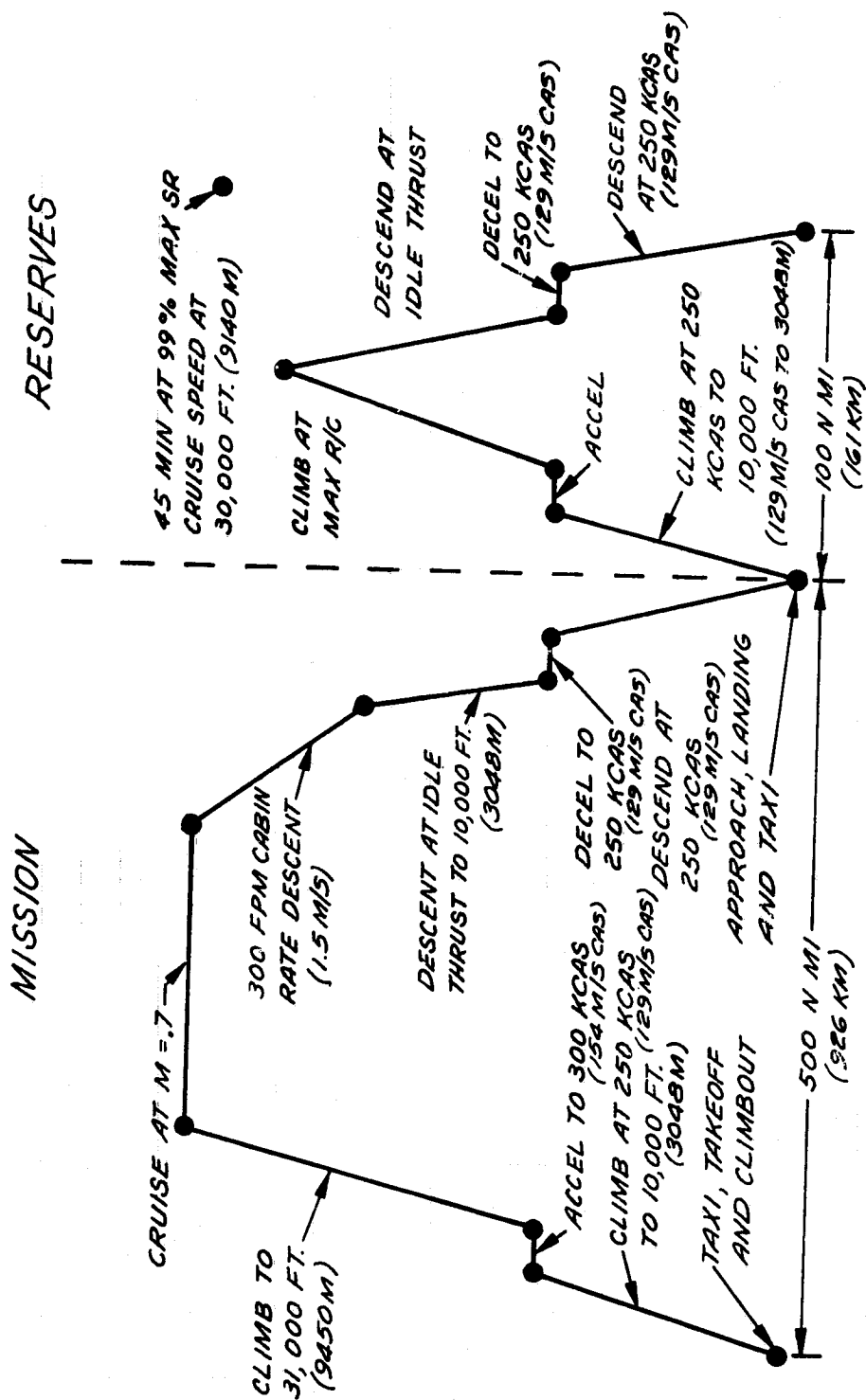


Figure 17-5. Mission Profile Used for Aircraft Sizing.

- 150 Passengers
- 914 m (3000 ft) Field Length

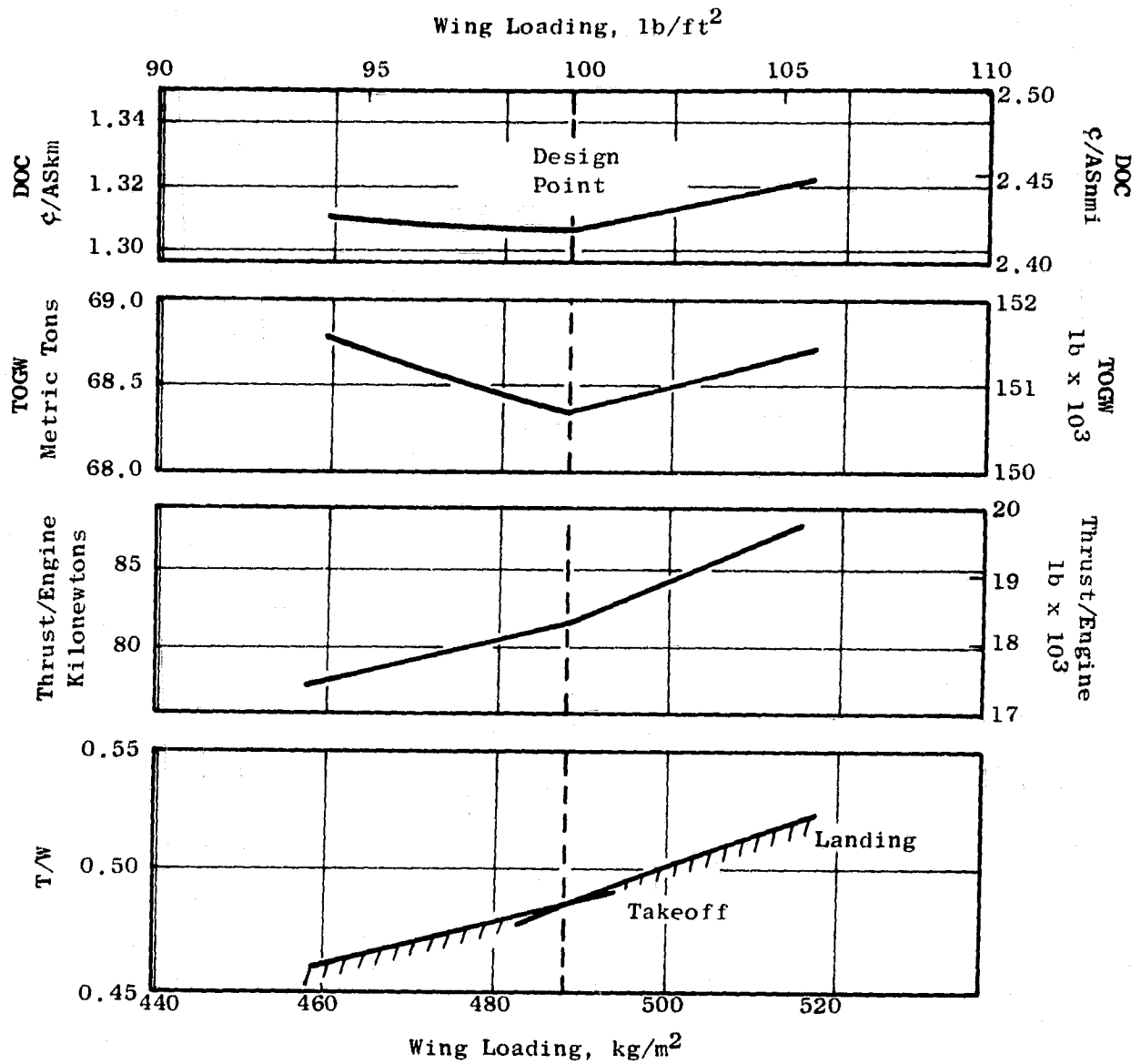


Figure 17-6. Baseline Aircraft Sizing Parameters.

Direct operating cost is relatively insensitive to design wing loading. A somewhat smaller engine could be used and still meet all design requirements without significant increase in DOC.

A summary of the basic UTW aircraft characteristics is shown in Table 17-V. The primary aircraft design requirement is to carry 150 passengers 926 m (500 nmi) from a 914 m (3000 ft) length field. An alternate mission is to carry the same payload 1389 km (750 nmi) from a longer runway. The 1389 km (750 nmi) mission requires the fuel load be increased by 2313 kg (5100 lb) which increases the required field length to 983 m (3225 ft). Both missions are flown at a cruise Mach number of 0.70 which represents a compromise between the high speed ($M = 0.75$) and long range ($M = 0.62$) cruise speeds.

Table 17-V. UTW Aircraft Characteristics

Design Field Length, m (ft)	914 (3,000)
Payload [150 passengers @ 91 kg (200 lb), kg (lb)	14,600 (30,000)
Design Range, km (nmi)	926 (500)
Max Range with Full Payload, km (nmi)	1,389 (750)
Design Takeoff Gross Weight, kg (lb)	68,300 (150,700)
Max Takeoff Gross Weight, kg (lb)	70,400 (155,700)
Max Landing Weight, kg (lb)	69,300 (150,700)
Wing Area, m^2 (ft^2)	140 (1,507)
Rated Thrust per Engine, N(lb)	81,400 (18,300)
W/S, kg/m^2 (lb/ft^2)	450 (100)
T/W Uninstalled	0.486
Cruise Mach Number	0.70
DOC @ 926 km (500 nmi)	2.16 ¢/ASNM

The group weight statement for the airplane is shown in Table-VI. Advanced construction techniques and materials are incorporated in the aircraft as follows:

- Composite Materials: Control surfaces and a limited amount of secondary structure.
- Advanced Metallic Structural Concepts: Integrally machined stiffeners, advanced alloys and honeycomb sandwich used in wing and tail boxes.
- Carbon Brakes.

Payload-range performance for the airplane is shown in Figure 17-7 for three operational conditions:

Table 17-VI. Group Weight Statement.

	Weight	
	<u>kg</u>	<u>(lb)</u>
Wing	7,760	17,107
Tail	1,702	3,752
Fuselage	10,386	22,896
Landing Gear	2,697	5,945
Surface Controls	1,609	3,548
Propulsion	9,048	19,946
Auxiliary Power Plant	431	950
Instruments and Navigational Equip.	533	1,175
Hydraulic	583	1,285
Pneumatic	460	1,013
Electrical	1,175	2,590
Electronics	798	1,760
Furnishings	6,210	13,690
Air Conditioning and Anti-Icing Equipment	892	1,968
Auxiliary Gear	14	30
Manufacturer's Empty Weight	44,296	97,655
Operational Items	1,291	2,845
Operational Empty Weight	45,587	100,500
Payload	13,608	30,000
Fuel	9,163	20,200
Design Takeoff Gross Weight	6,836	150,700

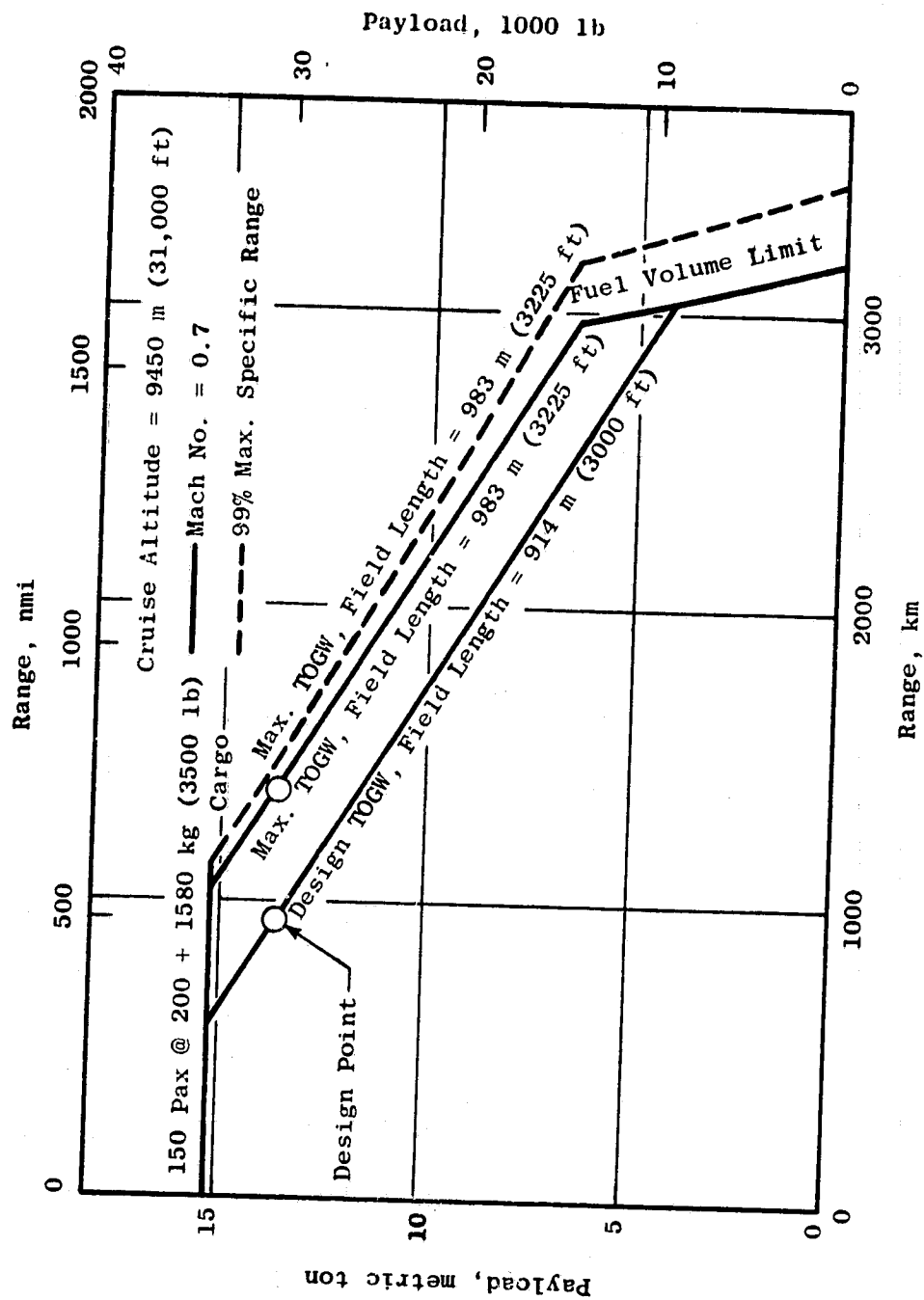


Figure 17-7. Payload Range Performance.

- Design takeoff gross weight: $M = 0.7$ cruise
- Maximum takeoff gross weight: $M = 0.7$ cruise
- Maximum takeoff gross weight: long range cruise speed

Maximum payload consists of 150 passengers and bags at 91 kg (200 lb) each plus 1588 kg (3500 lb) of cargo. All fuel is carried in the wing outside the fuselage. Maximum fuel capacity is 18,600 kg (41,000 lb).

Figure 17-8 shows how direct operating cost (DOC) varies with stage length. The airplane reaches the maximum gross weight limit at 1389 km (750 nmi). For longer stage lengths, payload must be reduced as fuel is increased so that this weight is not exceeded. The reduction in payload causes DOC to increase.

A breakdown of the direct operating cost for the design point is shown in Table 17-VII. Fuel cost is the largest single contributor to DOC making up almost a third of the total. A fuel cost of 7.93¢/liter (30 cents per gallon) was used in the calculations.

Trade factors or sensitivity factors in terms of aircraft gross weight, required engine size, and direct operating cost are presented in Table 17-VIII for changes in engine weight, cost and SFC. Of these the aircraft is most sensitive to SFC due to the high fuel price.

17.6 OTW BASELINE AIRCRAFT CHARACTERISTICS

Presented in this section are the preliminary results of the Boeing OTW baseline aircraft system sizing and economic study. The objectives of the study are:

1. Determine the size and characteristics of an OTW airplane using the upper surface blowing propulsive lift technique.
2. Evaluate the resulting airplane operating costs.

The design conditions are shown in Table 17-IX. Thus, the basic design task was to size the aircraft to the QCSEE OTW engine which is based on the use of the F101 core.

The propulsion system data was furnished by GE to Boeing as shown on Table 17-X. These data established the basic thrust, fuel consumption, and propulsion weights used in the study.

The resulting baseline aircraft sized to a takeoff gross weight of 91,500 kg (201,200 lb) with a payload of 195 passengers. The aircraft general arrangement is shown on Figure 17-9. For this size of aircraft, seven abreast seating with 86 cm (34 in) pitch was used to limit body length for adequate rotation at takeoff. The overall length is 46 m (154 ft) and the wing span is 37.5 m (125 ft). The airplane features double-slotted flaps blown by the OTW engines. During engine operation the flap slots are sealed to provide a smooth Coanda

C-4

- Cruise at $M = 0.7$, 9.45 km (31,000 ft)
- 150 Seats

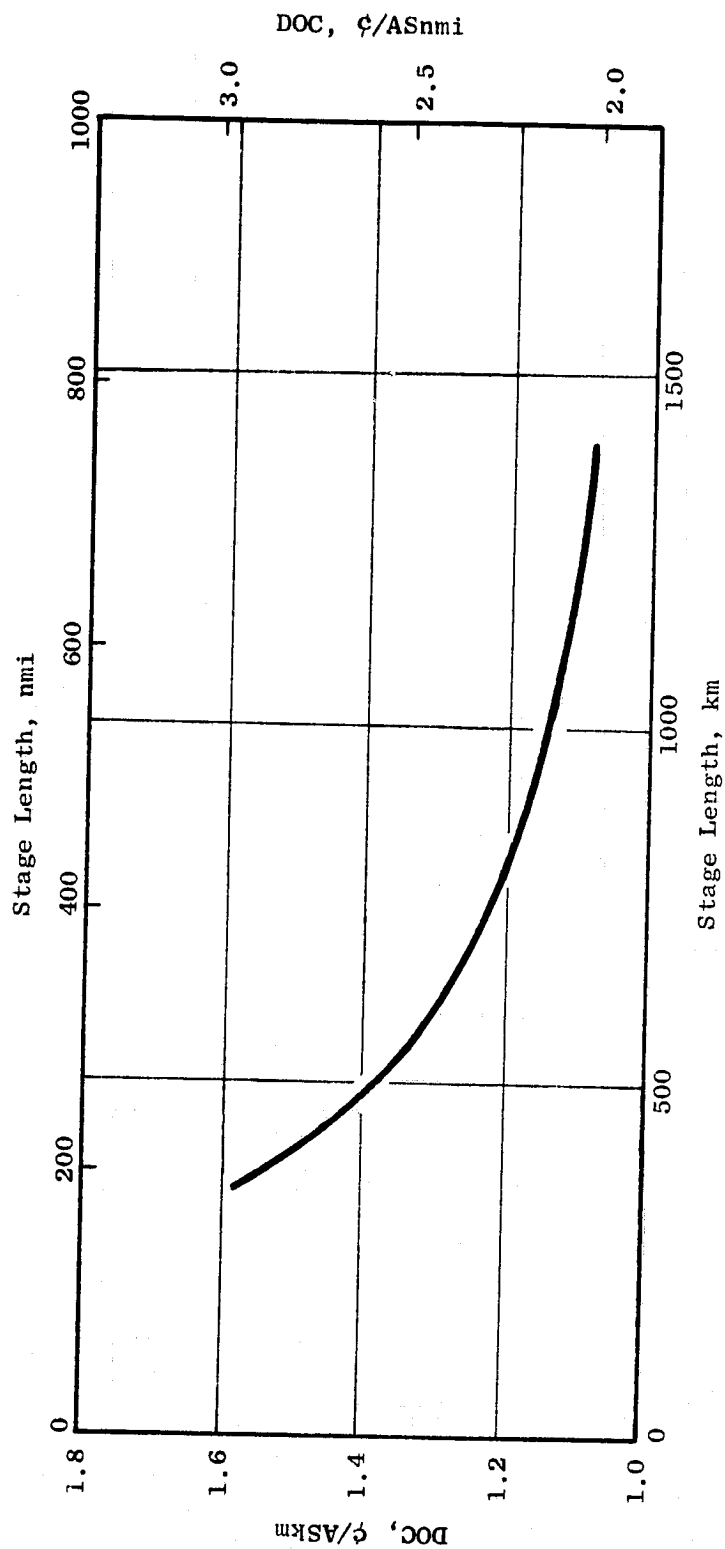


Figure 17-8. DOC Vs Stage Length.

Table 17-VII. Direct Operating Cost Breakdown.

Stage Length - 926 m (500 nmi)

<u>Component</u>	<u>\$/Flt. Cycle</u>	<u>Percent of Total</u>
Crew	229	14
Insurance	48	3
Depreciation	302	19
Fuel	572	35
Airframe Maintenance	212	13
Engine Maintenance	<u>257</u>	<u>16</u>
Total	1620	100

Table 17-VIII. Engine Trade Factors .

- A 10% increase in bare engine weight
will increase TOGW by 1.5%

$F_{N \text{ Req'd}}$ by 1.5%

DOC_{500} by 0.9%
- A 10% increase in bare engine cost
will increase DOC_{500} by 2.1%
- A 5% increase in climb and cruise SFC
will increase TOGW by 1.1%

$F_{N \text{ Req'd}}$ by 1.1%

DOC_{500} by 2.2%

Table 17-IX. Design Conditions.

• Field Length	914 m (3000 ft) [32° C(90° F) Sea Level]
• Stage Length	925 km (500 nmi)
• Cruise Speed	0.72 Mach
• Cruise Altitude	9,100 m (30,000 ft)
• Four GE19/F4E2 Engines	91,000 N (20,500 lb)/engine Rated
• Extended Range (P/L Off Load)	1389 km (750 nmi)

Table 17-X. Propulsion System,
(GE19/F4E2)

• Bypass Ratio	10
• F_N (Uninstalled)	91,000 N (20,500 lb[SLS T.O., 32° C(90° F)])
• F_N (Installed)	87,200 N (19,700 lb[SLS T.O., 32° C(90° F)])
• SFC (Cruise)	0.00002 kg/sec/N (0.71 lb/hr/lb)
• Weights kg (lbs/engine)	
• Engine	1290 (2,850)
• Nacelle and Systems	<u>665</u> (<u>1,470</u>)
Total	1955 (4,320)

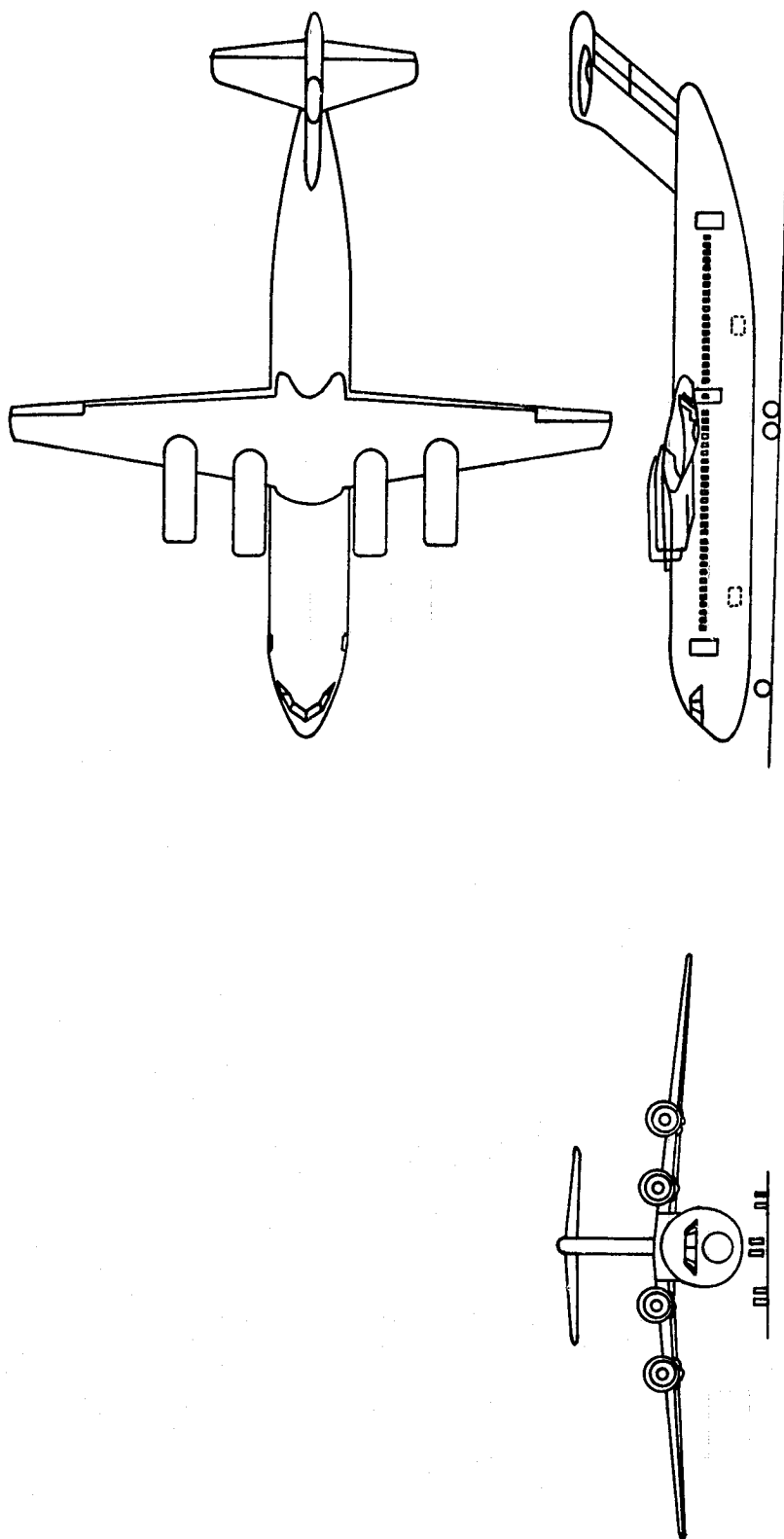


Figure 17-9. QCSEE Baseline OTW Aircraft.

turning surface and to reduce noise radiated below the aircraft. During engine out operation, the flap slots behind the inoperative engine are opened and the flaps further extended. The blown flaps on the opposite engine are partially retracted. This technique considerably reduces the engine out rolling moment which allows the lateral control system to trim the airplane with less drag.

A group weight summary is presented on Table 17-XI. With full passenger payload and fueled for the design range of 926 km (500 nmi) (including reserves), a takeoff gross weight of 91,500 kg (201,200 lb) will be reached. A 742 kg (1,530 lb) weight provision was made for nacelle-to-wing attachment. These include items such as engine mounts, wing heat shields, nacelle wing fittings, strut shells, and remote aircraft accessories.

The payload-range performance is shown on Figure 17-10. With a payload of 17,800 kg (39,400 lb), the airplane can be loaded with increasing amounts of fuel until the maximum takeoff gross weight of 91,500 kg (201,200 lb) is reached. At this point the takeoff field length is 914 m (3,000 ft) and a 926 km (500 nmi) range can be achieved. For an extended range of 1390 km (750 nmi), the payload must be reduced to 15,600 kg (34,400 lb) (170 passengers) to compensate for the additional fuel needed. The payload-fuel tradeoff can be continued until the wing tank fuel volume limit is reached corresponding to a 2220 km (1,200 nmi) mission capability with a 133 passenger payload.

A summary of the OTW baseline aircraft characteristics is shown on Table 17-XII. Takeoff and landing performance is provided for use in community noise analyses.

An economic analysis was conducted for the baseline QCSEE OTW airplane using the input data shown on Table 17-XIII. The propulsion system costs were provided by GE.

The direct operating cost as a function of range is shown on Figure 17-11. The DOC minimizes at the design range. At this point the DOC is 1.72 cents per available seat statute mile. Beyond this point the DOC will increase since the payload off loading reduces the number of available seats. At the extended range of 390 km (750 nmi) the DOC is 1.96/ASM.

The DOC sensitivity to airframe and engine price is presented in Figure 17-12. The sensitivity to fuel price and aircraft utilization is presented in Figure 17-13. These sensitivities can be applied to the basic DOC shown in Figure 17-11 at the 926 km (500 nmi) range condition.

The cost elements for a 926 km (500 nmi) trip is shown in the right hand column on Table 17-XIV for the QCSEE airplane. The short-haul 1974 costs are based on the 1967 ATA cost format updated with operational data as reported by regional carriers. A comparison is also shown for the baseline airplane when utilizing cost formula based on domestic trunk (CTOL) operating experience.

Similar data is presented on Table 17-XV for the indirect operating costs. This comparative data reflects short-haul operation from the smaller secondary airports expected to be in operation in the 1980 time period. IOC cost sensitivities are shown on Figure 17-14.

Table 17-XI. Basic Weights.

● Airplane

	<u>kg</u>	<u>lbs</u>
Structure	36,406	80,260
Propulsion (Engine Starting Control, and Fuel System)	6,015	13,260
Equipment Systems	16,017	35,310
Manufacturer's Empty Weight	58,437	128,830
Std and Operational Items	2,118	4,670
OEW	60,556	133,500
Payload (195 passengers)	17,872	39,400
Fuel	<u>12,836</u>	<u>28,300</u>
Maximum T.O. Gross Weight	91,264	201,200

● Propulsion Installation

	<u>kg</u>	<u>lbs</u>
Engine and Nacelle	1,950	4,320
Nacelle to Wing Attach	<u>694</u>	<u>1,530</u>
Installed Propulsion Weight Per Engine	2,654	5,850

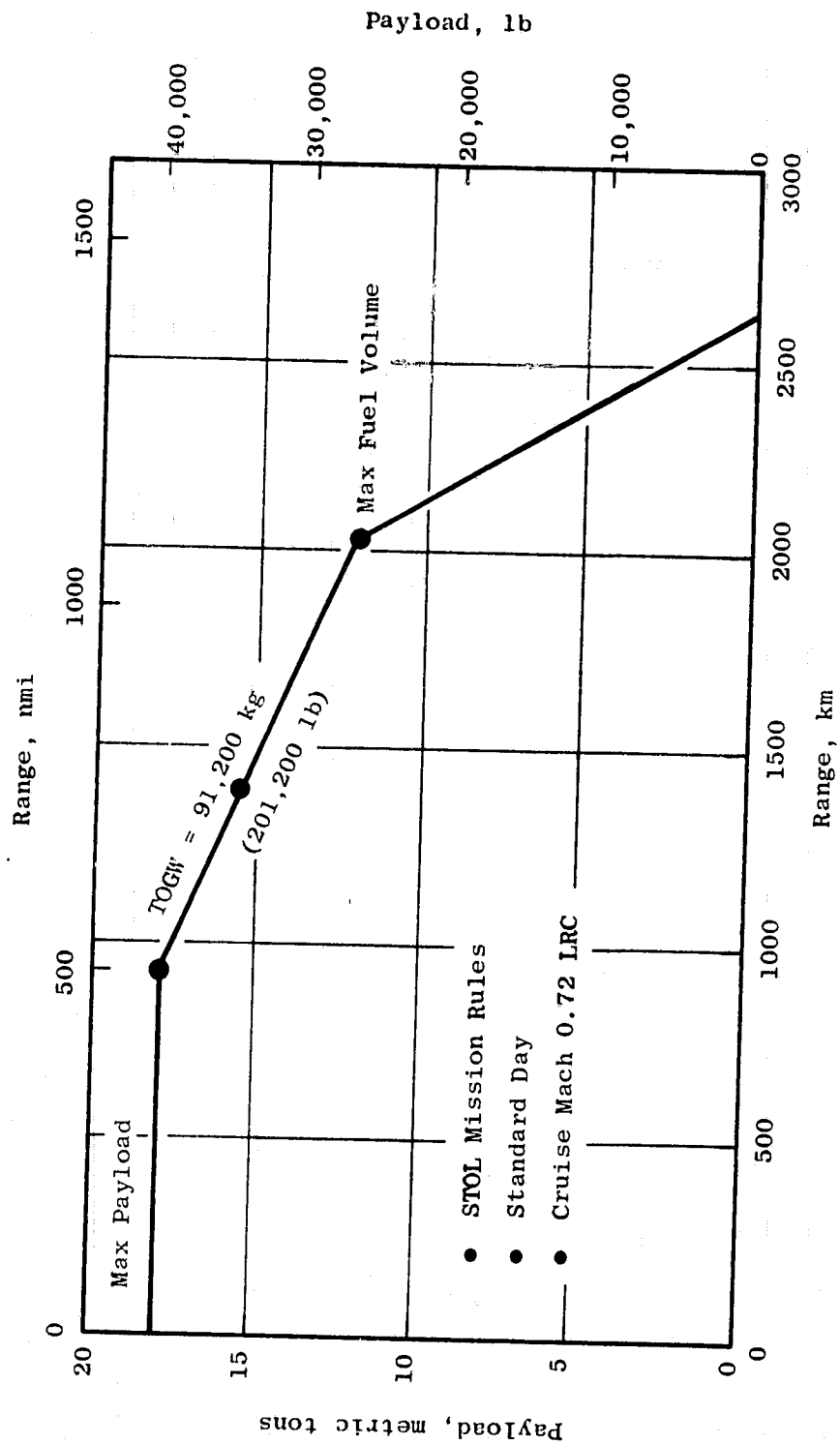


Figure 17-10. OTW Mission Performance.

Table 17-XII. Baseline Aircraft Characteristics.

Maximum Takeoff Gross Weight, kg (lb)	89,200 (201,200)
Operating Empty Weight, kg (lb)	61,300 (133,500)
Fuel Capacity, kg (lb)	18,600 (41,300)
Maximum Payload (195 Passengers), kg (lb)	17,750 (39,400)
Range, m (nmi)	926 (500)
Wing Area/Aspect Ratio, m ² (ft ²)	164 (1830)/8.6
Body Length, m (ft)	415 (139)
SLST, N (lb)	91,180 (20,500)
Engine Bypass Ratio	10
Cruise Mach/Alt, m (ft)	0.72/9140(30,000)
Wing Loading, kg/m ² (lb/f ²)	495 (110)
T/W	0.41
TOFL, m (ft)	914 (3000)
Climb Gradient, radians (degrees)	0.15 (9)
Speed @ (35 ft) Obstacle, m/sec (knots)	58.2 (113)
Landing FL, m (ft)	914 (3000)
Approach Speed, m/sec (knots)	48 (93)
Power Settings ($\gamma = 6^\circ$)	50%

Table 17-XIII. Data for Economic Analysis.

Block Fuel: 1217 lbs + 21.0 lb/st.mi.

Block Time: 18 Min. + 0.123 Min./st.mi.

Utilization: 2555 Block hrs/yr

2 Man Crew

Fuel: 30¢ per U.S. gallon

Study Prices: (1974 Dollars)

- Airframe (Including Nacelles and Avionics): \$15,200,000
- Engines: \$997,000
- Spares: 6% Airframe: 30% Engines

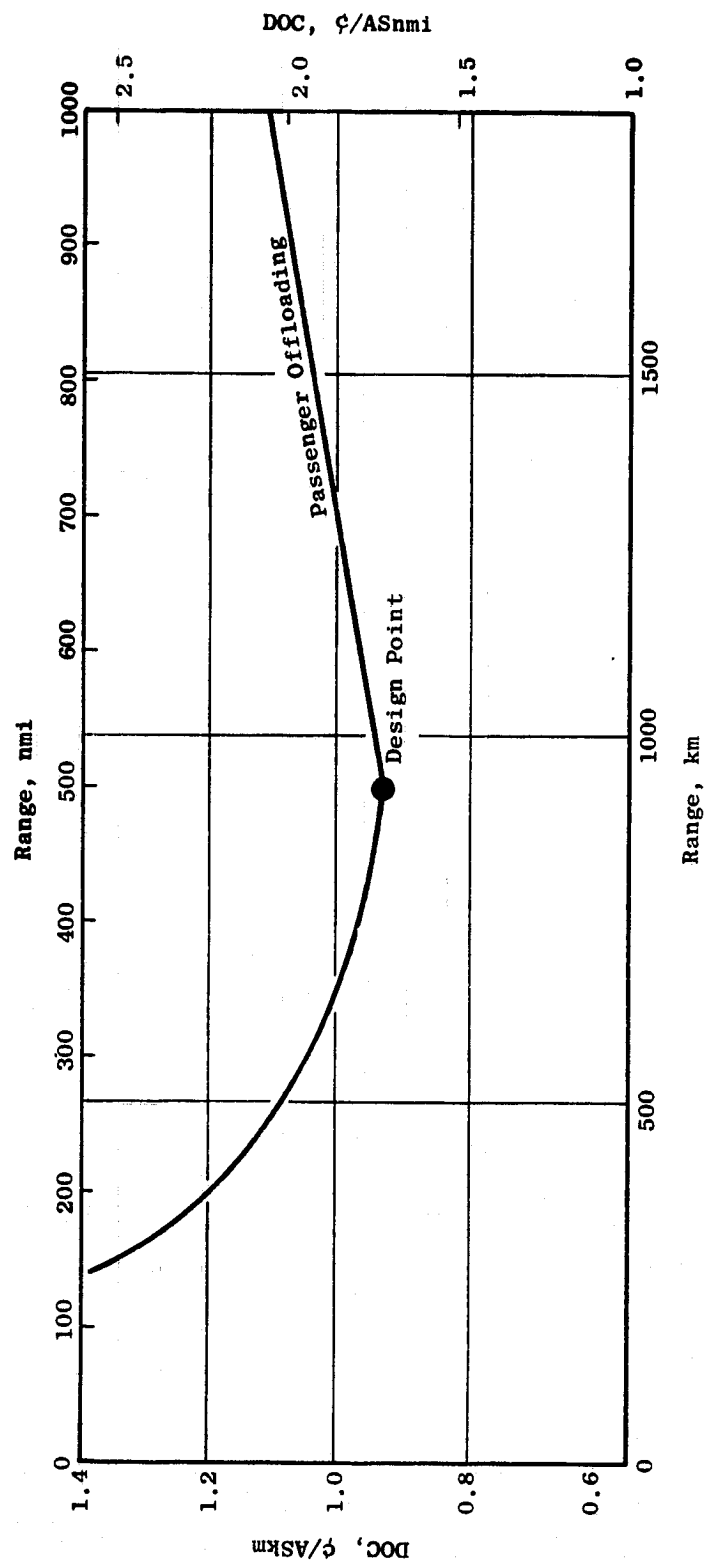


Figure 17-11. OTW Direct Operating Cost.

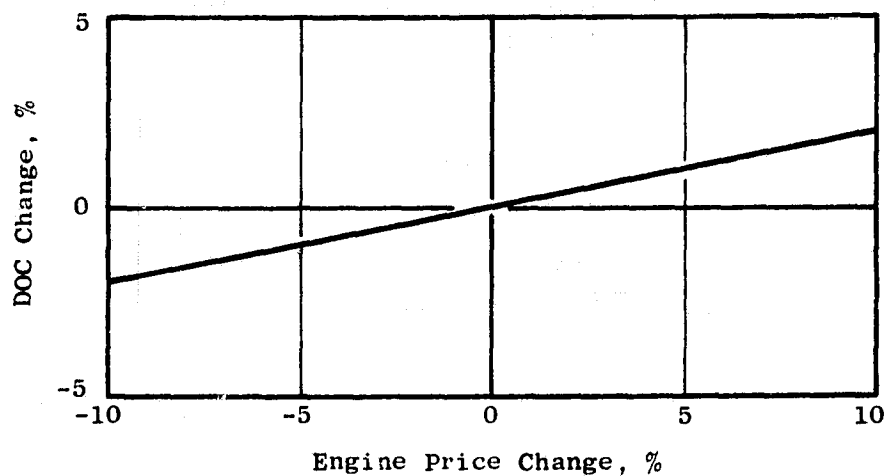
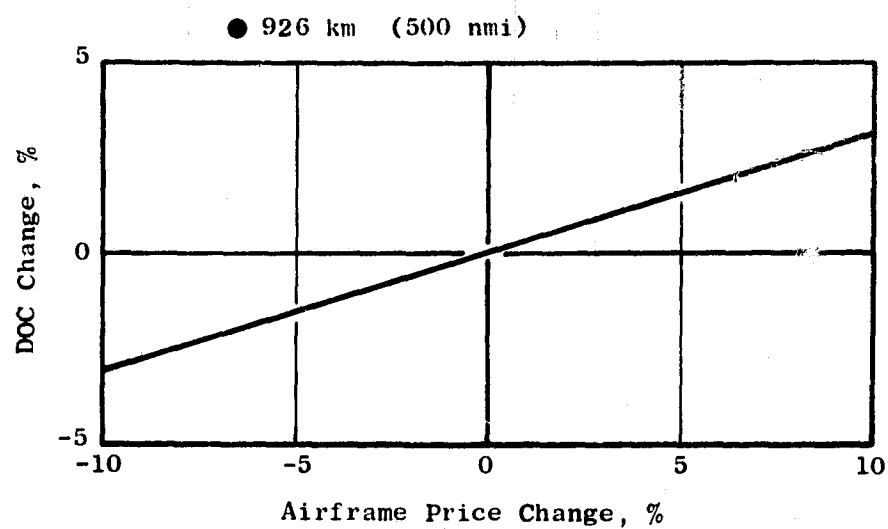


Figure 17-12. Operating Cost Sensitivities to Airframe and Engine Price.

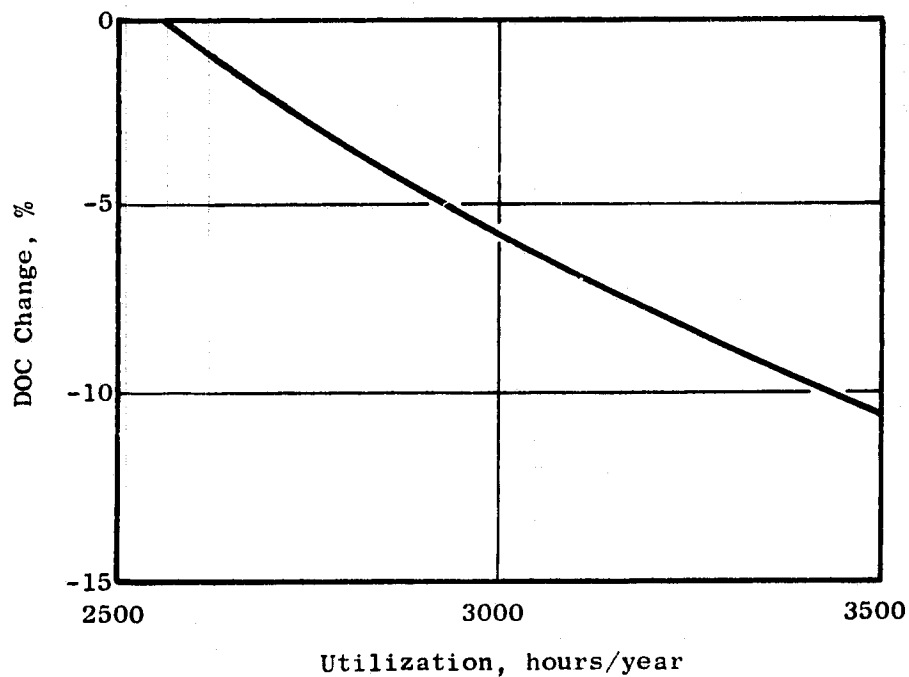
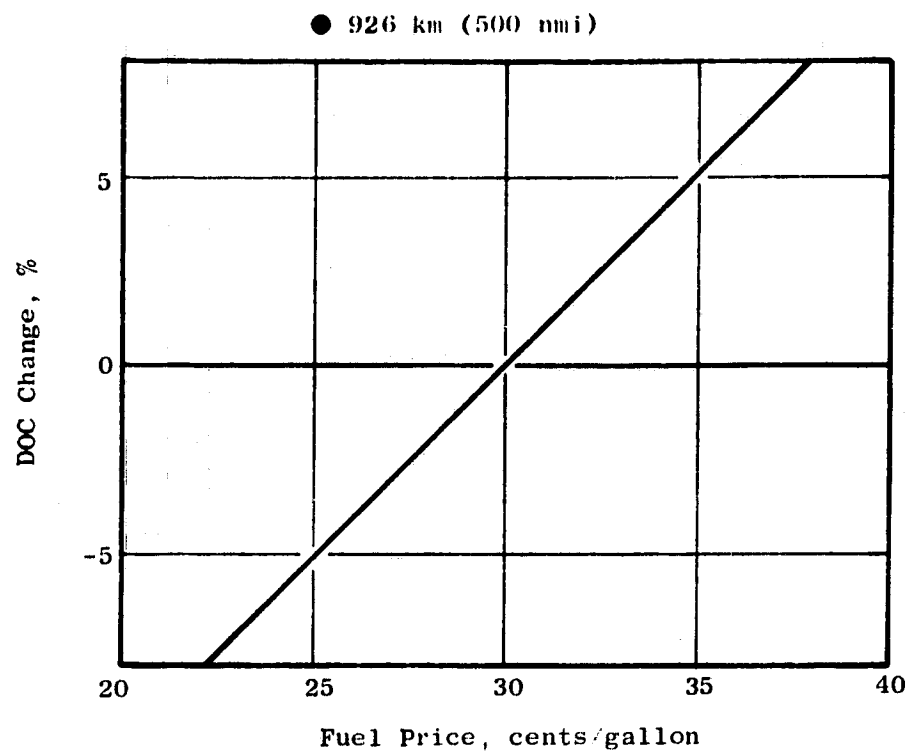


Figure 17-13. Operating Cost Sensitivities to Fuel Price and Aircraft Utilization.

Table 17-XIV. Direct Operating Cost Comparison.

Configuration: Baseline QCSEE OTW, 914 m
(3000 ft)

Base: Trip Cost in Dollars at 926 m
(500 nmi)

Utilization = 2555 hr/yr

<u>No.</u>	<u>Cost Item</u>	<u>1967 ATA</u>	<u>Boeing 1974 CTOL</u>	<u>Boeing 1974 Short Haul</u>
1	Flight Crew	162.89	232.18	212.31
2	Fuel	607.43	607.43	594.80
3	Insurance	88.12	88.12	88.12
4	Depreciation	727.01	692.63	690.67
5	Airframe Direct Labor/Cycle	89.11	77.89	24.71
6	Airframe Direct Labor/Hr			37.26
7	Airframe Material/Cycle	56.28	56.86	22.09
8	Airframe Material/Hr			22.80
9	Engine Direct Labor/Cycle	52.28	37.02	4.64
10	Engine Direct Labor/Hr			24.66
11	Engine Material/Cycle	101.20	119.52	26.64
12	Engine Material/Hr			89.82
13	Maintenance Burden	298.85	290.29	126.31
	Total DOC	2183.17	2201.96	1964.84

Table 17-XV. Indirect Operating Cost Comparison.

Configuration: Baseline QCSEE OTW, 914 m (3000 ft)

Base: Trip Cost in Dollars at 926 km
(500 Nautical Miles)

No.	Cost Item	Boeing Lockheed	Boeing 1974 CTOL	Boeing 1974 Short Haul
1	Cabin Attendant Pay and Exp.	230.36	268.70	173.68
2	Passenger Food	156.02	272.28	81.60
3	Passenger Liability Insurance			31.57
4	Other Passenger Service	28.53	15.56	42.84
5	Control and Communication	67.00	59.00	3.80
6	Aircraft Servicing	147.72	148.40	17.30
7	Landing Fees	73.97	82.80	84.05
8	Passenger Handling	227.58	276.21	241.90
9	Baggage Handling	165.34	114.76	Included in (8)
10	Passenger Reservation	339.43	291.78	92.45
11	Commission (Passenger)	127.72	153.00	75.54
12	Advertising			
		84.28	90.76	62.01
13	Misc. Promotion and Sales			
14	General and Administration	184.36	198.45	147.60
15	Amortization			52.56
		80.00	81.00	
16	G.E. and F. Depreciation			50.70
17	G.E. and F. Maintenance			8.46
		74.56	81.00	
18	G.E. and F. Maintenance Burden			3.26
	Total IOC	1986.88	2133.71	1169.33

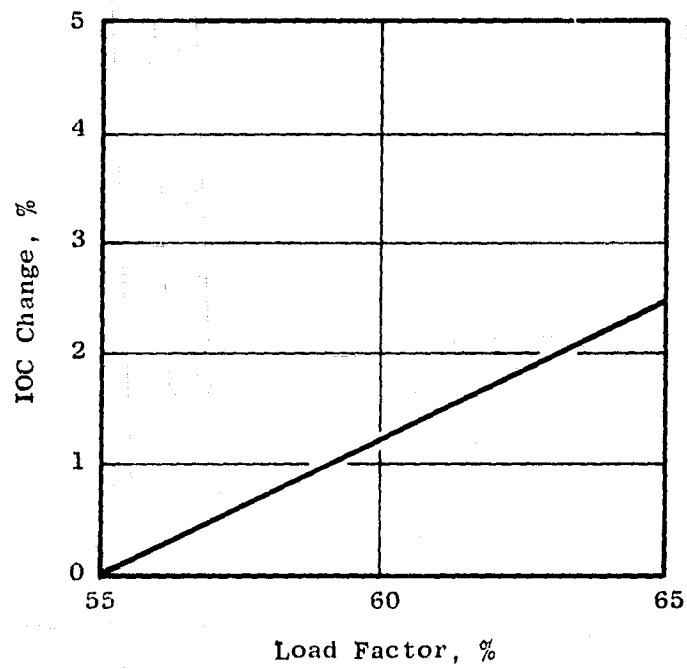
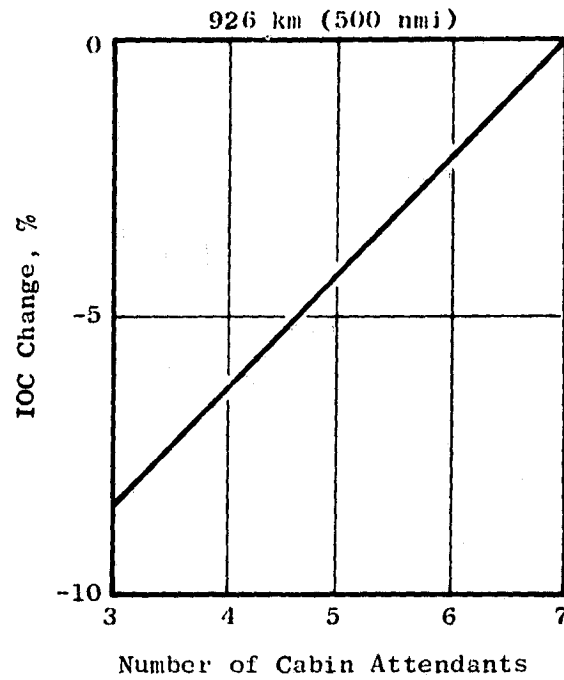


Figure 17-14: Indirect Operating Cost Sensitivities.

APPENDIX A

INFLIGHT AND REVERSE THRUST NOISE CALCULATION PROCEDURE

1.0 INTRODUCTION

A major technical objective of this contract is to develop quiet propulsion systems. Specifically the contract calls for:

The UTW and OTW propulsion systems to be designed with the objective of achieving and demonstrating the total powered lift system noise levels delineated below when the installed thrust of either system is scaled to 90,000 pounds (equivalent to a four engine aircraft installation):

- a. 95 EPNdB - 500 ft either side of the flight path during take-off and approach; and
- b. 100 PNdB - 500 ft either side of the aircraft during reverser operation on the ground with a reverse thrust level equal to 35 percent of the static take-off thrust.

For other thrust levels the noise levels shall be scaled based on 10 times the logarithm, to the base 10, of the thrust ratio. The noise levels given above shall include the noise from the propulsion system exhaust interacting with the wing and/or flap.

The procedure delineated in the appendix shall be used to calculate the expected inflight and reverse thrust noise levels of the QCSEE propulsion systems using measured acoustic data obtained from static ground tests. This procedure shall also be used in the QCSEE acoustic design program to predict the inflight and reverse thrust noise. This shall be accomplished by the substitution of predicted QCSEE acoustic data for the measured data as input to the calculation procedure. Whenever measured data is made available (e.g., through model test, component test, or engine test), the measured data shall be substituted for the calculated data upon recommendation by GE and approval of the NASA Project Manager.

2.0 SUMMARY OF CALCULATION PROCEDURE

Inflight EPNL values and reverse thrust PNL values for the QCSEE propulsion systems shall be computed from the measured maximum forward and maximum aft total propulsion system spectra obtained from ground tests without wings and flaps. The maximum forward and aft total spectra shall be obtained experimentally at the directions in the forward and aft quadrants, respectively, at which the 500 ft sideline PNL of the total spectrum is maximum. The aft spectra are obtained by measurements with a massive inlet acoustic suppressor. Forward spectra are assumed to be the total propulsion system spectra less the aft spectra.

A number of adjustments are made to relate static ground test acoustic data to inflight or reverse thrust noise levels for a 90,000 lb SLS thrust EBF airplane equipped with four QCSEE engines.

For inflight noise levels, the jet noise spectrum is removed from the total spectrum and replaced by the jet-flap interaction noise spectrum. The jet-flap noise spectrum is computed from empirical correlations based on scale model and engine jet-flap noise test results.

The spectra are extrapolated to a 500 ft sideline with the aircraft at the altitude at which maximum noise levels occur (200 ft or as otherwise determined), and are adjusted for atmospheric attenuation, Doppler shift, the source velocity, and extra ground attention.

The spectra are then converted to perceived noise levels (PNL) and further corrections for the number and thrust from the engines, shielding, reflection, acoustic absorption by the ground, inlet clean up, angle of attack, and relative velocity effects are made.

The differences between the UTW and OTW aircraft are considered in the shielding corrections.

The calculated jet-flap PNL values are then added to the measured and corrected maximum forward and maximum aft PNL values to obtain total aircraft perceived noise levels, which are in turn converted to EPNL values by a specified correlation.

A similar procedure is specified for acoustic design, differing primarily in that the propulsion system initial spectra are obtained analytically from correlations of model and full-scale engine data.

Reverse thrust noise calculations from either measured or predicted source noise spectra require only an abbreviated version of the complete procedure used for inflight noise calculations. A number of steps associated with forward velocity are eliminated by the assumption that maximum reverse thrust noise occurs with the aircraft at static ground conditions.

3.0 AIRCRAFT FLIGHT CHARACTERISTICS, PROPULSION SYSTEM LOCATION, AND OPERATING CONDITIONS

The calculation procedures for EBF inflight and reverse thrust noise levels require a definition of the aircraft flight characteristics, propulsion system location with reference to the wing and flap system, and operating conditions of the engines at takeoff, approach, and in reverse thrust operations. Aircraft flight and engine characteristics for takeoff, approach, and reverse thrust to be used for noise calculations at each condition are given in Tables A-I and A-II. All engine operating parameters shall be corrected to SLS ambient conditions of 59° F and 2116 lb/ft².

Table A-I. UTW and OTW Engine and Aircraft Design Flight Characteristics for Acoustic Calculations.

<u>Flight Conditions</u>	<u>Takeoff</u>	<u>Landing</u>
Aircraft Speed, knots	80	80
Flap Angle, degrees	30	60
Climb or Glide Angle, degrees	12.5	6.0
Angle of Attack, degrees	6.0	2.0
Upwash Angle, degrees	15.0	11.0
Installed Net Thrust, %	100	65

Table A-II. Propulsion System Reverse Thrust Static Test Conditions.

UTW Propulsion System

Fan blade position	-	through flat pitch or stall
Thrust	-	35 percent of SLS takeoff thrust
Flap Angle	-	30 degrees
Aircraft Speed	-	0 knots

OTW Propulsion System

Thrust	-	35 percent of SLS takeoff thrust
Flap Angle	-	30 degrees
Aircraft Speed	-	0 knots

It has been assumed that maximum EPNL values for inflight noise correspond to a 200 ft altitude for the aircraft. In the event that more detailed analyses from the QCSEE Fly-Over Noise Program (QFONP Computer Program) determine a significantly different altitude for maximum fly-over noise, such altitude shall be used in place of the 200 ft value for all inflight 500 ft sideline noise calculations in Sections 4.0 and 5.0.

The UTW and OTW engine and exhaust arrangements at the inboard position with respect to the wing flaps and flap geometry are shown in Figures A-1 through A-4 for the UTW and OTW aircraft, respectively. The upper surface contours of the OTW wing are designed such that flap interfaces form a closed surface.

4.0 CALCULATION OF IN-FLIGHT NOISE FROM PREDICTED DATA

This procedure shall be used for the QCSEE UTW and OTW propulsion system acoustic designs. The EPNL for a powered-lift EBF aircraft on takeoff and approach shall be computed according to the following steps.

Step 1 - Source Noise Spectra. The noise spectra for the following noise sources at maximum forward and maximum aft conditions shall be estimated from available test data or QCSEE component tests.

- a. Fan inlet noise
- b. Fan exhaust noise
- c. Turbine noise
- d. Combustor noise
- e. Gear noise
- f. Jet/flap noise

All spectra used in the estimations shall be approved by the NASA Project Manager.

Step 2 - Sideline Conditions. Correct the maximum forward and maximum aft individual spectra to a 500 ft sideline, 200 ft altitude basis. The maximum forward and maximum aft sideline locations are the positions relative to the flight path at which the total propulsion system perceived noise level is a maximum with the aircraft at 200 ft altitude.

Step 3 - Jet-Flap Spectra. Calculate 500 ft sideline, 200 ft altitude maximum forward and maximum aft jet-flap spectra for the aircraft defined in Table A-I and Figures A-1 through A-4 using the procedure defined in AIAA Paper 73-1028. For the UTW configuration, the equation

$$K = 83.0 + 0.14\psi$$

shall be substituted for equation (4) in the AIAA Paper. Similarly, for the OTW configuraition, the equation

$$k = 84.5 + 0.01\psi$$

shall be used in place of equation (6) in the paper. The calculated effective velocity for the installed propulsion system shall not be adjusted for inflight relative velocity.

Step 4 - Spectrum Adjustments. Adjust the source noise spectra and the jet-flap spectra for prescribed inflight conditions with the following corrections:

- a. Atmospheric Attenuation - Calculate per SAE ARP 866 to acoustic standard day conditions of 77° F and 70 percent RH.
- b. Doppler Shift - A frequency shift that occurs for a moving source relative to a fixed observer. This shift is calculated using the equation in Figure A-5.
- c. Extra Ground Attenuation - Apply the 0°-2° attenuation curves of Figure 4, SAE AIR 923, to that portion of the acoustic range that lies within an assumed 100 ft turbulent boundary layer above the ground.
- d. Dynamic Effect - A change in SPL occurs due to the motion of a moving source. The correction is computed from the equation given in Figure A-6. The variables θ and M are defined in the illustration of Figure A-5.

Step 5 - Perceived Noise Levels. Calculate PNL for each spectrum using SAE ARP 865A.

Step 6 - PNL Adjustments. Correct the Calculated PNL values for the following:

- a. Engine Size - This calculation provides a Δ PNL increment for adjustment of the calculated acoustic levels to the corresponding levels for a four-engine airplane with 90,000 lb total installed thrust. For the OTW propulsion system add

$$\Delta\text{PNL} = 10 \log \frac{22,500}{F} \text{ PNdB}$$

where $F = 17,400$ lb SLS installed thrust or the actual cycle calculated value.

For the OTW propulsion system, add

$$\Delta\text{PNL} = 10 \log \frac{22,500}{F} \text{ PNdB}$$

where $F = 20,300$ lb SLS installed thrust or the actual cycle calculated value.

The ΔPNL values shall be added for both takeoff and approach.

- b. No. of engines - Add the following

$$\Delta PNL = 10 \log 4 = +6 \text{ PNdB}$$

- c. Fuselage shielding and aircraft reflections:
for 200 ft altitude, 500 ft sidelines, add

$$\Delta PNL = 10 \log 3/4 = -1.2 \text{ PNdB}$$

- d. Dirt/grass ground sound absorption, add:

Forward and aft engine noise,

$$\Delta PNL = -1.5 \text{ PNdB}$$

Jet-flap noise,

$$\Delta PNL = -0.5 \text{ PNdB}$$

or where individual spectra can be defined:

High frequency sources (e.g., fan, turbine)

$$\Delta PNL = -1.5 \text{ PNdB}$$

Low frequency sources (e.g., combustor)

$$\Delta PNL = -0.5 \text{ PNdB}$$

Step 7 - Inlet Noise Adjustment. Adjust the fan inlet radiated noise for inlet cleanup effects as determined by forward velocity and engine inlet upwash angle by adding the values from Figure A-7. Figure A-7 presents an estimate from CTOL aircraft which shall be used for preliminary calculations. Figure A-7 shall be modified to include upwash angle data obtained from wind tunnel model tests with high Mach number QCSEE inlets when these data become available.

Step 8 - Relative Velocity. Correct jet-flap noise for inflight, relative velocity effects using Figure A-8, adding the indicated values.

Step 9 - OTW Wing Shielding. The levels of the following noise sources shall be adjusted by adding the indicated amounts to correct for OTW wing shielding:

OTW combustor $\Delta PNL = -3.5 \text{ PNdB}$

OTW turbine $\Delta PNL = -5.0 \text{ PNdB}$

OTW fan exhaust $\Delta PNL = -5.0 \text{ PNdB}$

Step 10 - Summation of Sources. The noise sources shall be summed at the maximum forward and maximum aft angles to obtain maximum forward and aft system PNdB levels. Noise sources with similar spectra (fan and turbine or core and jet-flap) shall be summed using Figure A-9. Then the combined spectra shall in turn be summed using Figure A-10. (Fan and turbine plus core and jet-flap).

Step 11 - Effective Perceived Noise Level. Convert the maximum PNdB level of Step 10 to EPNdB using Figure A-11.

5.0 CALCULATION OF INFIGHT NOISE FROM MEASURED DATA

This procedure shall be used in the evaluation of the UTW and OTW propulsion system acoustic performance as determined by forward thrust static ground tests.

The UTW and OTW propulsion systems shall be acoustically tested at conditions representative of takeoff and approach operations as specified in Table A-I. The approach conditions shall also be compatible with engine response requirements.

The engine operating points to be used during acoustic testing for the simulated takeoff and approach acoustic reference conditions must be approved by the NASA Project Manager. No compromise to the basic engine performance and operating requirements (i.e., response time, pollution, etc) shall be used to achieve minimum noise. Engine operating conditions for takeoff and approach shall be consistent with ordinary aircraft engine operating procedures compatible with flight safety.

For the acquisition of measured propulsion system acoustic data, ground static acoustic propulsion system tests shall be conducted by the contractor with the UTW and OTW systems but without EBF wings. Data shall be obtained on a microphone arc over a hard ground surface (crushed rock). The contractor shall obtain the approval of the NASA Project Manager on the test setup, data acquisition systems, and data reduction procedure prior to testing.

Step 1 - Total Aft Noise. The propulsion system aft noise spectra shall be obtained from propulsion system tests at the required conditions with a massive inlet acoustic suppressor designed to reduce inlet radiated noise 10 dB below the aft suppressed radiated noise in the inlet quadrant. Aft noise shall be defined as the noise measured with the inlet suppressor in place.

Step 2 - Inlet Noise. The inlet radiated noise spectra shall be obtained from a propulsion system test without a massive inlet suppressor. The aft noise shall then be subtracted from this data to provide the inlet noise spectra.

Step 3 - Jet Velocity. The fan and core jet velocities shall be calculated from propulsion system tests at the specified takeoff and approach operating conditions, using instrumentation and a procedure mutually agreed to by NASA and the Contractor.

Step 4 - Jet Noise. The calculation of inflight noise levels for an EBF propulsion system requires that the jet noise component of the engine noise system be replaced with the appropriate jet/flap noise spectrum. Jet noise shall be calculated for the UTW and OTW propulsion systems using the General Electric Company - Annular Jet Noise Computer Program dated 3/7/74. These jet noise calculations shall be modified, as appropriate, in accordance with data obtained from the OTW Scale Model noise tests.

Step 5 - Aft Fan and Core Noise. The jet-noise-free exhaust spectrum (fan exhaust and core noise) shall be obtained by subtracting the calculated jet noise spectrum from the total propulsion system aft noise spectrum. The procedures used in making these adjustments shall be mutually agreed to by NASA and the Contractor.

Step 6 - Sideline Conditions. Correct the maximum forward and maximum aft individual spectra less jet noise to a 500 ft sideline at 200 ft altitude as prescribed in Step 2, Section 4.0.

Step 7 - Jet-Flap Noise. Calculate the 500 ft sideline, 200 ft altitude, maximum forward and maximum aft jet-flap spectra using the Aircraft defined in Table A-1 and Figures A-1 through A-4 in accordance with the procedure prescribed in Step 3, Section 4.0.

Step 8 - Spectrum Adjustments. The engine inlet spectra, engine exhaust spectra and the jet-flap spectra shall be corrected to inflight conditions using the procedures specified in Step 4 of Section 4.0.

Step 9 - Perceived Noise Levels. Calculate PNL values for each spectrum using SAE ARP 865A.

Step 10 - PNL Adjustments. Same as Step 6 of Section 4.0 except for the following modification:

- a. Engine size - Add the following corrections for the UTW and OTW propulsion systems at takeoff and approach:

$$\Delta \text{PNL} = 10 \log \frac{22,500}{F} \quad \text{PNdB}$$

Step 11 - Inlet Noise Adjustment. Same as Step 7, Section 4.0.

Step 12 - Relative Velocity. Same as Step 8, Section 4.0.

Step 13 - OTW Wing Shielding - The level of the engine exhaust shall be corrected by adding -5 PNdB. If spectrum is low frequency noise dominated, add -3.5 PNdB to the engine exhaust noise value.

Step 14 - Summation of Sources. The inlet radiated and aft radiated PNL values shall be added at the maximum forward and maximum aft angles using Figure A-9. These sums shall then be added to the jet-flap noise at the maximum forward and aft angles, respectively, using Figure A-10 to obtain maximum forward and aft total propulsion system PNL's.

Step 15 - Effective Perceived Noise Levels. Same as Step 11, Section 4.0.

6.0 CALCULATION OF REVERSE THRUST NOISE FROM PROPULSION SYSTEM PREDICTED AREA

The basic calculation procedure of Section 4.0 shall be used for reverse thrust noise calculation by modifying some steps and omitting others. A basic difference occurs in that the reverse thrust design condition is ground static so no inflight corrections are needed. Fundamental differences in reverse thrust fan flow require separate treatment of the UTW and OTW propulsion systems for reverse thrust noise calculations. In the reverse thrust mode in static ground conditions only the maximum PNL is required and the time dependent EPNL calculations are omitted.

6.1 UTW Reverse Thrust Noise

The maximum 500 ft sideline PNL for the UTW propulsion system in the reverse thrust mode shall be computed from predicted design source noise spectra in accordance with the following steps:

Step 1 - Source Noise Spectra. Spectra for the maximum forward and maximum aft directions for each of the following noise sources shall be estimated from existing experimental reverse flow acoustic data correlations and from QCSEE component and model fan test data as such data becomes available:

- a. Fan inflow noise radiated from the exhaust nozzle or exlet
- b. Fan exhaust noise radiated from the fan inlet
- c. Fan jet noise radiated from the fan inlet
- d. Turbine noise
- e. Combustor noise
- f. Gear noise
- g. Core jet flap impingement noise

The spectra used in the calculations shall be approved by the NASA Project Manager.

Step 2 - Sideline Conditions. Correct the data to a 500 ft ground plane sideline. The maximum forward and maximum aft sideline locations are the positions, respectively, on a 500 ft sideline parallel to the aircraft heading at which the total propulsion system reverse thrust perceived noise level is a maximum with the aircraft on the ground.

Step 3 - Core Jet-Flap Spectra. Calculate 500 ft ground plane sideline, maximum forward, and maximum aft core jet-flap spectra for the reverse thrust mode with the flap configuration as defined in Figure A-1 using the procedure prescribed in Step 3, Section 4.0 and the core jet velocity from design engine cycle data.

Step 4 - Spectrum Adjustments. Adjust the individual spectra and the jet-flap spectra for reverse thrust conditions with the following corrections:

- a. Atmospheric Attenuation - Calculate per SAE ARP 866 to acoustic standard day conditions of 77° F and 70 percent RH.
- b. Extra Ground Attenuation - Use Figure 4, SAE AIR 923.

Step 5 - Perceived Noise Level. Calculate PNL values for each spectrum using SAE ARP 865A.

Step 6 - PNL Adjustments. Adjust the calculated PNL values by adding the following increments:

- a. Engine size Same as Step 6(a), Section 4.0.
- b. No. of Engines $\Delta\text{PNL} = 10 \log 4 = + 6 \text{ PNdB}$
- c. Fuselage shielding and aircraft reflections from 500 ft ground plane sideline

$$\Delta\text{PNL} = 10 \log 2/4 = -3.0 \text{ PNdB}$$

- d. Dirt/grass ground absorption:

High frequency sources (fan, turbine) use

$$\Delta\text{PNL} = -1.0 \text{ PNdB}$$

Low frequency sources (core jet-flap, combustor, gears) use:

$$\Delta\text{PNL} = - 0.5 \text{ PNdB}$$

Step 7 - Summation of Sources. Same as Step 10, Section 4.0. The greater of the two values shall be taken as the maximum reverse thrust PNL.

6.2 OTW Reverse Thrust Noise

The maximum 500 ft sideline PNL for the OTW propulsion system in the reverse thrust mode shall be computed from predicted design source noise spectra in accordance with the following steps:

Step 1 - Source Noise Spectra. Spectra for the maximum forward and maximum aft directions for each of the following noise sources shall be estimated from existing experimental data on reverse thrust noise and from the results of QCSEE model and component tests, including the results of the OTW thrust reverser scale model tests if such data are available.

- a. Fan inlet noise
- b. Fan exhaust noise*
- c. Jet/Reverser*
- d. Turbine noise*
- e. Combustor noise*
- f. Gear noise*

*redirected by the thrust reverser mechanism

Directivity patterns for the deflected fan and core jet shall be updated by the results of component noise tests when data become available.

The spectra used in the calculations shall be approved by the NASA Project Manager.

Step 2 - Sideline Conditions. Correct the data to a 500 ft ground plane sideline as prescribed in Step 2, Section 6.1.

Step 3 - Spectrum Adjustments. Adjust the individual spectra for reverse thrust conditions with the following corrections:

- a. Atmospheric Attenuation - Calculate per SAE ARP 866 to acoustic standard day conditions of 77° F and 70 percent RH.
- b. Extra Ground Attenuation - Use Figure 4, SAE AIR 923.

Step 4 - Perceived Noise Level. Calculate PNL for each spectrum using SAE ARP 865A.

Step 5 - PNL Adjustments. Adjust the calculated PNL values by adding the following increments:

- a. Engine Size - Same as Step 6(a), Section 4.0.
- b. No. of engines - Same as Step 6(b), Section 4.0.
- c. Fuselage shielding and aircraft reflections:

for 500 ft ground plane sideline:

$$\Delta \text{PNL} = 10 \log 3/4 = -1.2 \text{ PNdB}$$

- d. Dirt/grass ground absorption

High frequency sources (fan, turbine) use:

$$\Delta \text{PNL} = -1.0 \text{ PNdB}$$

Low frequency sources (jet noise, combustor) use:

$$\Delta \text{PNL} = - 0.5 \text{ PNdB}$$

Step 6 - Summation of Sources. Same as Step 10, Section 4.0. The greater of the two values shall be taken as the maximum reverse thrust PNL.

7.0 CALCULATION OF REVERSE THRUST NOISE FROM PROPULSION SYSTEM TEST DATA

The degree to which the QCSEE propulsion systems meet the reverse thrust noise objectives shall be determined by extrapolating the single engine reverse thrust acoustic test data without a wing in place to a four engine aircraft.

This section delineates the procedures to be followed in obtaining the single engine reverse thrust test data and extrapolating it to an aircraft in reverse thrust operation at zero velocity on a hard surface runway.

The contractor shall obtain the UTW and OTW propulsion system acoustic test data using test set ups, data acquisition procedures, and data reduction procedures which have been approved by the NASA Project Manager. The engines shall be tested in reverse thrust at the conditions specified in Table A-II.

7.1 UTW Reverse Thrust Noise

The following procedure shall be used to determine the UTW propulsion system reverse thrust noise:

Noise sources to be accounted for in the UTW procedure are:

1. The measured total engine noise.
2. Calculated jet flap noise resulting from the interaction of the core jet and the wing flaps.

Step 1 - Measurement of Total Engine Noise. The propulsion system total forward and aft noise spectra shall be obtained from reverse thrust tests at 35 percent of maximum takeoff thrust.

Step 2 - Jet Velocity. The core jet velocity shall be calculated from propulsion system tests at the conditions specified in Table A-II, using instrumentation and a procedure mutually agreed to by NASA and the Contractor.

Step 3 - Core Jet-Flap Noise. The calculation of the core jet flap noise levels for an EBF propulsion system requires that the core jet noise component of the engine noise system be replaced with the appropriate jet-flap noise spectrum. Core-jet noise shall be calculated for the UTW propulsion systems using the General Electric Company - Annular Jet Noise Computer Program dated 3/7/74 and the calculated core jet velocity from Step 2 above.

Step 4 - Engine Noise. The engine noise spectrum shall be obtained by subtracting the calculated core jet noise from the total propulsion system noise using procedures mutually agreed to by NASA and the Contractor.

Step 5 - Sideline Conditions. Correct the maximum forward and maximum aft spectra to a 500 ft ground plane sideline as prescribed in Step 2 of Section 6.1.

Step 6 - Jet-Flap Spectra. Calculate 500 ft ground plane sideline, maximum forward and maximum aft jet-flap noise due to the core jet impacting the jet flap system shown in Figure A-2 using the procedure prescribed in Step 3, Section 4 and the core jet velocities calculated per Step 2.

Step 7 - Spectrum Adjustments. Adjust the engine noise spectra and the jet-flap spectra for reverse thrust conditions with the following corrections:

- a. Atmospheric Attenuation - Calculate per SAE ARP 866 to acoustic standard day conditions of 77° F and 70 percent RH.
- b. Extra Ground Attenuation - Use Figure 4, SAE AIR 923.

Step 8 - Perceived Noise Level. Calculate PNL for each spectrum using SAE ARP 865A.

Step 9 - PNL Adjustments. Adjust the calculated PNL values by adding the following increments:

- a. Engine size -

$$\Delta \text{PNL} = 10 \log \frac{0.35 \times 22,500}{F} \quad \text{PNdB}$$

where F is the measured reverse thrust in pounds.

- b. No. of engines - Same as Step 6(b) of Section 4.0.
- c. Fuselage shielding and aircraft reflections for 500 ft ground plane sideline.

$$\Delta \text{PNL} = 10 \log 2/4 = - 3.0 \text{ PndB}$$

- d. Dirt/grass ground absorption.

measured engine noise use $\Delta \text{PNL} = - 1.0 \text{ PndB}$.

calculated jet-flap noise use $\Delta \text{PNL} = - 0.5 \text{ PndB}$

Step 10 - Summation of Sources. The noise sources shall be summed at the maximum forward and maximum aft angles to obtain maximum forward and aft system PNL levels. Noise sources with similar spectra shall be summed using Figure A-9 and those with dissimilar spectra using Figure A-10.

Step 11 - Reverse Thrust Noise. The maximum of the two values from Step 10, maximum forward or maximum aft noise, shall be selected as the reverse thrust noise.

7.2 OTW Reverse Thrust Noise

The following procedures shall be used to determine the reverse thrust noise of the OTW propulsion system:

Step 1 - Measurement of Total Engine Noise. Same as Step 1, Section 7.1.

Step 2 - Ground Impingement Noise. Remove noise due to ground impingement of the jet from the jet reverser by applying a correction to forward and aft maximum spectra using data obtained from the scale model thrust reverser test program. (WBS 2.13) if such data are available.

Step 3 - Sideline Conditions. Adjustment to 500 ft ground plane sideline. Same as Step 5, Section 7.1.

Step 4 - Spectrum Adjustments. Same as Step 7, Section 7.1.

Step 5 - Perceived Noise Levels. Same as Step 8, Section 7.1.

Step 6 - PNL Adjustments. Same as Step 9 of Section 7.1 except for the following:

- a. Fuselage shielding and aircraft reflections for 500 ft ground plane sideline

$$\Delta \text{PNL} = 10 \log 3/4 = - 1.2 \text{ PNdB}$$

- b. Dirt/Grass ground absorption

$$\Delta \text{PNL} = - 0.5 \text{ PNdB}$$

If fan noise dominates

$$\Delta \text{PNL} = - 1.0 \text{ PNdB}$$

Step 7 - Reverse Thrust Noise. The maximum of the two values from Step 6, maximum forward or maximum aft total noise, shall be selected as the reverser thrust noise.

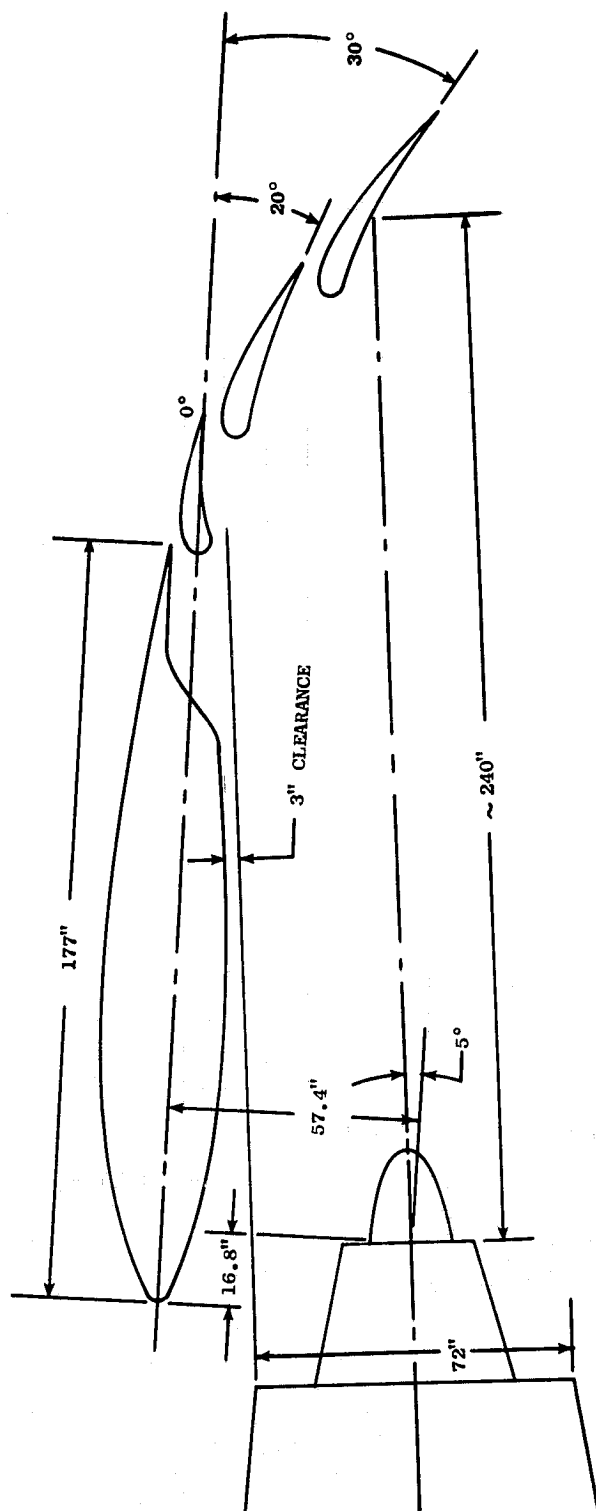


Figure A-1. UTW Propulsion System Takeoff Configuration - UTW Reference Nozzle, Wing Orientation, and Flap Location; Inboard Engine, Wing Chord, $C = 17.9$ ft; Dimensions Based on 18,300 Pound Thrust Engine.

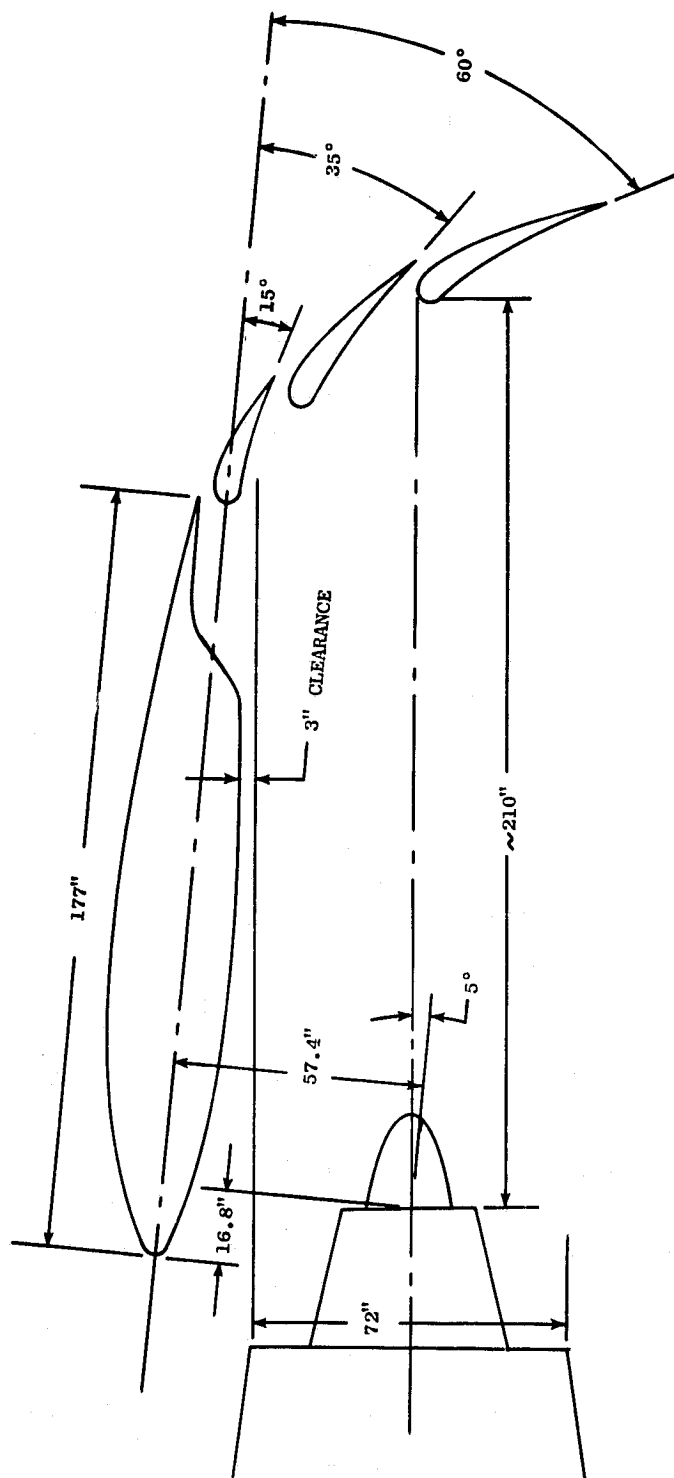


Figure A-2. UTW Propulsion System Approach Configuration - UTW Reference Nozzle, Wing Orientation, and Flap Location; Inboard Engine, Wing Chord, $C = 17.9$ ft; Dimensions Based on 18,300 Pound Thrust Engine.

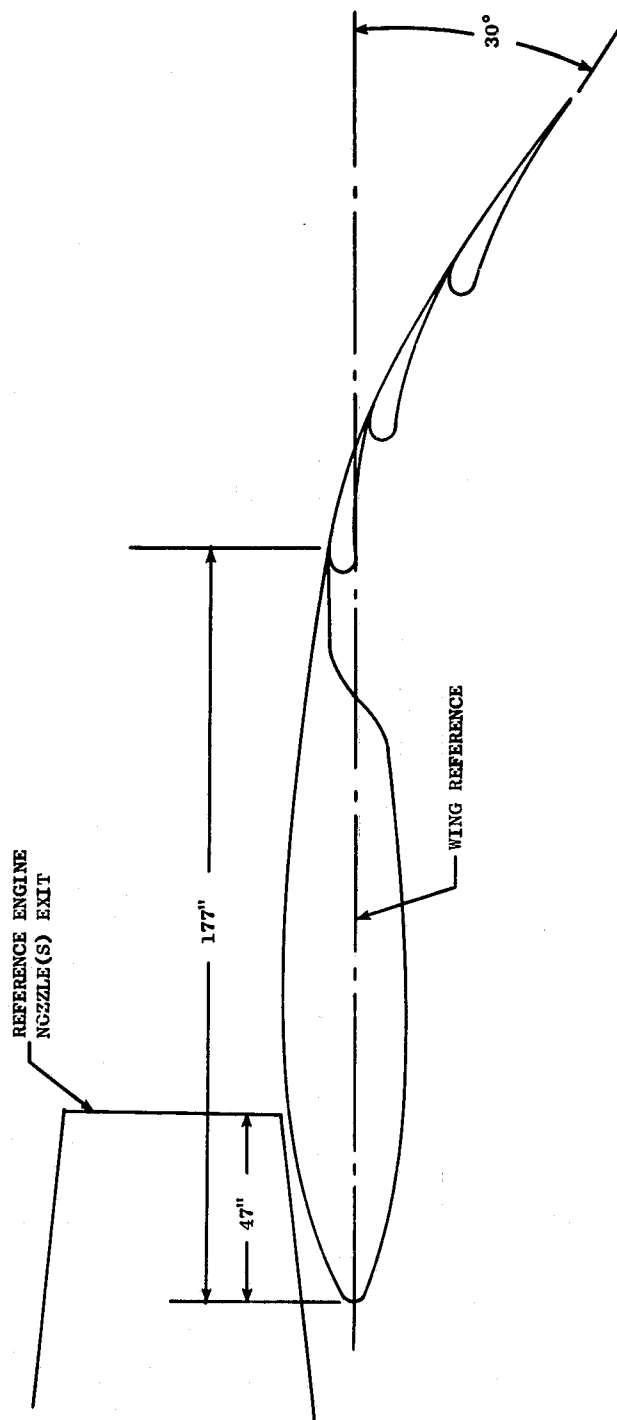


Figure A-3. OTW Propulsion System Takeoff Configuration - OTW Reference Nozzle, Wing Orientation, and Flap Location; Inboard Engine, Wing Chord, $C = 17.9$ ft; Dimensions Based on 21,000 Pound Thrust Engine.

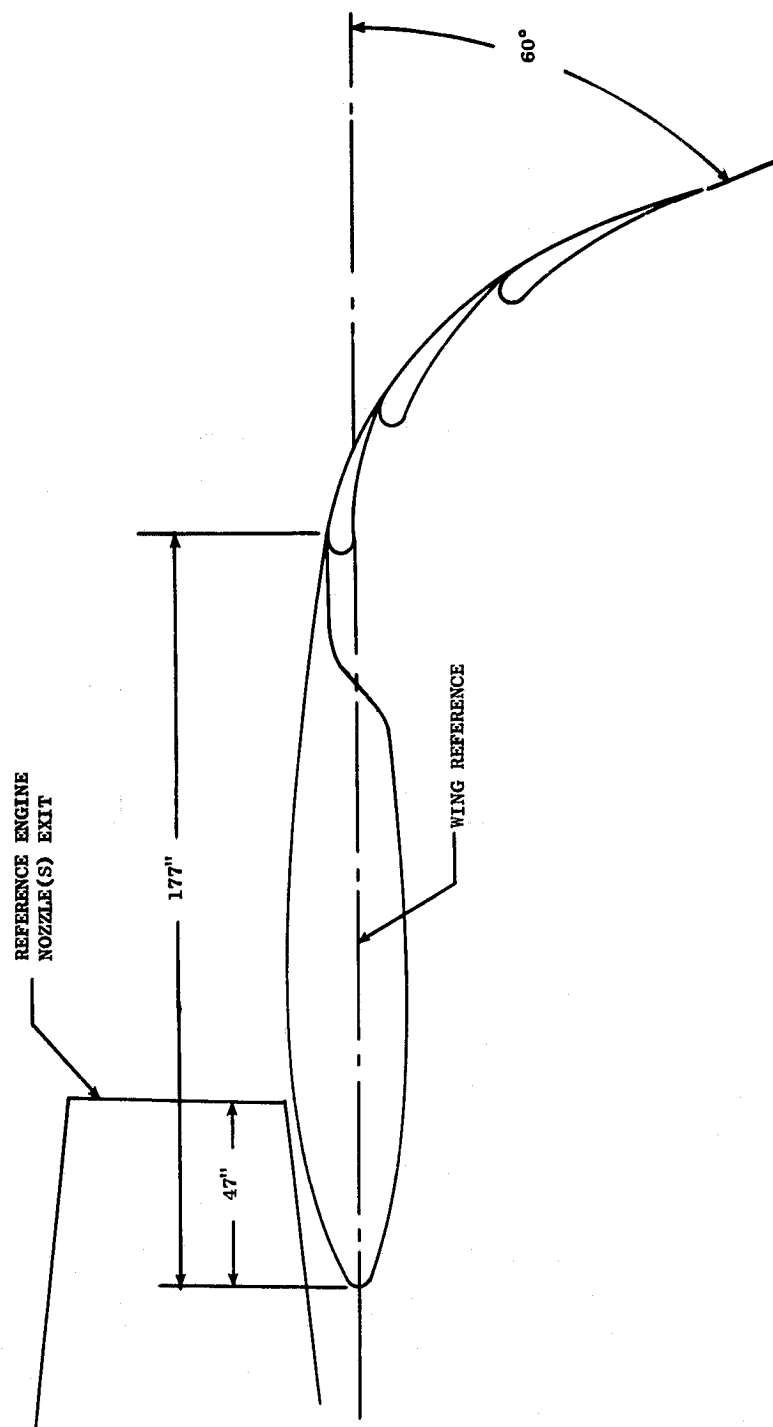
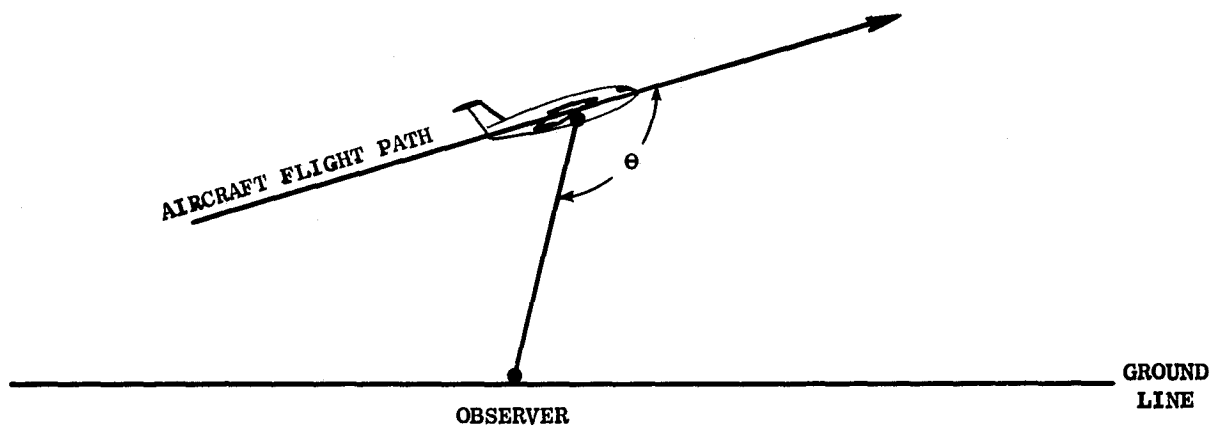


Figure A-4. OTW Propulsion System Approach Configuration - OTW Reference Nozzle, Wing Orientation, and Flap Location; Inboard Engine, Wing Chord, $C = 17.9$ ft; Dimensions Based on 21,000 Pound Thrust Engine.



$$f_o = \frac{f_s}{1 - M \cos \theta}$$

f_o = OBSERVED FREQUENCY

M = AIRCRAFT MACH NUMBER

f_s = SOURCE FREQUENCY

θ = ANGLE FROM FLIGHT DIRECTION TO OBSERVER

Figure A-5. Doppler Frequency Shift.

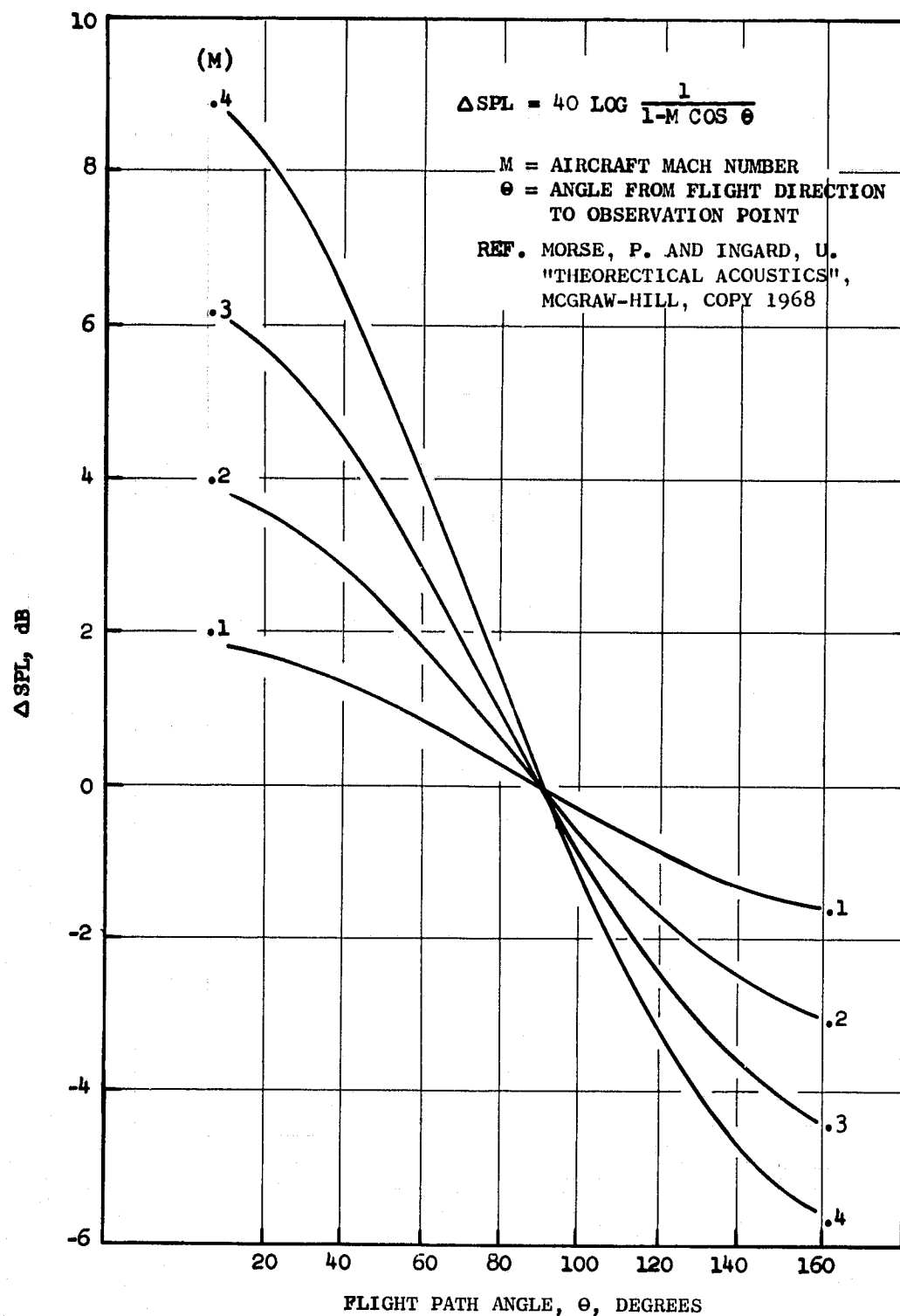


Figure A-6. Dynamic Effect - Correction Curves.

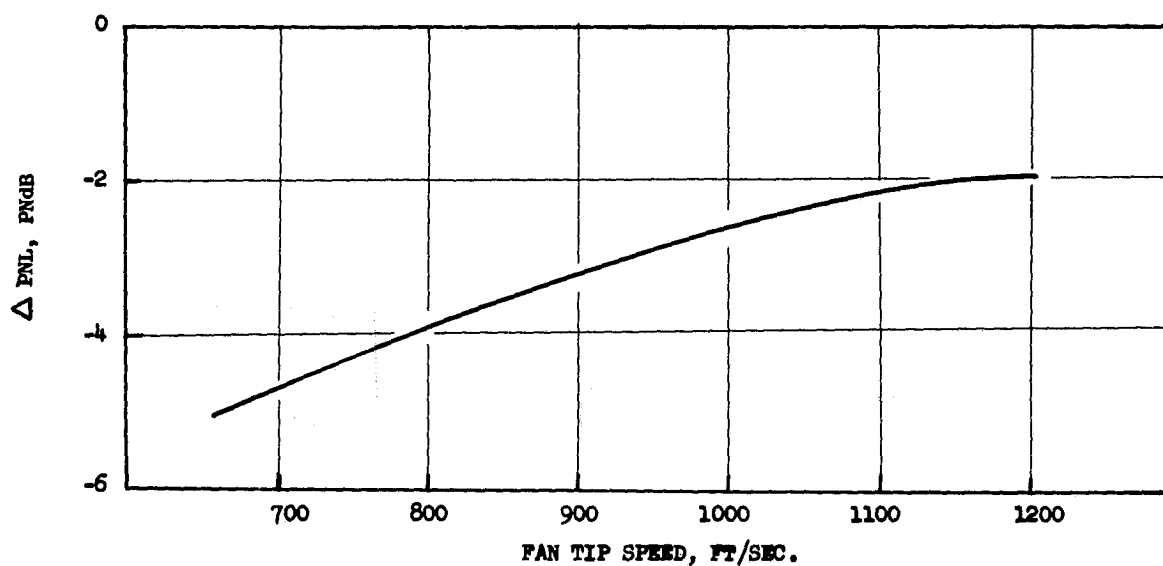


Figure A-7. In-Flight Clean-Up and Upwash Angle Correction.

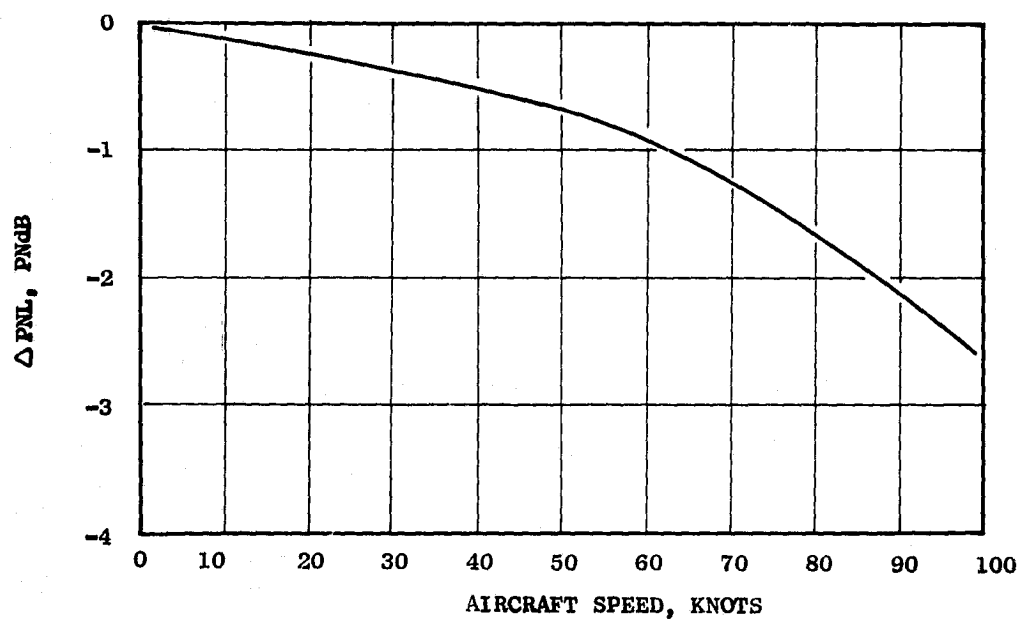


Figure A-8. Correction to OTW and UTW Jet/Flap Noise for In-Flight Effect.

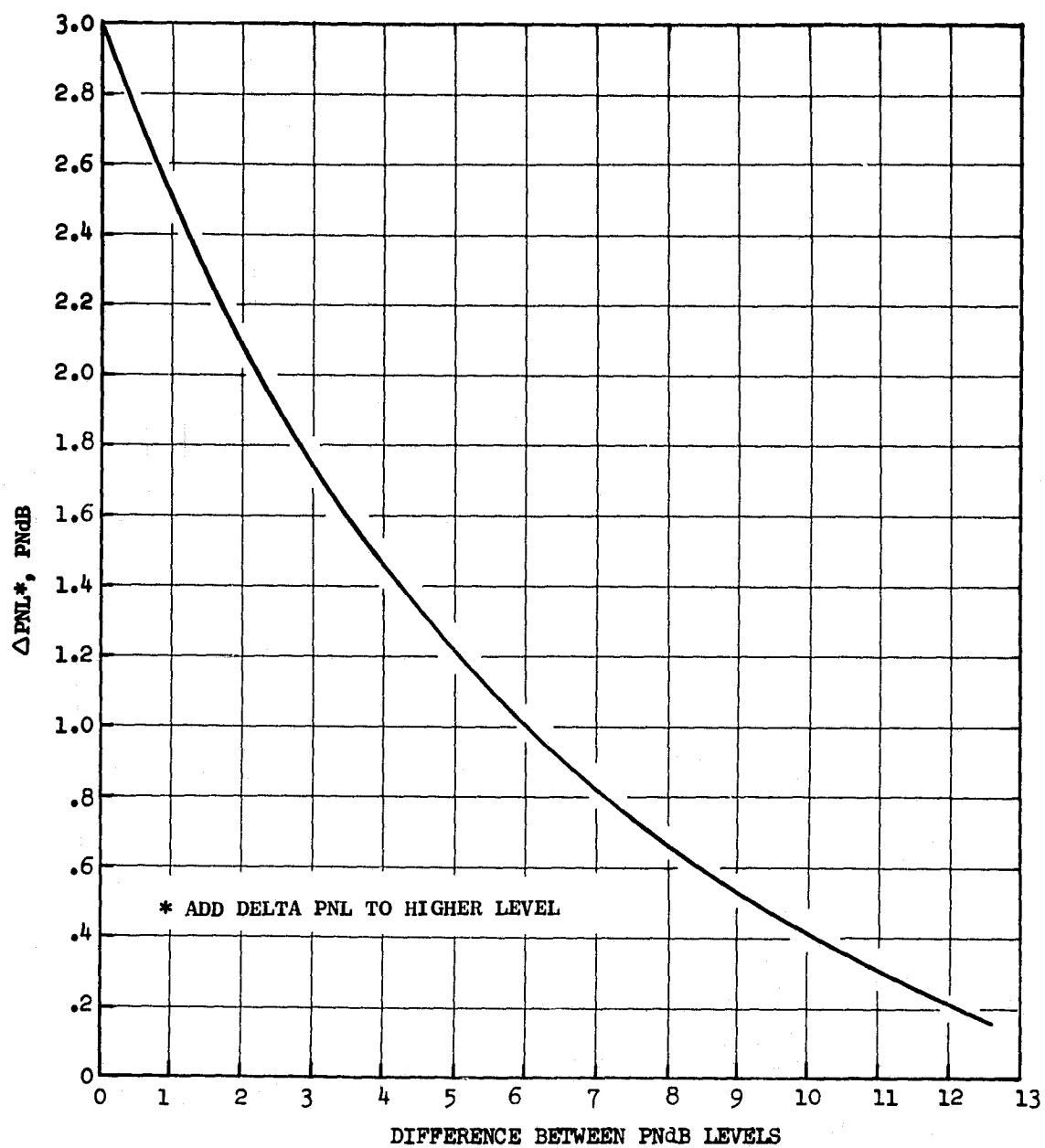


Figure A-9. Curve for Adding Constituent PNdB Levels with Similar Spectra.

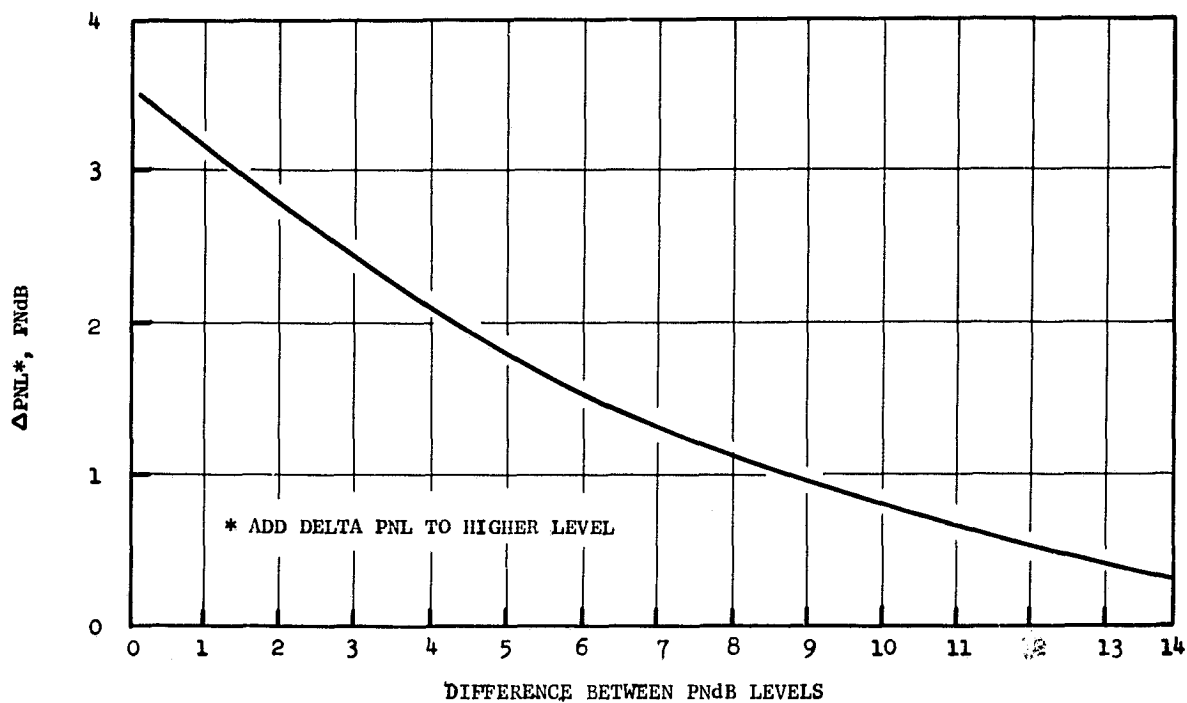


Figure A-10. Curve for Adding Constituent PNdB with Nonsimilar Spectra.

- AIRCRAFT VELOCITY = 80 KNOTS
- FOR AIRCRAFT MACH NUMBER DIFFERENT FROM 80 KNOTS, CORRECT BY $\Delta \text{dB} = 10 \text{ LOG (SPEED RATIO)}$
- TONE CORRECTION = 0

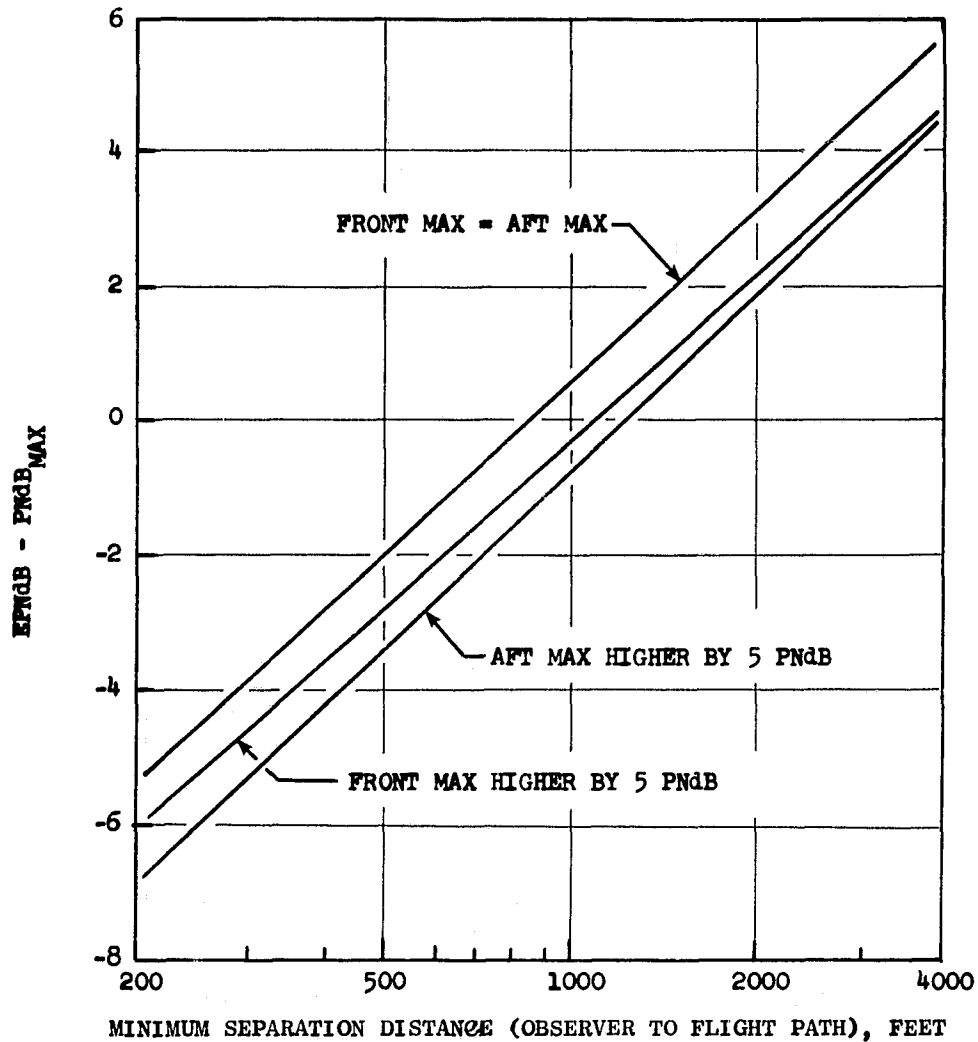


Figure A-11. PNdB to EPNdB Conversion for Highly Suppressed Engines.